

**STEREOSELECTIVE CARBON-CARBON BOND CONSTRUCTION USING
INDIUM AND BISMUTH: NEW METHODS IN GREEN CHEMISTRY**

**A Dissertation
Submitted to the Graduate Faculty
of the
North Dakota State University
of Agriculture and Applied Science**

By

Narayanaganesh Balasubramanian

**In Partial Fulfillment of the Requirements
For the Degree of
DOCTOR OF PHILOSOPHY**

**Major Department:
Chemistry & Biochemistry**

August 2012

Fargo, North Dakota

North Dakota State University
Graduate School

Title

Stereoselective Carbon-Carbon Bond Construction Using Indium and Bismuth:

New Methods in Green Chemistry

By

Narayanaganesh Balasubramanian

The Supervisory Committee certifies that this **disquisition** complies with North Dakota State University's regulations and meets the accepted standards for the degree of

Doctor of Philosophy

SUPERVISORY COMMITTEE:

Prof. Gregory R. Cook

Chair

Prof. Mukund P. Sibi

Prof. Pinjing Zhao

Prof. Chengwen Sun

Approved by Department Chair:

6th September 2012

Date

Prof. Gregory R. Cook

Department Chair

ABSTRACT

Selective chemical reactions that can be accomplished with minimal waste using non-toxic catalysts and reagents will allow for new greener chemical processes for future environmentally sustainable technologies. This work will present an account on enantioselective nucleophilic addition to carbon-nitrogen and carbon-oxygen double bonds mediated by the environmentally benign indium and bismuth metals.

The dissertation entitled “ Stereoselective carbon-carbon bond construction using indium and bismuth: new methods in green chemistry” is divided into three chapters. Chapter one outlines a few concepts in green chemistry and background information on the vital role of indium and bismuth in present day organic synthesis.

The development of a procedure for using allylic alcohol derivatives for umpolung type allylation of chiral hydrazones is described in chapter two. This procedure affords homo allylic amines in good yields and excellent diastereoselectivity. An interesting study with respect to the mechanism of the reaction has been conducted. Switching gears towards the end of this chapter, ultrasound-promoted indium-mediated Reformatsky reaction of chiral hydrazones is described. This chapter describes a potential green chemical method for making β -amino acids.

In chapter three, indium mediated enantioselective allylation of α -ketoamides is described. The developed procedure is applied in the allylation of linear and cyclic α -ketoamides. Overall, an operationally simple and environmentally benign strategy development has been explained. The later section of this chapter discusses the Reformatsky reaction in isatin series using the same protocol applied for imines.

To fully explore any organometallic reaction, it is important to understand the mechanism with which they operate at molecular level. Chapter three outlines some of our attempts to understand the enantioselective indium and bismuth mediated allylation and the nature of chiral- indium and bismuth Lewis acids. A positive non-linear effect has been observed and studied in bismuth-mediated allylation. Key findings obtained in each chapter and their implications to the future of our research is also discussed in each chapter. The chapters also details on what we understood about the potentials of organoindium and organobismuth chemistry towards developing new green chemical methods.

ACKNOWLEDGEMENTS

I wish to express my deepest gratitude to the following people who made it possible for me achieve my goal:

Prof. Gregory R. Cook, I would like to thank you for providing me with the opportunity to conduct my graduate research in your laboratory. I appreciate all the helpful mentoring you provided me to become a proficient synthetic organic chemist. **My graduate committee: Prof. Mukund P. Sibi, Prof. Pinjing Zhao and Prof. Chengwen Sun.** Thank you all for your helpful guidance and advice during my stay at NDSU. **Prof. Seth C. Rasmussen** for his helpful advice all through my graduate carrierand for introducing me to the field of chemical history.

My former group members: Robert, Ruyuji, Yoko and Xixi. Thank you all for the all the help you provided. **Dr. Tanmay Mandal**, I enjoyed the moments we worked together through our successes and failures in all the research we performed. Thank you for your guidance and help during my intial days as a graduate student. I would like to express my sincere appreciation to **Anthony J. Ostlund** and **Dr. Vesela Ugrinova** for being excellent lab mates and providing me all the support I needed. A very special thanks to my dear friend **Taj** for encouraging me and supporting me throughout this process.

I would like to express my sincere appreciation to the Department of Chemistry and Biochemistry, NDSU and Center for Protease Research, NDSU for providing me with financial assistance through my graduate program. A big thanks is owed to my family for being very supportive in every decision I made through my life.

DEDICATION

This work is dedicated to my beloved parents

TABLE OF CONTENTS

ABSTRACT	iii
ACKNOWLEDGMENTS	v
DEDICATION.....	vi
LIST OF TABLES.....	xii
LIST OF FIGURES	xiv
LIST OF SCHEMES	xvi
GLOSSARY	xxi
LIST OF APPENDIX TABLES.....	xxv
LIST OF APPENDIX FIGURES	xxvii
CHAPTER 1. GREEN CHEMICAL METHODS USING INDIUM AND BISMUTH.....	1
1.1. Introduction.....	1
1.2. Green Chemistry: Evolution and Principles	1
1.3. Concepts and Applications	2
1.3.1. Green Solvents	3
1.3.2. Ultrasound in Organic Synthesis.....	4
1.3.3. Microwave Irradiation in Organic Synthesis	6
1.4. Measuring the Efficiency.....	7
1.5. Metal-Mediated Reactions.....	9
1.6. Metal-Mediated Allylations	10
1.7. Green Chemistry with Indium Reagents.....	27
1.8. Green Chemistry with Bismuth Reagents.....	30
1.9. Conclusions.....	34

1.10. References.....	35
CHAPTER 2. INDIUM-MEDIATED STEREOSELECTIVE NUCLEOPHILIC ADDITION TO IMINES.....	51
2.1. Introduction.....	51
2.2. Allyl Nucleophile Addition to Imines	52
2.2.1. Ümpolung Allylation of Imines	60
2.2.2. Results and Discussion	64
2.2.3. Summary of Ümpolung Allylation of Hydrazones	71
2.3. Enolate Addition to Imines	71
2.3.1. Stereoselective Reformatsky Reaction of Imines	72
2.3.2. Ultrasound-Promoted Reformatsky Reaction.....	75
2.3.3. Applications of Reformatsky Reaction and Unsolved Problems.....	79
2.3.4. Results and Discussion.....	83
2.3.5. Summary of Indium-Mediated Reformatsky Reaction	95
2.4. Supporting Information	96
2.4.1. Experimental Section	96
2.4.2. General Procedure for Preparation of Chiral Hydrazones	96
2.4.3. General Procedure for Allylation of Chiral Hydrazones.....	102
2.4.4. General Procedure for Indium-Mediated Reformatsky Reaction of Chiral Hydrazones.....	108
2.5. References	116
CHAPTER 3. STEREOSELECTIVE NUCLEOPHILIC ADDITION TO α -KETOAMIDES.....	128
3.1. Introduction.....	128
3.2. Cyclic α -Ketoamides: Isatin	129

3.2.1. 3-Substituted-3-hydroxy oxindoles from Isatin	129
3.2.2. Alkylation of Isatin	135
3.2.3. Results and Discussion.....	140
3.2.3.1. Solvent Screening and Optimization	140
3.2.3.2. Ligand Screening	142
3.2.3.3. Survey of Lewis-Acids	149
3.2.3.4. Scope of Isatins.....	150
3.2.3.5. Scope of Nucleophilic Precursors: Preliminary Results	153
3.2.3.6. Synthesis of Isatins	156
3.2.4. Summary of Isatin Alkylation.....	162
3.3. Expanding the Utility: Addition of Enolates to Isatin	163
3.4. Mechanistic Studies in Alkylation of Isatins.....	165
3.4.1. Non-Linear Effects	166
3.4.2. Mechanism of Bismuth-Mediated Reactions.....	170
3.4.3. Studies Towards Understanding Chiral-Bismuth Lewis Acids	171
3.4.4. Non-Linear Effects in Bismuth-Mediated Alkylation.....	178
3.4.5. Mechanism of Indium-Mediated Reaction	180
3.4.6. Studies Towards Understanding Chiral Indium-LewisAcids	184
3.4.7. Non-Linear Effects in Indium-Mediated Alkylation.....	190
3.4.8. Summary.....	191
3.5. Linear α -Ketoamides	191
3.5.1. Biological Significance of Linear α -Ketoamides	192
3.5.2. Alkylation of Linear α -Ketoamides	193

3.5.3. Results and Discussion	194
3.5.3.1. Ligand Screening	194
3.5.3.2. Substrate Scope	196
3.5.3.3. Choice of Nucleophilic Precursors	199
3.6. Stereochemical Reasoning	200
3.7. Conclusion	203
3.8. Supporting Information	203
3.8.1. General Procedure for the Preparation of Isatins	204
3.8.2. General Procedure for the Preparation of 1-Aryl-1 <i>H</i> -indole-2,4-diones	205
3.8.3. General Procedure for Indium-Mediated Allylation of Isatins	206
3.8.4. General Procedure for the Preparation of Linear Ketoamides	213
3.8.5. General Procedure for the Preparation of Pyruvanilides	217
3.8.6. General Procedure for Indium-Mediated Allylation of Linear Ketoamides ..	220
3.9. References	225
APPENDIX A. X-RAY ANALYSIS OF ALLYLISATIN 3.17	237
A.1. Crystal Data and Structure Refinement for Allylisatin 3.17	238
APPENDIX B. X-RAY ANALYSIS OF CROTYLISATIN 3.75	244
B.1. Crystal Data and Structure Refinement for Crotylisatin 3.75	245
APPENDIX C. X-RAY ANALYSIS OF REFORMATSKY PRODUCT 2.130h	251
C.1. Crystal Data and Structure Refinement for Reformatsky Product 2.130h	252
APPENDIX D. X-RAY ANALYSIS OF REFORMATSKY PRODUCT 2.132h	261
D.1. Crystal Data and Structure Refinement for Reformatsky Product 2.132h	262
APPENDIX E. X-RAY ANALYSIS OF CHIRAL LIGAND-BISMUTH COMPLEX	277

E.1. Crystal Data and Structure Refinement for Chiral Ligand-Bismuth Complex	278
APPENDIX F. X-RAY ANALYSIS OF RACEMIC LIGAND-BISMUTH COMPLEX.	293
F.1. Crystal Data and Structure Refinement for Racemic Ligand-Bismuth Complex ...	294
APPENDIX G. X-RAY ANALYSIS OF LIGAND-INDIUM COMPLEX	315
G.1. Crystal Data and Structure Refinement for Ligand-Indium Complex.....	316

LIST OF TABLES

<u>Table</u>	<u>Page</u>
1.1 Green Chemisty Metrics	8
1.2 Cost and Toxicity of Commonly Used Salts	33
2.1. Solvent Screening for Ümpolung Allylation of Chiral Hydrazone	65
2.2. Substrate Screening Ümpolung Allylation of Chiral Hydrazone	67
2.3. Role of Phosphines in Ümpolung Allylation of Chiral Hydrazone	69
2.4. Lewis-Acid Screening for Indium-Mediated Reformatsky Reaction	84
2.5. Solvent-free Conditions for Indium-Mediated Reformatsky Reaction.....	85
2.6. Solvent Study for Benzaldehyde Derived Achiral Hydrazones.....	86
2.7. Solvent Study with Chiral Hydrazones.....	87
2.8. Substrate Scope in Indium-mediated Reformatsky Reaction	89
2.9. Substrate Scope Continued	90
3.1. Optimizing Indium-mediated Allylation of Isatins.....	141
3.2. Initial Ligand Screening for Allylation of Isatins.....	143
3.3. Ligand Screening- BINOL Derivatives	145
3.4. Ligand Screening- BOX Ligands	147
3.5. Ligand Screening- BOX Ligands	148
3.6. Lewis Acid Screening.....	150
3.7. Substrate Scope for Isatins.....	151
3.8. Scope of Nucleophilic Precursors.....	155
3.9. Synthesis of N-Arylated Isatins	162
3.10. Solvent Screening in Bismuth-Mediated Allylation of Isatins.	173

3.11. Trials with (<i>S</i>)-Phenyl glycinol.....	176
3.12. Ligand Screening for Linear Ketoamides.....	195
3.13. Allylation of Linear Ketoamides: Substrate Scope.....	198
3.14. Allylation of Pyruvanilides.....	199

LIST OF FIGURES

<u>Figure</u>	<u>Page</u>
2.1. Thermal Ellipsoid Plot of 2.130h at 50% Probability.	94
2.2. Thermal Ellipsoid Plot of 2.132h at 50% Probability.	95
3.1. Thermal Ellipsoid Plot of (<i>R</i>)- Allyl isatin at 50% Probability Level.	153
3.2. Thermal Ellipsoid Plot of Crotylated Product at 50% Probability Level.	156
3.3. Non-Linear Effects in Asymmetric Catalysis.	167
3.4. Asymmetric Model.	168
3.5. Reservoir Model.	169
3.6. ¹ H-NMR Showing Symmetric Complex in Methanol- <i>d</i> ₄	172
3.7. Mass Spectral Analysis of Symmetrical Complex.	172
3.8. ¹ H-NMR of Bi-Lewis Acid complex in Acetonitrile- <i>d</i> ₃	173
3.9. Mass spectra of Unsymmetrical Bi-Complex.	174
3.10. ¹ H-NMR of the Reaction Mixture after 24h in Methanol- <i>d</i> ₄	174
3.11. ¹ H-NMR showing Possible Presence of Phenyl glycinol.	175
3.12. Thermal Ellipsoid Plot of (<i>S</i>)-Ph PyBOX –BiBr ₃ at 50% Probability.	177
3.13. Thermal Ellipsoid Plot of Racemic Complex at 50% Probability.	178
3.14. Non-Linear Effect Observed in Bismuth-Mediated Allylation.	179
3.15. Positive Non-Linear Effect in Reaction of Et ₂ Zn with Benzaldehyde.	180
3.16. Indium-PyBOXComplex-Formation Monitored by ¹ H-NMR.	185
3.17. Mass Spectra of Ligand + InBr ₃ in Methanol- <i>d</i> ₄	186
3.18. Complex-Formation in CD ₂ Cl ₂	187
3.19. Two Species Observed with InCl ₃ and InBr ₃	187

3.20. Complexes Observed in ^1H -NMR in Different Solvents.....	188
3.21. Mass Spectra of Various Indium Complexes.	189
3.22. Thermal Ellipsoid Plot of 2:1 Ligand:Indium Complex at 50% Probability	190

LIST OF SCHEMES

<u>Scheme</u>	<u>Page</u>
1.1. Reactions with Water as Solvent.	4
1.2. Ultrasound Promoted Reactions.	5
1.3. Microwave Promoted Reactions.	7
1.4. Useful Synthetic Transformations From Allylation.	10
1.5. Allylation of Aldehydes using Allyllithium.	13
1.6. Synthesis of Pheromone 1.27 using Allyllithium.	13
1.7. Allylation of Silylketones using Allylmagnesium.	14
1.8. Structure of Lithium, Potassium and Magnesium Allylmetals.	14
1.9. Barium-Mediated Allylation of Ketones.	15
1.10. Origin of Selectivity in Metal-Mediated Allylation.	16
1.11. Preparation of Allylzinc Reagent.	16
1.12. Zinc-Mediated Allylation.	17
1.13. Allylation of Aldehydes using Triallylborane.	17
1.14. Preparation of Chiralborane Reagent.	18
1.15. Chiralborane Reagents and Ligands.	18
1.16. Allylation using Allylsilanes.	19
1.17. Allylation of Aldehydes using Allyltributyltin.	20
1.18. Indium-Mediated Allylation of Aldehydes.	21
1.19. Allylindium Preparation and Synthesis of Yomogi Alcohol.	21
1.20. Origin of Selectivity Using Allylstannane and Indium trichloride.	22
1.21. Enantioselective Allylation Using Indium-PyBox Complex.	23

1.22. Ümpolung Allylation Using Pd(0) / In(I).	23
1.23. π -Allylpalladium from Aryl iodide and Allene.	24
1.24. Bismuth-Mediated Allylations.....	25
1.25. Cross-Coupling Reaction Using Organoindium.	28
1.26. Indium-Mediated Reformatsky Reaction.....	29
1.27. Reactions Using Aryl Bismuth Reagents.	31
1.28. Triphenyl bismuth in Organic Synthesis.	31
1.29. Bismuth(III)- Catalyzed Pechmann Condensation.	33
2.1. Drug Molecules Containing Chiral Amine Moiety	51
2.2. Metal-Mediated Allylation of Imines	52
2.3. Imines With Chiral Auxiliary	52
2.4. Aluminum-Mediated Diastereoselective-Allylation of Imines.....	53
2.5. Stereochemical Outcome of Titanium-Aluminum Mediated Allylation	54
2.6. Allylation of Imines Using Magnesium Reagent	55
2.7. Allylation of Aldimines Using Allylboron Reagents	56
2.8. Asymmetric Allylation of <i>N</i> -Silylimines.....	56
2.9. Allylation of Chiral Hydrazones using Allylsilanes.....	57
2.10. N-Linked Auxiliary Approach for Imines.	58
2.11. Indium-Mediated Diastereoselective Allylation of Chiral Hydrazones.	58
2.12. Indium-Mediated Enantioselective Allylation of Hydrazones.	59
2.13. Enantioselective Indium-Mediated Allylation of Imine.	59
2.14. Ümpolung Reactivity of π -Allylpalladium complex.....	61
2.15. Allylation of Aldehydes using Pd/Sn and Pd/B.....	62

2.16. Allylation of Imines using Pd/Sn and Pd/B.....	62
2.17. Mechanism of Ümpolung Allylation.....	63
2.18. Diastereoselective Allylation of Imines.....	63
2.19. Pd(0)/In(I)-mediated Allylation of Benzaldehyde.....	64
2.20. Proposed Mechanism for Phosphine Inhibition.....	70
2.21. Removal of Chiral Auxiliary.....	71
2.22. Classical Reformatsky Reaction.....	72
2.23. Chromium- and Magnesium-mediated Reformatsky Reaction.....	73
2.24. Manganese-Mediated Reformatsky Reaction.....	74
2.25. Zinc-Mediated Diastereoselective Reformatsky Reaction.....	74
2.26. Dimethylzinc-Mediated Enantioselective Reformatsky Reaction of Ketones.....	75
2.27. One-pot Enantioselective Reformatsky Reaction of Imines.....	75
2.28. Zinc-Silver couple Mediated Reformatsky Reaction.....	76
2.29. Ultrasound-Promoted Zinc-Mediated Reformatsky Reaction.....	77
2.30. Indium-Mediated Diastereoselective Reformatsky Reaction.....	78
2.31. Indium-Mediated Ultrasound-Promoted Reformatsky Reaction.....	78
2.32. Total Synthesis of (+)-Acutiphycin using Reformatsky Reaction.....	79
2.33. Total Synthesis of Taxol.....	80
2.34. Total Synthesis of Maistemoneine.....	80
2.35. Total Synthesis of Epothilone B.....	81
2.36. Total Syntheses of Dolaproine.....	82
2.37. Initial Screening for Indium-Mediated Reformatsky Reaction.....	83
2.38. Pathway for Zinc-Mediated Reformatsky Reaction.....	91

2.39. Indium-Mediated <i>anti</i> -Selective Reformatsky Reaction.	92
2.40. Proposed Pathway for Indium-Mediated Reformatsky Reaction.	92
2.41. Attempts to Cleave the Chiral Auxiliary.	93
2.42. Indium-mediated Reformatsky Reaction with Substrate 2.62k	93
3.1. Linear and Cyclic α -ketoamides.	128
3.2. 3-Substituted-3-Hydroxyoxindole Based Molecules.	130
3.3. Preparation of Convolutamydine A through Aldol reaction on Dibromoisatin.	132
3.4. 3-Hydroxylation of Oxindole Using Zinc acetate as Catalyst.	133
3.5. Palladium Catalyzed Intramolecular Arylation of Oxindoles.	133
3.6. Hydroxylation of 3-allyl oxindole.	134
3.7. Allylboration of Isatin.	135
3.8. Indium-Mediated Allylation of Isatin.	135
3.9. Allylation of Isatin in Aqueous-Solvent Mixtures.	136
3.10. Syntheses of a CPC Analogue Through Allylation of Isatin.	137
3.11. Allylation of Isatins Through Transfer Hydrogenation.	137
3.12. Palladium-Catalyzed Asymmetric Allylation of Isatin.	138
3.13. Allylation of Isatin Using Chiral-Allyltin Reagent.	139
3.14. Hosomi-Sakurai type Allylation of Isatin using a Scandium Complex.	139
3.15. Sandmeyer's Synthesis.	157
3.16. Stolle's Procedure For Synthesis of Melosatin A.	158
3.17. Gassmann's Procedure.	158
3.18. Synthesis of Isatins from Indole.	159
3.19. Modified Stolle's Procedure.	160

3.20. Common N-Arylation Procedures.	161
3.21. Reformatsky Reaction of N-Protected Isatins.	163
3.22. Zinc-Mediated Reformatsky Reaction on Isatin.	164
3.23. Indium-Mediated Reformatsky Reaction on Isatin.	164
3.24. Potential Targets from Reformatsky Reaction on Isatins.	165
3.25. Stereochemical Similarities in In(0) and Bi(0)-Mediated Reactions.	166
3.26. Pre-generation of the Catalyst.	171
3.27. Alkylation of Benzaldehyde with Et ₂ Zn.	179
3.28. Generation of Allylindium(I) through Different Methods.	181
3.29. Proposed Active Species in Indium-Mediated Allylation.	181
3.30. Proposed Equations for Organoindium(I) Formation.	182
3.31. Proposed Equations for Organoindium(III) Formation.	183
3.32. Activation of Electrophile by Cationic Indium.	184
3.33. Pre-generation of Chiral Indium-Lewis acid.	185
3.34. Diastereoselective Allylation of Ketoamides.	194
3.35. Substrate Scope for Linear Ketoamides.	196
3.36. Allylation of Mesitylglyoxalic Acid Derived Ketoamide.	199
3.37. Nucleophilic Precursor scope with Linear Ketoamide.	200
3.38. Allylation of Linear Ketoamides with Indium and Bismuth.	201
3.39. Proposed Modes of Binding for Substrates to Chiral-Lewis acid.	202

GLOSSARY

Ac.....	Acetyl
AIBN.....	2,2'-Azabisobutyronitrile
aq.....	Aqueous
Ar.....	Aryl
9-BBN.....	9-Borabicyclo[3.3.1]nonane
BINAP.....	2,2'-bis(diphenylphosphino)-1,1'-binaphthyl
BINOL.....	1,1'-Bi-2-naphthol
Bn.....	Benzyl
BOC.....	<i>tert</i> -Butyloxycarbonyl
Bu.....	Butyl
<i>n</i> -BuLi.....	<i>n</i> -Butyllithium
<i>t</i> -Bu.....	<i>tert</i> -Butyl
Bu ₂ BOTf.....	Dibutyl Boron Triflate
Bu ₃ SnH.....	Tributyl tin hydride
C.....	Carbon
cat.....	Catalyst
CBZ.....	Carboxybenzoyl
<i>c</i> -hex.....	Cyclohexyl
CLA.....	Chiral Lewis Acid
COD.....	Cyclooctadiene
Config.....	Configuration
Cp.....	Cyclopentadienyl

DCC	Dicyclohexylcarbodiimide
de	Diastereomeric Excess
DIBAL	Diisobutylaluminum Hydride
DMF	Dimethylformamide
DMS	Dimethylsulfide
dr	Diastereomeric Ratio
E ⁺	Electrophile
ee	Enantiomeric Excess
eq	Equivalent
equiv	Equivalent
Et	Ethyl
Et ₃ B	Triethylborane
EtOAc	Ethyl Acetate
EtOH	Ethanol
fod	tris-6,6,7,7,8,8,8-Heptafluoro-2,2-dimethyl-3,5-octanedionato
GC	Gas Chromatography
h	Hours
HPLC	High Pressure Liquid Chromatography
<i>i</i> -Pr	<i>iso</i> -Propyl
L	Ligand
L*	Chiral Ligand
LA	Lewis Acid
LDA	Lithium Diisopropylamide

lit.	Literature
MAD	Methylaluminum bis(4-methyl-di- <i>t</i> -butylphenoxide)
<i>m</i> -CPBA	<i>m</i> -Chloroperbenzoic Acid
Me	Methyl
Menth	Menthol
MeOH	Methanol
min	Minutes
M	Metal
ML _n *	Chiral Lewis Acid Complex
mol	Molar
mol sieves	Molecular Sieves
Ms	Methanesulfonyl
NaH	Sodium Hydride
NOE	Nuclear Overhauser Effect
NMR	Nuclear Magnetic Resonance
Nu	Nucleophile
OTf	Triflate
ox.	Oxidation
PDC	Pyridinium Dichromate
Ph	Phenyl
piv-Cl	Pivaloyl Chloride
Prod.	Product
pyr	Pyridine

Ra-Ni.....	Raney Nickel
RT	Room temperature
SbF ₆	Antimony Hexafluoride
TADDOL.....	<i>trans</i> -2,2-dimethyl-a,a,a'-tetraphenyl-1,3-dioxolane-4,5-dimethanol
TBAF	Tetrabutylammonium Fluoride
TBDMS.....	<i>tert</i> -Butyldimethylsilyl
TBDPS.....	<i>tert</i> -Butyldiphenylsilyl
TBS	<i>tert</i> -Butyldimethylsilyl
Temp.....	Temperature
THF	Tetrahydrofuran
THP	Tetrahydropyran
TLC.....	Thin Layer Chromatography
TMSCl.....	Trimethylsilyl Chloride
TMSI.....	Trimethylsilyl Iodide
tol.....	Toluene
TsOH.....	Toluenesulfonic acid
TTMS.....	Tris(trimethylsilyl)silane
X	Halogen Ligand

LIST OF APPENDIX TABLES

<u>Table</u>	<u>Page</u>
A.1. Atomic Coordinates and Equivalent Isotropic Displacement Parameters for Allylisatin 3.17	240
A.2. Symmetry Operations for Allylisatin 3.17	241
A.3. Bond Lengths for Allylisatin 3.17	241
A.4. Bond Angles for Allylisatin 3.17	242
B.1. Atomic Coordinates and Equivalent Isotropic Displacement Parameters for Crotylisatin 3.75	247
B.2. Symmetry Operations for Crotylisatin 3.75	247
B.3. Bond Lengths for Crotylisatin 3.75	248
B.4. Bond Angles for Crotylisatin 3.75	249
C.1. Atomic Coordinates and Equivalent Isotropic Displacement Parameters for Reformatsky Product 2.130h	254
C.2. Symmetry Operations for Reformatsky Product 2.130h	255
C.3. Bond Lengths for Reformatsky Product 2.130h	256
C.4. Bond Angles for Reformatsky Product 2.130h	257
D.1. Atomic Coordinates and Equivalent Isotropic Displacement Parameters for Reformatsky Product 2.132h	264
D.2. Bond Lengths for Reformatsky Product 2.132h	267
D.3. Bond Lengths for Reformatsky Product 2.132h	270
E.1. Atomic Coordinates and Equivalent Isotropic Displacement Parameters for Chiral Ligand-Bismuth Complex	280
E.2. Symmetry Operations for Chiral Ligand-Bismuth Complex	283
E.3. Bond Lengths for Chiral Ligand-Bismuth Complex	283
E.4. Bond Angles for Chiral Ligand-Bismuth Complex	286

F.1. Atomic Coordinates and Equivalent Isotropic Displacement Parameters for Racemic Ligand-Bismuth Complex.....	295
F.2. Bond Lengths for Racemic Ligand-Bismuth Complex	299
F.3. Bond Lengths for Racemic Ligand-Bismuth Complex	299
F.4. Bond Angles for Racemic Ligand-Bismuth Complex.....	303
G.1. Atomic Coordinates and Equivalent Isotropic Displacement Parameters for Ligand-Indium Complex	317
G.2. Symmetry Operations for Ligand -Indium Complex.....	323
G.3. Bond Lengths for Ligand-Indium Complex	324
G.4. Bond Angles for Ligand-Indium Complex	330

LIST OF APPENDIX FIGURES

<u>Figure</u>	<u>Page</u>
A.1. Thermal Ellipsoid Plot of Allylisatin 3.17	237
A.2. Crystal Packing of Allylisatin 3.17	237
B.1. Thermal Ellipsoid Plot of Crotylisatin 3.75	244
B.2. Crystal Packing of Crotylisatin 3.75	244
C.1. Thermal Ellipsoid Plot of Reformatsky Product 2.130h	251
C.2. Crystal Packing of Reformatsky Product 2.130h	251
D.1. Thermal Ellipsoid Plot of Reformatsky Product 2.132h	261
D.2. Crystal Packing of Reformatsky Product 2.132h	261
E.1. Thermal Ellipsoid Plot of Chiral Ligand-Bismuth Complex	277
E.2. Crystal Packing for Chiral Ligand-Bismuth Complex	277
F.1. Thermal Ellipsoid Plot of Racemic Ligand-Bismuth Complex	293
F.2. Crystal Packing of Racemic Ligand-Bismuth Complex	293
G.1. Thermal Ellipsoid Plot of Ligand-Indium Complex	315
G.2. Crystal Packing of Ligand-Indium Complex	315

CHAPTER 1. GREEN CHEMICAL METHODS USING INDIUM AND BISMUTH

1.1. Introduction

For the past century, metal-mediated reactions have played an important role in defining the path of organic synthesis. In the last decade, two metals in particular have emerged as “green metals” in this field: indium and bismuth. Reactions employing these metals or compounds containing these metals embrace the principles of green chemistry. This research work consists of environmentally benign stereoselective methods developed using indium and bismuth.

1.2. Green Chemistry: Evolution and Principles

Towards the end of the twentieth century, with the alarming increased rate of emission of greenhouse gases and increasing safety concerns about industrial accidents due with the non-eco-friendly practices in chemical industries,¹ a big revolution started. In 1990 the EPA established a policy to either prevent pollution or reduce it at its source. Paul Anastas, the science advisor to EPA coined the term “green chemistry” in 1991.² Later Paul and John C. Warner developed the twelve principles of green chemistry.³

“The twelve principles of green chemistry are as follows

1. It is better to prevent waste than to treat or clean up waste after it is formed.
2. Synthetic methods should be designed to maximize the incorporation of all materials used in the process into the final product.
3. Wherever practicable, synthetic methodologies should be designed to use and generate substances that possess little or no toxicity to human health and the environment
4. Chemical products should be designed to preserve efficacy of function while

reducing toxicity.

5. The use of auxiliary substances (e.g. solvents, separation agents, etc.) should be made unnecessary whenever possible and innocuous when used.
6. Energy requirements should be recognized for their environmental and economic impacts and should be minimized. Synthetic methods should be conducted at ambient temperature and pressure.
7. A raw material feedstock should be renewable rather than depleting whenever technically and economically practical.
8. Unnecessary derivatization (blocking group, protection/deprotection, temporary modification of physical/chemical processes) should be avoided whenever possible.
9. Catalytic reagents (as selective as possible) are superior to stoichiometric reagents.
10. Chemical products should be designed so that at the end of their function they do not persist in the environment and break down in innocuous degradation products.
11. Analytical methodologies need to be further developed to allow for real-time in-process monitoring and control prior to the formation of hazardous substances.
12. Substances and the form of a substance used in a chemical process should be chosen so as to minimize the potential for chemical accidents, including releases, explosions, and fires.”

1.3. Concepts and Applications

A major aspect of conducting organic reactions in a benign fashion is to look carefully at the properties of the reaction medium. One of the major factors of pollution from reactions carried out in large scale by industries is the toxic solvent waste. Industrial effluents mixing with drinking water supply is one of the major issues in third-world

countries. The rest of this chapter will focus mainly on green solvents and how indium and bismuth are compatible with these methods and able to promote the concept of green chemistry.

Some of the notable advancements made due to the advent of green chemistry are: H-beta catalyzed Friedel-Crafts acylation,⁴ 100% atom-efficient amidocarbonylation,⁵ Diels-Alder reactions with water compatible Lewis-acids, synthesis of cumene from benzene using zeolites and polymer-supported recyclable catalysts.

1.3.1. Green Solvents

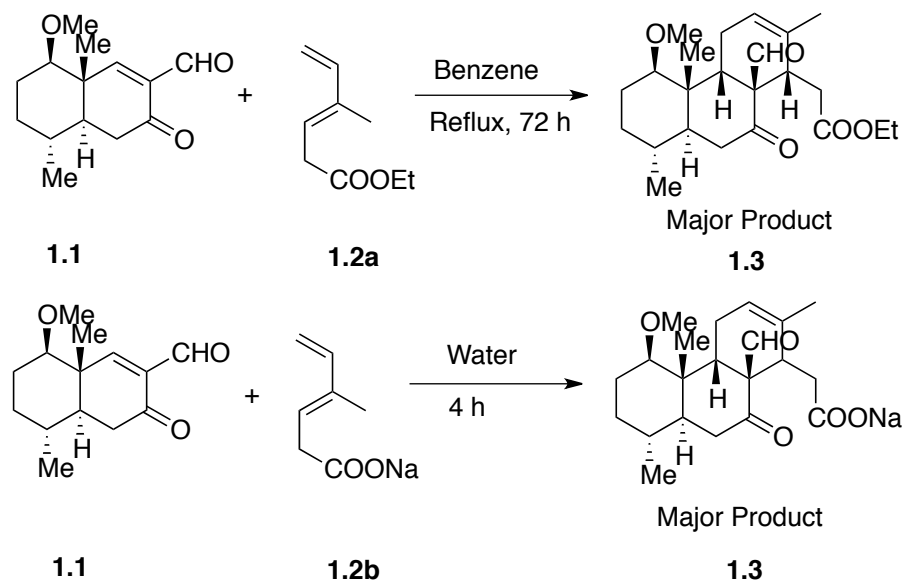
The green chemical institute identified the following reaction mediums to be efficient and have a lower impact on environment, health and safety. The “greener” solvent is determined by the method developed by EHS.⁶

1. Water and aqueous solvent mixtures⁷
2. Solvents derived from bio-mass such as ethanol and methanol⁸
3. Supercritical fluids⁹
4. Non-volatile ionic liquids¹⁰

Water as a solvent for synthesis was ignored for a long time due to the insolubility of numerous organic compounds. Water has several beneficial characteristics including high heat capacity, high cohesive energy, very large surface tension and very good hydrogen bonding property. The hydrophobicity of many compounds in an aqueous media can actually be useful in organic synthesis. A natural example of this principle is found in the human body. Numerous reactions in our body happen in aqueous medium.¹¹ The hydrophobic effect is a main reason for the binding of enzymes to substrates in biological

systems. All these reactions that are ubiquitous to human survival happen in an aqueous environment.

Ronald Breslow is a pioneer in the field of organic reactions in aqueous media.¹² He initiated a detailed study of pericyclic reactions in water and found that many organic transformations proceed more rapidly and effectively in water than in common organic solvents.¹³ It appeared as if water was the missing ingredient in these reactions. Diels-Alder reactions have been reported to have an enhanced rate under aqueous conditions. Grieco et al reported a notable example of bio-molecule synthesis using a Diels-Alder reaction (Scheme 1.1).¹⁴ The reaction of **1.1** with the diene **1.2a** took 72 hours for completion under reflux in benzene. Whereas in water, when the sodium salt **1.2b** is used, the reaction was complete in 4 hours.



Scheme 1.1. Reactions with Water as Solvent

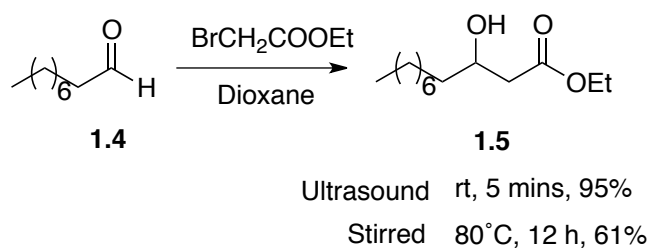
1.3.2. Ultrasound in Organic Synthesis

The development of ultrasound-mediated reactions is a field that is still in the developing stages.¹⁵ Ultrasound is considered to be a non-classical form of energy source

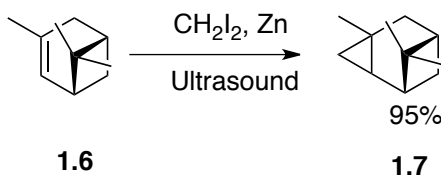
for reactions. The main areas of its applications include cleaning metal surfaces, Emulsification, degassing liquids, sterilization and extraction.¹⁶ Ultrasound was first used for surface activation of metals in the Reformatsky reaction. Later on, the extent of the applications has increased. Today, sonochemical methods are used in organic synthesis for variety of reasons.¹⁷ These include, increasing the speed and improving the yield of a reaction, switching the reaction pathways, improving particle synthesis, avoiding phase transfer catalysis and efficient energy usage.

In 1982, Han and Boudjouk reported the benefit of ultrasound in organic synthesis. They presented a comparative picture for a Reformatsky type reaction of 1-octanal **1.4** under ultrasound condition and normal stirring to produce the β -hydroxy ester. The reaction took twelve hours under heating to produce average yield. Where as under ultrasound promoted condition, it took five minutes for excellent yield of **1.5**. Following this report and similar reports, the use of this method in organic synthesis has become increasingly important (Scheme 1.2).¹⁸

Reformatsky Reaction



Simons-Smith Cyclopropanation



Scheme 1.2. Ultrasound Promoted Reactions

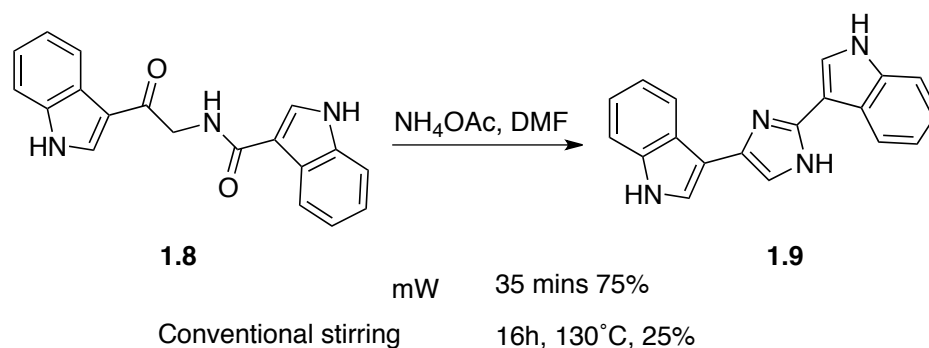
Following the Reformatsky reaction, cyclopropanation¹⁹ and other reactions have been performed under ultrasound-mediated condition. The chemical effects of ultrasound are primarily due to the cavitation effect. The collapse of the bubbles that are formed during sonication results in the generation of large amounts of energy.²⁰ Due to this energy the interfacial region between the bubbles has temperatures about 5000°C and pressure of several hundred atmospheres. The heating and cooling rates are on the order of 10¹⁰ K/s. The high degree of temperature and pressure could be beneficially used in organic synthesis.²¹

Today ultrasound has not only found its application in organic synthesis, but also for making nano-particles,²² making protein microspheres used in MRI,²³ drug delivery²⁴ and polymer synthesis.²⁵ Chapter two discusses the use of ultrasound in the Reformatsky reaction of chiral hydrazones under solvent free conditions. It is worth mentioning that the amount of literature available in stereoselective reactions promoted by ultrasound is very low.

1.3.3. Microwave Irradiation in Organic Synthesis

Microwave is one of the unconventional energy sources for organic reactions.²⁶ Generally non-polar molecules are inert to microwave radiation. Only molecules with a net dipole moment can absorb microwave energy. Microwave is a non-ionizing radiation and it cannot break bonds. In the case of many reactions, microwave produces the heating effect, which accelerates the reaction. Microwaves have been shown to facilitate the hydrolysis of amides, esters, nitriles and peptides. Tertiary amides, which are stable to hydrolysis even under reflux conditions, are successfully hydrolyzed under microwave irradiation.²⁷

Microwave has both thermal effects and non-thermal effects. The former is due to the ability of molecules possessing a dipole and thereby absorbing the microwave energy and convert it to thermal energy. The non-thermal effects of microwave irradiation are still under debate.²⁸ The amount of literature that exists in the asymmetric microwave induced reactions suggests that the increased temperature results in the loss of selectivity. Gedye et al compared a set of reactions under thermal and microwave induction and demonstrated the advantages of microwave.²⁹ An illustrative example of the synthesis of the diindolyl compound **1.9** is described in Scheme 1.3. A cyclization that requires longer reaction time and high temperature was facilitated in minutes with a higher yield by using microwave.³⁰



Scheme 1.3. Microwave Promoted Reactions

1.4. Measuring the Efficiency

Implementing the methods and principles of green chemistry is as important as developing a measuring system for those processes. Several works have been disclosed for measuring the processes that claim to be “green”. Some well-known concepts of green chemistry are outlined in Table 1.1. Measuring the efficiency of a process or a reaction is imperative. To date, no generalized method has been developed to access any process or

method that claims to be eco-benign.³¹ As early as 1995, Trost introduced the concept of atom economy, which remained widely used way to analyze processes for a decade.³²

Hudlicky proposed to consider only the mass of non-benign reagents while analyzing a process and came up with the idea of effective mass-yield. This term often has been criticized because most of the substances used in industry are non-benign. The pharmaceutical manufacturer GSK came up with concepts such as carbon efficiency and reaction mass efficiency.³³ Instead of considering all the atoms, carbon efficiency considered as the name stands, considered only carbons. Both of these concepts were relatively unused in the present scenario.

Table 1.1. Green Chemistry Metrics³⁴

Concept	Introduced by	Calculation
Effective Mass Yield	Hudlicky	$\frac{\text{Mass of Products}}{\text{Mass of non-benign reagents}} \times 100$
Carbon Efficiency	GSK	$\frac{\text{Amount of C in pdt} \times 100}{\text{Total C in the reactants}}$
Atom Economy	Barry Trost	How much of reactants remain in the final product
Reaction Mass Efficiency	GSK	$\frac{\text{A + B} \rightarrow \text{C}}{\text{Mass of Pdt C}} \times 100$ $\frac{\text{Mass of Pdt C}}{\text{Mass of A + Mass of B}}$
E-Factor	Roger Sheldon	$\frac{\text{Total Waste (Kg)}}{\text{Product (Kg)}}$

Recently Roger Sheldon proposed the concept of E factor. The E-factor is the ratio of the amount of waste produced with respect to the amount of product obtained.³⁵ Instead of using the concepts separately, atom economy, effective mass yield and carbon efficiency have been used in conjunction with other methods. Eco scale is a semi-quantitative tool developed by researchers in Switzerland, which utilizes a complex calculation for computing economical and ecological parameters.³⁶

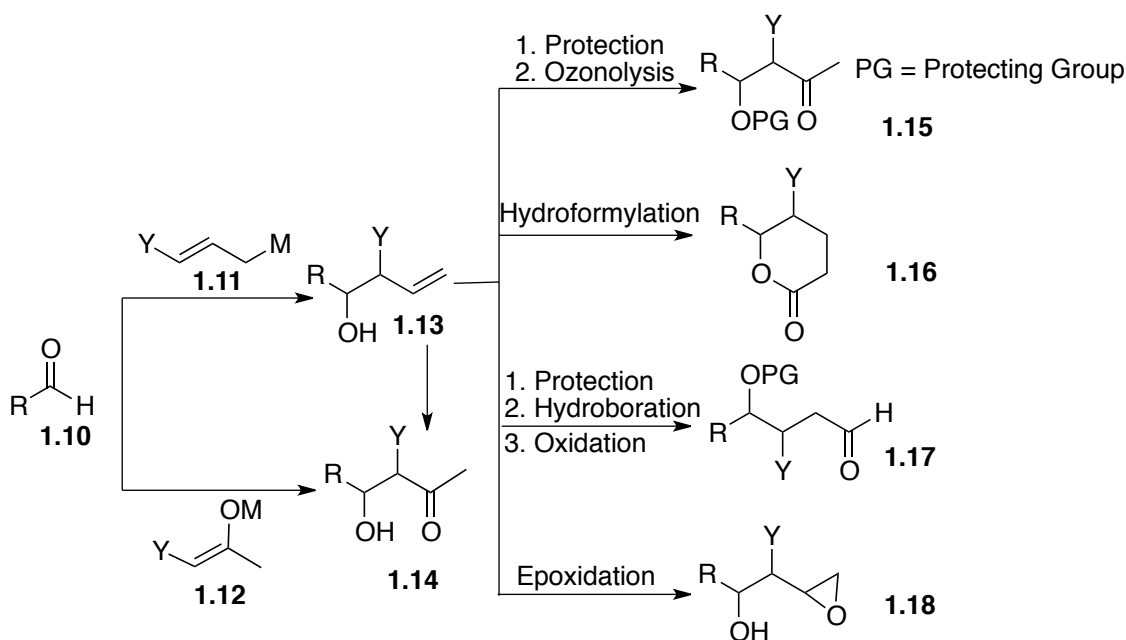
1.5. Metal-Mediated Reactions

Metal-mediated reactions are fundamental in organic synthesis.³⁷ Whether it is a transition metal mediated reaction, or a Lewis-acid catalyzed reaction, the use of metals and their compounds are ubiquitous in organic synthesis. The discovery and development of stereoselective carbon-carbon bond forming reactions is one of the major achievements in synthetic organic chemistry in the past century.³⁸ This achievement would not be possible without metal mediated reactions. The advent of Barbier and Grignard type reactions has changed the course of constructing complex molecular architectures.³⁹

The addition of carbon nucleophiles to various electrophiles is a field that evolved in the mid-eighteenth century. In the past century it has been found that a number of metals can mediate these transformations. Metals such as Mg, Zn, Sb, Sn, Pb, Ga, Bi and In are used in Barbier and Grignard type reactions for C-C bond formation.⁴⁰ The salts of the main group metals as well as transition metals have significant utility in carbon-carbon bond forming reactions as Lewis acids or Lewis bases or chelating templates. Excellent monographs have been written in this area and many of these reactions are applied in a large-scale chemical and pharmaceutical industries.⁴¹

1.6. Metal-Mediated Allylations

Of all carbon functionality that could be introduced to an electrophilic carbon, with substantial argument allyl group is one of the most versatile. The latent allyl functional group is attractive for synthetic elaboration (Scheme 1.4).⁴²



Scheme 1.4. Useful Synthetic Transformations From Allylation

The most common strategy to introduce the allyl group is the use of allyl metal reagents. Stereoselective metal-mediated allylations are performed with the use of chiral ligands, or the addition of allyl metal reagents are assisted using chiral Lewis acids. An existing problem of metal-mediated allylations is the generation of metal salts as by-products. The toxicity of the waste generated depends on the nature of the metal used. A desired ideal metal-mediated allylation will use a minimum amount of the metal and the nucleophilic precursor to achieve a good yield of the product in high stereoselectivity. As mentioned before allylation methods are often used in the earlier stages of an elaborate

synthesis and performed in large scales hence reducing toxic metal waste in this step would be attractive.

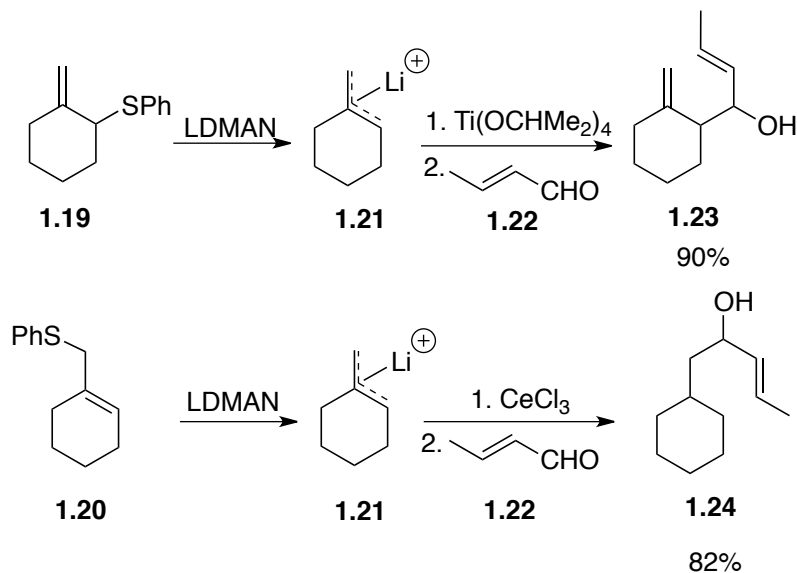
As early as 1970's people started investigating allyl metal reagents for synthetic purpose.⁴³ Prior to those major investigations, allyl metal reagents have been primarily investigated for structural studies.⁴⁴ The 1,3-transposition of allyl metals was also widespread area of interest.⁴⁵ The below discussion outline some allyl metal reagents, their structure, reactivity and application.

The following metals were explored in general for allylations of electrophilic carbons.

1. Group 1 (lithium, sodium and potassium)
2. Group 2 (magnesium and barium)
3. Group 3 (cerium, lanthanum, Neodymium, Samarium and ytterbium)
4. Group 4 (titanium and zirconium)
5. Group 6 (chromium and molybdenum)
6. Group 7 (Manganese)
7. Group 8 to 10 (iron, cobalt and nickel)
8. Group 11 (copper)
9. Group 12 (cadmium)
10. Group 13 (boron, aluminum and indium)
11. Group 14 (silicon, germanium, tin and lead)
12. Group 15 (arsenic, antimony and bismuth)
13. Group 16 (tellurium)

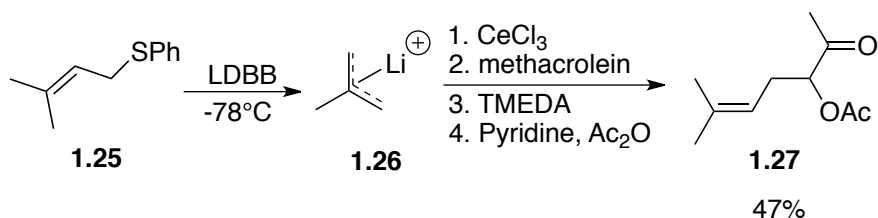
The following discussion outlines only the metals that made a major impact with their selectivity and applicability in organic synthesis. Different groups have extensively reviewed the addition of allyl metal reagents to electrophilic carbons.

Among the group one metals, allyllithiums have been known to exist for a long time. Unlike alkylolithium compounds, allyllithium cannot be prepared by halogen metal exchange since that would cause substitution reaction. They are prepared by transmetallation from allyltin reagents and allyllead reagents with alkylolithium.⁴⁶ The most common method for the preparation of allyllithium is to react alkylolithium with allylmethyl or allylphenyl selenides and cleaving the ethers with lithium or lithium biphenyls.⁴⁷ Substituted allyllithium reagents react with poor selectivity. Unsymmetrical allyllithium reagents react with aldehydes producing mixture of products with slightly higher preference for the attack at more substituted position. In the presence of a Lewis acid the selectivity changes. For instance, simple aldehyde reacted with unsymmetrical allyl lithium in the presence of titanium Lewis acid resulted in attack from the more substituted site giving the allyl alcohol **1.23**. When the Lewis acid was modified to cerium chloride the reaction occurred from the less substituted site yielding the allylic alcohol **1.24** (Scheme 1.5).⁴⁸



Scheme 1.5. Alkylation of Aldehydes using Allyllithium

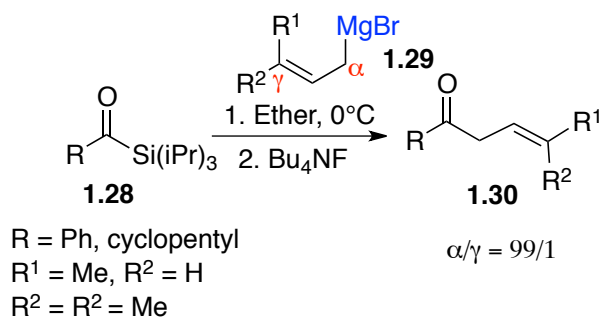
This observation was beneficial for the synthesis of Comstock mealybug pheromone **1.27**. The allyl lithium generated at low temperature from the thioether **1.25** is reacted with methacrolein. Acetylation of the resulting homoallylic alcohol produced the product pheromone **1.27** in average yields (Scheme 1.6).⁴⁹



Scheme 1.6. Synthesis of Pheromone **1.27** using Allyllithium

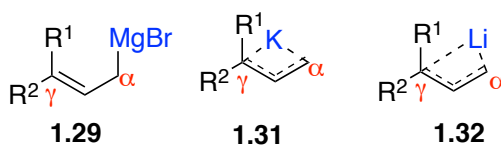
Allylsodium and allylpotassium reagents are relatively less explored compared to allyl lithium reagents. Allylmagnesium reagents or most commonly referred to as allyl Grignard reagents are well known and have been used for allylation for more than a century. Substituted Grignard reagents such as crotylmagnesium bromide and prenylmagnesium bromide react selectively with aromatic aldehydes at the γ -position. For example

triisopropylsilyl ketones react with substituted magnesium reagents to produce the α -products in great selectivity (Scheme 1.7).⁵⁰



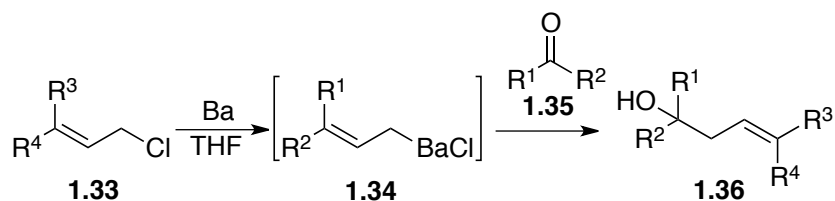
Scheme 1.7. Alkylation of Silylketones using Allylmagnesium

The structures of the allyl magnesium, lithium and potassium reagents were studied using isotopic perturbation method and NMR technique. These studies indicated that crotyl magnesium reagent **1.29** has σ -structure and the magnesium metal is attached to the least substituted carbon. Potassium **1.31** and lithium reagents **1.32** on the other hand are π -structures. Studies also indicated that the carbon-metal bond length in crotylpotassium reagent is equal and there are unequal bond length's observed with crotyllithium reagent (Scheme 1.8).⁵¹



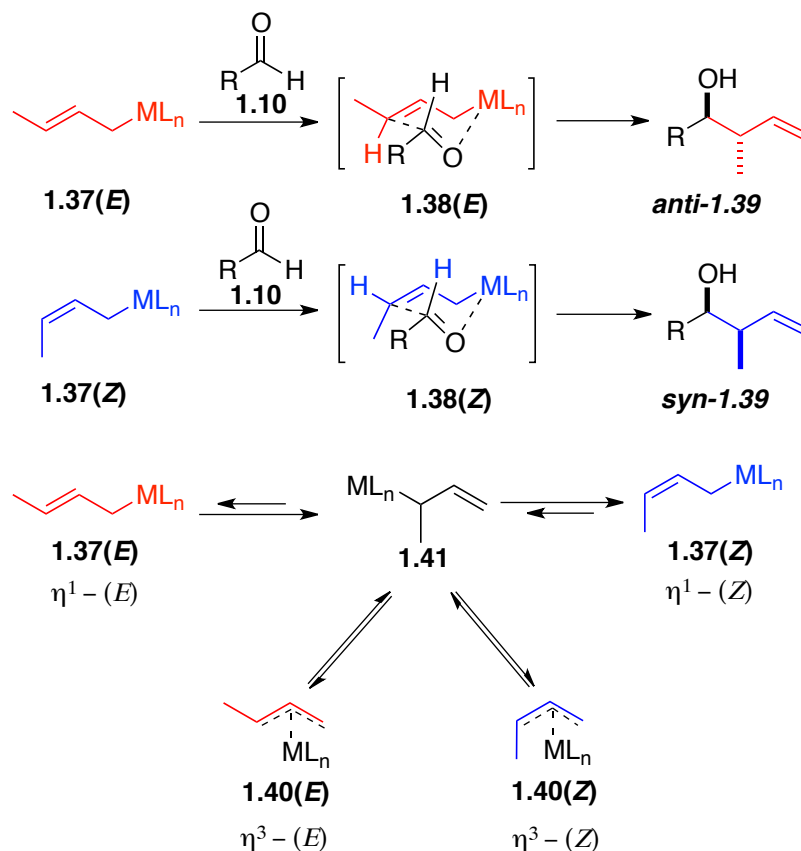
Scheme 1.8. Structure of Lithium, Potassium and Magnesium Allylmetals

Allylbarium reagents are prepared from the reaction of barium metal with allylic chlorides. Allylbarium reagents react with a high α -selectivity. The reaction of prenyl chloride with barium metal in THF resulted in the formation of prenylbarium species **1.33**. This further reacts with aldehydes or ketones to produce α -adduct **1.36** exclusively (Scheme 1.9).⁵²



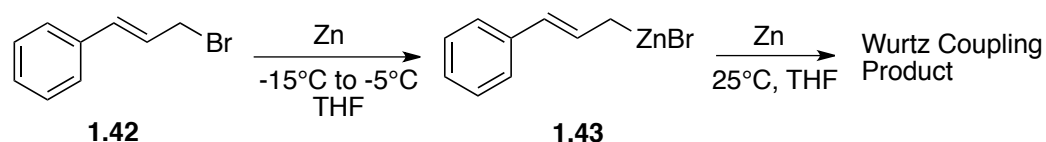
Scheme 1.9. Barium-mediated Allylation of Ketones

Considering the stereoselective C-C bond formation, substituted allylmetal reagents can exist in two different forms η_1 - σ -complex and η_3 - π -complex. This will reflect in their reactivity and thus the observed product selectivity. Considering crotylmetal reagent as an example, if the *E* crotyl reagent **1.37**(*E*) reacts with the aldehyde **1.10**, it produces the *anti*-isomer *anti*-**1.39**. The *Z* crotylmetal reagent **1.37**(*Z*) reacts with the aldehyde **1.10** to produce the *syn*- isomer *syn*-**1.39**. Thus the stereochemical information present in the reagent is transmitted to the product as *syn*- or *anti*- relationship. This would be possible if the crotylmetal reagent is configurationally stable. Generally the η_1 crotylmetal reagent **1.37** is not configurationally stable they undergo metallotropic rearrangement. For instance, the *E*- crotylmetal **1.37**(*E*) can rearrange to a methallyl species **1.41**. This species can undergo isomerization to η_3 -allyl metal **1.40**, which could be a η_3 -*E*-crotylmetal **1.40**(*E*) or a η_3 *Z*-crotylmetal reagent **1.40**(*Z*). Thus the stereochemical information that is supplied in the preliminary stage of a reaction cannot be successfully transmitted to the product because of the effects of the isomerization. This stability of the η_1 crotylmetal reagent changes with the nature of the metal. In some cases it has been successfully demonstrated that the selectivity could be changed with the addition of Lewis acid.⁵³



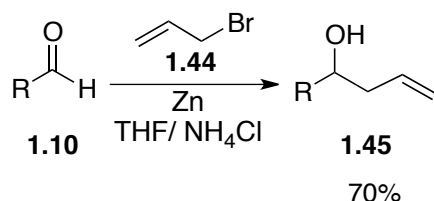
Scheme 1.10. Origin of Selectivity in Metal-Mediated Allylation

Next to organomagnesium and organolithium reagents, the oldest known organometallic reagents are the zinc compounds.⁵⁴ Allylzinc halides are similar in reactivity to allylmagnesium reagents as well as they could be prepared similar to Grignard reagents. Allylzinc reagent **1.43** from cinnamyl bromide **1.42** could be prepared at low temperatures in THF.⁵⁵ Similar to Allyllithium and allylmagnesium reagents, allylzinc reagents undergo Wurtz type homo coupling.⁵⁶



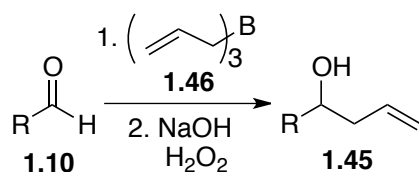
Scheme 1.11. Preparation of Allylzinc reagent

Luche showed that zinc could mediate allylation of aldehydes in mixture of saturated ammonium chloride and THF to produce the homoallylic alcohol **1.45** in average yield. The other byproducts include the homocoupled product from *in situ* generated allylzinc (Scheme 1.12).⁵⁷

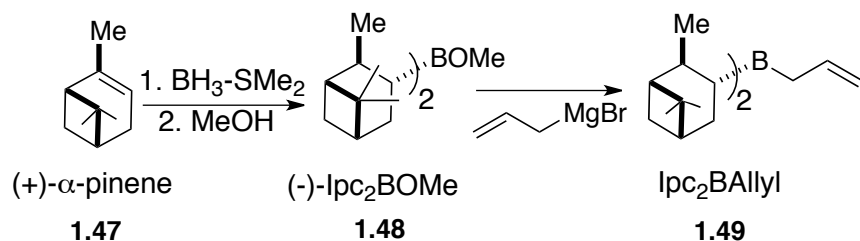


Scheme 1.12. Zinc-mediated Allylation

In 1964, Mikhailov and Bubnov showed that triallylborane adds to aldehydes and ketones effectively to form borane esters.⁵⁸ Under hydrolytic conditions, these esters yield homoallylic alcohols in good yield (Scheme 1.13). The attractive feature of boron reagents is that there are different chiral boron reagents available to carry out asymmetric transformations. A major disadvantage in using boron reagents is the stoichiometric amount of the bulky groups present in the reaction, which is not atom economical. Brown and co-workers demonstrated the synthesis of chiral borane reagents for allylation. A major disadvantage with borane reagents is that their preparation involves multiple steps (Scheme 1.14).⁵⁹

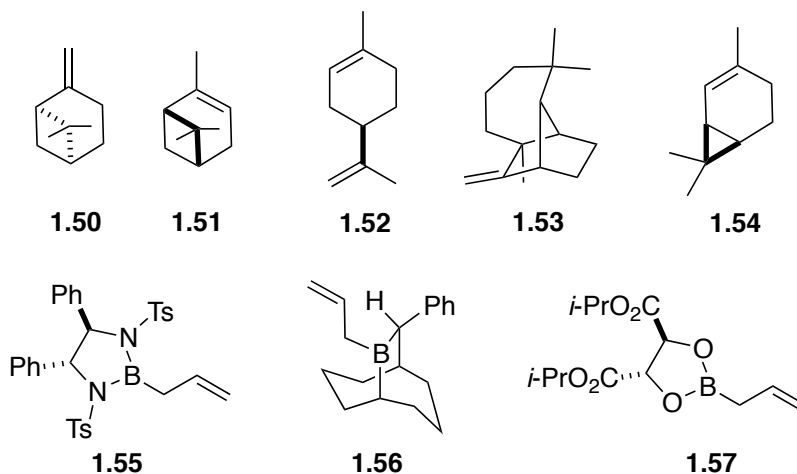


Scheme 1.13. Allylation of Aldehydes using Triallylborane



Scheme 1.14. Preparation of Chiralborane Reagent

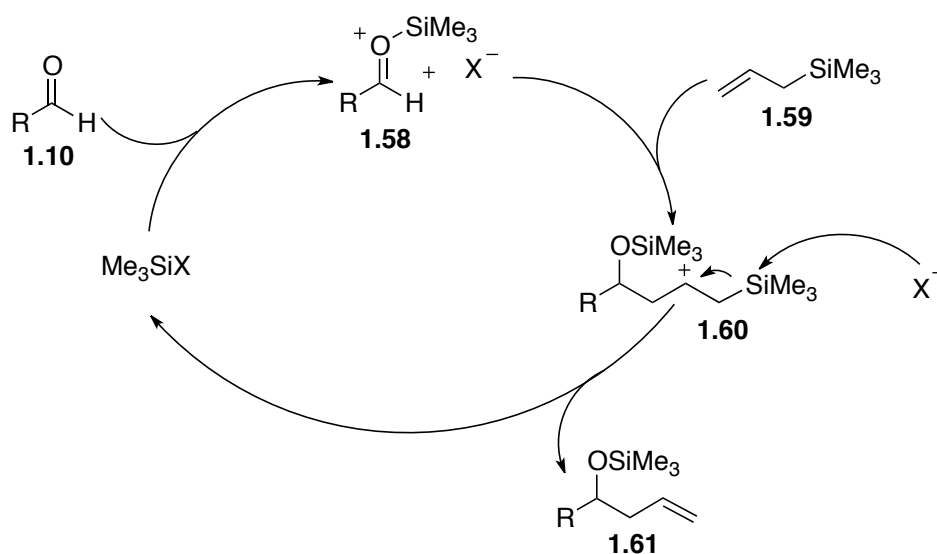
B-allyldialkylboranes are usually prepared from naturally available chiral materials such as (+)- α -pinene **1.47**, (-)- β -pinene **1.50**, (+)-limonene **1.52**, (+)-longifolene **1.53**, (+)-2-carene **1.54** (Scheme 1.15).⁶⁰ A highly moisture sensitive chiral boronate **1.57** was prepared by Roush from diisopropyl tartaric acid and have been applied for allylation of aldehydes and ketones.⁶¹ The reactivity of chiral boranes with ketones was relatively slow. To overcome this problem Solderquist introduced 9-BBN derived chiral boranes **1.56**.⁶²



Scheme 1.15. Chiralborane Reagents and Ligands

Allylsilanes and allylstannanes are relatively stable than allylboron reagents. One major setback with their reactivity is that they are not Lewis acidic in nature and hence they need external Lewis acids to promote their addition. Diastereoselective addition of allylsilanes and stannanes in the presence of a Lewis acid is a well-explored arena. The stereoselectivity and regioselectivity depends mainly on the nature of the Lewis acid used

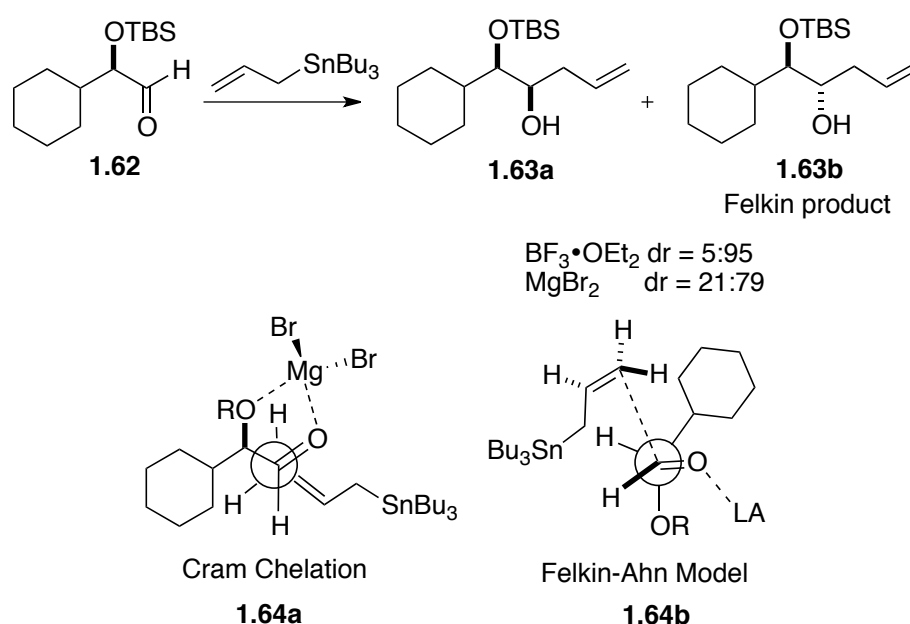
and the binding mode. Among the group fourteen elements, allylgermanium and allyllead reagents are also known. Allylation through silicon and tin reagents are known to proceed through the formation of a carbenium ion. These carbenium ions are stabilized by hyperconjugation of silicon-carbon and tin-carbon bonds that are present in the β -position. The Lewis acid mediated allylation of aldehydes proceed through a proposed pathway involving a silylated aldehyde that initiates the catalytic cycle. This activated aldehyde will react with allyltrimethyl silane followed by the attack of counter anion produces the homoallylic silyl ether. Chan and Fleming proposed the pathway for allylation of aldehydes using allyltrimethyl silane (Scheme 1.16).⁶³



Scheme 1.16. Allylation using Allylsilanes

In the proposed pathway, the trimethyl silyl group activates the carbonyl oxygen to form an activated complex **1.58** and this complex undergoes nucleophilic attack by allyltrimethyl silane **1.59**. Regeneration of the trimethylsilyl halide resulted in the allylated silylether **1.61**. Usually an work up of the reaction using ammonium fluoride yields homoallylic alcohol. Allylstannanes are similar in reactivity to allylsilanes. Activation of

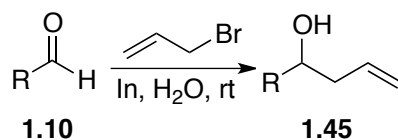
the electrophile with a Lewis acid is often necessary. Not all allylmetals would react through a cyclic transition state. In the case of silicon and tin reagent, their reactivity is often explained through an open transition state. One major reason for this difference is that the addition of Lewis acid changes the nature of binding. In the cases where cyclic transition state is discussed, the allylmetal is Lewis acidic enough to activate the carbonyl oxygen. For instance, the diastereoselection observed in the addition of allyltributyltin reagent to the aldehyde **1.62** changes drastically with the Lewis acid. The Felkin-model describes the reason for the *anti* product **1.63b** observed in a high selectivity with borontrifluoride etherate. The Cram's model **1.64a** explains the observed selectivity with magnesium bromide.⁶⁴



Scheme 1.17. Alkylation of Aldehydes using Allyltributyltin

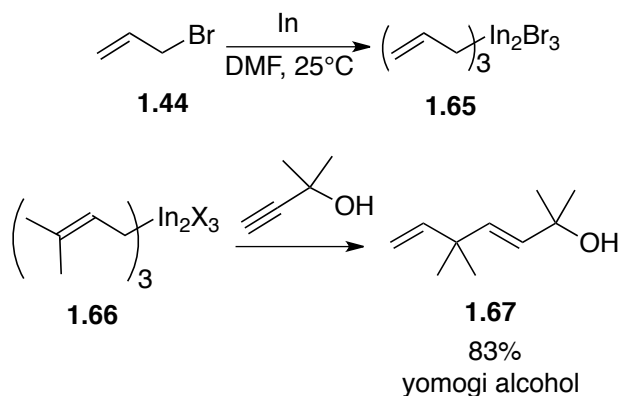
One of the recent additions to the list of allylmetal reagent is the allylindium reagent. In 1988, Araki and Butsugan demonstrated the utility of indium in allylation of a variety of aldehydes and ketones.⁶⁵ Aldehydes and ketones reacted smoothly in water in

the presence of indium metal with allylhalides to produce homoallylic alcohols in good yields (Scheme 1.18).



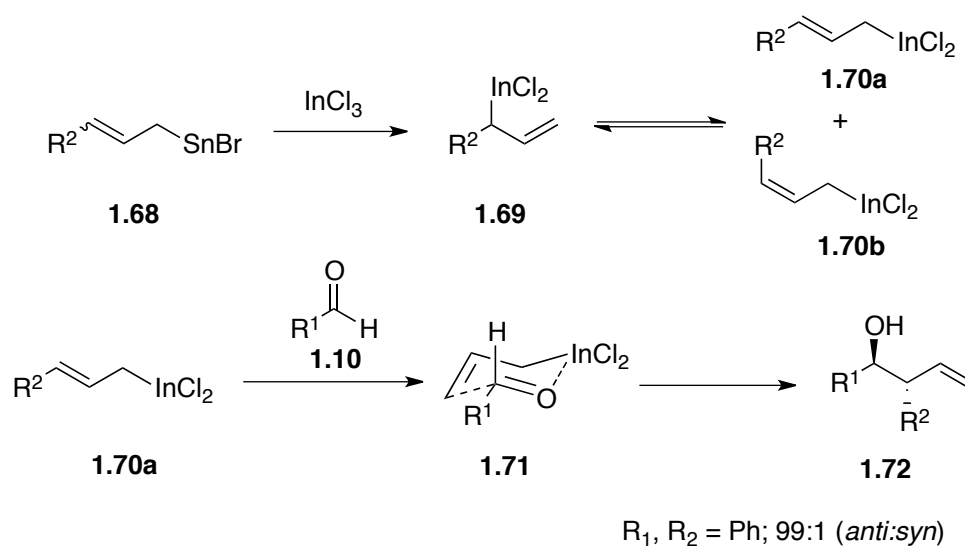
Scheme 1.18. Indium-Mediated Allylation of Aldehydes

In 1992, Araki and Butsugan demonstrated the utility of allylindium reagent by the total synthesis of yomogi alcohol **1.67** (Scheme 1.19). A prenyl indium reagent **1.66** was prepared from the corresponding halide in DMF. The reaction was highly selective, the allyl group added predominantly to the terminus of the triple bond (*anti*-markovnikov addition).⁶⁶



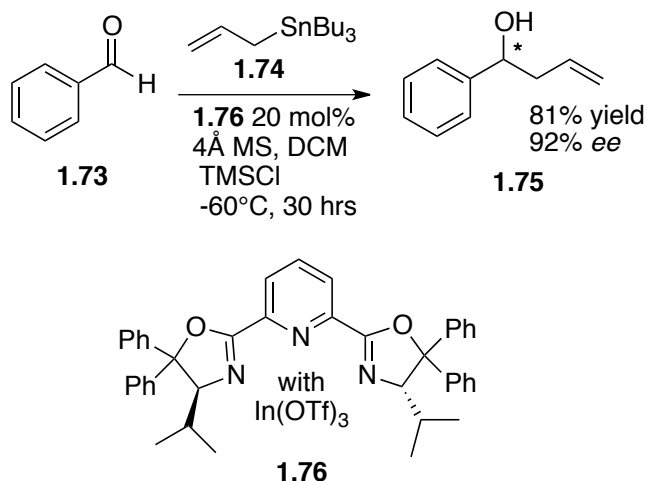
Scheme 1.19. Allylindium Preparation and Synthesis of Yomogi Alcohol

Marshal and Hinkel explored the addition of allyl tin reagent to simple aldehydes in the presence of Lewis acid.⁶⁷ The anti-selectivity of the reaction was attributed to the six-membered transition state **1.71** as shown in Scheme 1.20. The observed regio- and stereoselectivity in indium Lewis-acids promoted allylation has been substantiated well in a comprehensive review published by Cook and Kargbo.⁶⁸



Scheme 1.20. Origin of Selectivity Using Allylstannane and Indium trichloride

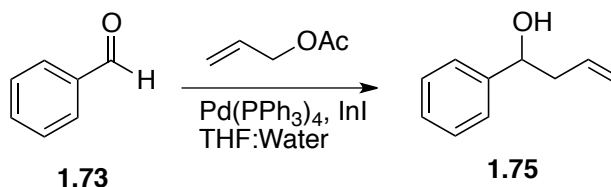
Allylindium reagents are attractive and easier to prepare compared to allylmagnesium and allyllithium reagents. The Wurtz-type coupled side products were not usually formed during the preparation of allylindium reagent. Another class of indium-mediated allylation was performed by using stoichiometric amount of allylating agents such as allylstannanes and allylboranes and used a catalytic amount of indium(III) salts.⁶⁹ A variety of indium(III) salts and chiral indium-complexes have been investigated to a great extent in allylation reaction.⁷⁰ The combination of allylstannane and indium trichloride was found to allylate simple aldehydes in highly diastereoselective fashion with high yields (Scheme 1.21),⁷¹ In a recent attempt, Loh and co-workers demonstrated the use of indium(III)-Lewis acids in the allylation of aldehydes and ketones with allylstannanes.⁷² Allylation of benzaldehyde **1.73** with allyltibutyltin **1.74** produced the homoallylic alcohol **1.75** in excellent yields and enantioselectivity. The allyl transfer to carbonyl carbon is facilitated by indium Lewis-acid complex pre-generated with indium triflate and the PyBOX ligand **1.76**.



Scheme 1.21. Enantioselective Allylation Using Indium-PyBox Complex

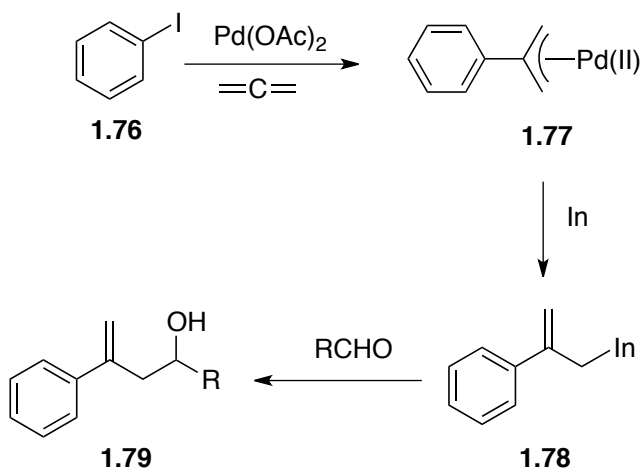
Amidst numerous reports, chiral indium complexes remain a field that has not been explored to its fullest. In 2007, Cook and Lloyd-Jones reported the possibility of generation of chiral indium(III)-Lewis acid *in situ* in a highly enantioselective allylation of aldimine-hydrazones.⁷³

Chemistry of indium in its low oxidation state is a relatively unexplored area.⁷⁴ Due to the presence of both free p orbitals and a lone pair of electrons, convincing evidence suggests that Indium (I) can behave as a Lewis acid as well as a Lewis base.⁷⁵ In 2000, Araki utilized indium(I) iodide and described a novel procedure for the generation of allyl indium reagent from pi-allyl palladium species. The allyl indium reagent can further react with an aldehyde **1.73** to produce homoallylic alcohol **1.75** (Scheme 1.22).



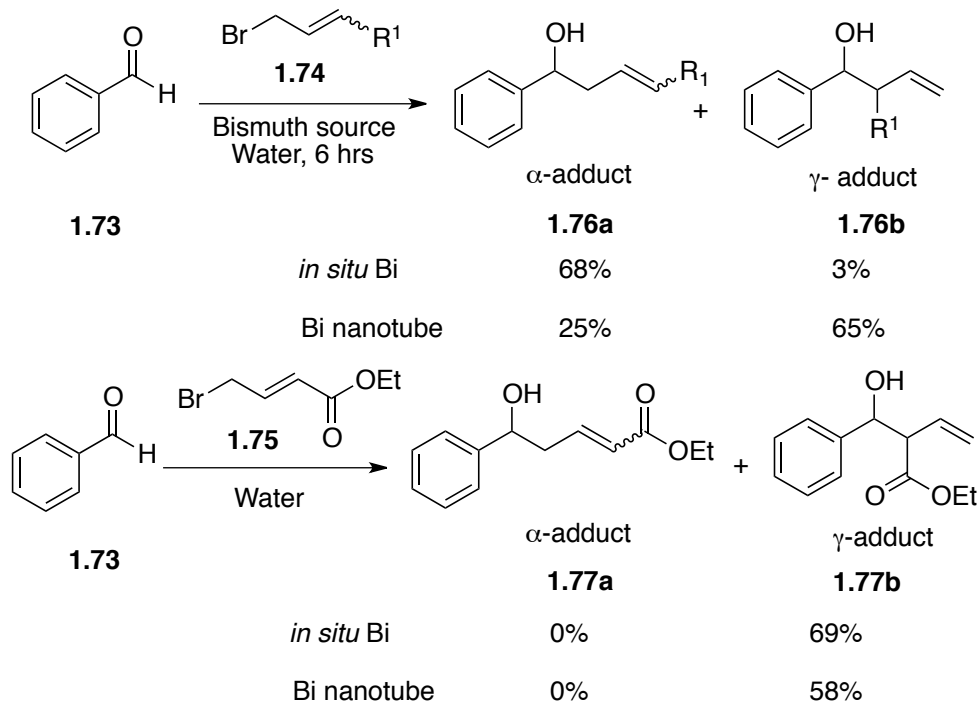
Scheme 1.22. Umpolung Allylation Using Pd(0) / In(I)

One notable example showing the utility of this procedure is found in a report from Cooper and Grigg (Scheme 1.23).⁷⁶ In 2002, they demonstrated the allylation of aldehydes with allenes. The π -allyl palladium(II) complex **1.77** was prepared from aryl iodide **1.76** and allene. This π -allyl complex is reacted with indium metal to produce the allylindium(I) species. The prepared allyl indium reagent reacts with aldehyde to produce the homoallylic alcohol **1.79**.



Scheme 1.23. π -Allylpalladium from Aryl iodide and Allene

In 1985, Wada and Akiba first reported the use of bismuth in allylation.⁷⁷ They were successful in using metallic bismuth scraped out of bismuth shots and allyl halides to react with aldehydes under mild conditions to produce homoallylic alcohols. The procedure was successful under Barbier and Grignard-type allylations.⁷⁸ In 1993, Sandhu and co-workers found that the addition of metal salts promoted bismuth mediated allylation.⁷⁹ This is one of the earliest examples of bismuth-mediated allylation. Following this, Thomas and Liu investigated the use of bismuth nanotubes *in situ* generated bismuth nanoparticles for allylation of aldehydes.⁸⁰ A difference in regioselectivity was observed with *in situ* bismuth and bismuth nanotubes (Scheme 1.24).



Scheme 1.24. Bismuth-Mediated Allylations

The reaction proceeded effectively with allylic bromides and allylic crotonates. With the crotonates the reversal of regiochemistry is not observed. The *in situ* Bi(0)-nanoparticles can be prepared by reduction of bismuth nitrate with potassium borohydride in water in the presence of cetyltrimethylammonium bromide. Bismuth mediated allylations under aqueous conditions are not very well known. In 2004, Wang reported a procedure of using nano meter sized bismuth with allyl bromide in water at room temperature for the allylation of aldehyde.⁸¹ Stereoselective allylation methods using bismuth under environmentally benign conditions or in green solvents have not been reported to date.

Analyzing the different allylmetal reagents discussed above, allyllithium, allylmagnesium reagents are reactive, more basic in nature resulting in side reactions such as deprotonation. The process involving the preparation of these reagents are tedious and sensitive to air and moisture. Allylboron reagents are relatively unstable compared to allyl

tin, silicon, indium and bismuth reagents and the asymmetric versions often involve the use of stoichiometric use of chiral source. Allylsilicon reagents require stoichiometric use of Lewis acid for activation and the reaction could not be performed in protic solvents. Allyltin reagents suffer from most of the disadvantages mentioned above. In addition to that tin byproducts generated from the reactions are very toxic to human life. From the above discussion of the reactivity and selectivity of allylmetal reagents we infer that even though allylation is an attractive protocol and the methods that are available currently could help to achieve desired selectivity, the path towards the goal is not green.

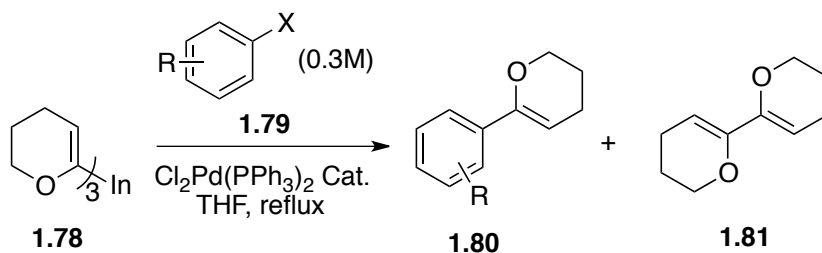
A critical question one would ask in present day scenario is: How many of these processes are green? If not how can we make these chemical transformations green? To answer this question, present day chemists work on solving the issue at its origin. i.e., developing environmentally benign methods that will replace the present toxic alternatives in all chemical industries. Considering this above transformation it is easy to note that indium and bismuth metal mediated allylations are relatively eco-friendly compared to other metals. This is due to the fact that the by-products from these metals are non-toxic to the environment and human beings. Organoindium and organobismuth reagents could be generated in water and in bio renewable protic solvents. For example organoindium species are found to be reactive in boiling water. The use of protic solvents is attractive and often stressed in current day organic synthesis because protic solvents such as methanol and ethanol are available from bio-sources. This minimizes the consumption of fossil fuels. This character of indium and bismuth reagents is not confined to allylation methodology but has wide range of application.

1.7. Green Chemistry with Indium Reagents

For a long time, scientists have been intrigued by the possible use of other metals in the classical Barbier/Grignard reactions. In 1972, Reike used indium for the classical Reformatsky reaction.⁸² This is the first recorded report of the use of indium in organic synthesis. Followed by Reike, Butsugan and co-workers demonstrated an indium mediated Reformatsky reaction.⁸³ These reactions were performed in DMF. It was not until Chan's 1991 report of the use of indium in aqueous solvents that people realized the potential use of indium in green chemistry.⁸⁴ In the past decade, the role of indium has been widened to a great extent. Indium metal and its compounds have found application in a variety of reactions. In recent times, Cook and Kargbo reviewed the stereoselective applications of indium-mediated allylations.⁸⁵ Yadav and Reddy described the role of indium and its salts in a microreview.⁸⁶ To date, a comprehensive idea regarding the use of organoindium species pertaining to green chemistry has not been presented. This part of the review focuses mainly on the various carbon-carbon bond-forming reactions achieved using organoindium reagents in an eco-benign fashion and the challenges remaining.

Transition metal-catalyzed cross-coupling reactions of organometallic reagents with electrophiles is one of the efficient carbon-carbon bond forming reactions that yielded the Nobel Prize for chemistry in 2010.⁸⁷ Classical Stille coupling involves the reaction between organostannanes and organic electrophiles, similarly Suzuki coupling involves organoboranes. Stille coupling is employed in magnificent scales in pharmaceutical industry for synthesis of several API's. One major environmental issue from these reactions is the toxic tin waste. To overcome this problem, Oshima in 2011 described the cross-coupling reaction between organoindiums and aryl halides in aqueous media.⁸⁸

Following by Oshima's report, Minehan reported cross coupling reactions between tris(dihydropyranyl)indium **1.10** and aryl halides **1.11** in THF (Scheme 1.4.).⁸⁹

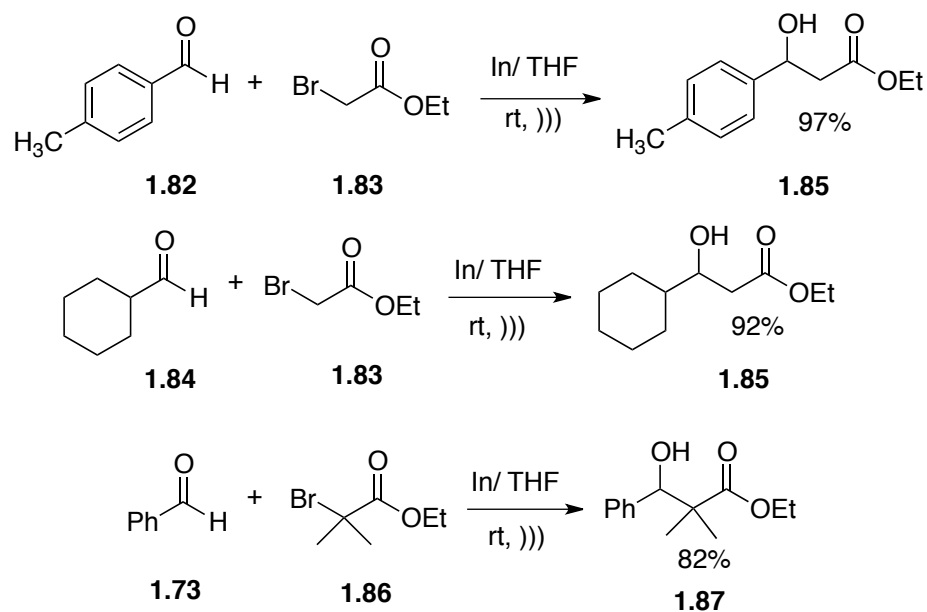


Scheme 1.25. Cross-Coupling Reaction Using Organoindium

As a consequence of the stability of organoindium species in aqueous solutions and its tolerance to non-inert reaction conditions, there are significant examples in the area of cross coupling reactions. Inter- and intramolecular coupling have been reported.⁹⁰ Within five years of the development of the cross coupling reactions using indium reagents and salts, Sakai and Konakahara were able to develop palladium-catalyzed cross coupling of terminal alkynes with aryl iodides in the presence of catalytic amount of indium tribromide.⁹¹ They also demonstrated the use of indium tribromide efficiently catalyzes the intramolecular cycloaddition of 2-phenylethynylaniline to indoles in excellent yields.⁹²

One of the continuing endeavors in the cross-coupling chemistry with indium resulted in the use of acetates as electrophilic partners. Unlike halides, acetates are readily accessible and easy to handle. Lee and co-workers first demonstrated the use of allylic acetates in an inter- and intramolecular cross coupling reactions.⁹³ The combination of In/InCl₃ as a reductive transmetalating agent for π -allylpalladium(II) species to produce desired cross-coupling products has been demonstrated and numerous variants of this procedure have been reported in literature⁹⁴ and will be discussed in detail in chapter two.

Reike and co-workers reported the first use of indium metal in organic synthesis in 1975 through a Reformatsky reaction. Aromatic aldehydes **1.82** and **1.73** and aliphatic aldehydes **1.84** reacted well under the ultrasound-promoted, indium-mediated Reformatsky conditions to produce the β -hydroxy esters in excellent yields (Scheme 1.26).



Scheme 1.26. Indium-Mediated Reformatsky Reaction

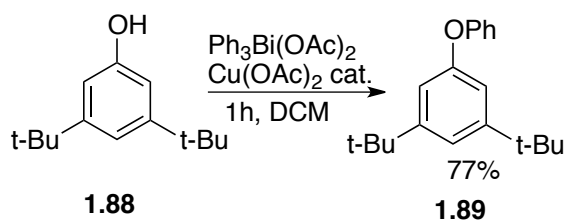
Even though, allylations are one of the most popular reactions using indium metal; the evolution of the use of indium for allylations did not come into the picture until the initial investigations on the Reformatsky reaction. Ultrasound promoted conditions have been reported for the enolate additions to aldehydes, ketones and imines. Although this topic is extensively reviewed in chapter two, it is worth mentioning that the ultrasound promoted Reformatsky reaction provides a direct access to variety of β -amino acids, and β -amino esters in an environmentally benign fashion.

1.8. Green Chemistry with Bismuth Reagents

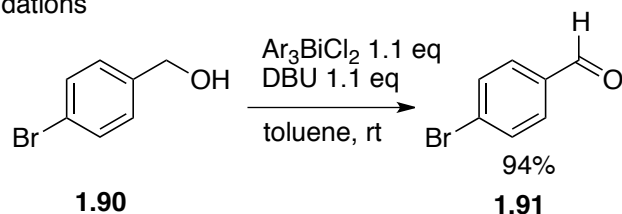
Humans have known about bismuth since the early ages. Early miners considered bismuth ores, bismuthinite (Bi_2S_3) and bismite (Bi_2O_3) as intermediate stages of the development of tin and lead ores.⁹⁵ Due to its remarkable similarities in appearance with tin and lead, it is often confused with these metals. It was not until 1753, when Claude Geoffroy the Younger showed it is a distinct element. Bismuth 209 was thought to be the heaviest isotope existing in nature. In 2002, experiments indicated that Bi-209 is radioactive with a half-life of 19×10^{18} years.⁹⁶ The pronounced metallic character of bismuth was expected to play a crucial role in organic synthesis. In the context to its application to organic reactions, bismuth is cheaper and less toxic than its neighbors in the periodic table.⁹⁷

The major applications of organobismuth(V) reagents are oxidation and arylation. Wittig in 1950, studied the synthesis of pentavalent bismuth derivatives.⁹⁸ Sir Barton first reported the arylation using bismuth reagents in 1980s.⁹⁹ Following his report, Suzuki studied various organobismuth(V) reagents and bismuthonium salts. Bismuth(V) reagents can be used for *O*-arylation of phenols.¹⁰⁰ Oxidation of benzylic alcohols could be performed using triarylbismuth dichloride in combination with DBU at room temperature in toluene to produce benaldehydes in high yields. (Scheme 1.27).

O-arylations

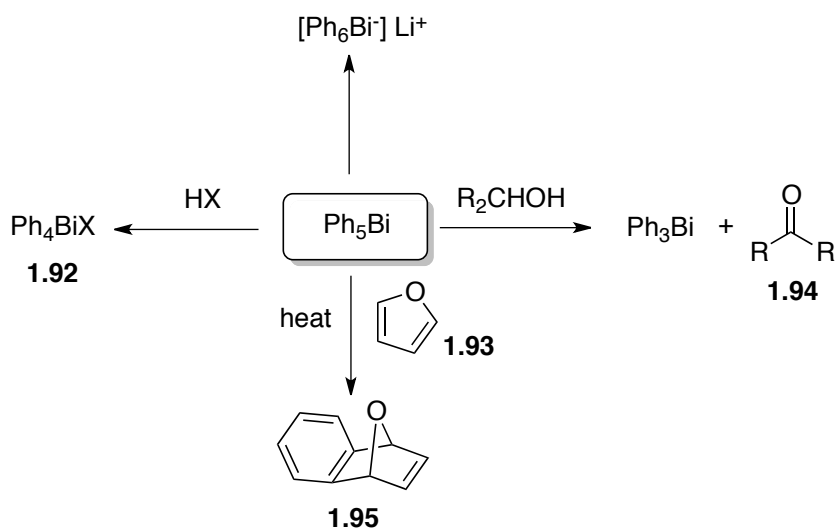


Oxidations



Scheme 1.27. Reactions Using Aryl Bismuth Reagents

Pentaphenyl bismuth can be utilized in a variety of reactions. Secondary alcohols could be successfully oxidized using pentaphenyl bismuth to produce ketones **1.94**. Under thermal conditions, it could undergo Diels-Alder reaction with furan **1.93** to make bicyclic compound **1.95** (Scheme 1.28).¹⁰¹



Scheme 1.28. Triphenyl bismuth in Organic Synthesis

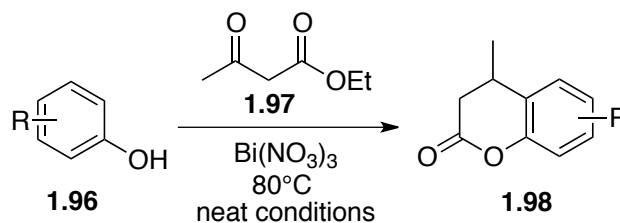
Organobismuth(III) reagents are mostly generated *in situ*. Although they are stable under standard atmospheric conditions, there are fewer examples of the use of these species

in reactions. The number of examples that reported the use of organobismuth reagents under aqueous conditions is rare. However bismuth salts were found to be compatible with aqueous-organic solvent mixtures as well as water.¹⁰² The remarkable Lewis-acidic features of bismuth might appear surprising on a first glance. Compounds of group 15 elements, such as phosphines and arsines, typically were Lewis-bases.¹⁰³ The contrasting Lewis-acidic property of bismuth is attributed to the relativistic effects. The electronic configuration of bismuth is $[\text{Xe}] 4f^{14}5d^{10}6s^26p^3$. Due to the poor shielding of the f-orbitals, the coordination could be extended around bismuth and thus helps in increased Lewis-acidity.¹⁰⁴ For the past two-decades, copious amounts of literature have been reported in the field of bismuth(III)-salts catalyzed reactions in aqueous conditions.¹⁰⁵ Though the discussion of bismuth(III)-catalyzed reactions is beyond the scope of this chapter, it is worth mentioning the ‘green’ properties of bismuth salts. Table 1.2 shows data on LD₅₀ values of bismuth salts and some common Lewis acids.¹⁰⁶ Bismuth oxychloride has an LD₅₀ value of 22 g/Kg in rats. It is commonly used in cosmetics. Other bismuth salts also have appreciably lower toxicity. This enables the use of salts of bismuth in several reactions to promote green chemistry.

Table 1.2. Cost and Toxicity of Commonly Used Salts

Compound	LD ₅₀ (g/Kg)	Cost \$/100g
BiOCl	22	100
Bi ₂ O ₃	5.0	48
Bi(NO ₃) ₃	4.4	40
ScCl ₃	3.9	200/g
NaCl	3.8	0.05
BiCl ₃	3.3	204
CeCl ₃	2.1	660
InCl ₃	1.1	600
NiCl ₂	0.105	68
HgCl ₂	0.001	56

The condensation of β -ketoesters with phenols to produce coumarin derivatives is known as the Pechmann condensation. The reaction is usually reported using main group catalysis. With the increased use of non-toxic bismuth Lewis-acids in organic synthesis, Gibbs disclosed the used of bismuth nitrate in Pechmann condensation in 2005. Substituted phenols **1.96** were successfully condensed with ethyl acetoacetate **1.97** in the presence of catalytic amount of bismuth nitrate under neat condition to produce coumarins **1.98** (Scheme 1.29).¹⁰⁷



Scheme 1.29. Bismuth(III)- Catalyzed Pechmann Condensation

Concurrent with this report, Bhatt reported the use of bismuth trichloride under solvent-free conditions as well as by ultrasound promoted conditions to produce the coumarin efficiently.¹⁰⁸ These methods served as defining examples of the utility of

bismuth(III)-Lewis-acids in organic synthesis and performing reactions under solvent-free conditions effectively promote green chemistry.

Bismuth compounds are reported to increase the yield and improve the kinetics of the Biginelli reactions.¹⁰⁹ Bismuth(III)- triflates, chlorides, nitrates and perchlorates have been reported to catalyze these reactions in acetonitrile under dry conditions.¹¹⁰ Efficient conditions promoting green chemistry including microwave heating or using ionic-liquids have been reported with bismuth salts for similar transformations.¹¹¹ Gangadsa et al reported in 2004 the use of polyaniline-bismoclite complex (PANI-BC) for promoting Biginelli reaction in ethanol.¹¹² The bismuth (III) catalysis examples were included in this chapter to distinguish the extent of research that needs to be performed in the area of organobismuth chemistry to make those methods clean and green.

1.9. Conclusions

Historically, bismuth has been known to humanity for a long period of time¹¹³. However, the first use of bismuth has not been identified so far and in the field of organic synthesis metallic bismuth is relatively a new entry; meanwhile, indium was recently discovered in 1863 and extent of the use of indium in organic synthesis has more examples than bismuth. Every metal has its own advantage and disadvantage. Indium, for example is expensive. The cost of the metal has increased dramatically due to the extensive use of indium tin oxide in the semiconductor industry.¹¹⁴ This makes the transfer of the technology developed based on indium from the bench top to a practical industrial scale difficult. In this present scenario one would envision bismuth as a possible alternative for those methods we have currently developed with indium. Bismuth is cheap and abundant

and seems to hold a prominent place in the next chapter in a story and a strategy that has been unfolding over a period of two decades now in green synthetic methods.

1.10. References

- (1) Cintas, P.; Luche, J.-L., Green chemistry. *Green Chemistry* **1999**, 1, (3), 115-125.
- (2) Mestres, R., Green chemistry--views and strategies. *Env. Sci. Res. Intl.*, **2005**, 12 (3), 128-32.
- (3) Jessop, P. G.; Trakhtenberg, S.; Warner, J., The twelve principles of green chemistry. *ACS Symposium Series* **2009**, 1000, (Innovations in Industrial and Engineering Chemistry), 401-436.
- (4) Hwang, K.-Y.; Rhee, H.-K. Friedel-Crafts acylation of 2-methoxynaphthalene over H-beta catalysts: effect of Si/Al ratio. *Reac. Kinet. Cat. Lett.*, **2003**, 79, 189-196.
- (5) Beller, M. A method to characterize the greenness of solvents used in pharmaceutical manufacture. *Med. Res. Rev.*, **1999**, 19, 357-369.
- (6) Slater, C. S.; Savelski, M. *J. Env. Sci. Res., Part A*: **2007**, 42, 1595-1605.
- (7) Wei, W.; Keh, C. C. K.; Li, C.-J.; Varma, R. S. *Clean Technologies and Environmental Policy* **2004**, 6, 250-257.
- (8) Albright, D. *Biogas and Alcohol Fuels Production* **1981**, 2, 153-8.
- (9) Selected examples: a) Poliakoff, M.; George, M. W.; Hamley, P. A.; Howdle, S. M. *Chimica e l'Industria (Milan)* **1999**, 81, 339-344. b) Poliakoff, M.; George, M. W.; Howdle, S. M.; Bagratashvili, V. N.; Han, B.-X.; Yan, H.-K. *Chinese Journal of Chemistry* **1999**, 17, 212-222. c) Ikariya, T. *Kagaku to Kyoiku* **2000**, 48, 127-129. d) Leitner, W.; Poliakoff, M. *Green Chemistry* **2008**, 10, 730. e) Sparks, D. L.; Antonio Estevez, L.; Hernandez, R. *Green Chemistry* **2009**, 11, 986-993.

- (10) a) Kuschnerow, J. C.; Wesche, M.; Scholl, S. *Chemie Ingenieur Technik*, **83**, 1582-1589. b) Suresh; Sandhu, J. *Green Chem. Lett. Rev.*, **4**, 289-310.
- (11) Cramer, C. J.; Truhlar, D. G. *ACS Symposium Series* **1994**, **568**, 1-7.
- (12) Breslow, R. *Acc. Chem. Res.*, **1991**, **24**, 159-64. and references cited there-in
- (13) Wei, W.; Keh, C. C. K.; Li, C.-J.; Varma, R. S. *Clean Technologies and Environmental Policy* **2004**, **6**, 250-257. B) Narayan, S.; Muldoon, J.; Finn, M. G.; Fokin, V. V.; Kolb, H. C.; Sharpless, K. B. *Angew. Chem. Int. Ed.*, **2005**, **44**, 3275-3279.
- (14) Grieco, P. A.; Garner, P.; He, Z. Micellar catalysis in the aqueous intermolecular diels-alder reaction: rate acceleration and enhanced selectivity. *Tetrahedron Lett.*, **1983**, **24**, 1897-1900.
- (15) Mojtahedi, M. M.; Abaee, M. S., Ultrasound applications in synthetic organic chemistry. *Handbook on Applications of Ultrasound*, 281-321.
- (16) Hayashi, Y.; Takizawa, H. Nanocomposite fabrications by sonochemical eco-design. *Materials Integration* **2005**, **18**, 33-38. B) Kardos, N.; Luche, J. L. Sonochemistry of carbohydrate compounds. *Carbohydr. Res.*, **2001**, **332**, 115-31. b) Baig, S.; Farooq, R.; Rehman, F. Sonochemistry and its industrial applications. *World Appl. Sci. J.*, **2010** **10**, 936-944.
- (17) a) Cintas, P.; Palmisano, G.; Cravotto, G. *Ultrasonics Sonochemistry*, **18**, 836-841. (b) Martin-Aranda, R. M. Calvino-Casilda, V. *Recent Patents on Chemical Engineering*, **3**, 82-98.
- (18) Boudjouk, P. R.; Han, B. H.; (North Dakota State University Development Foundation, USA). Application: US, 1984, 19830614.

- (19) a) Repic, O.; Vogt, S. Ultrasound in organic synthesis: cyclopropanation of olefins with zinc-diiodomethane. *Tetrahedron Lett.*, **1982**, *23*, 2729-32. b) Bose, A. K.; Gupta, K.; Manhas, M. S. δ -Lactam formation by ultrasound-promoted Reformatskii type reaction. *J. Chem. Soc: Chem. Commun.*, **1984**, 86-7. c) Oguni, N.; Tomago, T.; Nagata, N. Stereoselective syntheses of δ -lactam derivatives by ultrasound promoted Reformatskii reaction *Chem. Exp.*, **1986**, *1*, 495-7. d) Kitazume, T. *Ultrasonics.*, **1990**, *28*, 322-5. e) Lee, P. H.; Bang, K.; Lee, K.; Sung, S.-Y.; Chang, S. Ultrasound promoted synthesis of hydroxy esters by Reformatskii reaction using indium metal. *Synth. Commun.*, **2001**, *31*, 3781-3789. f) Ross, N. A.; Bartsch, R. A.; Marchand, A. P. *Arkivoc.*, (Gainesville, FL, United States) **2003**, 27-30.
- (20) Krasovitski, B.; Frenkel, V.; Shoham, S.; Kimmel, E. *Proceedings of the National Academy of Sciences of the United States of America*, *108*, 3258-3263, S3258/1-S3258/5.
- (21) Suslick, K. S. The chemical effects of ultrasound. *Scientific American* **1989**, *260*, 80-6.
- (22) Hayashi, Y.; Takizawa, H. Nanocomposite fabrications by sonochemical eco-design. *Mat. Intg.*, **2005**, *18*, 33-38.
- (23) Gedanken, A.; Shimanovich, U.; Perelshtein, I.; (Bar-Ilan University, Israel). Application:US, p 12pp , *Cont -in-part of U S Ser No 997,276*.
- (24) Pua, E. C.; Zhong, P., Ultrasound-Mediated Drug Delivery Range of Ultrasonic Interactions and Applications in Biological Systems. *Ieee Med & Biol. Engg.*, **2009**, *28* (1), 64-75.

- (25) Chen, J.; Chen, Y.; Li, H.; Lai, S.-Y.; Jow, J. Physical and chemical effects of ultrasound vibration on polymer melt in extrusion. *Ultrason Sonochem.*, **2010**, *17*, 66-71.
- (26) Polshettiwar, V.; Varma, R. S., Non-conventional energy sources for green synthesis in water (microwave, ultrasound, and photo). *Handbook of Green Chemistry* **5**, 273-290.
- (27) Jaipuri, F. A.; Francisca Jofre, M.; Schwarz, K. A.; Pohl, N. L. *Tetrahedron Lett.*, **2004**, *45*, 4149-4152.
- (28) de la Hoz, A.; Diaz-Ortiz, A.; Moreno, A. Microwaves in organic synthesis. Thermal and non-thermal microwave effects. *Chem. Soc. Rev.*, **2005**, *34*, 164-178.
- (29) Gedye, R.; Smith, F.; Westaway, K.; Ali, H.; Baldisera, L.; Laberge, L.; Rousell, J., The use of microwave ovens for rapid organic synthesis. *Tetrahedron Lett.*, **1986**, *27* (3), 279-282.
- (30) Martins, M. A. P.; Frizzo, C. P.; Moreira, D. N.; Buriol, L.; Machado, P., Solvent-Free Heterocyclic Synthesis. *Chem. Rev. (Washington, DC, U. S.)* **2009**, *109* (9), 4140-4182. Wei, B.; Guo, J.; Fu, N.-Y.; Yuan, Y.-F., Green synthesis of ferrocenyl-substituted heterocycles. *Youji Huaxue* **2008**, *28* (5), 791-796.
- (31) D. J. C. Constable, A. D. Curzons, V. L. Cunningham, An improved preparation of ionic liquids by ultrasound. *Green Chem.* **2002**, *4*, 521.
- (32) Trost, B. M., Atom Economy—A Challenge for Organic Synthesis: Homogeneous Catalysis Leads the Way. *Angew. Chem. Int. Ed.*, **1995**, *34* (3), 259-281.
- (33) Kang, C.; Zhou, T.; Chen, Q.; Xu, Q.; Xia, Q.; Ji, Z., Carbon Emission Flow in Networks. *Sci. Rep.* **2**.

- (34) Constable, D. J. C.; Curzons, A. D.; Cunningham, V. L., Metrics to 'green' chemistry-which are the best? *Green Chemistry.*, **2002**, *4* (6), 521-527.
- (35) Sheldon, R. A., The E Factor: fifteen years on. *Green Chemistry.*, **2007**, *9* (12), 1273-1283.
- (36) Van Aken, K.; Streckowski, L.; Patiny, L., EcoScale, a semi-quantitative tool to select an organic preparation based on economical and ecological parameters. *Beilstein J Org Chem.*, **2006**, *2*.
- (37) Motherwell, W. B. In Some recent studies on the development of new metal mediated reactions for organic synthesis, Kluwer Academic/Plenum Publishers. **1999**, 247-257.
- (38) C.-J. Li, Organic Reactions in Aqueous Media with a Focus on Carbon-Carbon Bond Formations: A Decade Update. *Chem. Rev.*, **2005**, *105*, 3095.
- (39) Selected examples: (a) Kyriakides, L. P., Some Barbier-Grignard reactions. *J. Am. Chem. Soc.*, **1914**, *36*, 657-63. (b) Obe, Y.; Sato, M.; Matsuda, T., Mobile metal salt catalysts and Grignard reactions. 2. Comparison between Grignard and Barbier-Grignard procedures in the alcohol synthesis from aldehydes. *Kyushu Daigaku Kogaku Shuho.*, **1971**, *44* (2), 208-12. (c) Liao, L.-A.; Li, Z.-M., The Barbier-Grignard reaction in aqueous media. *Youji Huaxue.*, **2000**, *20* (3), 306-318.
- (40) Barbier-type reactions: (a) Alonso, F.; Yus, M., Recent developments in Barbier-type reactions. *Recent Res. Dev. Org. Chem.*, **1997**, *1*, 397-436. (b) Haberman, J. X.; Yi, X.-H.; Li, C.-J. In *Solvent-free metal-mediated Barbier-type reactions*, American Chemical Society: 1998; pp ORGN-199. (c) Kouznetsov, V. V.; Mendez, L. Y. V., Recent developments in three-component Grignard-Barbier-type

- reactions. *Synthesis.*, **2008**, (4), 491-506. Grignard type reactions: (d) Agnes, G.; Chiusoli, G. P.; Marraccini, A., Grignard-type reactions with transition metals. Alkylation of carbon compounds in protic solvents. *J. Organometal. Chem.*, **1973**, 49 (1), 239-41. (e) Chiusoli, G. P.; Salerno, G.; Bersellini, U.; Dallatomasina, F.; Preseglio, S., Grignard-type reactions with zerovalent nickel complexes. *Transition Met. Chem. (Weinheim, Ger.)*, **1978**, 3 (3), 174-6. (f) Wei, X.-F., Pd-catalyzed Grignard-type reactions. *Youji Huaxue.*, **2005**, 25 (2), 234-237. (g) Li, C.-J. In *Metal-mediated C-C bond formations in aqueous media*, Blackwell Publishing Ltd.: **2007**; pp 92-145.
- (41) Trost, B. M., Basic Aspects of Organic Synthesis with Transition Metals. In *Transition Metals for Organic Synthesis*, Wiley-VCH Verlag GmbH: 2004; pp 2-14. Keim, W., Concepts for the Use of Transition Metals in Industrial Fine Chemical Synthesis. In *Transition Metals for Organic Synthesis*, Wiley-VCH Verlag GmbH: 2004; pp 15-25.
- (42) Yamamoto, Y.; Asao, N., Selective Reactions Using Allylic Metals. *Chem. Rev.*, **1993**, 93 (6), 2207-2293.
- (43) Okude, Y.; Hirano, S.; Hiyama, T.; Nozaki, H., Grignard-type carbonyl addition of allyl halides by means of chromous salt. A chemospecific synthesis of homoallyl alcohols. *J. Am. Chem. Soc.*, **1977**, 99 (9), 3179-3181.
- (44) Courtois, G.; Mauze, B.; Miginiac, L., Addition of Saturated Allyl Organometallic and Organolithium Compounds to Functional and Simple Conjugated Enynes. *J. Organomett. Chem.*, **1974**, 72 (3), 309-322. Courtois, G.; Miginiac, L., Reactivity of Allylic Organometallic Compounds of Lithium, Sodium, Magnesium, Zinc,

- Cadmium and Aluminum - Recent Advances. *J. Organomett. Chem.*, **1974**, *69* (1), 1-44.
- (45) Buechi, G.; Vederas, J. C., Interchange of functionality in conjugated carbonyl compounds through isoxazoles. *J. Am. Chem. Soc.*, **1972**, *94* (26), 9128-9132.
- (46) Seyferth, D.; Weiner, M. A., The Preparation of Organolithium Compounds by the Transmetalation Reaction. IV. Some Factors Affecting the Transmetalation Reaction. *J. Am. Chem. Soc.*, **1962**, *84* (3), 361-364.
- (47) Eisch, J. J.; Jacobs, A. M., A Convenient Preparation of Allyllithium¹. *J. Org. Chem.*, **1963**, *28* (8), 2145-2146.
- (48) Cohen, T.; Guo, B. S., Reductive Metalation - a General Preparative Method for Hydrocarbon Allylmetallic Compounds. *Tetrahedron* **1986**, *42* (11), 2803-2808.
- (49) Guo, B. S.; Doubleday, W.; Cohen, T., Allylcerium(III) compounds, powerful new synthetic reagents. A new stereocontrolled approach to olefins and methylene-interrupted polyenes. *J. Am. Chem. Soc.*, **1987**, *109* (15), 4710-4711.
- (50) Yanagisawa, A.; Habaue, S.; Yamamoto, H., Propargyl and allyl Grignard and zinc reagents. Regioselective alkylation and its application to the synthesis of PGE₃ and F₃.alpha. methyl ester. *J. Org. Chem.*, **1989**, *54* (22), 5198-5200.
- (51) Schlosser, M.; Stähle, M., Allylic Compounds of Magnesium, Lithium, and Potassium: σ - or π -Structures? *Angew Chem. Int. Ed.*, **1980**, *19* (6), 487-489.
- (52) Yanagisawa, A.; Habaue, S.; Yamamoto, H., Allylbarium in organic synthesis: unprecedented .alpha.-selective and stereospecific allylation of carbonyl compounds. *J. Am. Chem. Soc.*, **1991**, *113* (23), 8955-8956.

- (53) (a) Yamamoto, Y.; Maruyama, K., Organo-Metallic Compounds for Stereoregulated Synthesis of Acyclic Systems - Their Application to the Synthesis of the Prelog-Djerassi Lactonic Acid. *Heterocycles.*, **1982**, *18*, 357-386. (b) Yamamoto, Y., Acyclic Stereocontrol Via Allylic Organometallic Compounds. *Acc of Chem. Res.*, **1987**, *20* (7), 243-249.
- (54) Seyferth, D., Zinc Alkyls, Edward Frankland, and the Beginnings of Main-Group Organometallic Chemistry. *Organometallics.*, **2001**, *20* (14), 2940-2955.
- (55) Hanessian, S.; Margarita, R.; Hall, A.; Johnstone, S.; Tremblay, M.; Parlanti, L., Total Synthesis and Structural Confirmation of the Marine Natural Product Dysinosin A: A Novel Inhibitor of Thrombin and Factor VIIa. *J. Am. Chem. Soc.*, **2002**, *124* (45), 13342-13343.
- (56) Wurtz, A., Ueber eine neue Klasse organischer Radicale. *Justus Liebigs Annalen der Chemie.*, **1855**, *96* (3), 364-375.
- (57) (a) Hanessian, S.; Margarita, R.; Hall, A.; Johnstone, S.; Tremblay, M.; Parlanti, L., Total Synthesis and Structural Confirmation of the Marine Natural Product Dysinosin A: A Novel Inhibitor of Thrombin and Factor VIIa. *J. Am. Chem. Soc.*, **2002**, *124* (45), 13342-13343. (b) Einhorn, C.; Luche, J. L., Selective Allylation of Carbonyl-Compounds in Aqueous-Media. *J. Organomett. Chem.*, **1987**, *322* (2), 177-183.
- (58) W. Kramer, G.; C. Brown, H., Organoboranes : XIX. The preparation and some unusual chemistry of β -allyl derivatives of 9-borabicyclo[3.3.1]Nonane. *J. Organomett. Chem.*, **1977**, *132* (1), 9-27.

- (59) (a) Brown, H. C.; Jadhav, P. K., Asymmetric carbon-carbon bond formation via .beta.-allyldiisopinocampheylborane. Simple synthesis of secondary homoallylic alcohols with excellent enantiomeric purities. *J. Am. Chem. Soc.*, **1983**, *105* (7), 2092-2093. (b) Brown, H. C.; Bhat, K. S., Chiral synthesis via organoboranes. 7. Diastereoselective and enantioselective synthesis of erythro- and threo-.beta.-methylhomoallyl alcohols via enantiomeric (Z)- and (E)-crotylboranes. *J. Am. Chem. Soc.*, **1986**, *108* (19), 5919-5923.
- (60) (a) Brown, H. C.; Bhat, K. S.; Randad, R. S., .beta.-Allyldiisopinocampheylborane: a remarkable reagent for the diastereoselective allylboration of .alpha.-substituted chiral aldehydes. *J. Org. Chem.*, **1987**, *52* (2), 319-320. (b) Brown, H. C.; Bhat, K. S.; Randad, R. S., Chiral synthesis via organoboranes. 21. Allyl- and crotylboration of .alpha.-chiral aldehydes with diisopinocampheylboron as the chiral auxiliary. *J. Org. Chem.*, **1989**, *54* (7), 1570-1576.
- (61) Roush, W. R.; Walts, A. E.; Hoong, L. K., Diastereo- and enantioselective aldehyde addition reactions of 2-allyl-1,3,2-dioxaborolane-4,5-dicarboxylic esters, a useful class of tartrate ester modified allylboronates. *J. Am. Chem. Soc.*, **1985**, *107* (26), 8186-8190.
- (62) Canales, E.; Prasad, K. G.; Soderquist, J. A., B-Allyl-10-Ph-9-borabicyclo[3.3.2]decanes: Strategically Designed for the Asymmetric Allylboration of Ketones. *J. Am. Chem. Soc.*, **2005**, *127* (33), 11572-11573.
- (63) Chan, T. H.; Fleming, I., Electrophilic Substitution of Organosilicon Compounds - Applications to Organic-Synthesis. *Synthesis-Stuttgart* **1979**, (10), 761-786.

- (64) (a) Hayashi, T.; Konishi, M.; Ito, H.; Kumada, M., Optically active allylsilanes. 1. Preparation by palladium-catalyzed asymmetric Grignard cross-coupling and anti stereochemistry in electrophilic substitution reactions. *J. Am. Chem. Soc.*, **1982**, *104* (18), 4962-4963. (b) Yamamoto, Y.; Yatagai, H.; Naruta, Y.; Maruyama, K., Erythro-selective addition of crotyltrialkyltins to aldehydes regardless of the geometry of the crotyl unit. Stereoselection independent of the stereochemistry of precursors. *J. Am. Chem. Soc.*, **1980**, *102* (23), 7107-7109. (c) Keck, G. E.; Savin, K. A.; Cressman, E. N. K.; Abbott, D. E., Effects of Olefin Geometry on the Stereochemistry of Lewis Acid Mediated Additions of Crotylstannanes to Aldehydes. *J. Org. Chem.*, **1994**, *59* (25), 7889-7896.
- (65) Araki, S.; Ito, H.; Butsugan, Y. *Synth. Commun.*, **1988**, *18*, 453-458.
- (66) Araki, S.; Imai, A.; Shimizu, K.; Butsugan, Y. Carboindation of alkynols. A facile synthesis of yomogi alcohol. *Tetrahedron Lett.*, **1992**, *33*, 2581.
- (67) Marshall, J. A.; Hinkle, K. *The Journal of Organic Chemistry* **1995**, *60*, 1920-1921. Marshall, J. A. *Chemtracts-Org. Chem.* **1997**, *10*, 481.
- (68) Kargbo, R. B.; Cook, G. R., Stereoselective indium-mediated allylation reactions. *Curr. Org. Chem.*, **2007**, *11* (15), 1287-1309.
- (69) Miura, K.; Fujisawa, N.; Hosomi, A. Indium(III) Chloride-Promoted Intramolecular Addition of Allylstannanes to Alkynes. *J. Org. Chem.*, **2004**, *69*, 2427-2430.
- (70) Teo, Y.-C.; Tan, K.-T.; Loh, T.-P. Catalytic asymmetric allylation of aldehydes via a chiral indium(III) complex. *Chem. Commun.*, **2005**, 1318-1320.

- (71) Li, X.-R.; Loh, T.-P. Indium trichloride-promoted tin-mediated carbonyl allylation in water: High simple diastereo- and diastereofacial selectivity. *Tetrahedron: Asymm.*, **1996**, *7*, 1535-1538.
- (72) Teo, Y.-C.; Goh, J.-D.; Loh, T.-P., Catalytic Enantioselective Allylation of Ketones via a Chiral Indium(III) Complex. *Org. Lett.*, **2005**, *7* (13), 2743-2745.
- (73) Kargbo, R.; Takahashi, Y.; Bhor, S.; Cook, G. R.; Lloyd-Jones, G. C.; Shepperson, I. R. Readily Accessible, Modular and Tuneable BINOL 3,3'-Perfluoroalkylsulfones: Highly Efficient Catalysts for Enantioselective In-Mediated Imine Allylation. *J. Am. Chem. Soc.*, **2007**, *129*, 3846-3847.
- (74) Tuck, D. G. The lower oxidation states of indium. *Chem. Soc. Rev.*, **1993**, *22*, 269-276.
- (75) Schneider, U.; Kobayashi, S. Catalytic Activation of Pinacolyl Allylboronate with Indium(I): Development of a General Catalytic Allylboration of Ketones. *Angew. Chem. Int. ed.*, **2007**, *119*, 6013-6016.
- (76) Cooper, I. R.; Grigg, R.; MacLachlan, W. S.; Thornton-Pett, M.; Sridharan, V., 3-Component palladium-indium mediated diastereoselective cascade allylation of imines with allenes and aryl iodides. *Chem. Commun.*, **2002**, (13), 1372-1373.
- (77) Wada, M.; Akiba, K. Metallic bismuth mediated allylation of aldehydes to homoallylic alcohols. *Tetrahedron Lett.*, **1985**, *26*, 4211-4212.
- (78) (a) Wada, S.; Hayashi, N.; Suzuki, H. Noticeable facilitation of the bismuth-mediated Barbier-type allylation of aromatic carbonyl compounds under solvent-free conditions. *Org. Biomol. Chem.*, **2003**, *1*, 2160-2163. (b) Smith, K.; Lock, S.; El-Hiti, G. A.; Wada, M.; Miyoshi, N. A convenient procedure for bismuth-

- mediated Barbier-type allylation of aldehydes in water containing fluoride ions.
Org & Biomol. Chem., **2004**, *2*, 935-938.
- (79) Bhuyan, P. J.; Prajapati, D.; Sandhu, J. S. Metallic Bismuth and Tantalum Mediated C-Allylation of Aldimines with Allyl Bromide. *Tetrahedron Lett.*, **1993**, *34*, 7975-7976.
- (80) Bazar, N.; Donnelly, S.; Liu, H.; Thomas, E. J. 1,5-Stereocontrol in Bismuth-Mediated Reactions Between Aldehydes and Allyl Bromides: Stereoselective Synthesis of Open-Chain all-syn- and anti,anti-1,3,5-Disposed Trimethylalkanes. *Synlett.*, **2010**, 575-578.
- (81) Xu, X. L.; Zha, Z. G.; Miao, Q.; Wang, Z. Y. Allylation of Carbonyl Compounds Mediated by Nanometer-Sized Bismuth in Water. *Synlett.*, **2004**, 1171-1174.
- (82) L. C. Chao, R. D. Rieke. Activated metals. IX. New reformatsky reagent involving activated indium for the preparation of β -hydroxy esters. *J. Org. Chem.* **1975**, *40*, 2253.
- (83) S. Araki, H. Ito, Y. Butsugan, Synthesis of β -Hydroxyesters by Reformatsky Reaction Using Indium Metal. *Synth. Commun.* **1988**, *18*, 453.
- (84) a) C.-J. Li, T.-H. Chan. Organic syntheses using indium-mediated and catalyzed reactions in aqueous media. *Tetrahedron.*, **1999**, *55*, 11149. b) V. J. Bryan, T.-H. Chan. Organometallic-type reactions in aqueous media mediated by indium. Allylation of acyloyl-imidazoles and pyrazoles. Regioselective synthesis of β,γ -unsaturated ketones. *Tetrahedron Lett.*, **1997**, *38*, 6493.
- (85) Kargbo, R. B.; Cook, G. R., Stereoselective indium-mediated allylation reactions. *Curr. Org. Chem.* **2007**, *11* (15), 1287-1309.

- (86) J. S. Yadav, A. Antony, J. George, B. V. Subba Reddy. Recent Developments in Indium Metal and Its Salts in Organic Synthesis. *Eur. J. Org. Chem.*, **2010**, 591.
- (87) Wu, X.-F.; Anbarasan, P.; Neumann, H.; Beller, M. From Noble Metal to Nobel Prize: Palladium-Catalyzed Coupling Reactions as Key Methods in Organic Synthesis *Angew. Chem. Int. Ed.*, **2010**, *49*, 9047-9050.
- (88) Papoian, V.; Minehan, T., Palladium-Catalyzed Reaction of Arylindium Reagents Prepared Directly from Aryl Iodides and Indium Metal. *J. Org. Chem.* **2008**, *73* (18), 7376-7379.
- (89) (a) Pham, M.; Allatabakhsh, A.; Minehan, T. G. *J Org Chem.*, **2008**, *73*, 741-4. (b) Moral, J. A.; Moon, S. J.; Rodriguez-Torres, S.; Minehan, T. G. *Org Lett.*, **2009**, *11*, 3734-7.
- (90) Jiang, N.; Hu, Q.; Reid, C. S.; Lu, Y.; Li, C. J. A novel palladium-catalyzed coupling of epoxides with allyl bromide mediated by indium(I) chloride: a cascade epoxide rearrangement–carbonyl allylation. *Chem Commun (Camb)*, **2003**, 2318-2319.
- (91) Fu, N.-Y.; Yuan, Y.-F.; Cao, Z.; Wang, S.-W.; Wang, J.-T.; Peppe, C. Indium(III) Bromide-Catalyzed Preparation of Dihydropyrimidinones: Improved Protocol Conditions for the Biginelli Reactions *Tetrahedron.*, **2002**, *58*, 4801-4807.
- (92) Sakai, N.; Annaka, K.; Konakahara, T. Palladium-Catalyzed Coupling Reaction of Terminal Alkynes with Aryl Iodides in the Presence of Indium Tribromide and Its Application to a One-Pot Synthesis of 2-Phenylindole. *Org. Lett.*, **2004**, *6*, 1527-1530.

- (93) Lee, P. H.; Seomoon, D.; Lee, K.; Kim, S.; Kim, H.; Kim, H.; Shim, E.; Lee, M.; Lee, S.; Kim, M.; Sridhar, M. *Adv. Synth. Cat.*, **2004**, *346*, 1641-1645.
- (94) Qian, M.; Huang, Z.; Negishi, E.-i. Use of InCl₃ as a Cocatalyst and a Cl₂Pd(DPEphos)—P(2-Furyl)₃ Catalyst System for One-Pot Hydrometalation—Cross-Coupling and Carbometalation—Cross-Coupling Tandem Processes. *Org. Lett.*, **2004**, *6*, 1531-1534.
- (95) Donaldson, E. M., Determination of bismuth in ores, concentrates and non-ferrous alloys by atomic-absorption spectrophotometry after separation by diethyldithiocarbamate extraction or iron collection. *Talanta* **1979**, *26* (12), 1119-1123.
- (96) (a) de Marcillac, P.; Coron, N.; Dambier, G.; Leblanc, J.; Moalic, J.-P. *Nature* **2003**, *422*, 876-878. (b) Riezler, W.; Porschen, W., Natural radioactivity of bismuth. *Z. Naturforsch.* **1952**, *7a*, 634-5.
- (97) Antoniotti, S.; Dunach, E., Recent uses of bismuth derivatives in organic synthesis. *C. R. Chim.* **2004**, *7* (6-7), 679-688.
- (98) Wittig, G.; Clauß, K. *Justus Liebigs Annalen der Chemie* **1952**, *578*, 136-146.
- (99) (a) Barton, D. H. R.; Kitchin, J. P.; Motherwell, W. B. *J. Chem. Soc: Chem. Commun.*, **1978**, 1099-1100. (b) Barton, D. H. R.; Lester, D. J.; Motherwell, W. B.; Papoula, M. T. B. *J. Chem. Soc: Chem. Commun.*, **1979**, 705-707. (c) Barton, D. H. R.; Blazejewski, J.-C.; Charpiot, B.; Motherwell, W. B. *J. Chem. Soc: Chem. Commun.*, **1981**, 503-504. (d) Barton, D. H. R.; Kitchin, J. P.; Lester, D. J.; Motherwell, W. B.; Papoula, M. T. B. *Tetrahedron* **1981**, *37*, 73-79. (e) Barton, D. H. R.; Finet, J. P. *Pure. & Appl. Chem.*, **1987**, *59*, 937-946.

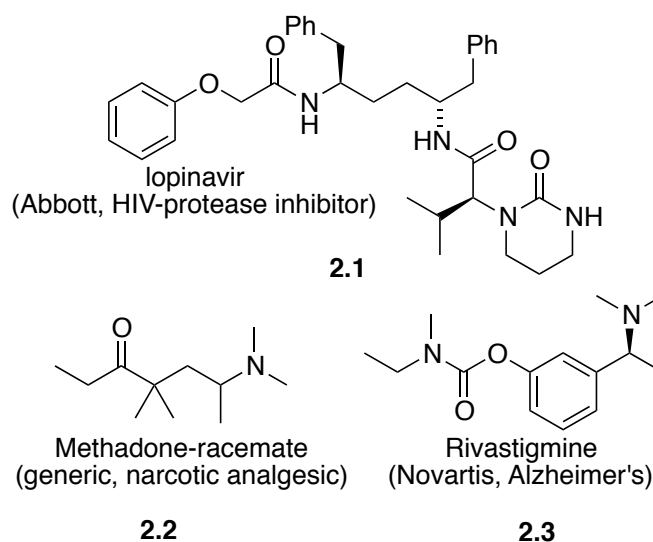
- (100) Barton, D. H. R.; Bhatnagar, N. Y.; Blazejewski, J. C.; Charpiot, B.; Finet, J. P.; Lester, D. J.; Motherwell, W. B.; Papoula, M. T. B.; Stanforth, S. P. *J. Chem. Soc-Perk. Trans-I*, **1985**, 2657-2665.
- (101) Matano, Y., Pentavalent organobismuth reagents in organic synthesis: alkylation, alcohol oxidation and cationic photopolymerization. *Top Curr Chem.*, **2012**, *311*, 19-44.
- (102) Hua, R. M. Recent Advances in Bismuth-Catalyzed Organic Synthesis. *Curr. Org. Synth.*, **2008**, *5*, 1-27.
- (103) Rueping, M.; Nachtsheim, B.; Ollevier, T., Bismuth Salts in Catalytic Alkylation Reactions. Bismuth-Mediated Organic Reactions. Springer Berlin / Heidelberg: **2012**, (31), 115-141
- (104) Leonard, N. M.; Wieland, L. C.; Mohan, R. S. Applications of bismuth(III) compounds in organic synthesis. *Tetrahedron.*, **2002**, *58*, 8373-8397.
- (105) (a) Salvador, J.; Silvestre, S.; Pinto, R.; Santos, R.; LeRoux, C.; Ollevier, T., New Applications for Bismuth(III) Salts in Organic Synthesis: From Bulk Chemicals to Steroid and Terpene Chemistry. (b) Bismuth-Mediated Organic Reactions. Springer Berlin / Heidelberg: **2012**, *311*, 143-177.
- (106) LD₅₀ value from MSDS of the compounds from OSHA database. Price as of June 2012 from Sigma Aldrich. Seppelt, K. *Angew. Chem. Int. Ed.*, **2002**, *41*, 2610-2611.
- (107) Alexander, V. M.; Bhat, R. P.; Samant, S. D., Bismuth(III) nitrate pentahydrate, a mild and inexpensive reagent for synthesis of coumarins under mild conditions. *Tetrahedron Lett.*, **2005**, *46* (40), 6957-6959.

- (108) Patil, S.; Bhat, R.; Raje, V.; Samant, S., Ultrasound-assisted Pechmann condensation of phenols with ketoesters to form coumarins, in the presence of bismuth(III) chloride catalyst. *Synth. Commun.* **2006**, *36* (4), 525-531.
- (109) Reddy, Y. T.; Rajitha, B.; Reddy, P. N.; Kumar, B. S.; Rao, V. P. *Synth. Commun.*, **2004**, *34*, 3821-3825.
- (110) Bothwell, J. M.; Krabbe, S. W.; Mohan, R. S., Applications of bismuth(III) compounds in organic synthesis. *Chem. Soc. Rev.*, **2011**, *40* (9), 4649-4707.
- (111) (a) Azurmendi, N.; Caro, I.; Caballero, A. C.; Jardiel, T.; Villegas, M., Microwave-Assisted Reaction Sintering of Bismuth Titanate-Based Ceramics. *J. Am. Cer. Soc.*, **2006**, *89* (4), 1232-1236. (b) Ollevier, T.; Li, Z., Bismuth Triflate Catalyzed Allylation of Aldehydes with Allylstannane under Microwave Assistance. *Eur. J. Org. Chem.*, **2007**, (34), 5665-5668.
- (112) Gangadasu, B.; Palaniappan, S.; Rao, V. J. One-pot synthesis of dihydropyrimidinones using polyaniline-bismoclite complex. A facile and reusable catalyst for the Biginelli reaction. *Synlett.*, **2004**, 1285-1287.
- (113) Gordon, R. B.; Rutledge, J. W., Bismuth Bronze from Machu Picchu, Peru. *Science.*, **1984**, *223* (4636), 585-586.
- (114) Zhu, X.-b.; Duan, X.-c., The present application and future development of indium. *Xiyou Jinshu Yu Yingzhi Hejin.*, **2008**, *36* (1), 51-55.

CHAPTER 2. INDIUM-MEDIATED STEREOSELECTIVE NUCLEOPHILIC ADDITION TO IMINES

2.1. Introduction

Nitrogen-containing compounds are found in variety of molecules in nature as well as in biologically important molecules. They served as important structural motifs in defining new pharmaceutical drug candidates. In those compounds, nitrogen is known to play a crucial role for their biological activity (Scheme 2.1).¹



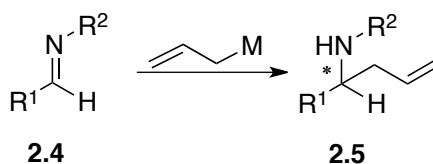
Scheme 2.1. Drug Molecules Containing Chiral Amine Moiety

Synthesis of these important molecules could be performed from a variety of starting materials. One well-known example is nucleophilic addition to imines.² Nucleophilic addition to these C=N in a stereo controlled fashion offers new carbon-carbon bond construction methods to the biologically relevant molecules. Among the plethora of methods that have been developed for nucleophilic addition to imines, allylation and Reformatsky reaction provide scaffolds that often facilitates the key starting materials to assemble useful pharmacophores. The collected projects that follow examine the preparation of chiral amines through an indium (I)-mediated allylation and indium (0)-

mediated Reformatsky reaction. These two projects are worked in collaboration with Dr. Tanmay Mandal who worked as a postdoctoral researcher at the Cook group.

2.2. Allyl Nucleophile Addition to Imines

Chiral homoallylic amines are valuable synthetic intermediates and are found in natural products of biological interest.³ Addition of allyl metals to C=N bonds with stereocontrol is one of the most studied areas (Scheme 2.2). The sense of asymmetric induction and the degree of stereoselectivity in the addition of allyl metal reagents to imines derived from aldehydes and ketones depends on two major factors, first, the nature of the metal and second, nature of the imine.⁴



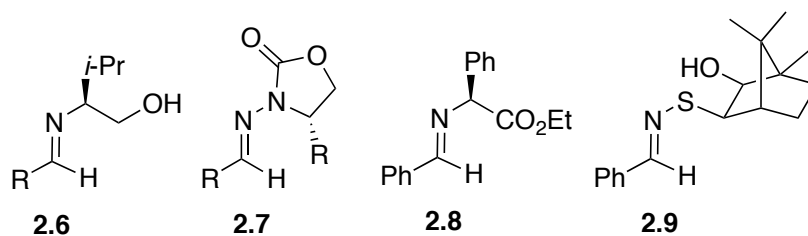
R¹ = alkyl, aryl, allyl, vinyl.

R² = alkyl, aryl, SiR₃, NR₂, POR₂, OR, BR₂

M = Li, Mg, Ba, B, Sn, Si, Ce, Yb, Cd, Cu, Zn, Zr, In

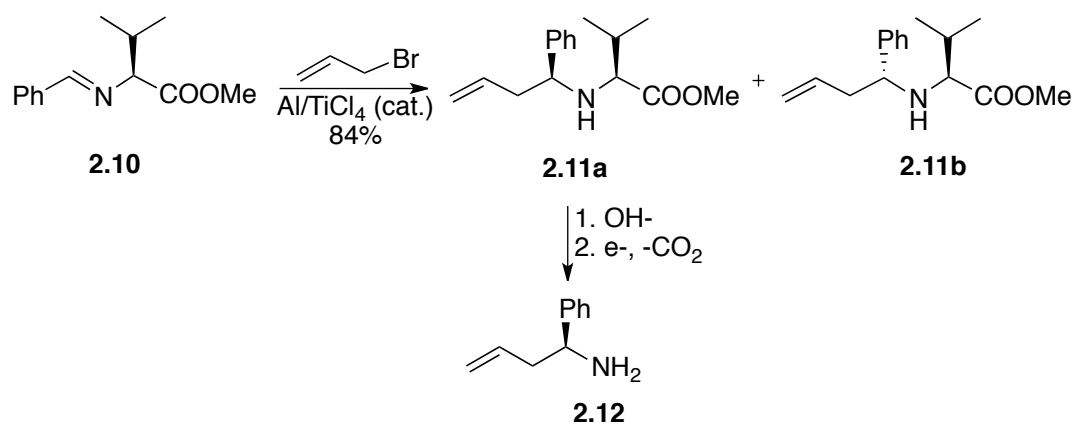
Scheme 2.2. Metal-Mediated Allylation of Imines

Among the metal-mediated reactions on imines, Barbier and Grignard type allylation of imines have been investigated in depth.⁵ Reports containing selective addition of allyl metal reagents to imines and their analogues such as oximes, hydrazones and nitrones have been known (Scheme 2.3).⁶



Scheme 2.3. Imines With Chiral Auxiliary

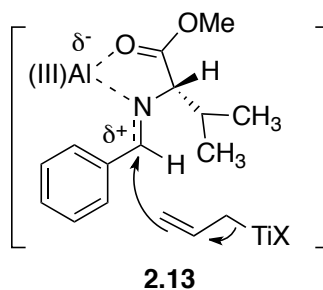
These chiral auxiliaries allow an effective stereocontrol during a nucleophilic addition to the imine carbon. Auxiliaries are proven to be selective with respect to the metal. After the completion of nucleophilic addition, the auxiliaries are removed using suitable procedures based on the *N*-substitution. Titanium is one of the pioneering metals in allylation. Usually in these reactions, a low valent titanium is generated by the reduction of Ti(III) or Ti(IV) with several reductants. In this example Tanaka and co-workers reported a diastereoselective allylation of imine derived from (*S*)-valine **2.10** using a Ti(0) generated from titanium tetrachloride and aluminum *in situ*. The allyl titanium reagent is formed *in situ* from Ti(0) and allyl bromide (Scheme 2.4).⁷



Scheme 2.4. Aluminum-Mediated Diastereoselective-Allylation of Imines

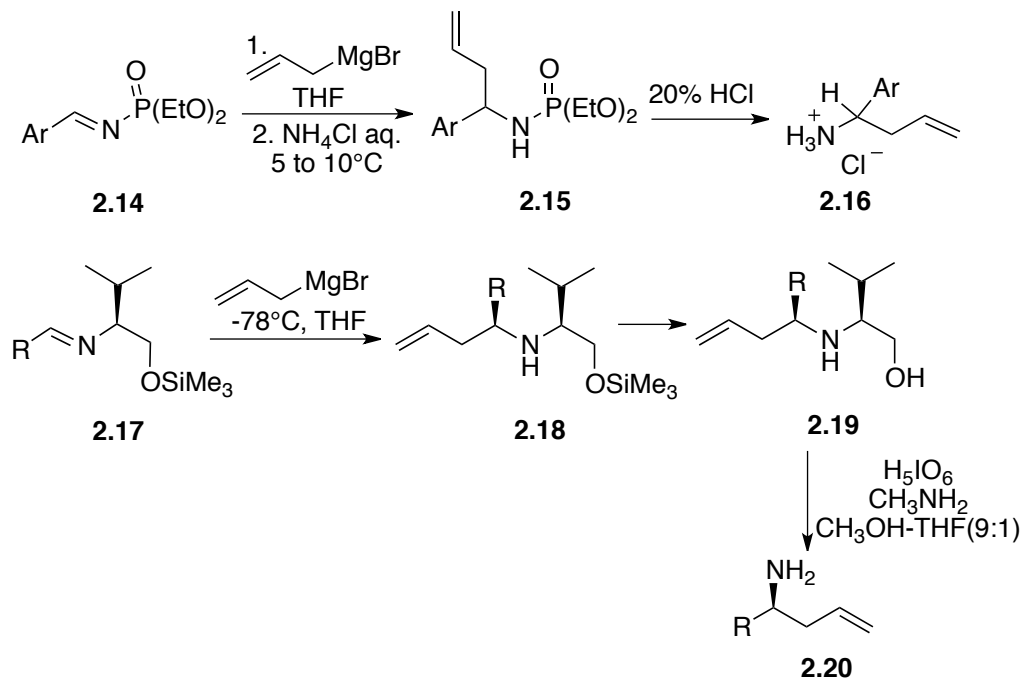
The valine esters **2.11a** and **2.11b** are obtained in 20:1 diastereoselectivity. The major isomer **2.11a** was separated using chromatography and the chiral auxiliary was removed using alkaline hydrolysis followed by decarboxylation using electrolysis producing the homoallylic amine **2.12**. Even though the procedure is titanium-mediated, it uses catalytic amount of titanium source and stoichiometric amount of aluminum for the redox cycle. The origin of diastereoselectivity was explained through an acyclic transition state model (Scheme 2.5). The ester carbonyl and the imine nitrogen could effectively

coordinate with the aluminum(III)-Lewis acid and the isopropyl group blocks a face there by this structure enables the preferential addition of allyl titanium reagent through one face. Thus model this explains the stereochemical outcome of this reaction.



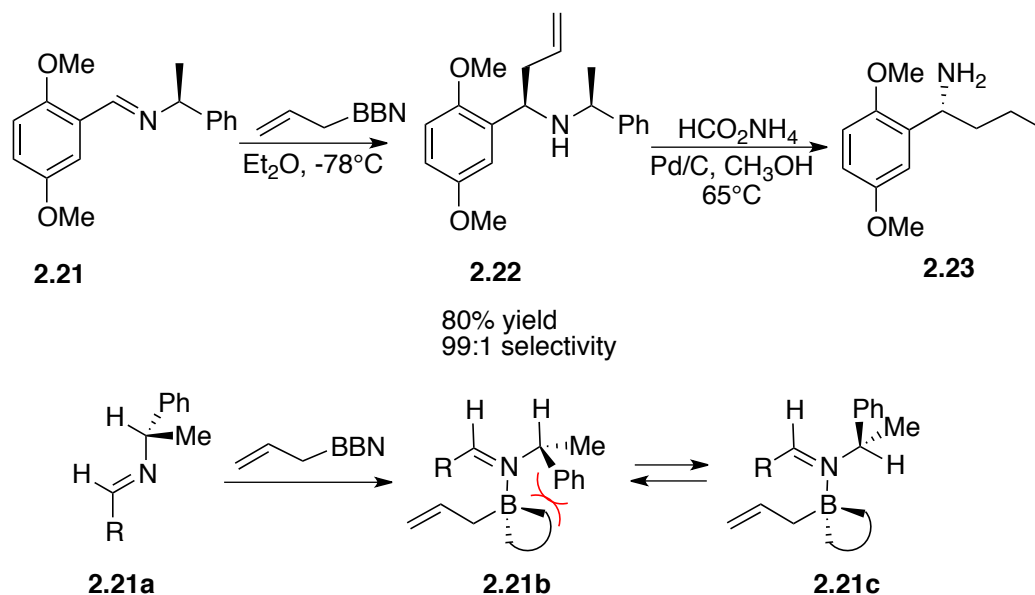
Scheme 2.5. Stereochemical Outcome of Titanium-Aluminum Mediated Allylation

Allyl magnesium reagents were also shown to add effectively to the imine carbons. Diastereoselective as well as racemic allylation methods have been reported with allyl magnesium halides (Scheme 2.6).⁸ *N*-Diphenylphosphinylimines **2.14** reacted effectively with allyl magnesium bromide to produce the diethyl-*N*-homoallylphosphoramidate **2.15** in good yields. Acid hydrolysis resulted in cleaving the phosphoramidate functional group yielding the homoallylic amine salt **2.16**. Valine derived silylestere were also proved to be efficient for the addition of allyl magnesium reagents, except the addition have to be performed at low temperatures.⁹ The cleaving of auxiliary also takes multiple steps to produce the homoallylic amine **2.20**.



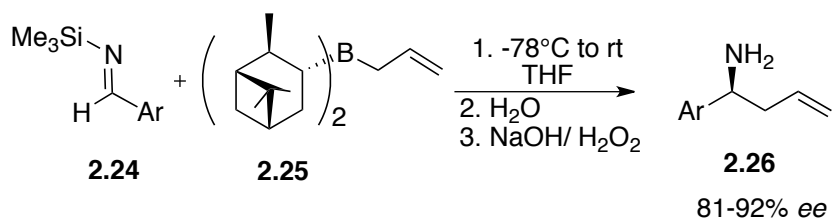
Scheme 2.6. Alkylation of Imines Using Magnesium Reagent

Cleaving chiral auxiliary sometimes does not lead to appreciable results. In an example of using allyl boronates with (S)- 2,5-dimethoxybenzalimine **2.21** resulted in 99:1 selectivity for the homoallylic amine **2.22** (Scheme 2.7). A pathway proposed, explained the origin of stereochemistry. The imines preferentially orient itself in conformation **2.21a** where the hydrogen atoms of the azomethine and the chiral auxiliary are in *syn* orientation. This was confirmed by NOE experiments. The complexation of the imine **2.21a** with the allyl boron species to form **2.21b**, the carbon-nitrogen bond rotates itself to avoid the steric interaction between the bulky group present on the boron and the chiral auxiliary and assumes the conformation **2.21c**. This conformation gives rise to the observed major isomer. The hydrogenolysis the homoallylic amine **2.22** leads to the chiral amine **2.23** without the useful allyl functionality for further elaboration.



Scheme 2.7. Alkylation of Aldimines Using Allylboron Reagents

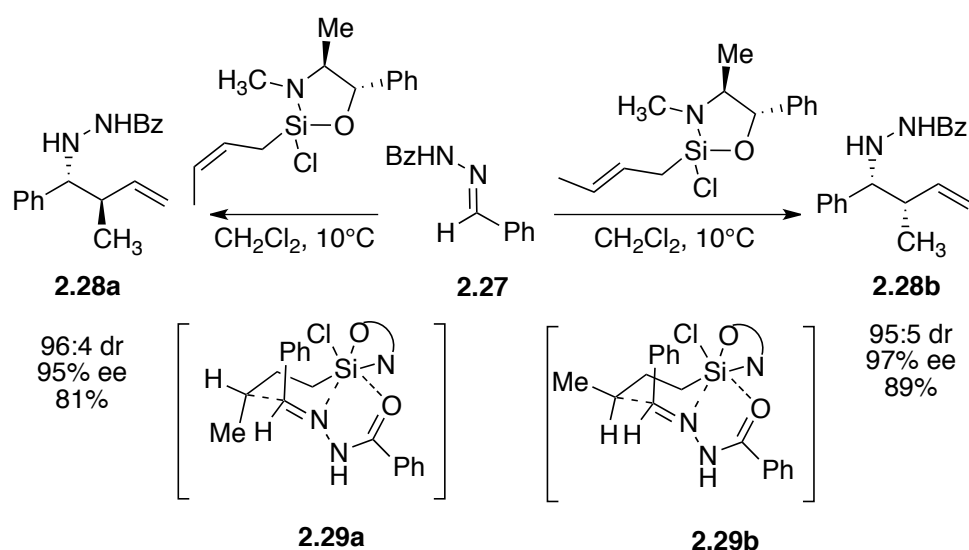
Having stereogenic centers in the allyl metal reagent could also be used for asymmetric induction in the product homoallylic amine. Brown and co-workers reported asymmetric allylation of allyl boron reagents with *N*-silylimines to produce homoallylic amine **2.26** (Scheme 2.8). In an atom economical stand point the use of stoichiometric amount of boron reagent with the heavy auxiliary such as pinene is not attractive. The oxidative cleavage of the boronate is necessary and could affect other functional groups when applied to relatively larger molecule.



Scheme 2.8. Asymmetric Allylation of *N*-Silylimines

Leighton reported an attractive strategy using chiral allylsilanes derived from pseudoephedrine. Both *E* and *Z*-crotylacetates reacted effectively with hydrazones to

produce *anti*-hydrazone **2.28a** and *syn*-hydrazone **2.28b** respectively in excellent yields and diastereoselection. The observed course of addition was opposite to that one performed with aldehydes. This could be reasoned out by the stereochemical models **2.29a** and **2.29b** where the two-point binding to silicon and double activation is playing a role (Scheme 2.9).

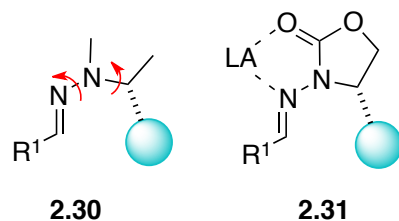


Scheme 2.9. Alkylation of Chiral Hydrazones using Allylsilanes

Hydrazone substrates provide additional binding sites to Lewis acids for obtaining stereoselection as observed in product **2.28b**. Cleaving the *N-N* bond after alkylation produces branched primary amines that are useful building blocks. Thus they could be considered as equivalents of imines from ammonia. Several interesting enantioselective methodologies have been developed using hydrazones as substrate. Hydrazones also provide an additional advantage of functional group tolerance compared to other aza precursors such as oximes, sulfinylimines and silylimines.

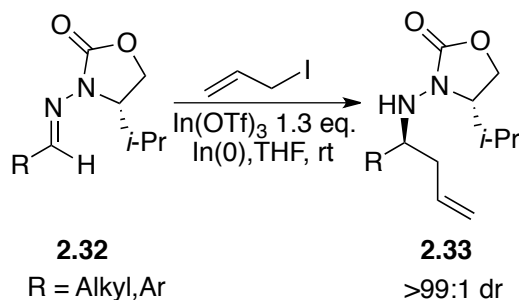
Gregory Friestad introduced unique chiral *N*-acylhydrazones as versatile imino acceptors for the synthesis of chiral amines. These substrates could be prepared from amination of 4-alkyl-2-oxazolidinones with NH_2^+ equivalents to afford *N*-(amino)-

oxazolidinones.¹⁰ These amines upon condensation with aldehydes and ketones will produce the aldimine hydrazones and ketimine hydrazones **2.31** respectively. These substrates incorporate two important features, the carbon-nitrogen bond is fixed due to the ring and the N-N bond is fixed due to Lewis acid chelation. These features are absent in the other common hydrazone substrate such as **2.30** (Scheme 2.10).



Scheme 2.10. N-Linked Auxiliary Approach for Imines

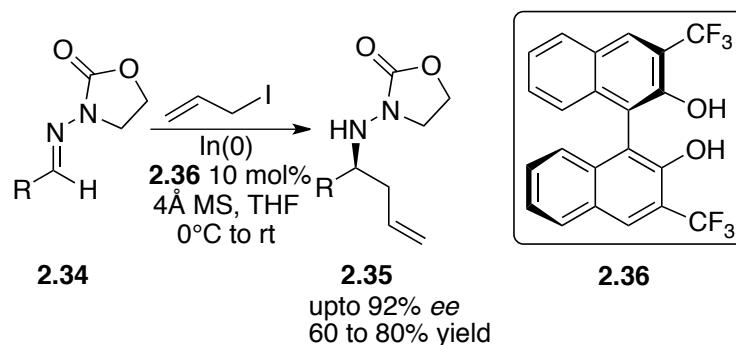
In 2004 our group reported a highly diastereoselective method for allylation of chiral hydrazones **2.32** using indium and allyl iodide (Scheme 2.11).¹¹ Near quantitative yields and high diastereoselectivity was observed for the product homoallyl amines **2.33**. The use of indium triflate effectively controlled the hydrazone rotamers as proposed in **2.31** and hence high diastereoselectivity was observed.



Scheme 2.11. Indium-Mediated Diastereoselective Allylation of Chiral Hydrazones

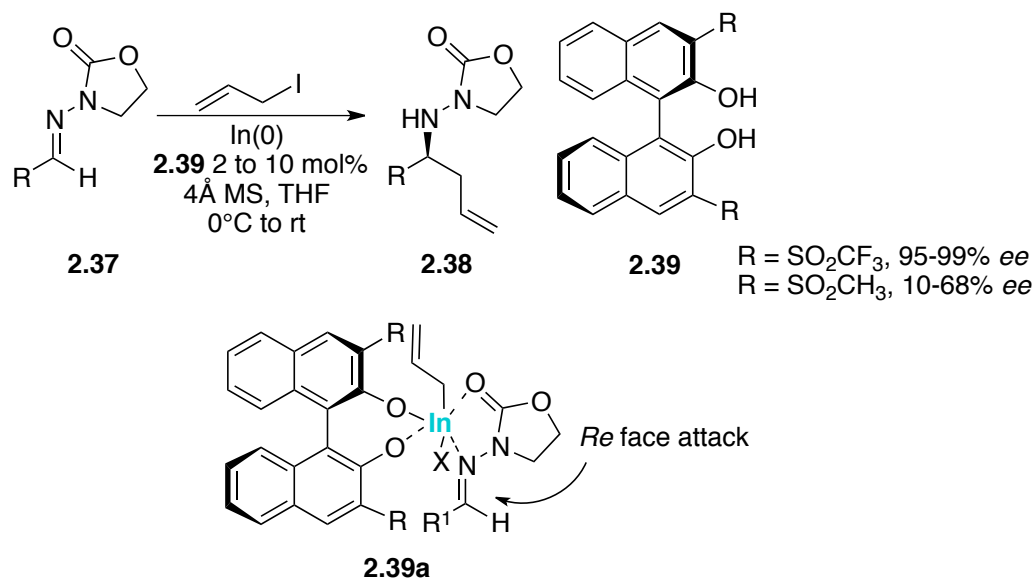
Followed by this report of diastereoselective allylation of hydrazones, our group investigated the use of the oxazolidinone derived hydrazone template for enantioselective allylation. The use of achiral oxazolidinone **2.34** under indium-mediated allylation with

chiral trifluoromethyl-BINOL **2.35** resulted in good yield and appreciable enantioselectivity (Scheme 2.12).¹² Stoichiometric use of ligand **2.36** resulted increase of the enantioselectivity up to 97%.



Scheme 2.12. Indium-Mediated Enantioselective Allylation of Hydrazones

The use of stoichiometric use of chiral source is not attractive in enantioselective catalysis. After a through study and investigation of this methodology our group reported the first highly enantioselective indium-mediated allylation of imines in 2007 (Scheme 2.13). This is the first example in the literature demonstrating the highest level of optical purity in the allylation of imines using indium-mediated method.¹³



Scheme 2.13. Enantioselective Indium-Mediated Allylation of Imine

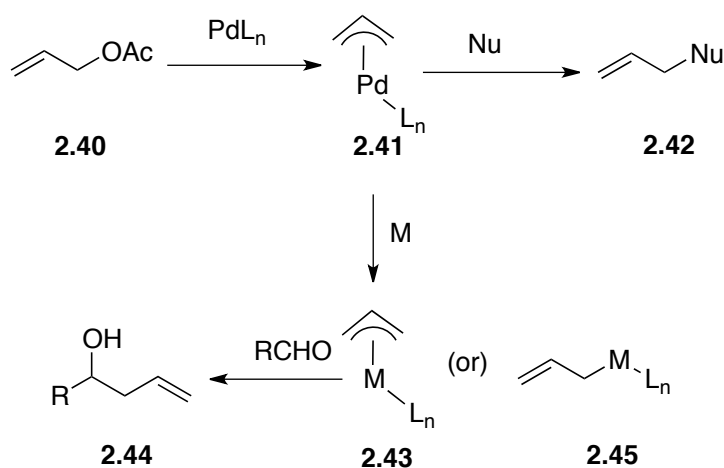
The sulfone-BINOL ligand **2.39** was prepared through thia-Fries rearrangement of perfluoroalkylsulfonated BINOL. The presence of perfluorosulfones was found to be crucial for the observed enantioselectivity, resulting up to 99% optical purity of the homoallylic amine **2.38**.

The methods discussed above utilizes allylic halides and indium metal in either Barbier-type or a Grignard-type reaction for the generation of allyl indium reagent. A mechanistically distinct Pd(0)-catalyzed generation of allyl indium reagent was reported by Araki and co-workers in 2000.¹⁴ This procedure used allylic alcohols and allylic acetates as nucleophilic precursors. This is procedure is referred to as *ümpolung* allylation. An advantage this protocol offers is the use of allylic alcohols that are readily available and convenient to use compared to allylic halides.

2.2.1. *Ümpolung* Allylation of Imines

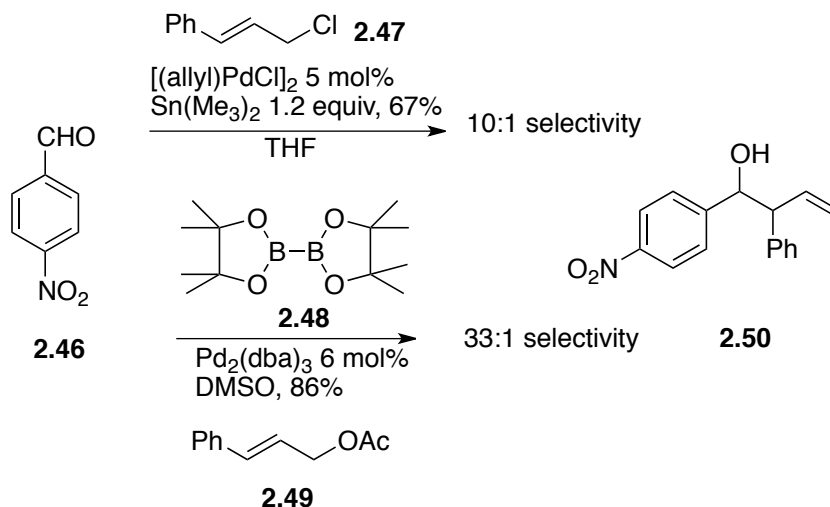
π -Allylpalladium complexes are well known to be electrophilic in nature. Thus, they allow a variety of nucleophiles to attack resulting in the formation of allylated product. When this electrophile is present along with a reducing agent, the electrophilic character of the π -allylpalladium complex is converted to nucleophilic character. This process may be referred to as a reductive transmetalation. This nucleophile can react with electrophilic sites to produce an allylated product. The nucleophilic reagent **2.43** reacts with an aldehyde to produce a homoallylic alcohol **2.44** (Scheme 2.14). The former, reaction of a π -allylpalladium complex with a nucleophile is commonly referred to as the Tsuji-Trost reaction.¹⁵ The latter is called a *ümpolung* allylation. This reversal of reactivity could be achieved using a variety of reductants such as Et_2Zn ¹⁶, SnCl_2 ¹⁷, Et_3B ¹⁸, Silanes¹⁹ and recently InI. An advantage of *ümpolung* allylation over other allylation methods is that

the reaction often uses readily available and easy to handle allylic alcohols and allylic acetates. The catalytic use of the expensive transition metal, palladium and the stoichiometric use of the relatively non-toxic and cheaper alternative led to many research groups exploring this area.



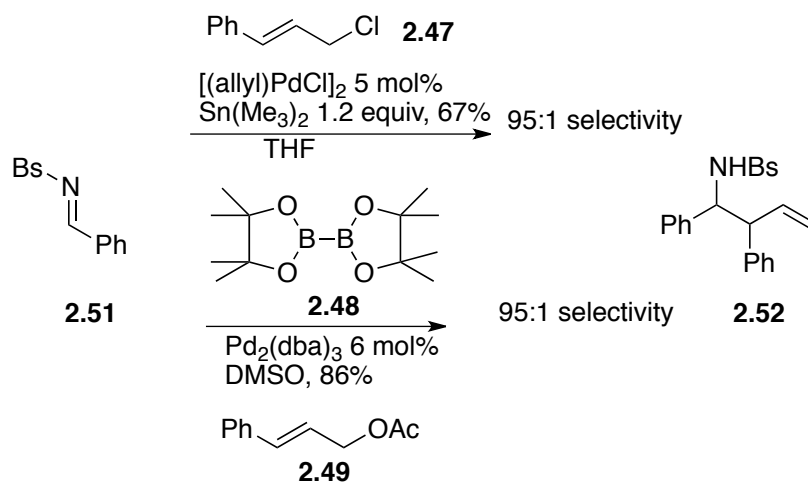
Scheme 2.14. Umpolung Reactivity of π -Allylpalladium Complex

Wallner and co-workers described allylation methods for aldehydes and imines using palladium/tin and palladium/boron systems.²⁰ As described in Scheme 2.15 hexamethyl ditin reacts with the π -allylpalladium complex from **2.47** to generate allyltin reagent that reacts with aldehyde **2.46** to yield the homoallylic alcohol **2.50** in 10:1 selectivity. The selectivity increases remarkably when the reaction is performed with an *in situ* generated allylboronate from BPin.



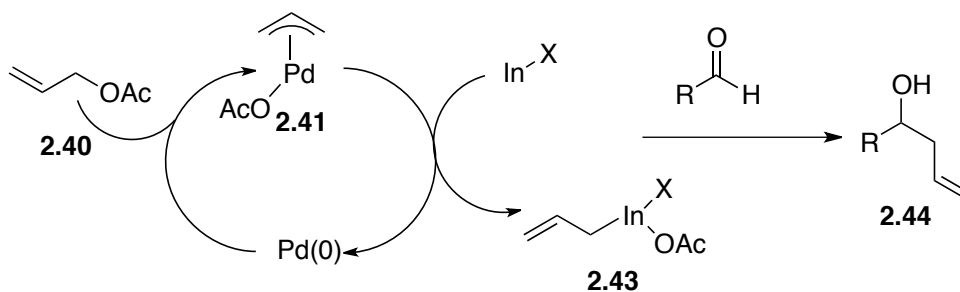
Scheme 2.15. Alkylation of Aldehydes using Pd/Sn and Pd/B

The same protocol was applied for the alkylation of imines. Unlike the difference in the selectivity observed in aldehydes with the change of metal, homoallylic amine **2.52** is obtained in excellent selectivity with boron as well as tin reagents (Scheme 2.16).



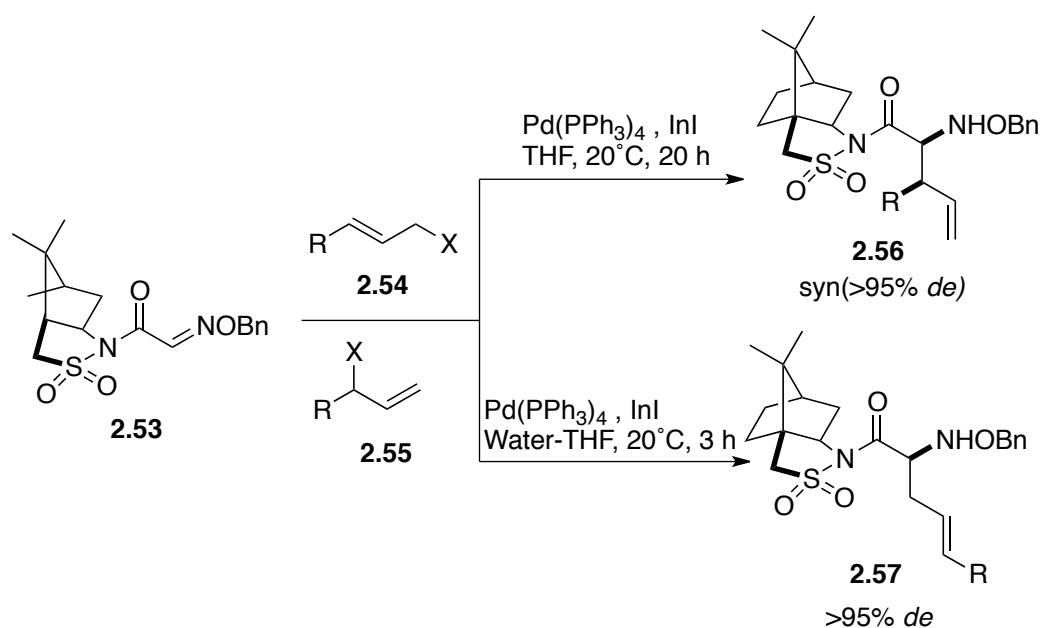
Scheme 2.16. Alkylation of Imines using Pd/Sn and Pd/B

Most methods for indium-mediated alkylation employ allylic bromides or iodides as the allyl metal precursor. In 2000, Araki and co-workers reported a new method for the preparation of allyl indium reagents **2.43** from allylic acetates and alcohols using a reductive transmetalation protocol catalyzed by Pd(0).¹⁴



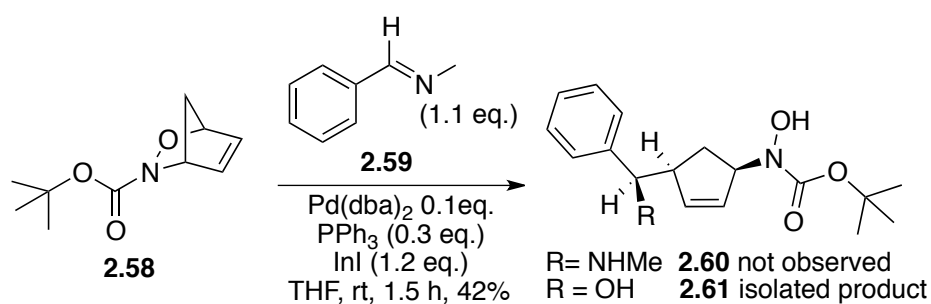
Scheme 2.17. Mechanism of Umpolung Allylation

This method is advantageous than conventional method of preparation of allyl indium reagents as it circumvents the use of more sensitive allylic halides and broadens the scope of nucleophiles that may be employed. Following Araki's work, multiple reports have appeared using this transmetalation protocol for various electrophiles. Takemoto and co-workers described a diastereoselective allylation of electron-deficient imines using a catalytic amount of palladium and indium(I) iodide.¹⁵ The α -adduct **2.56** was observed when anhydrous THF was used as a solvent. γ -adduct **2.57** was observed when THF: water mixture was used as a solvent (Scheme 2.18).



Scheme 2.18. Diastereoselective Allylation of Imines

Marvin Miller's group explored a diverse range of electrophiles including hetero Diels-Alder adducts for Pd(0)/In(I) allylations.²¹ A representative example described below uses N-benzylidenemethylamine **2.59** as a precursor for the allylation of benzaldehyde (generated *in situ*) (Scheme 2.19).²² The allyl indium reagent generated from **2.58** reacts with benzaldehyde to produce the biological useful structure **2.61** in average yield.



Scheme 2.19. Pd(0)/In(I)-mediated Allylation of Benzaldehyde

Indium serves as an attractive alternative to other toxic metals used as a reductant. Organoindium reagents are known to be mild towards a variety of functionalities and stable in aqueous conditions. Taking into account all these rationales, we decided to investigate diastereoselective allylation of chiral hydrazone substrates using a palladium catalyzed, indium-mediated allylation methodology.

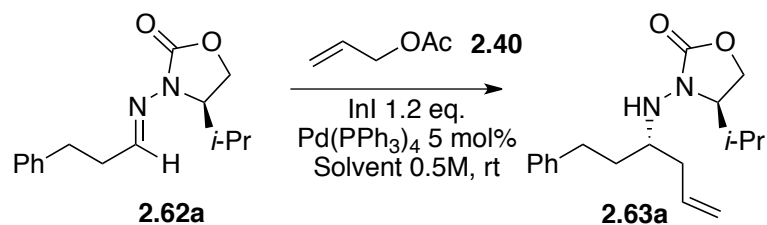
2.2.2. Results and Discussion

To the best of our knowledge, stereoselective palladium-catalyzed, indium-mediated *umpolung* allylation has not been explored thoroughly for imine substrates. From the current standpoint on the importance of chiral amine based molecules, developing allylation protocol for the synthesis of homoallylic amines would be beneficial. Our research group reported the first use of allylindium reagents generated from allylic iodides and indium metal with chiral hydrazone substrates. With the help of *umpolung* procedure,

convenient allylic acetates could be used as precursors. We envisioned that this method would improve the operational simplicity and easy handling options to the allylation of chiral hydrazones.

We first examined the optimum conditions for the allylation of chiral hydrazones. Table 2.1 (entry 1 to 8) shows the variation of yields and *dr* with various common solvents. A variety of solvents gave good yield (Table 2.1, entries 2, 4, 6). In THF (Table 2.1, entry 4) the yield was good but the *dr* was low compared to THF /water (Table 2.1, entry 5). With the exception of acetonitrile (Table 2.1, entry 3) the product **2.63a** was observed for all solvents. Allyl acetate, indium(I) iodide and catalytic amount (5 mol%) of Pd(PPh₃)₄ were mixed with imine in a Barbier-type reaction at room temperature.

Table 2.1. Solvent Screening for Umpolung Allylation of Chiral Hydrazone



Entry ^a	Solvent	% Yield ^b	<i>dr</i> ^c
1	CHCl ₃	65	97:3
2	Et ₂ O	78	98:2
3	CH ₃ CN	0	-
4	DMF	60	98:2
5	CH ₃ OH	84	98:2
6	Toluene	60	98:2
7	THF	79	96:4
8	THF:Water(3:1)	81	98:2
9	THF:H ₂ O (1:1)	81	99:1
10	THF:H ₂ O (1:3)	76	97:3
11	H ₂ O	0	-

^a Reactions performed at 0.5 mmol scale ^b isolated yield ^c*dr* calculated by ¹H-NMR

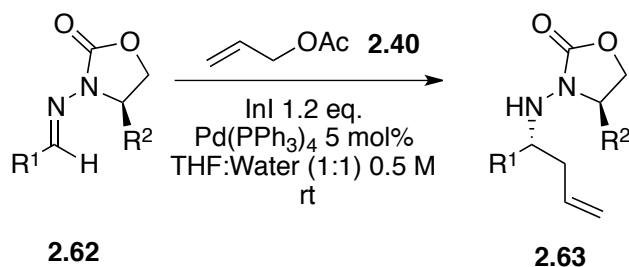
On the basis of these results obtained from the initial solvent study we further investigated the effect of the ratio of THF and water (1:1). We found that a 1:1 ratio of THF:Water (Table 2.1, entry 9) was found to give high diastereoselectivity. From the data in Table 2.1 it is also evident that increase in THF or water composition in the mixture slightly decreases diastereoselectivity (table 2.1, entry 4, 5, 10, 11, 12).

The substrate scope for indium(I) iodide mediated *umpolung* allylation was investigated next and the results are presented in Table 2.2. The reaction times for most of the substrates varied from 36 to 42 hrs. Excellent diastereoselectivity was observed in most cases.

In Table 2.2, the substrates with chiral oxazolidinones containing isopropyl and benzyl auxiliaries derived from (L)-valine and (L)-phenyl alanine respectively were screened. The isopropyl auxiliary effectively blocked a face for the attack of the nucleophile resulting in the formation of the product in high diastereoselectivity. Aliphatic substrates derived from linear aldehydes (Table 2.2, entry 1, 2) with isopropyl auxiliary reacted effectively giving moderate to good yields. Branched aldehydes derived hydrazones also reacted effectively (Table 2.2, Entry 3, 4) producing the corresponding β -amino esters. The diastereoselectivity although observed to be controlled by the auxiliary, substrate **2.62f** (Table 2.2, entry 5) gave average diastereomeric purity when subjected to the reaction condition. This lower dr could be attributed to the orientation of the ester functionality in the substrate, which might not effectively allow the auxiliary to block a face of the reaction center. Benzyl auxiliary gave slightly lower diastereoselectivity compared to isopropyl auxiliary. This is due to the steric difference provided by the benzyl group compared to isopropyl group (Table 2.2, entry 9, 10). Phenyl auxiliary on the other

hand gave us the lowest diastereoselectivity (Table 2.2, entry 12). This is due to the planar nature of the phenyl ring, which is not effective in controlling the nucleophile attack.

Table 2.2. Substrate Screening *Ümpolung* Allylation of Chiral Hydrazone



Entry ^a	SM	R ¹	R ²	Time (h)	%Yield ^b	dr ^c
1	2.62b	Et	<i>i</i> -Pr	36	92 (2.63b)	99:1
2	2.62c	<i>n</i> -Pr	<i>i</i> -Pr	36	91 (2.63c)	99:1
3	2.62d	<i>i</i> -Pr	<i>i</i> -Pr	48	81 (2.63d)	99:1
4	2.62e	<i>i</i> -Pr	<i>i</i> -Pr	48	74 (2.63e)	99:1
5	2.62f	EtOCO	<i>i</i> -Pr	30	80 (2.63f)	80:20
6	2.62g	<i>c</i> -C ₅ H ₉	<i>i</i> -Pr	34	92 (2.63g)	99:1
7	2.62h	<i>c</i> -C ₆ H ₁₁	<i>i</i> -Pr	38	83 (2.63h)	99:1
8	2.62i	PhCH ₂	<i>i</i> -Pr	40	77 (2.63i)	99:1
9	2.62j	Et	PhCH ₂	32	70 (2.63j)	98:2
10	2.62k	<i>i</i> -Bu	PhCH ₂	42	79 (2.63k)	97:3
11	2.62l	Ph(CH ₂) ₂	PhCH ₂	32	91 (2.63l)	99:1
12	2.62m	<i>i</i> -Bu	Ph	40	69 (2.63m)	86:14

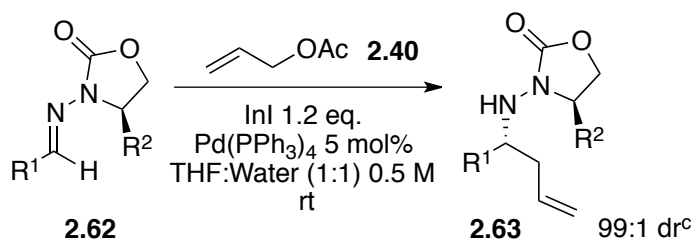
^a Reactions performed at 0.5 mmol scale ^b isolated yield ^cdr calculated by ¹H-NMR

To summarize the substrate scope, the isopropyl auxiliaries gave excellent diastereoselectivity (Table 2.2, Imine **2.21b-f**, **2.23a-c**). Phenyl auxiliary gave lower *dr* compared to isopropyl and benzyl auxiliaries (Table 2.2, Imine **2.27a**). The optical rotation of the diastereomerically pure isolated products were determined and compared with the literature values.

Despite the intensive research in Pd/In mediated α -allylation, studies are rare on the underlying mechanism of the reaction. The selectivity observed with changes in solvent as well as introducing additives in α -allylation of imines was well explored in the mid 2000's.²³ But the mechanism of the α -allylation-type addition to electrophilic carbon is not well studied.

The most plausible catalytic cycle for the α -allylation proposed by Araki and co-workers is shown in Scheme 2.4. The first step is the formation of π -allyl palladium complex, which undergoes a reductive transmetalation with indium(I) iodide to produce allyl indium. The nucleophilic allyl indium species attacks the electrophilic imine carbon to form the allylated product. In our studies about the mechanism of this reaction we found that an increase in the amount of catalyst decreased the yield of the reaction. One major cause for this lowering of yield could be the phosphine ligand interfering with the reaction at some point. To investigate the possibility of ligand effects we used a convenient Pd(0) source which is Pd₂(dba)₃ and varied the amount of phosphine ligand. Table 2.3 shows the variation of yields with increase in the amount of phosphine. The reaction proceeded efficiently with 1 phosphine per palladium (Table 2.3, entry 1). A significant difference in isolated yields of the reactions were observed in the cases of 15 mol % and 20 mol % of triphenyl phosphine with 2.5 mol % of palladium (Table 2.3 entry 4, 5). The same result was observed with 5 mol % of palladium (Table 2.3, entry 7 to 11).

Table 2.3. Role of Phosphines in Ümpolung Allylation of Chiral Hydrazone



Entry ^a	X	Y	PPh ₃ /Pd	%Yield ^b
1	2.5	2.5	0.5	86
2	2.5	5	1	81
3	2.5	10	2	72
4	2.5	15	3	61
5	2.5	20	4	40
6	5	0	-	0
7	5	2.5	0.25	78
8	5	5	0.5	75
9	5	10	1	65
10	5	20	2	54
11	5	30	3	37

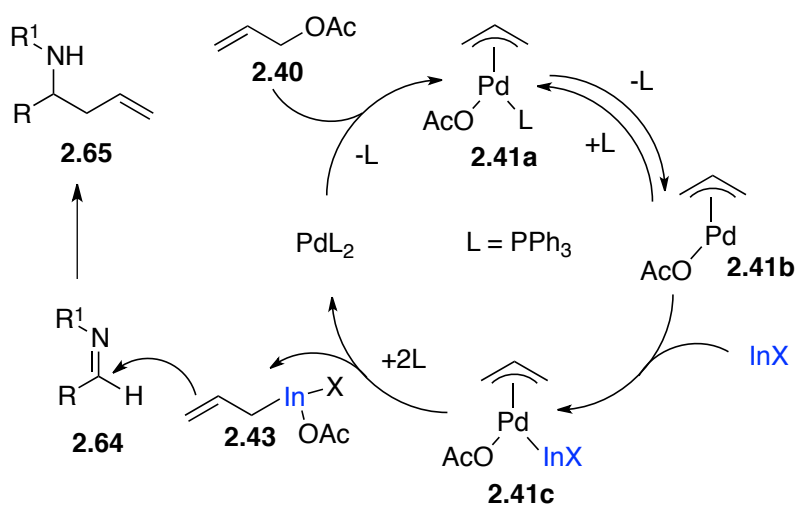
^a Reactions performed at 0.5 mmol scale ^b isolated yield ^cdr calculated by ¹H-NMR

We also probed into the ratio of phosphine to palladium. The reaction has an excellent yield when the ratio is 0.5 at low catalyst loading. When the ratio is kept constant and the catalyst loading is increased, we observe a decrease in the yield. This observation is consistent when comparing entry 2 and 9, 3 and 10 and 4 and 11.

With the observation that the reaction did not precede in the absence of the phosphine ligand (Table 2.3, Entry 6) we arrived with a possible mechanism (Scheme 2.7) that describes a possible way the phosphine ligands may inhibit the reaction. When allylic acetate is interfered with palladium it forms the π -allylpalladium complex **2.41a**. This complex should undergo a ligand dissociation to form **2.41b** and thereby coordination of

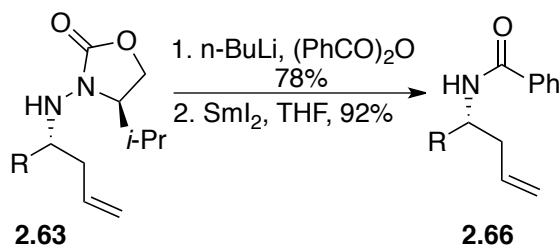
indium(I) iodide is enabled resulting in **2.41c**. In case there is excess of phosphine ligands present in the system, the rate of dissociation will be lower than the association step. This will affect the next step where indium coordinates with π -allyl palladium complex. The precedence for the formation of palladium-indium bond is well known in literature. The formation of these type of complexes are known to occur most likely with indium (I) species which supports our system where we use indium(I) iodide for the reaction.²⁴

Reductive transmetalation from **2.41c** results in the regeneration of Pd(0) catalyst and allylindium reagent **2.43**. This allyl indium reagent reacts with the imine **2.64** resulting in homoallylic amine **2.65** as the product (Scheme 2.20).



Scheme 2.20. Proposed Mechanism for Phosphine Inhibition

The chiral auxiliary could be readily cleaved in couple of steps effectively as reported by our group previously in the report on the enantioselective allylation of imines using sulfone-BINOL ligand. The absolute stereochemistry of the resulted product was confirmed by comparing the optical rotation values of the product obtained through our diastereoselective indium-mediated allylation (Scheme 2.21).⁵



Scheme 2.21. Removal of Chiral Auxiliary

We are hoping to expand the scope of the reaction beyond allylic acetates.

Exploring other leaving groups such as carbamates and benzoates would also be beneficial.

Unprotected allylic alcohols on the other hand are attractive for the methodology and have been reported to be effective for aldehyde substrates and less reactive for imines.

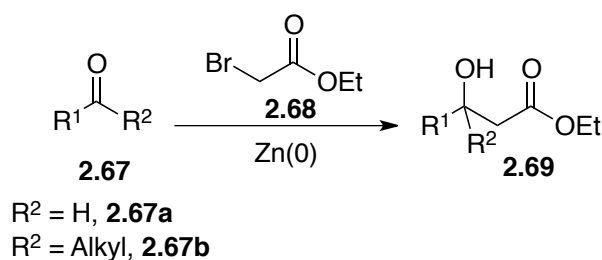
2.2.3. Summary of *Ü*mpolung Allylation of Hydrazones

In conclusion, we have developed a highly diastereoselective allylation method for chiral hydrazones. The reaction is operationally simple and produces excellent diastereoselectivity. This procedure for making homoallylic amines could be considered green supported by the facts that it uses toxic palladium in a catalytic amount and non-toxic indium in stoichiometric amount. An interesting study with respect to the mechanism of the reaction has been conducted. We also speculate that not just the phosphine to palladium ratio, but the total concentration of the catalyst is also having an effect on the conversion. A thorough mechanistic study is necessary to arrive at a viable pathway. Following the development of this diastereoselective procedure, our group has developed an enantioselective allylation method for achiral hydrazone substrates using triflone-BINOL ligand.

2.3. Enolate Addition to Imines

Metal-mediated reactions that form C-C bonds have a long history in organic chemistry and have been used in many industrial processes. A classical example is the

Reformatsky reaction. In 1887, Sergey Nikolayevich Reformatsky reported that zinc metal could mediate the addition of α -halo carbonyl compounds to aldehydes and ketones to produce β -hydroxyalkonates (Scheme 2.22).²⁵ Unlike to the aldol reaction, the Reformatsky reaction has been successfully performed with highly substituted ketones and imines. An advantage of Reformatsky reaction over the classical aldol reaction is, it is difficult to form an ester enolate selectively in the presence of enolizable aldehyde or ketone using a base.²⁶



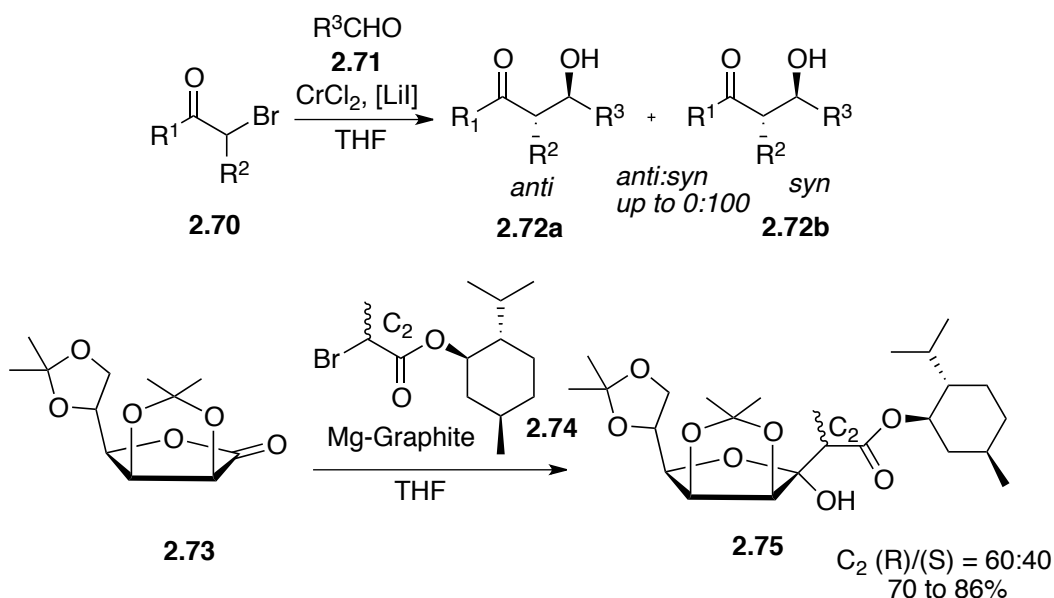
Scheme 2.22. Classical Reformatsky Reaction

Over the past century numerous variants of the Reformatsky reaction have been developed to achieve high yields and selectivity.²⁷ Reike and co-workers reported one major improvement to classical Reformatsky reaction in 1975.²⁸ They described an ultrasound promoted method for the formation of β -ketoesters and the reaction was mediated by indium. Historically this new method increased the attention of the scientific community towards the utility of indium.

2.3.1. Stereoselective Reformatsky Reaction of Imines

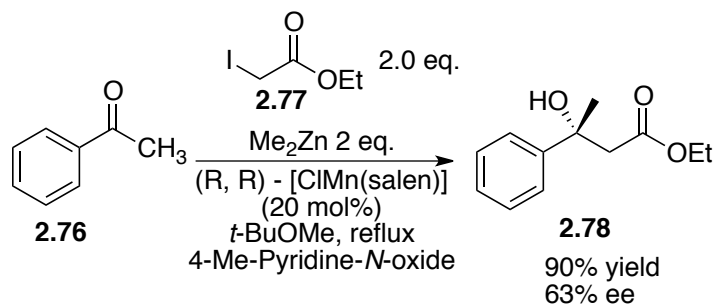
The original reaction developed by Reformatsky was mediated by zinc metal. The success of the reaction largely depended upon the ability to activate the zinc metal and performed in a strictly anhydrous atmosphere. In order to overcome these problems, numerous alternatives emerged over the years. Metals such as titanium,²⁹ cadmium,³⁰

germanium,³¹ gallium,³² samarium,³³ nickel,³⁴ cerium,³⁵ chromium,³⁶ cobalt,³⁷ copper,³⁸ manganese,³⁹ rhodium,⁴⁰ iron⁴¹ and other transition metals⁴² have been used as an alternative to zinc. Scheme 2.23 describes a chromium-mediated Reformatsky reaction of simple aldehydes **2.71**. The *syn*-selectivity is the result of the intermediate formed from the metal. The use of metal couples such as zinc-copper⁴³ and zinc-silver-graphite⁴⁴ have also been reported. The second equation in Scheme 2.23 describes magnesium-graphite mediated diastereoselective Reformatsky reaction of protected sugar **2.73**.



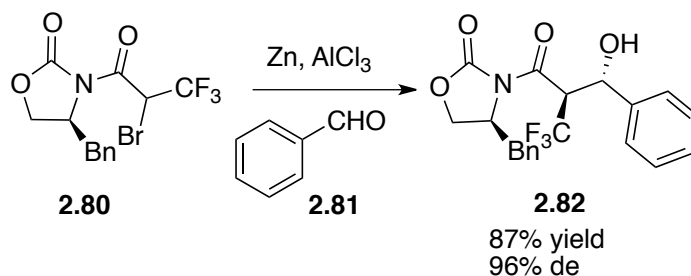
Scheme 2.23. Chromium- and Magnesium-mediated Reformatsky Reaction

Cozzi and co-workers in 2006 reported the first catalytic enantioselective Reformatsky reaction of ketones mediated by dimethyl zinc (Scheme 2.24).⁴⁵ Their system consisted of a salen-ligand for transferring the chiral information. The reaction sometimes used 4-methylpyridine-*N*-oxide, a common additive used in enantioselective epoxidation with salen ligands.



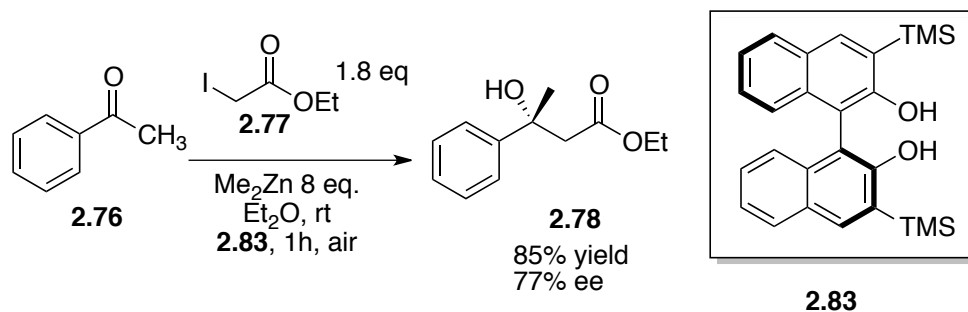
Scheme 2.24. Manganese-Mediated Reformatsky Reaction

In 1991, Ito and Sasaki described highly stereo controlled Reformatsky reaction with the use of oxazolidinone-derived bromides. Scheme 2.25 describes the successful enantioinduction on benzaldehyde obtained through a zinc-mediated diastereoselective Reformatsky reaction of benzaldehyde **2.81** with **2.80**. High levels of diastereoselectivity have been achieved using oxazolidinone auxiliary.



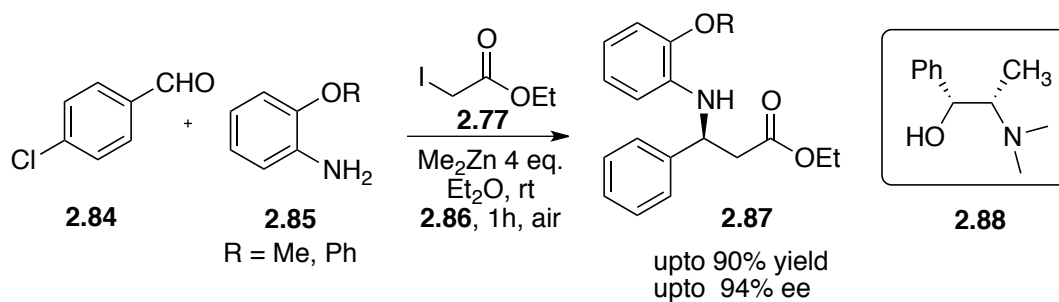
Scheme 2.25. Zinc-Mediated Diastereoselective Reformatsky Reaction

Followed by Cozzi's first report, in 2008, Feringa and co-workers reported an enantioselective Reformatsky reaction of ketone **2.76** with BINOL-derived ligand **2.83** (Scheme 2.26).⁴⁶ Compared to the longer reaction times (typically >50h) of Cozzi's method, this reaction was complete within a few hours. Also, this report consisted of the first successful enantioselective Reformatsky reaction on diaryl ketones.



Scheme 2.26. Dimethylzinc-Mediated Enantioselective Reformatsky Reaction of Ketones

Reformatsky reaction on imines is relatively difficult to achieve compared to aldehydes and ketones. Cozzi and co-workers reported a one-pot enantioselective reaction of imines prepared from simple aldehyde **2.84** and anilines **2.85**.⁴⁷ The reaction utilized four equivalents of dimethyl zinc to produce the product **2.87** in high yields and appreciable enantioselectivity. It is interesting to note that the reaction was promoted by air. The role of air is proposed to be crucial for the formation of the Reformatsky reagent from dimethyl zinc and ethyl iodoacetate **2.77** (Scheme 2.27).



Scheme 2.27. One-pot Enantioselective Reformatsky Reaction of Imines

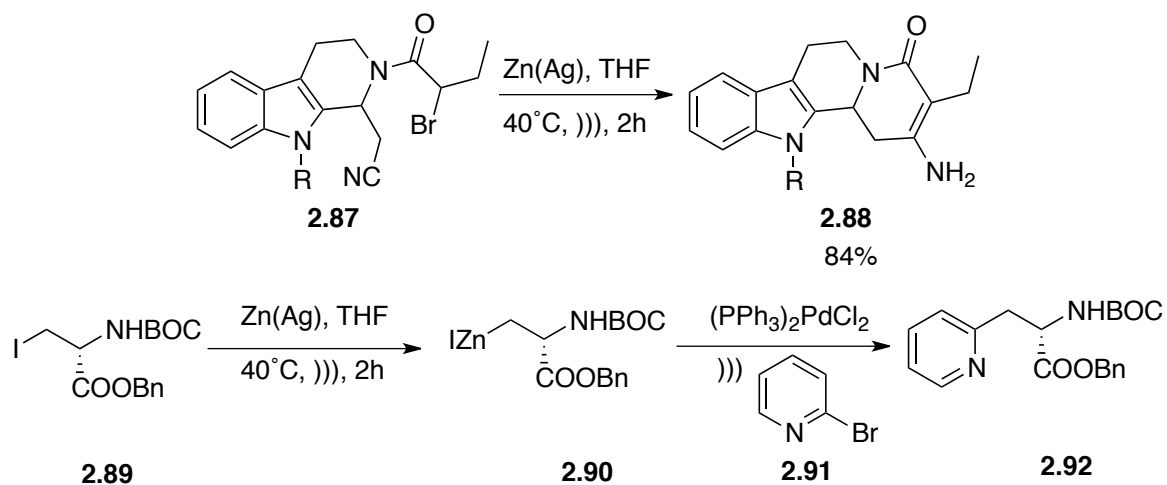
2.3.2. Ultrasound-Promoted Reformatsky Reaction

Milder alternatives developed for the Reformatsky reaction include activation of zinc using the Reike protocol,⁴⁸ Knochel's protocol,⁴⁹ using zinc-copper couple and zinc-silver on graphite as discussed earlier. An alternate route to the pre-activation methods uses ultrasound-promoted activation of the metal. Loomis reported the first use of ultrasound in

1927. This was followed by a period of intense interest in ultrasound into the 1940's. After that there was a dormant period until the 1970's, when commercial ultrasound equipment became readily available. This promoted the research in ultrasound-mediated organic reactions. Ultrasound has been used in promoting various reactions such as Simon-Smith's reaction, Ullman coupling, Heck coupling, Sonagashira coupling and Pauson-Khand reaction.⁵⁰ From a series of monographs published by Luche in the 1990's, it is understood that ultrasound promotion could be beneficial for three kinds of reactions:⁵¹

1. Reaction that involves radical intermediates.
2. Any heterogeneous reaction that could be enhanced by mixing or activation of metal surfaces.
3. Heterogeneous reaction that proceeds through a radical or an ionic pathway.

Ultrasound is also used in combination with other activation methods such as using metal couples (Scheme 2.28).

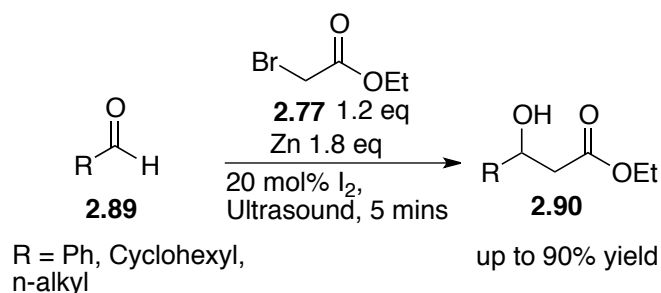


Scheme 2.28. Zinc-Silver couple Mediated Reformatsky Reaction

Meyers, in 1991, used an intramolecular Reformatsky reaction promoted by zinc-silver couple to produce **2.88** in 84% yield. A similar report from Jackson used zinc-

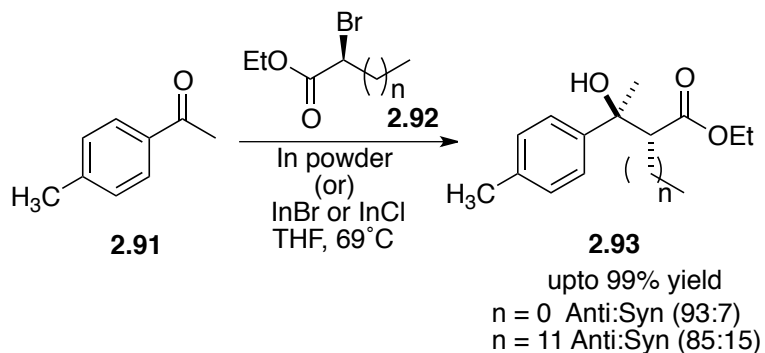
copper couple in combination with ultrasound to form the Reformatsky intermediate **2.90**, which, upon coupling with 2-bromopyridine, produced the unusual amino acid derivative **2.92**.

An interesting alternative way to activate zinc metal for Reformatsky reaction is by using a combination of ultrasound and iodine (Scheme 2.29). This is a commonly observed characteristic of ultrasound promoted Reformatsky reactions employing zinc. Simple aldehydes **2.89** undergo zinc-mediated ultrasound-promoted Reformatsky reaction with ethyl bromoacetate **2.77** in the presence of catalytic amount of iodine.



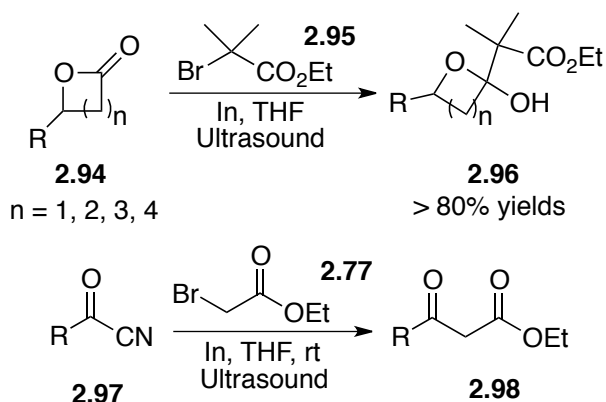
Scheme 2.29. Ultrasound-Promoted Zinc-Mediated Reformatsky Reaction

While zinc requires a pre-activation using iodine even under ultrasound promoted conditions, indium metal was reported to mediate Reformatsky reaction without pre-activation just under sonication. Lo and co-workers reported a diastereoselective sonochemical Reformatsky reaction of aldehydes and ketones mediated by indium metal. An excellent *anti*-selectivity was observed when ketone **2.91** reacted with the chiral α -bromo acetate **2.92** in the presence of indium powder to produce the product α -hydroxy- β -disubstituted ester **2.93** (Scheme 2.30).



Scheme 2.30. Indium-Mediated Diastereoselective Reformatsky Reaction

In recent examples lactones and acyl nitriles and lactones have been used in indium promoted Reformatsky reactions as shown in Scheme 2.31. Substituted lactone **2.94** reacted effectively under ultrasound-promoted indium-mediated Reformatsky condition to produce unique β -hydroxy ester in high yields. Acyl nitriles **2.97** on the other hand shows a different addition pattern under the same reaction conditions to produce β -ketoester **2.98** in good yield (Scheme 2.31).

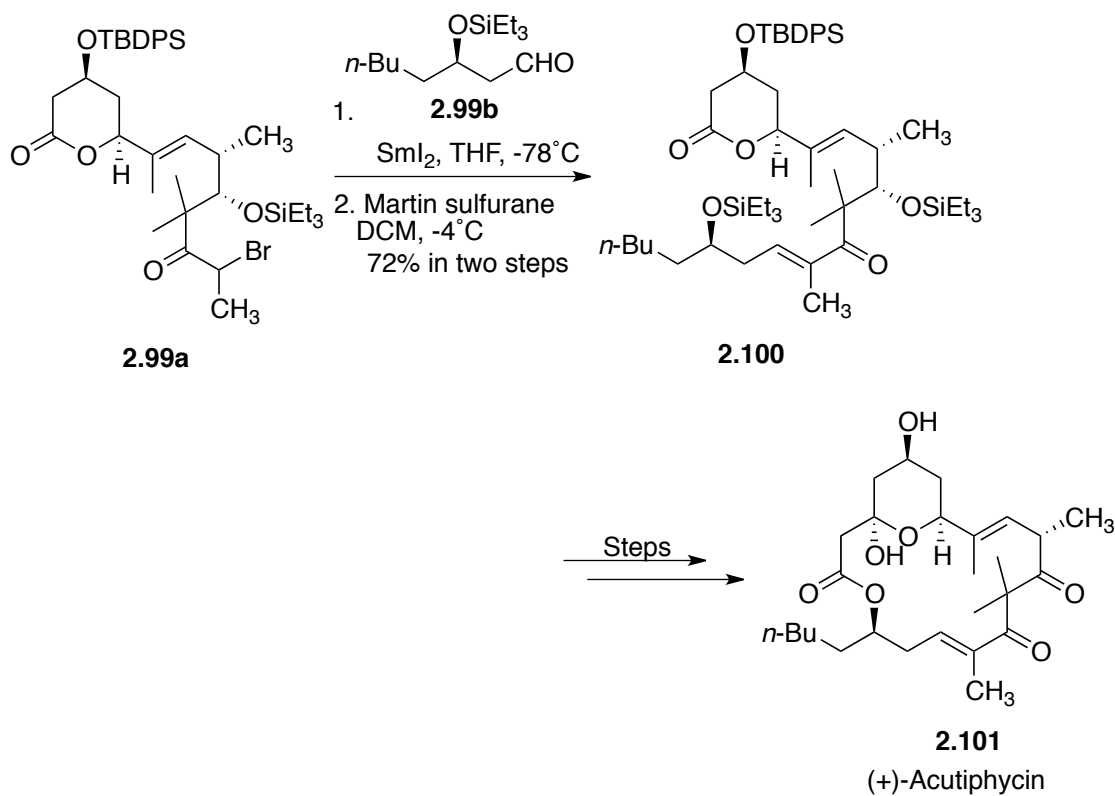


Scheme 2.31. Indium-Mediated Ultrasound-Promoted Reformatsky Reaction

Though ultrasound has various applications other than organic synthesis. The power of the ultrasound produced varies in each application. Ultrasonic bath used in laboratories generally range from 45-55 KHz.

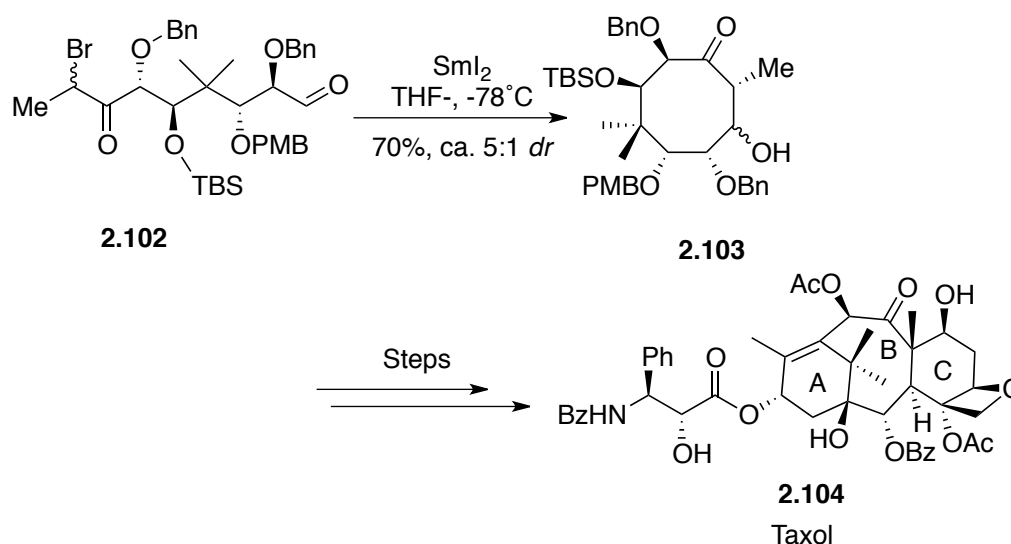
2.3.3. Applications of Reformatsky Reaction and Unsolved Problems

Complex natural product syntheses do not always demand new reagents and reactions. At times, simple reagents and classical transformations can perform formidable tasks. Several groups have demonstrated illustrative examples of the application of the Reformatsky reaction in total synthesis. In 1977, Henry Kagan introduced samarium diiodide to the synthetic community. SmI_2 has been largely used in radical transformations and also Reformatsky-type reactions.⁵² Moslin and Jamison reported the first example of the use of samarium diiodide in the total synthesis of acutiphycin (Scheme 2.32).⁵³ They effectively demonstrated the use of intermolecular Reformatsky reaction of **2.99a** with the aldehyde **2.99b** to produce **2.100**, which would cyclize through a series of transformations to produce the desired compound (+)-Acutiphycin **2.101**.



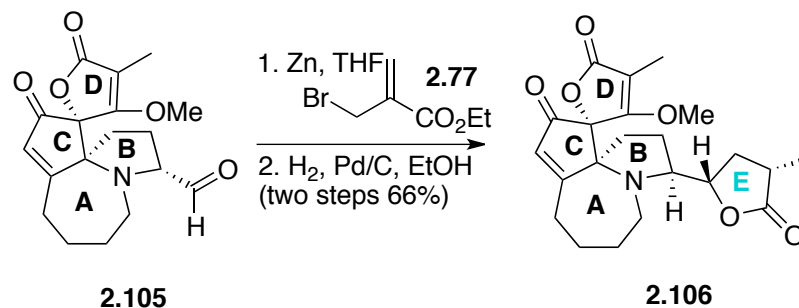
Scheme 2.32. Total Synthesis of (+)-Acutiphycin using Reformatsky Reaction

The second example comes from the Mukaiyama group's total synthesis of taxol **2.104**. Again an intramolecular SmI_2 -mediated Reformatsky was used to solve the problem of constructing the B-ring precursor **2.103** as shown in Scheme 2.33. An intramolecular SmI_2 -mediated Reformatsky reaction in closing a macrocyclic ring structure **2.104**.



Scheme 2.33. Total Synthesis of Taxol

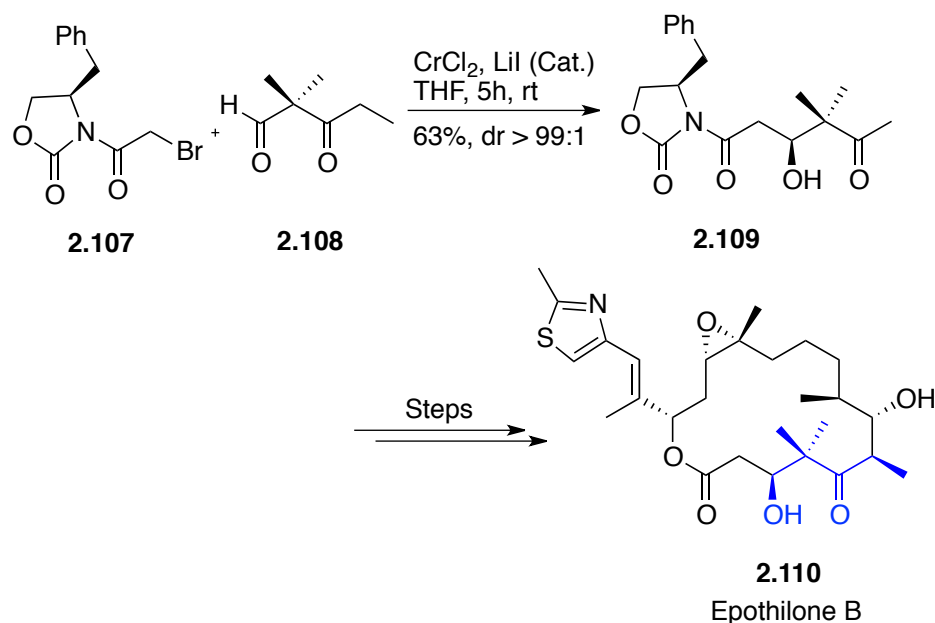
It is interesting to note that in both cases the substrates were highly functionalized and the authors were still able to perform the transformation successfully with fewer or no side products. Another prominent example is Zhang's report on the total synthesis of a stemona alkaloid, (\pm)-maistemonine (Scheme 2.34).⁵⁴



Scheme 2.34. Total Synthesis of Maistemonine

As above cases a late stage Reformatsky reaction under the classical conditions was used to construct E ring of the product **2.106** as described in Scheme 2.34. Similar to these examples shown above, numerous synthetic routes use the Reformatsky reaction as a key C-C bond-forming step. The most common application of Reformatsky reaction is the synthesis of β -hydroxy acids and non-proteogenic β -amino acids. For example, Soengas group used an indium-mediated Reformatsky reaction of oximes to prepare methyl aspartic acid in a fewer steps.⁵⁵

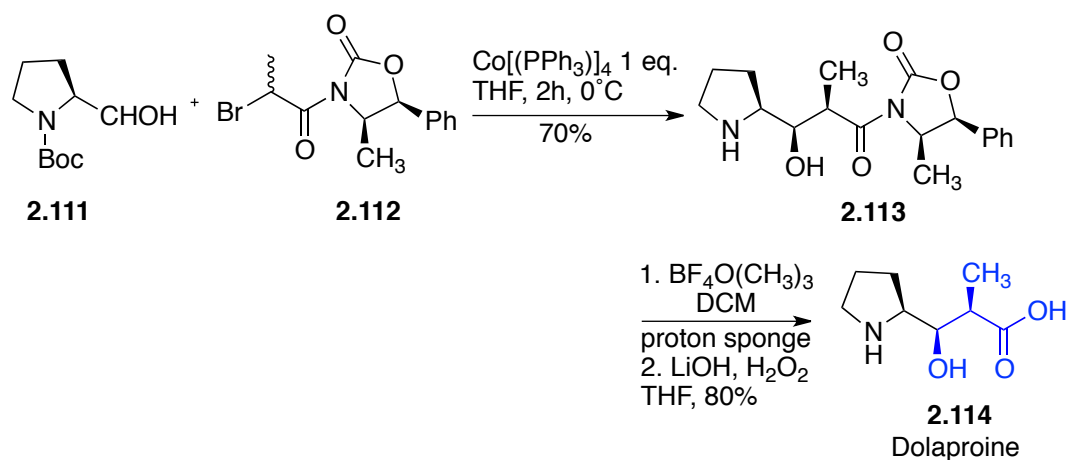
Epithilones are similar to taxanes in their biological activity and have a better bioavailability than compounds like paclitaxel (Scheme 2.35).



Scheme 2.35. Total Synthesis of Epithilone B

In scheme 2.35, Wessjohn used a chromium promoted diastereoselective Reformatsky reaction to construct the C-3 chiral center. The product **2.109** is obtained as a single diastereomer and is further converted to Epithilone B **2.110**.

In an example from Pettit's group, diastereoselective cobalt mediated Reformatsky reaction was used to prepare Dolaproine **2.114**, a linear peptide isolated from the sea hare *Dolabella auricularia* found in the western Indian Ocean (Scheme 2.36). The scarcity of compounds from the natural resources makes a synthetic route like this very attractive.



Scheme 2.36. Total Syntheses of Dolaproine

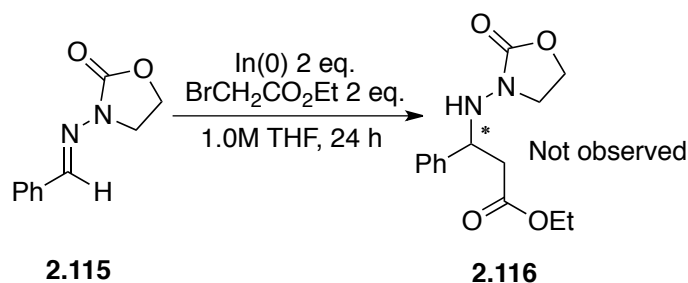
Despite the usefulness of the Reformatsky reaction, very few examples are operationally simple and environmentally benign stereoselective methods are known so far. Operationally simple reaction using ultrasound has been reported but the important issue in the realm of ultrasound promoted Reformatsky reactions is enantioselectivity.

Very few reports on enantioselective Reformatsky reaction of imines have been reported to date. Cozzi and co-workers reported the first enantioselective Reformatsky reaction of imines through a one-pot synthesis. The reaction was mediated by dimethyl zinc and N-methyl ephedrine as a ligand. The use of excess ligand to substrate (1.2 eq.) makes this method unattractive. The current literature suffers from the lack of highly stereoselective Reformatsky reactions that could be performed on imine substrates without employing sensitive reagents or expensive ligands. With this problem, we set out to explore a stereoselective Reformatsky reaction of imines mediated by imines. With our group's

expertise in using hydrazone template, we began our investigation of exploring Reformatsky reaction of hydrazones.

2.3.4. Results and Discussion

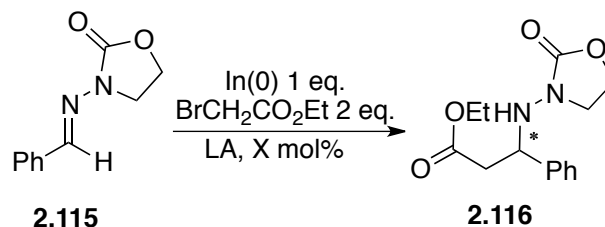
We started the investigation with the achiral hydrazone substrate **2.115**, which is a simple benzaldehyde derived hydrazone with a hope of developing an enantioselective methodology. A mixture of substrate **2.115**, indium powder and ethyl bromoacetate was stirred in THF for one day did not give any amount of product (Scheme 2.37).



Scheme 2.37. Initial Screening for Indium-Mediated Reformatsky Reaction

As a method of activating the imine substrate, we decided to perform a Lewis acid screening (Table 2.4). Addition of 1 equivalent of indium triflate resulted in a trace amounts of product by $^1\text{H-NMR}$ (Table 2.4, entry 1). When the amount of Lewis acid is reduced similar conversion was observed (Table 2.4, entry 2). Stoichiometric use of Lewis acid is not appreciable hence we decided to screen some Lewis acids in catalytic amounts. Indium halides did not effect the reaction and quantitative amount of starting material was recovered from the reaction (Table 2.4, entry 3 to 6). Lanthanide Lewis-acids gave trace amount of product (Table 2.4, entry 7, 8.) similar to indium triflate. Employing bismuth triflate (Table 2.4, entry 9) as Lewis acid resulted in 11% conversion by $^1\text{H-NMR}$.

Table 2.4. Lewis-Acid Screening for Indium-Mediated Reformatsky Reaction

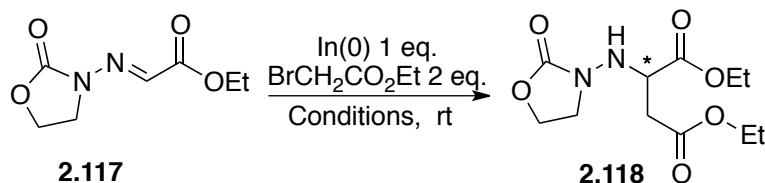


Entry ^a	LA	X	% Conv by NMR
1	In(OTf) ₃	100	6
2	In(OTf) ₃	10	5
3	InCl ₃	10	0
4	InBr ₃	10	0
5	InI ₃	10	0
6	InF ₃	10	0
7	Yb(OTf) ₃	10	9
8	Sc(OTf) ₃	10	4
9	Bi(OTf) ₃	10	11

^a Reactions were performed in a scintillation vial under argon atmosphere

From the above two tables one could interpret easily that substrate reactivity is a limiting factor. Also, It would be too early to reject substrate **2.115**. To identify some initial conditions to proceed with we prepared an activated substrate **2.117** from ethyl glyoxalate. Initially we decided to screen the reaction with increased concentration of the substrate, a variation compared to the previous table. Stirring at room temperature in THF (Table 2.5, entry 1) did not produce the desired β -amino ester **2.118**. Deleting the solvent from the reaction system and performing it under near conditions surprisingly produced the desired product in moderate yield (Table 2.5, entry 2). Recalling the examples of ultrasound promoted Reformatsky reactions, sonochemical activation of indium metal would have positive effect on the conversion. This motivated us to perform the reaction under ultrasound which gave the product β -amino ester in near quantitative yield.

Table 2.5. Solvent-free Conditions for Indium-Mediated Reformatsky Reaction

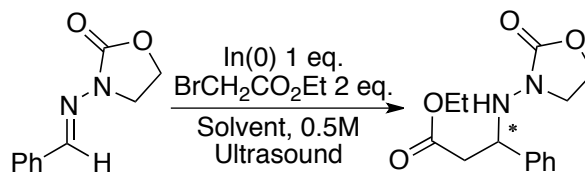


Entry ^a	Solvent	Time	Conditions	Yield ^b
1	THF (0.5M)	48h	rt, stirring	0%
2	Neat	24h	rt, stirring	57%
3	Neat	3.5	Ultrasound	93%

^a Reactions were performed in a scintillation vial under argon atmosphere, Monitored by TLC. ^b Isolated yields

From the screening performed we realized that ultrasound promoted conditions would be beneficial. With this information we track back to our original substrate, the achiral benzaldehyde derived hydrazone **2.115** for a solvent screening (Table 2.6). Initial reaction conditions were performed in THF. The use of other solvents such as 1,4-dioxane has also been reported in literature. The use of several aprotic solvents under ultrasound promoted condition did not produce desired result of good yield (Table 2.6, entry 1 to 5). Although under neat condition the so far unreactive aromatic hydrazone reacted to an appreciable extent to produce the β -amino ester in 21% yield. The starting material was recovered after the indicated time.

Table 2.6. Solvent Study for Benzaldehyde Derived Achiral Hydrazones



2.115		2.116	
Entry	Solvent	Time	%Yield
1	THF	48h	0
2	CH ₂ Cl ₂	48h	0
3	1,4 Dioxane	48h	0
4	DMF	48h	0
5	THF	48h	0
6	Neat	6	21

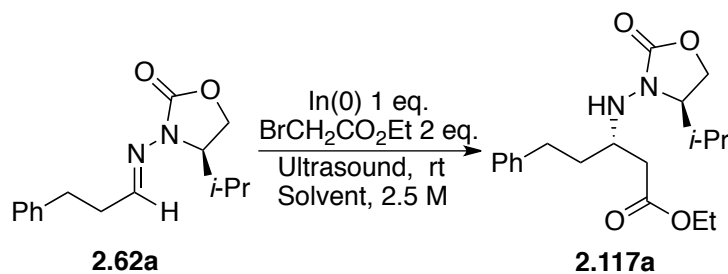
^a Reactions were performed in a scintillation vial under argon atmosphere, Monitored by TLC. ^b Isolated yields

From the above experiments we inferred that aromatic imines were less reactive than aliphatic imines under the set of conditions examined. And the reaction proceeded only under neat conditions. These two factors motivated us to prepare a chiral hydrazone **2.62a**, similar to the one used in indium-mediated allylation reported from our group and subject it to a Reformatsky reaction under neat conditions.

This result motivated us to explore the synthetic scope of the reaction. From the observations from screening the aromatic hydrazones, it appears that they are less reactive under ultrasound promoted Reformatsky reaction. As Table 2.5 details, we were able to successfully isolate 21% of the β -amino ester **2.116** under neat conditions. The potential problem we face is the nature of the substrate. We decided to screen aliphatic hydrazones for the above solvents. Also employing a chiral auxiliary would give us an idea about the stereocontrol that could be achieved under the developed reaction conditions. With this goal in mind, we used substrate **2.62a** that was used for our indium-mediated *umpolung*-

type allylation of chiral hydrazones for Reformatsky reaction condition screening. The reaction was performed using water, THF, dichloromethane, DMF (Table 2.7, entry 1 to 5). None of those solvents gave the desired product **2.117a**. With no added solvent and under ultrasound promoted condition, the chiral hydrazone **2.62a** produced β -amino ester **2.117a** in high yield and high diastereoselectivity (Table 2.7, entry 6).

Table 2.7. Solvent Study with Chiral Hydrazones



Entry ^a	Solvent	Time	Yield ^b	dr ^c
1	THF	6h	0	-
2	(THF:Water)	6h	0	-
3	Water	6h	0	-
4	DCM	6h	0	-
5	DMF	6h	0	-
6	Neat	4h	90	98:2

^a Reactions were performed in a scintillation vial under monitored by TLC. ^b Isolated yields. ^c *dr* by ¹H NMR

Thus from the above optimization experiments we understood that ultrasound promoted Reformatsky reaction can be performed with indium metal effectively under neat conditions for chiral hydrazones. Usually imine substrates are sensitive to the basicity of the nucleophiles. In the presence of strongly basic-nucleophile there is a potential problem of deprotonating the α -position to form the metalloenamine for aldimine substrates. Under indium-mediated Reformatsky reaction, we did not observe the deprotonation and thus organoindium reagents can be applied effectively with great functional group tolerance.

The Reformatsky reaction was conducted in a 25°C thermostated ultrasound bath to minimize the frictional heating produced by the molecules subjected to ultrasound. The vial was partially immersed into the bath so as the contents will experience the ultrasound irradiation. The reaction was performed with indium (1.0 eq.) and α -bromoacetate (2.0 eq.). Table 2.8 and Table 2.9 shows the results of indium-mediated ultrasound promoted Reformatsky reaction of chiral hydrazones. In table 2.8 the substrates with chiral oxazolidinones containing isopropyl and benzyl auxiliaries derived from (L)-valine and (L)-phenyl alanine respectively were screened. The isopropyl auxiliary effectively blocked a face for the attack of the nucleophile resulting in the formation of the product in high diastereoselectivity. α -Bromo acetates such as methyl, ethyl and phenyl bromo acetates were screened. Aliphatic substrates derived from linear aldehydes (Table 2.8, entry 1, 2 and 7) reacted effectively giving moderate to good yields. Branched aldehydes derived hydrazones also reacted effectively (Table 2.8, Entry 3, 4 and 5) producing the corresponding β -amino esters in moderate to good yields. The diastereoselectivity although observed to be controlled by the auxiliary, Substrate **2.62h** (Table 2.8, entry 10) gave average yield when subjected to the reaction condition. The observed diastereoselectivity was very low compared to the other entries in the table with isopropyl auxiliary. This could be attributed to the nature of the substrate. The conjugated nature of this cinnamaldehyde derived hydrazone; makes it relatively inert to the nucleophilic addition. The geometry of the substrate could play role in the observed diastereoselection, which is still under investigation.

Table 2.8. Substrate Scope in Indium-mediated Reformatsky Reaction

In(0) 1 eq.
 $\text{BrCH}_2\text{CO}_2\text{R}^3 \text{ 2 eq.}$
 $\xrightarrow[\text{Solvent, 2.5 M}]{\text{Ultrasound, rt}}$

2.62 **2.117:** R³ = Et
2.118: R³ = Me
2.119: R³ = Ph

Entry ^a	SM	R ¹	R ²	R ³	Time	Yield ^b	dr ^c
1	2.62a	PhCH ₂ CH ₂	i-Pr	Me	4.5	91 (2.118a)	99:1
2	2.62c	n-C ₃ H ₇	i-Pr	Et	5	70 (2.117c)	99:1
3	2.62d	i-Pr	i-pr	Et	5	75 (2.117d)	99:1
4	2.62d	i-Pr	i-Pr	Ph	5	78 (2.119d)	99:1
5	2.62e	i-C ₄ H ₉	i-Pr	Et	4	79 (2.117e)	99:1
6	2.62f	EtOCO	i-Pr	Et	6	73 (2.117f)	99:1
7	2.62b	Et	i-Pr	Et	2.5	92 (2.117b)	99:1
8	2.62a	PhCH ₂ CH ₂	i-pr	Et	4	90 (2.117a)	98:2
9	2.62a	PhCH ₂ CH ₂	i-Pr	Ph	5	78 (2.119a)	99:1
10	2.62h	PhCH=CH	i-Pr	Et	4.5	55 (2.117h)	71:29
11	2.62k	i-C ₄ H ₉	PhCH ₂	Et	5	83 (2.117k)	96:4

^a Reactions performed at 0.5 mmol scale ^b isolated yield ^cdr calculated by ¹H-NMR

The facial selection provided by the benzyl auxiliary was less than the isopropyl auxiliary (Table 2.8, entry 11).

Table 2.9 describes the substrates screening with the oxazolidinone containing isopropyl, benzyl and phenyl prepared from (D)-valine, (D)-phenyl alanine and (D)-phenyl glycine respectively. Cyclic derivatives such as cyclohexyl and cyclopentyl derivatives (Table 2.9, substrates **2.62g** and **2.62h**) reacted effectively under the reaction condition with different nucleophilic precursors yielding the β-amino esters in good yields and diastereoselectivity (Table 2.9, Entry 1 to 4). The use of benzyl auxiliary slightly decreased the diastereoselectivity as discussed before (Table 2.9, Entry 9, 10). The phenyl auxiliary

gave the lowest diastereoselectivity (Table 2.9, Entry 11). The planar phenyl ring is ineffective in blocking a face for the addition of the nucleophile resulting in a poor diastereomeric purity of the product

Table 2.9. Substrate Scope Continued

$$\text{2.62} \xrightarrow[\text{Solvent, 2.5 M}]{\text{In(0) 1 eq.}, \text{BrCH}_2\text{CO}_2\text{R}^3 \text{ 2 eq.}, \text{Ultrasound, rt}}$$

2.117: R³ = Et
2.118: R³ = Me
2.119: R³ = Ph

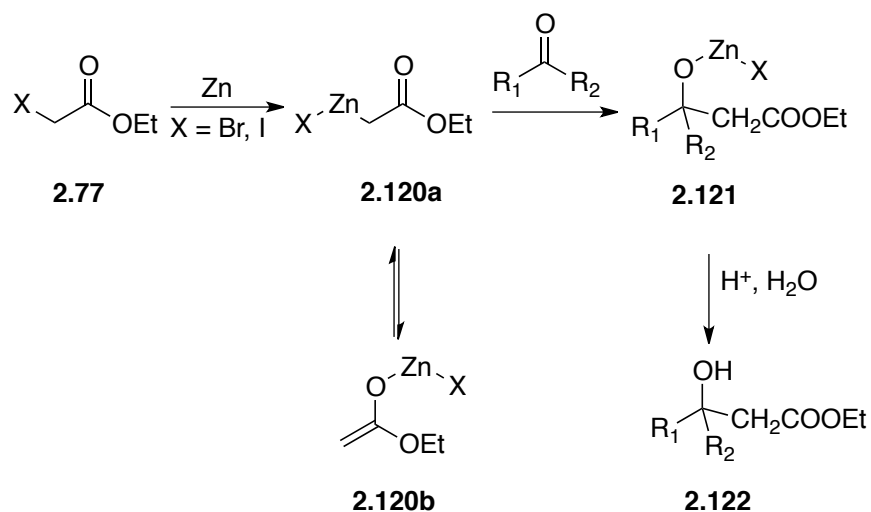
Entry ^a	SM	R ¹	R ²	R ³	Time	%Yield ^b	dr ^c
1	2.62g	C-C ₅ H ₉	i-Pr	Et	3	84 (2.117g)	99:1
2	2.62h	C-C ₆ H ₁₁	i-Pr	Et	2.5	91 (2.117h)	99:1
3	2.62h	C-C ₆ H ₁₁	i-Pr	Me	3	80 (2.118h)	99:1
4	2.62h	C-C ₆ H ₁₁	i-Pr	Bn	7	72 (2.119h)	99:1
5	2.62i	PHCH ₂	i-pr	Et	2.5	91 (2.117i)	99:1
6	2.62j	Et	i-Pr	Et	4.5	73 (2.117j)	99:1
7	2.62k	i-C ₄ H ₉	i-Pr	Et	5	66 (2.117k)	99:1
8	2.62l	PhCH ₂ CH ₂ PhCH ₂		Et	5	83 (2.117l)	99:1
9	2.62n	i-C ₄ H ₉	PhCH ₂	Et	4.5	78 (2.117n)	98:2
10	2.62n	i-C ₄ H ₉	PhCH ₂	Me	4	78 (2.118n)	98:2
11	2.62m	i-C ₄ H ₉	Ph	Me	5.5	76 (2.118m)	54:46

^a reactions performed at 0.5 mmol scale. ^b isolated yields. ^c dr calculated by ¹H NMR

Thus summarizing the substrate scope examination we infer that this methodology enabled an expanded range of aldimine hydrazones to participate in the indium mediated Reformatsky reaction. The isopropyl-derived auxiliary was successful in enforcing high levels of enantiofacial discrimination to deliver a broad range of β-amino esters.

After expanding the substrate scope we decided to understand the mechanism of the reaction. In classical Reformatsky reaction zinc metal inserts between the carbon halogen

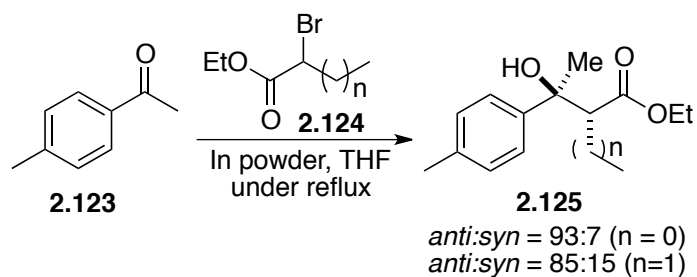
bond of the α -haloacetate and reacts with the aldehyde or ketone to produce β -hydroxyalkanoates as shown in Scheme 2.38.



Scheme 2.38. Pathway for Zinc-Mediated Reformatsky Reaction

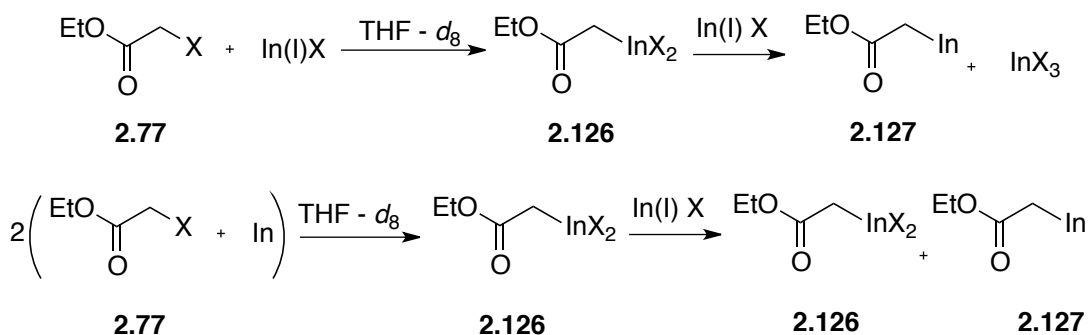
The mechanism of Reformatsky type reaction changes with the change in the metal. Samarium mediated Reformatsky involves the intermediacy of a different kind of species than the zinc-mediated reaction. Similarly, indium-mediated Reformatsky reactions have been proposed to go through a radical pathway rather than an ionic pathway. To date, the clearest example showing the mechanism of the Reformatsky reaction has been reported by Akoi Baba and co-workers.⁵⁶

Investigation of In(0)- and In(I)-mediated addition of the branched α -halo esters to ketones revealed that the degree of stereoselection depended on the steric demand between the two substituents that are present in the ketone and the steric conformation of a six membered cyclic transition state from the indium enolate. The formation of *anti*-isomer in major amount suggested the involvement of an *E* enolate (Scheme 2.39).



Scheme 2.39. Indium-Mediated *anti*-Selective Reformatsky Reaction

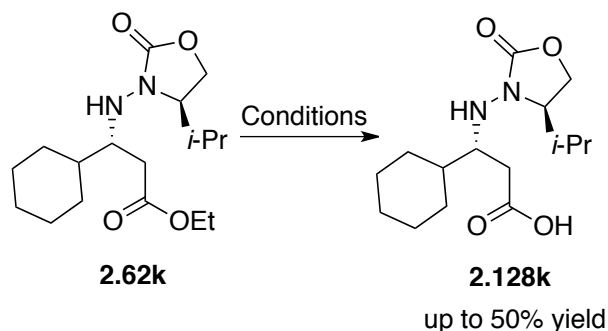
The report also suggested that some kind of transient species was formed irrespective of the source In(0) or In(I). $^1\text{H-NMR}$ spectra in THF- d_8 revealed that the active species was RIn(III)X_2 not RIn(I) and the interconversion has been studied and reported (Scheme 2.40).



Scheme 2.40. Proposed Pathway for Indium-Mediated Reformatsky Reaction

We did not make any attempt to decipher the active species. But, this brief note would set up the stage for the next chapter, where we discuss our attempts to study indium- and bismuth- reagents in allylation reaction. The underlying mechanism for metal-mediated, ultrasound-promoted reaction is presumably the activation of the metal surface

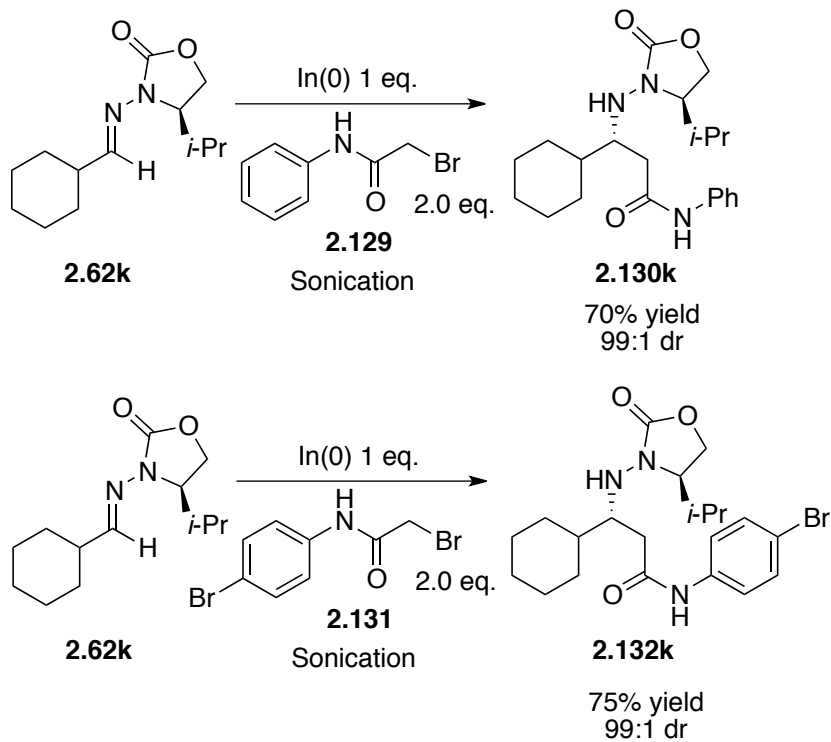
Absolute stereochemistry was determined unambiguously by X-ray crystallographic analysis. Attempts to cleave the N-N bond of the hydrazone were not successful (Scheme 2.41). The chemical integrity of the ester group over the course of N-N bond cleavage was questionable.



Conditions: SmI_2 (or) $\text{Li}(0)$, Liq NH_3 (or) Base hydrolysis

Scheme 2.41. Attempts to Cleave the Chiral Auxiliary

Our attempts to cleave the chiral auxiliary resulted in hydrolysis. Hence we decided to obtain the crystal structure of the major isomer in order to confirm the absolute stereochemistry. Reformatsky products from ethyl bromoacetate and our substrates remained were oily liquids hence we utilized the α -bromoacetates **2.129** and **2.131** shown in Scheme 4.20..



Scheme 2.42. Indium-mediated Reformatsky Reaction with Substrate **2.62k**

To our great interest the reaction proceeded smoothly to obtain **2.130h** and **2.132h** in appreciable yield and excellent diastereoselectivity. Products from both reactions were separated and crystallized using ethyl acetate/hexane mixture. Compound **4.65k** and **4.65l** were analyzed by X-Ray crystallography (Figure 4.1 and 4.2).

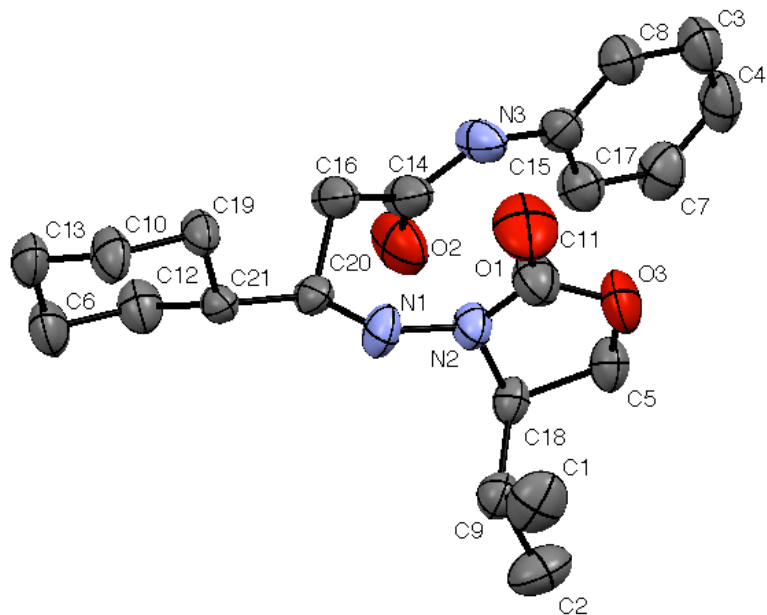


Figure 2.1. Thermal Ellipsoid Plot of **2.130h** at 50% Probability

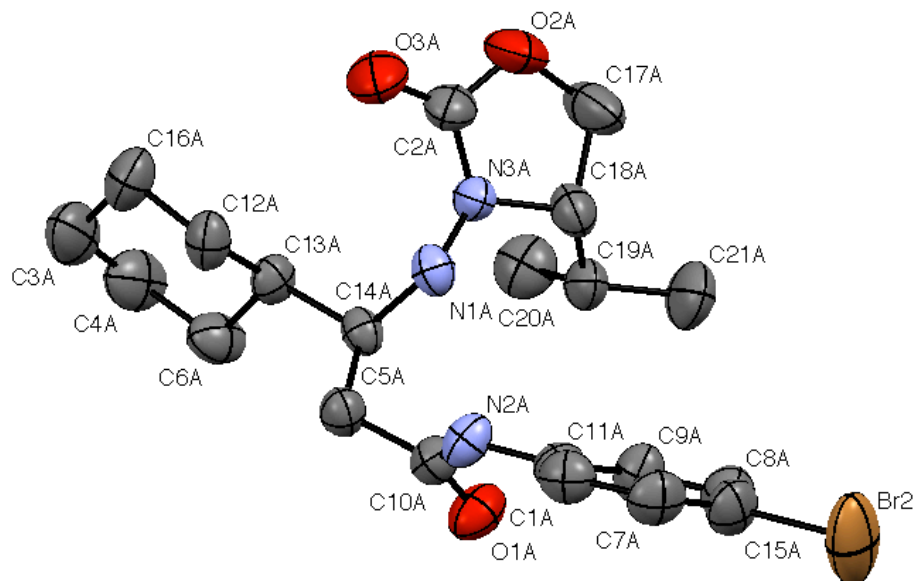


Figure 2.2. Thermal Ellipsoid Plot of **2.132h** at 50% Probability

2.3.5. Summary of Indium-Mediated Reformatsky Reaction

The greatest joy of an organic chemist relies in creating molecules; molecules that have never existed, but may exist on a distant cosmological entity. The myriad proteins found in humans, plants and animals all are made of simple structure called amino acids. Human life on earth is based on proteins and other complex structures built on α -amino acids. Studying these structures were always fruitful, but β -amino acids do exist in nature, as well, In fact they are found on earth as well as, in some samples of meteorites analyzed. In this regard β -amino acids are very interesting scaffolds. We have devised a highly stereoselective protocol using indium metal to prepare β -amino acids.

This methodology describes capacity to access several non-proteogenic amino acids with stereoselection; further this method underscores the utility of ultrasound in stereoselective organic synthesis. We quickly realized that this procedure is also applicable

to ketimine -derived hydrazones. This would enable our access to interesting quaternary centers.

2.4. Supporting Information

2.4.1. Experimental Section

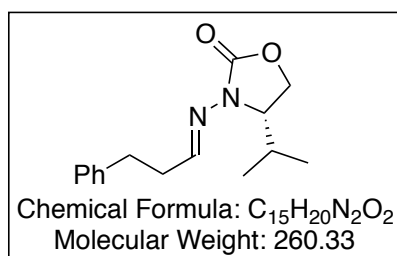
Thin Layer Chromatography (TLC) was performed on a silica gel Whatman-60F glass plates, and components were visualized by illumination of UV light at 254 nm or by staining with iodine vapors or ammonium molybdate solution or vanillin solution or potassium permanganate solution, Melting points were measured with a Fisher-Johns melting point apparatus and are uncorrected. ¹H-NMR was recorded on a Varian Innova-500NB (500MHz), Varian Innova-400NB (400MHz), or Varian Mercury-300 (300MHz). Chemical shifts are reported in parts per million (ppm) downfield from TMS, using residual CDCl₃ (7.24ppm) as an internal standard. Data are reported as follows: Chemical shift, multiplicity (s = singlet, d = doublet, t = triplet, q = quartet, m = multiplet), coupling constant and integration. ¹³C-NMR was recorded on varian Innova-500 NB (125 MHz), Varian Innova-400 NB (100MHz), and Varian Mercury-300 (75MHz) spectrometers, using broadband proton decoupling. Chemical shifts are reported in parts per million (ppm) downfield from TMS, using the middle resonance of CDCl₃ (77.9 ppm) as an internal standard. Rotations were recorded on a JASCO-DIP-370 instrument. High Resolution Mass Spectra (HRMS) (ESI⁺) were obtained on a BioTof –mass spectrometer

2.4.2. General Procedure for Preparation of Chiral Hydrazones

Hydrazones were prepared by a modified literature procedure. To a solution of the appropriate 2-oxazolidinone in THF (0.05M) was added *n*-BuLi (2.2 M in hexanes, 1.1 eq.) at -78°C. After 50 mins, *O*-(2,4-diphenylphosphinyl) hydroxylamine (1.2 eq.) was added,

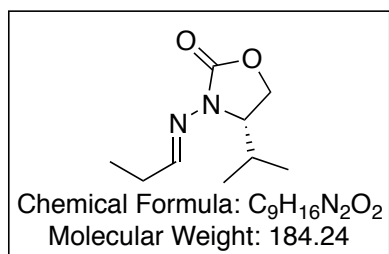
the reaction was allowed to warm to room temperature and further stirred for 14 hours. The mixture was filtered and concentrated to afford the corresponding *N*-amino-2-oxazolidinone. Without purification, the amino-oxazolidinone was dissolved in toluene (0.5 M) and aldehyde (2 eq.), magnesium sulfate (4 eq.) and *p*-toluene sulfonic acid (0.01 eq.) were added. The mixture was stirred under reflux until the completion as indicated by TLC. The crude reaction mixture is then concentrated and purified by flash column chromatography.

(S)-3-(3-Phenylpropylideneamino)-4-isopropylloxazolidin-2-one. (2.62a)



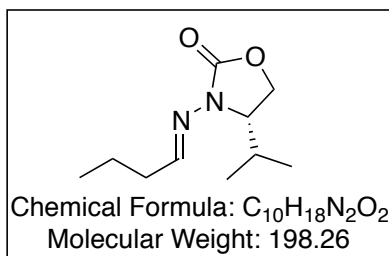
Pale yellow solid (60% yield); m.p = 38 - 40 °C; $[\alpha]_D^{23} = 46.9$ (c = 1.0 in CHCl₃); IR (film): 3427, 2955, 1756, 1640 cm⁻¹; ¹H NMR (CDCl₃, 500 MHz): $\delta = 8.06$ (t, *J* = 5.5 Hz, 1H), 7.32-7.28 (m, 2H), 7.23-7.20 (m, 3H), 4.31 (t, *J* = 8.5 Hz, 1H), 4.14-4.11 (m, 1H), 4.07-4.04 (m, 1H), 2.91 (t, *J* = 7.5 Hz, 2H), 2.75-2.66 (m, 2H), 2.18-2.12 (m, 1H), 0.91 (d, *J* = 7.5 Hz, 3H), 0.84 (d, *J* = 7.5 Hz, 3H); ¹³C NMR (CDCl₃, 125 MHz): $\delta = 155.4, 155.0, 140.8, 128.6, 126.4, 62.8, 61.0, 35.0, 32.8, 27.9, 17.9, 15.0$. HRMS Calcd for C₁₅H₂₀N₂O₂ (M+Na)⁺: 283.1417; Found: 283.1416.

(S)-4-Isopropyl-3-(propylideneamino)oxazolidin-2-one(2.62b):



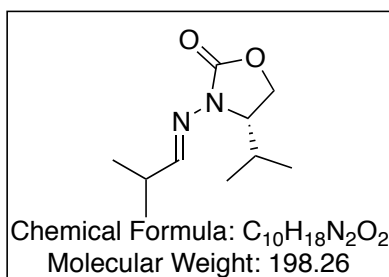
Colorless liquid (55% yield); $[\alpha]_D^{23} = -45.5$ (c = 1.0 in CHCl₃); ¹H NMR (400 MHz): $\delta = 7.93$ (t, *J* = 5.2 Hz, 1H), 4.24 (dd, *J* = 10.0, 9.0 Hz, 1H), 4.06 (dd, *J* = 9.0, 8.5 Hz, 1H), 4.00 (m, 1H), 2.29 (m, 2H), 2.16 (m, 1H), 1.05 (t, *J* = 7.5, 3H), 0.86 (d, *J* = 7.0 Hz, 3H), 0.82 (d, *J* = 7.0 Hz, 3H); ¹³C NMR (100 MHz): $\delta = 157.5, 155.1, 62.9, 61.1, 28.1, 26.8, 17.9, 15.1, 10.8$.

(S)-3-(Butylideneamino)-4-isopropylloxazolidin-2-one (2.62c)



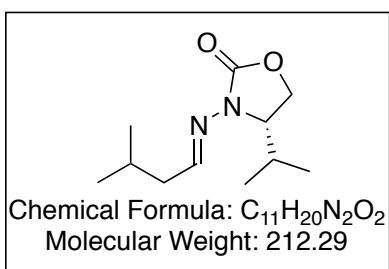
Colorless liquid (54% yield); $[\alpha]_D^{23} = -2.2$ (c = 0.8 in CH₃OH); ¹H NMR (400 MHz): $\delta = 7.90$ (t, $J = 5.6$ Hz, 1H), 4.25 (m, 1H), 4.07 (dd, $J = 4.4, 4$ Hz, 2H), 2.60 (q, $J = 7.2$ Hz, 2H), 2.16 (m, 1H), 1.52 (m, 2H), 0.90 (d, $J = 7.0$ Hz, 3H), 0.87 (d, $J = 7.0$ Hz, 3H), 0.81 (d, $J = 7.0$ Hz, 3H); ¹³C NMR (125.5 MHz): $\delta = 157.1, 155.1, 62.9, 61.4, 28.3, 26.9, 17.9, 15.2, 10.8$.

(S)-4-Isopropyl-3-(2-methylpropylideneamino)oxazolidin-2-one(2.62d)



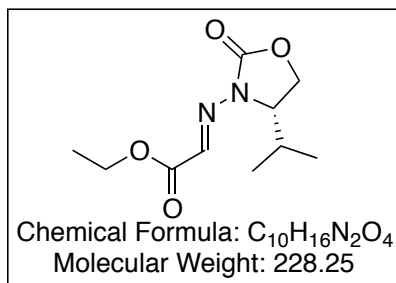
Colorless liquid (73% yield); $[\alpha]_D^{23} = -44.9$ (c = 1.0 in CHCl₃); ¹H NMR (400 MHz): $\delta = 7.96$ (d, $J = 5.5$ Hz, 1H), 4.28 (t, $J = 8.5$ Hz, 1H), 4.10 (dd, $J = 9.0, 9.0$ Hz, 1H), 4.05 (m, 1H), 2.59 (m, 1H), 2.19 (m, 1H), 1.12 (d, $J = 3.0$ Hz, 3H), 0.95 (d, $J = 3.5$ Hz, 3H), 0.92 (d, $J = 7.0$ Hz, 3H), 0.88 (d, $J = 7.0$ Hz, 3H); ¹³C NMR (100 MHz): $\delta = 161.8, 155.0, 63.0, 61.5, 32.6, 28.5, 20.0, 18.0, 15.3$.

(S)-3-(3-Methylbutylideneamino)-4-isopropylloxazolidin-2-one. (2.62e)



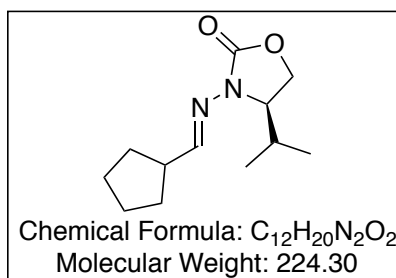
Colorless oil (58% yield); $[\alpha]_D^{23} = -59.8$ (c = 1.02 in CHCl₃); IR (film): 3420, 2959, 1751, 1652 cm⁻¹; ¹H NMR (CDCl₃, 400 MHz): $\delta = 7.98$ (t, $J = 6.0$ Hz, 1H), 4.27 (t, $J = 8.4$ Hz, 1H), 4.09-4.03 (m, 2H), 2.25-2.13 (m, 3H), 1.93-1.82 (m, 1H), 0.94-0.89 (m, 9H), 0.84 (d, $J = 6.8$ Hz, 3H); ¹³C NMR (CDCl₃, 100 MHz): $\delta = 157.2, 155.2, 62.9, 61.4, 42.3, 28.3, 26.9, 22.6, 22.5, 17.9, 15.1$. HRMS Calcd for C₁₁H₂₀N₂O₂ (M+Na)⁺: 235.1417; Found: 235.1423.

(S)-Ethyl 2-(4-isopropyl-2-oxooxazolidin-3-ylimino)acetate (2.62f)



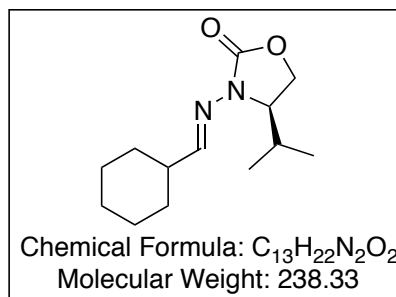
Colorless oil (64% yield); $[\alpha]_D^{23} = -0.7$ (c = 0.9 in CH₃OH); IR (film): 3420, 2959, 1751, 1652 cm⁻¹; ¹H NMR (CDCl₃, 400 MHz): $\delta = 7.98$ (t, $J = 6.0$ Hz, 1H), 4.27 (t, $J = 8.4$ Hz, 1H), 4.09-4.03 (m, 2H), 2.25-2.13 (m, 3H), 1.93-1.82 (m, 1H), 0.94-0.89 (m, 9H), 0.84 (d, $J = 6.8$ Hz, 3H); ¹³C NMR (CDCl₃, 100 MHz): $\delta = 157.2, 155.2, 62.9, 61.4, 42.3, 28.3, 26.9, 22.6, 22.5, 17.9, 15.1$. HRMS Calcd for C₁₁H₂₀N₂O₂ (M+Na)⁺: 235.1417; Found: 235.1423.

(R)-3-(Cyclopentylmethyleneamino)-4-isopropylloxazolidin-2-one (2.62g)



Pale yellow viscous liquid (62% yield); $[\alpha]_D^{23} = +53.8$ (c = 1.0 in CHCl₃); IR (film): 3422, 2958, 1751, 1636 cm⁻¹; ¹H NMR (CDCl₃, 400 MHz): $\delta = 7.91$ (d, $J = 6.4$ Hz, 1H), 4.26 (t, $J = 8.8$ Hz, 1H), 4.10-4.01 (m, 2H), 2.76-2.67 (m, 1H), 2.24-2.12 (m, 1H), 1.88-1.80 (m, 2H), 1.68-1.51 (m, 6H), 0.90 (d, $J = 7.2$ Hz, 3H), 0.85 (d, $J = 7.2$ Hz, 3H); ¹³C NMR (CDCl₃, 100 MHz): $\delta = 160.3, 155.1, 62.9, 61.3, 43.5, 30.9, 30.6, 28.2, 25.7, 17.9, 15.2$. HRMS Calcd for C₁₂H₂₀N₂O₂ (M+Na)⁺: 247.1417; Found: 247.1405.

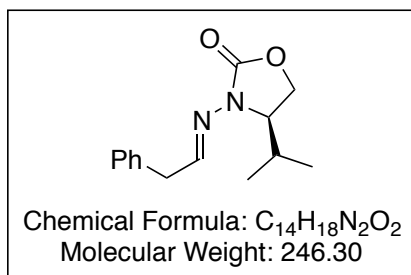
(R)-3-(Cyclohexylmethyleneamino)-4-isopropylloxazolidin-2-one (2.62h):



Colorless solid (76% yield); m.p. 46-48°C; $[\alpha]_D^{23} = +51.3$ (c = 1.0 in CHCl₃); ¹H NMR (400 MHz): $\delta = 7.80$ (d, $J = 5.6$ Hz, 1H), 4.26 (t, $J = 8.5$ Hz, 1H), 4.08 (dd, $J = 9.0, 6.0$ Hz, 1H), 4.01 (m, 1H), 2.30-2.20 (m, 1H), 2.18 (m, 1H), 1.81-1.71 (m, 5H), 1.66-1.59 (m, 5H), 1.30-1.16 (m,

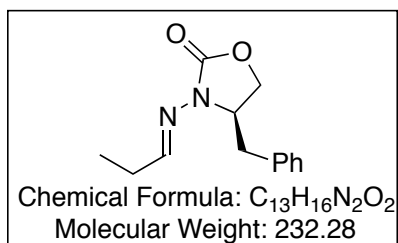
6H), 0.90 (d, $J = 7.0$ Hz, 3H), 0.85 (d, $J = 7.0$ Hz, 3H); ^{13}C NMR (125.5 MHz): $\delta = 160.7$, 155.0, 62.9, 61.4, 41.8, 30.3, 30.1, 28.3, 26.1, 25.6, 25.5, 17.9, 15.3.

(R)-3-(2-Phenylethylideneamino)-4-isopropylloxazolidin-2-one. (2.62i)



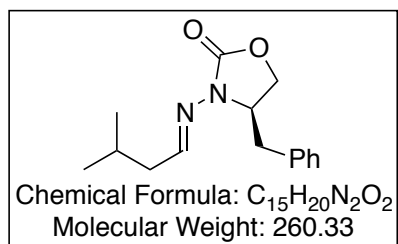
Pale yellow viscous liquid (65% yield); $[\alpha]_{\text{D}}^{23} = -105.1$ ($c = 1.0$ in CHCl_3); IR (film): 3434, 2955, 1757 cm^{-1} ; ^1H NMR (CDCl_3 , 400 MHz): $\delta = 7.98$ (t, $J = 6.0$ Hz, 1H), 4.27 (t, $J = 8.4$ Hz, 1H), 4.09-4.03 (m, 2H), 2.25-2.13 (m, 3H), 1.93-1.82 (m, 1H), 0.94-0.89 (m, 9H), 0.84 (d, $J = 6.8$ Hz, 3H); ^{13}C NMR (CDCl_3 , 100 MHz): $\delta = 154.8$, 153.9, 136.4, 129.1, 129.0, 127.1, 62.9, 61.0, 40.1, 28.1, 17.9, 15.1. HRMS Calcd for $\text{C}_{14}\text{H}_{18}\text{N}_2\text{O}_2$ ($\text{M}+\text{Na}$) $^+$: 269.1260; Found: 269.1258.

(R,E)-4-Benzyl-3-(propylideneamino)oxazolidin-2-one (2.62j)



Colorless oil (69% yield); $[\alpha]_{\text{D}}^{23} = -7.6$ ($c = 1.0$ in CHCl_3); ^1H NMR (400 MHz): $\delta = 8.04$ (d, $J = 6.0$ Hz, 1H), 7.30 (dd, $J = 5.6, 1.2$ Hz, 2H), 7.26 (dd, $J = 9.2, 1.0$ Hz, 1H), 7.14 (s, 1H), 4.32 (dd, $J = 8.5, 8.5$ Hz, 1H), 4.21 (t, $J = 9.0$ Hz, 1H), 4.06 (m, 1H), 3.20 (dd, $J = 10.4, 3.6$ Hz, 1H), 2.75-2.80 (m, 1H), 2.38 (m, 2H), 1.13 (q, $J = 4.0$ Hz, 3H); ^{13}C NMR (125.5 MHz): $\delta = 157.9$, 154.7, 135.6, 129.5, 129.1, 128.6, 127.4, 65.9, 58.1, 37.5, 26.9, 10.9.

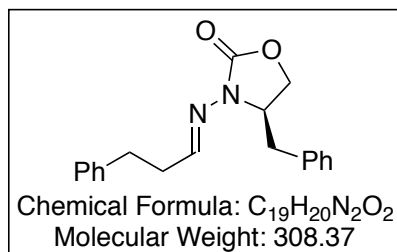
(R,E)-4-Benzyl-3-(3-methylbutylideneamino)oxazolidin-2-one (2.62k)



Colorless oil (62% yield); $[\alpha]_{\text{D}}^{23} = +160.0$ ($c = 1.0$, CHCl_3); ^1H NMR (400 MHz, CDCl_3) $\delta = 8.05$ (t, $J = 5.5$ Hz, 1H), 7.30 (dd, $J = 7.6, 7.6$ Hz, 2H), 7.24 (dd, $J = 7.3, 7.3$ Hz, 1H), 7.15 (d, $J = 7.0$ Hz, 2H), 4.38-4.32 (m, 1H), 4.23 (t, J

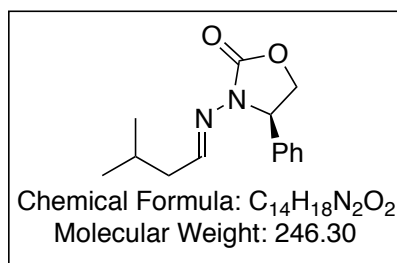
= 8.4 Hz, 1H), 4.06 (dd, $J = 8.4, 5.8$ Hz, 1H), 3.20 (dd, $J = 13.8, 3.6$ Hz, 1H), 2.79 (dd, $J = 13.8, 8.8$ Hz, 1H), 2.26 (t, $J = 6.4$ Hz, 2H), 1.97-1.90 (m, 1H), 1.00 (s, 3H), 0.99 (s, 3H); ^{13}C NMR (125 MHz, CDCl_3) $\delta = 157.2, 154.8, 135.5, 129.5, 129.1, 127.4, 65.8, 58.2, 42.4, 37.5, 26.9, 22.7, 22.6$

(R)-3-(3-Phenylpropylideneamino)-4-benzylloxazolidin-2-one. (2.62l)



Pale yellow viscous liquid (51% yield); $[\alpha]_{\text{D}}^{23} = -2.1$ ($c = 1.08$ in CHCl_3); IR (film): 3446, 2924, 1762, 1652 cm^{-1} ; ^1H NMR (CDCl_3 , 400 MHz): $\delta = 8.05-8.01$ (m, 1H), 7.32-7.17 (m, 8H), 7.09-7.07 (m, 2H), 4.32-4.26 (m, 1H), 4.20 (t, $J = 8.0$ Hz, 1H), 4.06 (dd, $J = 8.8, 5.2$ Hz, 1H), 3.11 (dd, $J = 14.0, 3.6$ Hz, 1H), 2.93-2.89 (m, 2H), 2.76-2.69 (m, 3H); ^{13}C NMR (CDCl_3 , 100 MHz): $\delta = 155.6, 154.6, 140.8, 135.5, 129.5, 129.1, 128.8, 128.7, 127.4, 126.5, 65.9, 57.9, 37.3, 35.0, 32.8$. HRMS Calcd for $\text{C}_{19}\text{H}_{20}\text{N}_2\text{O}_2$ ($\text{M}+\text{Na}$) $^+$: 331.1417; Found: 331.1440.

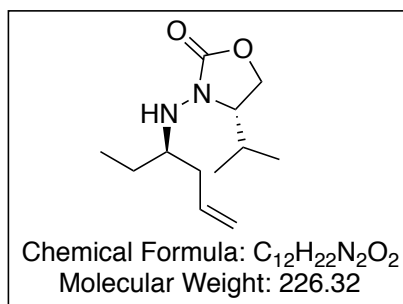
(S)-3-(3-Methylbutylideneamino)-4-phenylloxazolidin-2-one. (2.62n)



White solid (42% yield); m.p = 124 - 126 $^{\circ}\text{C}$; $[\alpha]_{\text{D}}^{23} = -94.4$ ($c = 1.0$ in CHCl_3); IR (film): 3434, 2955, 1757 cm^{-1} ; ^1H NMR (CDCl_3 , 500 MHz): $\delta = 7.43-7.35$ (m, 3H), 7.29-7.26 (m, 2H), 7.09 (t, $J = 6.0$ Hz, 1H), 5.19 (dd, $J = 9.0, 6.0$ Hz, 1H), 4.76 (t, $J = 8.5$ Hz, 1H), 4.16 (dd, $J = 9.0, 6.0$ Hz, 1H), 2.19-2.07 (m, 2H), 1.70-1.61 (m, 1H), 0.75-0.72 (m, 6H); ^{13}C NMR (CDCl_3 , 125 MHz): $\delta = 155.2, 152.0, 137.0, 129.8, 129.2, 126.2, 69.8, 59.1, 41.6, 27.2, 22.2$. HRMS Calcd for $\text{C}_{14}\text{H}_{18}\text{N}_2\text{O}_2$ ($\text{M}+\text{Na}$) $^+$: 269.1260; Found: 269.1254.

2.4.3 General Procedure for Allylation of Chiral Hydrazones: A mixture of hydrazone (1 eq.), indium(I) iodide (1.2 eq.), allyl acetate (2.0 eq.) and palladium tetrakis triphenylphosphine (5 mol%) in THF:Water (1:1) were stirred at room temperature. After the indicated period the reaction mixture was washed with water and extracted with ethyl acetate. The crude reaction mixture was subjected to flash column chromatography (30% ethyl acetate: 70% Hexane) to afford the allylated product.

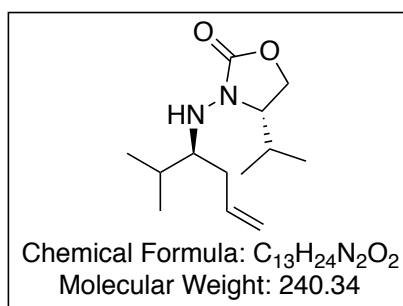
(S)-3-((R)-Hex-5-en-3-ylamino)-4-isopropylloxazolidin-2-one (2.63b)³



Colorless oil; $[\alpha]_D^{23} = -2.0$ (c = 2.11 in CHCl₃); ¹H NMR (400 MHz): δ 5.90-5.80 (m, 1H), 5.14 (dd, *J* = 17.0 Hz, 1.0 Hz, 1H), 5.09 (d, *J* = 10.0 Hz, 1H) 4.20 (t, *J* = 9.0 Hz, 1H), 4.03 (dd, *J* = 9.0 Hz, 4.0 Hz, 1H), 3.91 (d, *J* = 3.2 Hz, 1H), 3.65-3.61 (m, 1H), 3.02-2.97 (m, 1H),

2.30-2.16 (m, 2H), 1.96-1.81 (m, 2H), 0.89-0.85 (m, 9H), 0.80 (d, *J* = 7.2 Hz, 1H); ¹³C NMR (100 MHz): δ = 158.4, 135.0, 117.9, 62.6, 62.6, 62.2, 32.3, 28.7, 27.7, 18.9, 17.9, 16.3, 15.2.

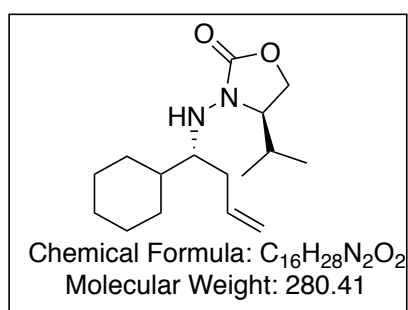
(S)-4-Isopropyl-3-((S)-2-methylhex-5-en-3-ylamino)oxazolidin-2-one (2.63d)³



Colorless oil; $[\alpha]_D^{23} = -6.9$ (c = 0.99 in CHCl₃); ¹H NMR (500 MHz): δ = 5.92-5.83 (m, 1H) 5.17 (d, *J* = 17.0 Hz, 1H), 5.12 (d, *J* = 10.5 Hz, 1H), 4.22 (t, *J* = 9.0 Hz, 1H), 4.06 (dd, *J* = 9.5 Hz, 3.5 Hz, 1H), 3.93 (d, *J* = 2.5 Hz, 1H), 3.66 (dt, *J* = 8.5, 3.5 Hz, 1H), 3.04-3.00 (m, 1H),

2.32-2.24 (m, 1H), 2.24-2.19 (m, 1H), 1.97-1.92 (m, 1H), 1.88-1.84 (m, 1H), 0.95-0.82 (m, 12H); ^{13}C NMR (125.5 MHz): $\delta = 158.4, 136.0, 117.9, 62.7, 62.6, 62.1, 32.2, 28.7, 27.7, 18.9, 17.8, 16.3, 15.1$.

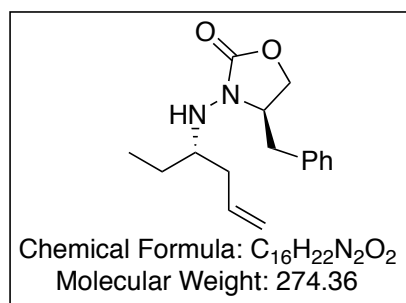
(R)-3-((R)-1-Cyclohexylbut-3-enylamino)-4-isopropylloxazolidin-2-one (2.63h)³



Colorless oil; $[\alpha]_{\text{D}}^{23} = -10.6$ (c = 1 in CHCl_3); ^1H NMR (400 MHz): $\delta = 6.03$ -5.93 (m, 1H) 5.21 (d, $J = 17.0$ Hz, 1H), 5.12 (d, $J = 10.5$ Hz, 1H), 4.10 (d, $J = 3.6$ Hz, 1H), 3.53 (dd, $J = 9.5$ Hz, 3.5 Hz, 1H), 3.49 (d, $J = 2.5$ Hz, 1H), 3.20 (dt, $J = 8.5, 3.5$ Hz, 1H), 3.08 (q, $J = 4.8$ Hz,

1H), 2.23-2.19 (m, 1H), 2.19-1.98 (m, 1H), 1.87-1.70 (m, 5H), 1.88-1.84 (m, 1H), 0.95-0.82 (m, 12H); ^{13}C NMR (100 MHz): $\delta = 158.4, 136.1, 117.7, 62.7, 62.6, 62.5, 62.1, 39.7, 33.4, 29.6, 27.7, 27.4, 27.0, 26.9, 17.9, 15.2$.

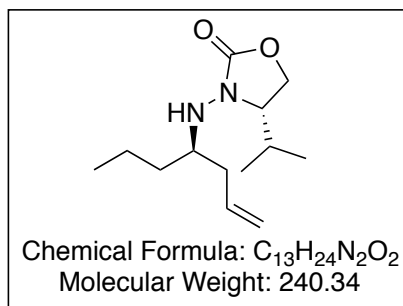
(R)-4-Benzyl-3-((S)-hex-5-en-3-ylamino)oxazolidin-2-one (2.63j)³



^1H NMR (500 MHz, CDCl_3) $\delta = 7.32$ -7.13 (m, 5H), 5.88 (dd, $J = 10.2, 10.2, 7.8, 6.2$ Hz, 1H), 5.18 (dd, $J = 17.1, 3.4, 1.6$ Hz), 5.13 (dd, $J = 6.5, 1.2$ Hz, 1H), 4.13 (dd, $J = 8.9, 4.5$ Hz, 1H), 4.00-3.98 (m, 1H), 3.95-3.86 (m, 2H), 3.30 (dd, $J = 13.1, 3.4, 3.4$ Hz, 1H), 2.30-2.21

(m, 3H), 1.51-1.48 (m, 2H), 0.98-0.90 (m, 3H); ^{13}C NMR (125 MHz, CDCl_3) $\delta = 158.4, 136.1, 135.0, 129.1, 128.9, 127.1, 117.6, 65.9, 65.7, 59.7, 59.3, 37.2, 36.3, 24.9, 9.3$.

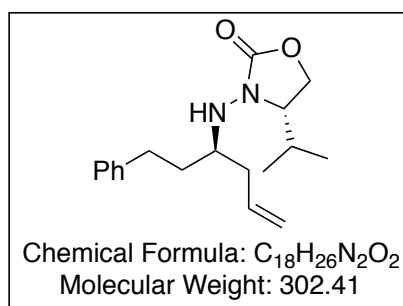
(S)-3-((R)-Hept-1-en-4-ylamino)-4-isopropylloxazolidin-2-one(2.63c)



Colorless oil; $[\alpha]_D^{23} = 3.87$ ($c = 1.06$ in MeOH); IR (film): 3287, 2926, 1756 cm^{-1} ; 1H NMR ($CDCl_3$, 400 MHz): $\delta = 5.86-5.76$ (m, 1H), 5.13-5.04 (m, 2H), 4.21 (dd, $J = 9.2, 8.4$ Hz, 1H), 4.03 (dd, $J = 9.2, 4.0$ Hz, 1H), 3.87 (d, $J = 4.0$ Hz, 1H), 3.66-3.62 (m, 1H), 3.11-3.05

(m, 1H), 2.26-2.17 (m, 2H), 2.11-2.04 (m, 1H), 1.42-1.27 (m, 4H), 0.90-0.85 (m, 6H), 0.80 (d, $J = 6.8$ Hz, 3H); ^{13}C NMR ($CDCl_3$, 100 MHz): $\delta = 158.7, 135.2, 117.7, 62.7, 62.3, 57.8, 37.1, 34.9, 27.6, 18.6, 17.9, 15.2, 14.6$. HRMS Calcd for $C_{13}H_{24}N_2O_2$ ($M+Na$) $^+$: 263.1730; Found: 263.1749.

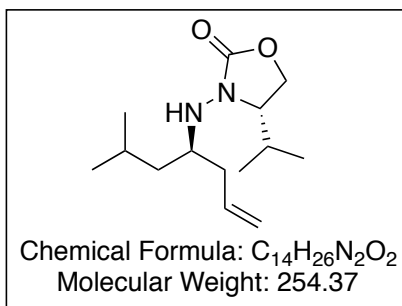
(S)-4-Isopropyl-3-((R)-1-phenylhex-5-en-3-ylamino)oxazolidin-2-one.(2.63a)



From **1a** by General Procedure was obtained **1b** (81% yield) as a Colorless oil; $[\alpha]_D^{23} = 13.8$ ($c = 1.0$ in $CHCl_3$); IR (film): 3434, 2955, 1757 cm^{-1} ; 1H NMR ($CDCl_3$, 400 MHz): $\delta = 7.17-7.13$ (m, 2H), 7.07-7.03 (m, 3H), 5.78-5.68 (m, 1H), 5.06-4.98 (m, 2H), 4.09 (t, $J = 8.8$ Hz, 1H),

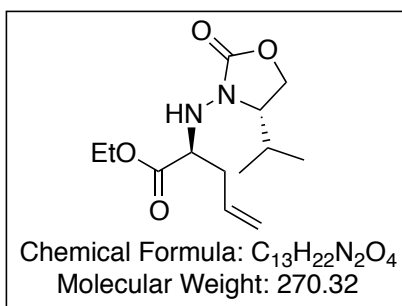
3.93 (dd, $J = 9.2, 3.6$ Hz, 1H), 3.85 (d, $J = 4.0$ Hz, 1H), 3.56-3.52 (m, 1H), 3.06-2.98 (m, 1H), 2.62-2.49 (m, 2H), 2.21-2.05 (m, 3H), 1.69-1.56 (m, 2H), 0.76 (d, $J = 7.2$ Hz, 3H), 0.69 (d, $J = 7.2$ Hz, 3H); ^{13}C NMR ($CDCl_3$, 100 MHz): $\delta = 158.7, 142.2, 134.8, 128.6, 128.4, 126.0, 117.9, 62.6, 62.0, 57.6, 36.9, 34.1, 31.4, 27.4, 17.8, 15.0$. HRMS Calcd for $C_{18}H_{26}N_2O_2$ ($M+Na$) $^+$: 325.1886; Found: 325.1885.

(S)-4-Isopropyl-3-((R)-6-methylhept-1-en-4-ylamino)oxazolidin-2-one(2.63e)



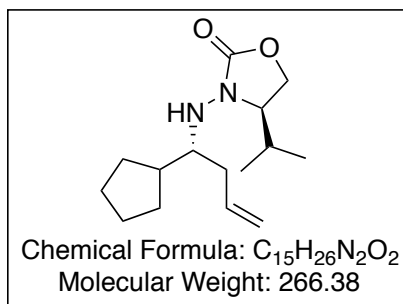
Colorless oil; $[\alpha]_D^{23} = 3.87$ ($c = 1.06$ in MeOH); IR (film): 3426, 2957, 1755, 1637 cm^{-1} ; ^1H NMR (CDCl_3 , 400 MHz): $\delta = 5.85\text{-}5.75$ (m, 1H), 5.10-5.02 (m, 2H), 4.19 (dd, $J = 8.8, 8.4$ Hz, 1H), 4.02 (dd, $J = 8.8, 4.0$ Hz, 1H), 3.84 (s, 1H), 3.66-3.62 (m, 1H), 3.11-3.04 (m, 1H), 2.25-2.16 (m, 2H), 2.12-2.05 (m, 1H), 1.70-1.61 (m, 1H), 1.29-1.18 (m, 2H), 0.86-0.83 (m, 9H), 0.78 (d, $J = 6.8$ Hz, 3H); ^{13}C NMR (CDCl_3 , 100 MHz): $\delta = 158.8, 135.2, 117.7, 62.6, 62.2, 56.2, 42.3, 37.7, 27.5, 25.0, 23.4, 22.8, 17.9, 15.1$. HRMS Calcd for C₁₄H₂₆N₂O₂ ($\text{M}+\text{Na}$)⁺: 277.1886; Found: 277.1891.

(S)-Ethyl-2-((S)-4-isopropyl-2-oxooxazolidin-3-ylamino)pent-4-enoate (2.63f)



Colorless oil; $[\alpha]_D^{23} = -150.5$ ($c = 0.58$ in CHCl_3); IR (film): 3426, 2957, 1755, 1637 cm^{-1} ; ^1H NMR (CDCl_3 , 400 MHz): $\delta = 5.89\text{-}5.77$ (m, 1H), 5.20-4.50 (m, 2H), 4.23-4.10 (m, 4H), 4.06-4.01 (m, 1H), 3.88-3.84 (m, 1H), 3.82-3.78 (m, 1H), 2.56-2.49 (m, 1H), 2.41-2.29 (m, 2H), 1.26 (t, $J = 7.2$ Hz, 3H), 0.87 (d, $J = 7.2$ Hz, 3H), 0.82 (d, $J = 7.2$ Hz, 3H); ^{13}C NMR (CDCl_3 , 100 MHz): $\delta = 172.6, 158.7, 133.0, 119.1, 63.0, 61.6, 61.5, 61.2, 35.7, 27.5, 17.9, 15.0, 14.4$. HRMS Calcd for C₁₃H₂₂N₂O₄ ($\text{M}+\text{Na}$)⁺: 277.1886; Found: 277.1891.

(R)-3-((R)-1-Cyclopentylbut-3-enylamino)-4-isopropylloxazolidin-2-one (2.63g)



Colorless oil; $[\alpha]_D^{23} = -7.5$ ($c = 1$ in $CHCl_3$); IR (film):

3434, 2951, 1754, 1632 cm^{-1} ; 1H NMR ($CDCl_3$, 400

MHz): $\delta = 5.97$ -5.89 (m, 1H), 5.17-5.08 (m, 2H), 4.22 (t,

$J = 9.0$ Hz, 1H), 4.07 (dd, $J = 9.0, 4.0$ Hz, 1H), 3.94 (d, J

$= 4.0$ Hz, 1H), 3.72-3.69 (m, 1H), 2.30-2.95 (m, 1H),

2.35-2.29 (m, 1H), 2.28-2.22 (m, 1H), 2.15-2.09 (m, 1H), 2.02-1.94 (m, 1H), 1.83-1.76 (m,

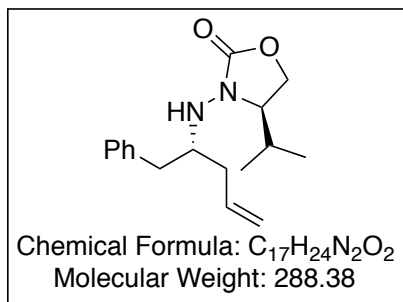
1H), 1.73-1.67 (m, 1H), 1.63-1.48 (m, 4H), 1.33-1.23 (m, 2H), 0.90 (d, $J = 7.0$ Hz, 3H),

0.84 (d, $J = 7.0$ Hz, 3H); ^{13}C NMR ($CDCl_3$, 100 MHz): $\delta = 158.6, 135.6, 117.6, 62.6, 61.6,$

61.1, 42.1, 35.3, 29.6, 28.9, 27.5, 25.9, 25.7, 18.0, 15.1. HRMS Calcd for $C_{15}H_{26}N_2O_2$

($M+Na$) $^+$: 289.1886; Found: 277.1877.

(R)-4-Isopropyl-3-((R)-1-phenylpent-4-en-2-ylamino)oxazolidin-2-one (2.63i)



Colorless oil; $[\alpha]_D^{23} = 9.7$ ($c = 1$ in $CHCl_3$); IR (film):

3287, 2926, 1756 cm^{-1} ; 1H NMR ($CDCl_3$, 400 MHz): $\delta =$

7.28-7.24 (m, 2H), 7.19-7.17 (m, 3H), 5.90-5.79 (m, 1H),

5.15-5.08 (m, 2H), 4.01-3.92 (m, 3H), 3.45-3.37 (m, 2H),

2.76 (dd, $J = 13.6, 6.8$ Hz, 1H), 2.66 (dd, $J = 13.6, 6.8$

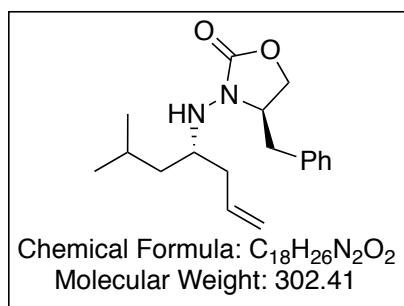
Hz, 1H), 2.26-2.19 (m, 1H), 2.15-2.08 (m, 1H), 1.99-1.91 (m, 1H), 0.78 (d, $J = 7.2$ Hz,

3H), 0.73 (d, $J = 7.2$ Hz, 3H); ^{13}C NMR ($CDCl_3$, 100 MHz): $\delta = 158.6, 139.1, 134.9,$

129.4, 128.6, 126.5, 118.3, 62.6, 61.6, 59.2, 40.0, 37.5, 27.4, 17.8, 15.0. HRMS Calcd for

$C_{17}H_{24}N_2O_2$ ($M+Na$) $^+$: 311.1730; Found: 311.1741.

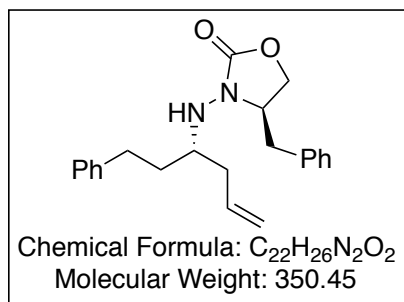
(R)-4-Benzyl-3-((S)-6-methylhept-1-en-4-ylamino)oxazolidin-2-one (2.63k)



Colorless oil; $[\alpha]_D^{23} = -37.2$ ($c = 0.97$ in $CHCl_3$); IR (film): 3287, 2926, 1756 cm^{-1} ; 1H NMR ($CDCl_3$, 500 MHz): $\delta = 7.36-7.32$ (m, 2H), 7.29-7.26 (m, 1H), 7.18 (d, $J = 7.5$ Hz, 2H), 5.94-5.85 (m, 1H), 5.19-5.13 (m, 2H), 4.18-4.15 (m, 1H), 4.07-4.05 (m, 2H), 3.94-3.89 (m, 1H),

3.34 (dd, $J = 13.5, 3.5$ Hz, 1H), 3.21-3.17 (m, 1H), 2.63 (dd, $J = 13.5, 8.5$ Hz, 1H), 2.30-2.21 (m, 2H), 1.82-1.74 (m, 1H), 1.34 (t, $J = 6.5$ Hz, 2H), 0.97 (d, $J = 6.5$ Hz, 3H), 0.94 (d, $J = 6.5$ Hz, 3H); ^{13}C NMR ($CDCl_3$, 125 MHz): $\delta = 158.9, 136.3, 135.3, 129.4, 129.2, 127.3, 117.8, 66.0, 60.0, 56.6, 42.3, 37.8, 37.2, 25.1, 23.3, 23.1$. HRMS Calcd for $C_{18}H_{26}N_2O_2$ ($M+Na$) $^+$: 325.1886; Found: 325.1876.

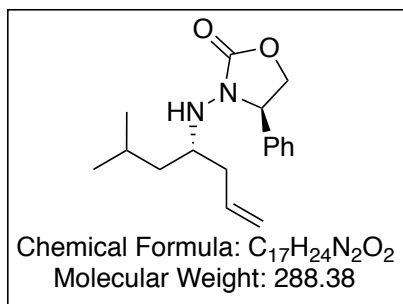
(R)-4-Benzyl-3-((S)-1-phenylhex-5-en-3-ylamino)oxazolidin-2-one (2.63l)



Colorless oil; $[\alpha]_D^{23} = -23.8$ ($c = 0.47$ in $CHCl_3$); IR (film): 3287, 2926, 1756 cm^{-1} ; 1H NMR ($CDCl_3$, 400 MHz): $\delta = 7.31-7.23$ (m, 5H), 7.22-7.17 (m, 3H), 7.13-7.11 (d, $J = 7.2$ Hz, 2H), 5.92-5.82 (m, 1H), 5.20-5.12 (m, 2H), 4.13-4.07 (m, 2H), 4.02 (dd, $J = 8.8, 4.4$ Hz,

1H), 3.90-3.84 (m, 1H), 3.29 (dd, $J = 13.6, 3.6$ Hz, 1H), 3.21-3.16 (m, 1H), 2.79-2.64 (m, 2H), 2.58 (dd, $J = 13.6, 9.6$ Hz, 1H), 2.36-2.22 (m, 2H), 1.81-1.75 (m, 2H); ^{13}C NMR ($CDCl_3$, 100 MHz): $\delta = 158.7, 142.3, 136.1, 134.9, 129.3, 129.1, 128.7, 128.6, 127.3, 126.2, 118.1, 65.9, 59.9, 58.1, 37.1, 34.3, 31.7$. HRMS Calcd for $C_{22}H_{26}N_2O_2$ ($M+Na$) $^+$: 373.1886; Found: 373.1884.

(R)-3-((S)-6-Methylhept-1-en-4-ylamino)-4-phenyloxazolidin-2-one(2.63m)

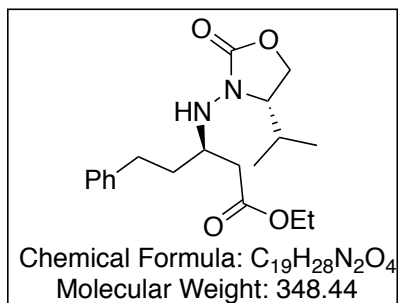


Colorless oil; $[\alpha]_D^{23} = -64.3$ ($c = 1.9$ in MeOH); IR (film): 3287, 2926, 1756 cm⁻¹; ¹H NMR (CDCl₃, 400 MHz): $\delta = 7.41-7.34$ (m, 3H), 7.30-7.26 (m, 2H), 5.74-5.63 (m, 1H), 5.01-4.95 (m, 2H), 4.82-4.78 (m, 1H), 4.61-4.57 (m, 1H), 4.19 (dd, $J = 8.8, 6.4$ Hz, 1H), 3.76 (bs, 1H), 3.94-3.88 (m, 1H), 2.10-2.00 (m, 2H), 1.42-1.35 (m, 1H), 1.26-1.15 (m, 2H), 0.75-0.71 (m, 6H); ¹³C NMR (CDCl₃, 100 MHz): $\delta = 158.5, 137.3, 135.1, 129.5, 129.4, 127.6, 117.5, 68.9, 61.5, 55.3, 41.9, 37.5, 24.8, 22.9, 22.8$. HRMS Calcd for C₁₇H₂₄N₂O₂ (M+Na)⁺: 311.1730; Found: 311.1737.

2.4.4. General Procedure for Indium-Mediated Reformatsky Reaction of Chiral Hydrazones

Chiral hydrazone (0.5 mmol scale, 1 equiv.), indium powder (0.5 mmol, 1.5 equiv.) and α -bromoacetate (1.0 mmol) were added to a 5 mL vial. The mixture was immersed in an ultrasound bath at room temperature until the substrate was totally consumed. The crude reaction mixture was mixed with silica gel and subjected to flash column chromatography hexane/ethyl acetate (50:50) to afford β -aminoesters.

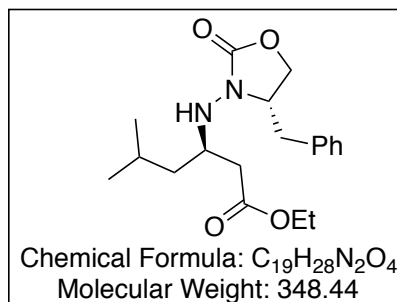
Ethyl-3-((S)-4-isopropyl-2-oxooxazolidin-3-ylamino)-5-phenylpentanoate (2.117a).



Colorless oil; $[\alpha]_D^{23} = -2.6$ ($c = 0.97$ in MeOH); ¹H NMR (CDCl₃, 500 MHz): $\delta = 7.19-7.16$ (m, 2H), 7.10-7.07 (m, 3H), 4.16 (d, $J = 7.0$ Hz, 1H), 4.11-4.00 (m, 3H), 3.97 (dd, $J = 9.0, 4.5$ Hz, 1H), 3.61-3.57 (m, 1H), 3.30-3.25 (m, 1H), 2.66-2.60 (m, 2H), 2.44-2.39 (m, 2H), 2.20-2.12 (m,

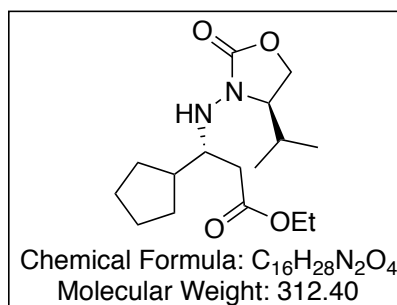
1H), 1.80-1.64 (m, 2H), 1.16 (t, $J = 7.0$ Hz, 3H), 0.79 (d, $J = 7.0$ Hz, 3H), 0.72 (d, $J = 7.0$ Hz, 3H); ^{13}C NMR (CDCl_3 , 125 MHz): $\delta = 172.1, 159.0, 141.7, 128.6, 128.5, 126.1, 62.7, 61.5, 60.7, 55.9, 38.5, 34.7, 32.0, 27.2, 17.9, 14.9, 14.3$. HRMS Calcd for $\text{C}_{19}\text{H}_{28}\text{N}_2\text{O}_4$ ($\text{M}+\text{Na}$) $^+$: 371.1941; Found: 371.1936.

Ethyl-3-((S)-4-benzyl-2-oxooxazolidin-3-ylamino)-5-methylhexanoate (2.117k).



Colorless oil; $[\alpha]_{\text{D}}^{22} = 23.6$ ($c = 0.55$ in MeOH); ^1H NMR (CDCl_3 , 400 MHz): $\delta = 7.31-7.28$ (m, 2H), 7.25-7.22 (m, 1H), 7.15-7.13 (m, 2H), 4.16-4.07 (m, 4H), 4.00 (dd, $J = 8.8, 4.8$ Hz, 1H), 3.97-3.90 (m, 1H), 3.49-3.40 (m, 1H), 3.28 (dd, $J = 13.6, 3.6$ Hz, 1H), 2.59 (dd, $J = 13.6, 9.6$ Hz, 1H), 2.50 (dd, $J = 16.0, 7.2$ Hz, 1H), 2.40 (dd, $J = 16.0, 5.6$ Hz, 1H), 1.78-1.70 (m, 1H), 1.43-1.36 (m, 1H), 1.30-1.22 (m, 4H), 0.96 (d, $J = 6.4$ Hz, 3H), 0.90 (d, $J = 6.4$ Hz, 3H); ^{13}C NMR (CDCl_3 , 100 MHz): $\delta = 172.5, 159.0, 136.2, 129.3, 129.1, 127.3, 66.1, 60.7, 59.2, 54.7, 42.5, 39.2, 37.0, 25.2, 23.1, 22.8, 14.4$. HRMS Calcd for $\text{C}_{19}\text{H}_{28}\text{N}_2\text{O}_4$ ($\text{M}+\text{Na}$) $^+$: 371.1941; Found: 371.1941.

Ethyl-3-((R)-4-isopropyl-2-oxooxazolidin-3-ylamino)-3-cyclopentylpropanoate (2.117g).

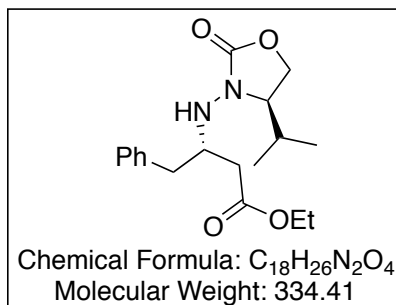


Colorless oil; $[\alpha]_{\text{D}}^{23} = 12.0$ ($c = 1.0$ in CHCl_3); ^1H NMR (CDCl_3 , 400 MHz): $\delta = 4.15-4.01$ (m, 5H), 3.74-3.70 (m, 1H), 3.22-3.16 (m, 1H), 2.45 (d, $J = 5.6$ Hz, 2H), 2.23-2.16 (m, 1H), 2.00-1.89 (m, 1H), 1.87-1.79 (m, 1H), 1.72-1.64 (m, 1H), 1.61-1.46 (m, 4H), 1.23-1.19 (m, 5H), 0.85 (d, $J = 7.2$ Hz, 3H), 0.78 (d, $J = 7.2$ Hz, 3H); ^{13}C NMR (CDCl_3 , 100 MHz): $\delta = 173.0, 158.6,$

62.7, 60.7, 60.2, 60.1, 42.8, 37.6, 30.0, 29.4, 27.3, 25.7, 25.6, 17.8, 15.0, 14.3. HRMS

Calcd for $C_{16}H_{28}N_2O_4$ ($M+Na$)⁺: 335.1941; Found: 335.1931.

Ethyl-3-((R)-4-isopropyl-2-oxooxazolidin-3-ylamino)-4-phenylbutanoate (2.117i).



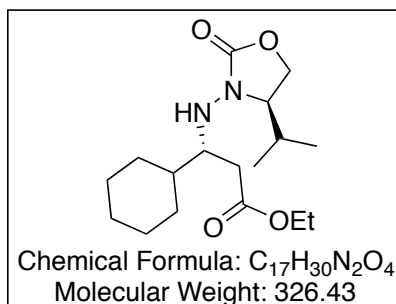
Colorless oil; $[a]_D^{23} = -3.14$ ($c = 1.02$ in $CHCl_3$); 1H NMR ($CDCl_3$, 400 MHz): $\delta = 7.29-7.24$ (m, 2H), 7.21-7.17 (m, 3H), 4.17 (d, $J = 5.2$ Hz, 1H), 4.12-4.06 (m, 3H), 3.97 (dd, $J = 9.2, 4.8$ Hz, 1H), 3.62-3.54 (m, 2H), 2.86 (dd, $J = 13.6, 7.2$ Hz, 1H), 2.70 (dd, $J = 13.6, 7.2$ Hz, 1H), 2.44-

2.42 (m, 2H), 1.90-1.82 (m, 1H), 1.22 (t, $J = 7.2$ Hz, 3H) 0.77 (d, $J = 7.2$ Hz, 3H), 0.73 (d, $J = 7.2$ Hz, 3H); ^{13}C NMR ($CDCl_3$, 100 MHz): $\delta = 172.2, 158.9, 138.3, 129.4, 128.8,$

126.8, 62.7, 61.0, 60.8, 57.4, 39.8, 38.2, 27.1, 17.9, 14.9, 14.4. HRMS Calcd for

$C_{18}H_{26}N_2O_4$ ($M+Na$)⁺: 357.1785; Found: 357.1782.

Ethyl-3-((R)-4-isopropyl-2-oxooxazolidin-3-ylamino)-3-cyclohexylpropanoate(2.117h).



Colorless oil; $[a]_D^{23} = 12.8$ ($c = 1.0$ in $CHCl_3$); 1H NMR ($CDCl_3$, 400 MHz): $\delta = 4.18-4.00$ (m, 5H), 3.67-3.63 (m, 1H), 3.19-3.14 (m, 1H), 2.44-2.30 (m, 2H), 2.27-2.19 (m, 1H), 1.74-1.61 (m, 5H), 1.50-1.42 (m, 1H), 1.24-1.17 (m, 4H), 1.15-1.05 (m, 2H), 1.02-0.92 (m, 2H), 0.85 (d, $J =$

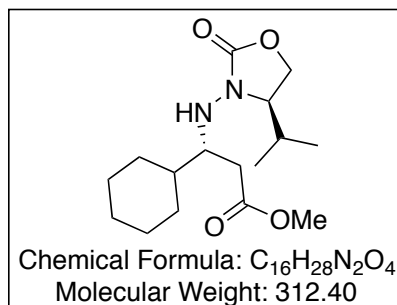
7.2 Hz, 3H), 0.79 (d, $J = 7.2$ Hz, 3H); ^{13}C NMR ($CDCl_3$, 100 MHz): $\delta = 173.0, 158.7, 62.7,$

61.0, 60.8, 60.6, 40.2, 35.5, 29.6, 28.3, 27.4, 26.7, 26.6, 26.5, 17.9, 15.0, 14.3. HRMS

Calcd for $C_{17}H_{30}N_2O_4$ ($M+Na$)⁺: 349.2098; Found: 349.2099.

Methyl-3-((R)-4-isopropyl-2-oxooxazolidin-3-ylamino)-3-cyclohexylpropanoate

(2.118h).

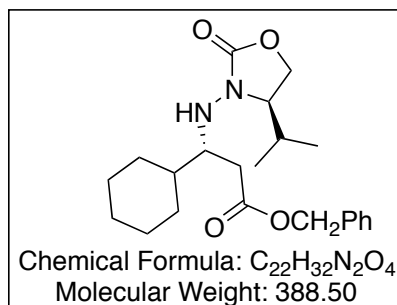


Colorless oil; $[\alpha]_D^{23} = -83.3$ ($c = 1.0$ in CHCl₃); ¹H NMR (CDCl₃, 400 MHz): $\delta = 4.18$ - 4.14 (m, 2H), 4.04 (dd, $J = 9.2, 4.0$ Hz, 1H), 3.69-3.64 (m, 4H), 3.21-3.15 (m, 1H), 2.47-2.35 (m, 2H), 2.28-2.20 (m, 1H), 1.77-1.63 (m, 5H), 1.52-1.43 (m, 1H), 1.24-1.07 (m, 3H), 1.05-0.92 (m, 2H),

0.87 (d, $J = 7.2$ Hz, 3H), 0.81 (d, $J = 7.2$ Hz, 3H); ¹³C NMR (CDCl₃, 100 MHz): $\delta = 173.5, 158.7, 62.7, 60.9, 60.7, 51.9, 40.2, 35.3, 29.6, 28.4, 27.4, 26.7, 26.6, 26.5, 17.9, 15.0$. HRMS Calcd for C₁₆H₂₈N₂O₄ (M+Na)⁺: 335.1941; Found: 335.1927.

Benzyl-3-((R)-4-isopropyl-2-oxooxazolidin-3-ylamino)-3-cyclohexylpropanoate

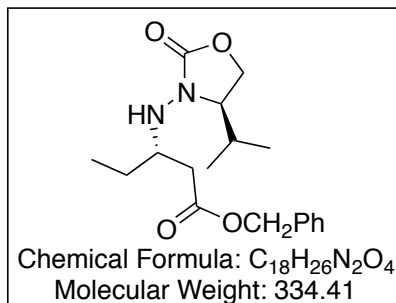
(2.119h).



Colorless oil; $[\alpha]_D^{23} = 13.33$ ($c = 0.87$ in CHCl₃); ¹H NMR (CDCl₃, 400 MHz): $\delta = 7.33$ - 7.27 (m, 5H), 5.09 (s, 2H), 4.18 (d, $J = 7.2$ Hz, 1H), 4.10-4.06 (m, 1H), 4.01-3.98 (m, 1H), 3.65-3.60 (m, 1H), 3.23-3.17 (m, 1H), 2.52-2.39 (m, 2H), 2.25-2.17 (m, 1H), 1.74-1.67 (m, 4H), 1.65-1.61 (m,

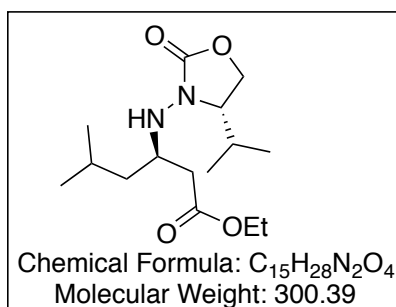
1H), 1.50-1.42 (m, 1H), 1.24-1.06 (m, 3H), 1.01-0.93 (m, 2H), 0.83 (d, $J = 6.8$ Hz, 3H), 0.78 (d, $J = 6.8$ Hz, 3H); ¹³C NMR (CDCl₃, 100 MHz): $\delta = 172.9, 158.8, 136.0, 128.7, 128.6, 128.4, 66.7, 62.7, 61.1, 60.8, 40.2, 35.6, 29.6, 28.4, 27.4, 26.7, 26.6, 26.5, 17.9, 15.0$. HRMS Calcd for C₂₂H₃₂N₂O₄ (M+Na)⁺: 411.2254; Found: 411.2242.

Ethyl-3-((S)-4-isopropyl-2-oxooxazolidin-3-ylamino)pentanoate (2.117j).



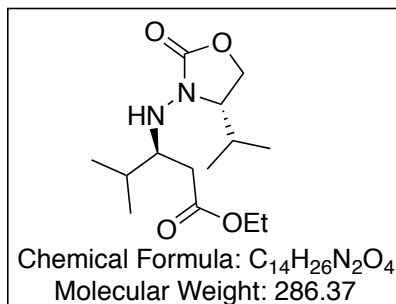
Colorless oil; $[a]_D^{23} = -3.62$ ($c = 1.05$ in $CHCl_3$); 1H NMR ($CDCl_3$, 500 MHz): $\delta = 4.17-4.13$ (m, 2H), 4.10-4.05 (m, 2H), 4.01 (dd, $J = 9.0, 4.5$ Hz, 1H), 3.67-3.64 (m, 1H), 3.28-3.23 (m, 1H), 2.37-2.35 (m, 2H), 2.23-2.16 (m, 1H), 1.55-1.48 (m, 1H), 1.44-1.37 (m, 1H), 1.20 (t, $J = 7.0$ Hz, 3H), 0.88 (t, $J = 7.0$ Hz, 3H), 0.84 (d, $J = 7.0$ Hz, 3H), 0.78 (d, $J = 7.0$ Hz, 3H); ^{13}C NMR ($CDCl_3$, 125 MHz): $\delta = 172.4, 159.0, 62.7, 61.6, 60.7, 57.4, 37.9, 27.4, 25.8, 17.9, 15.1, 14.4, 10.0$. HRMS Calcd for $C_{13}H_{24}N_2O_4$ ($M+Na$) $^+$: 295.1628; Found: 295.1610.

Ethyl-3-((S)-4-isopropyl-2-oxooxazolidin-3-ylamino)-5-methylhexanoate (2.117e)



Colorless oil; $[a]_D^{23} = 3.17$ ($c = 1.04$ in $CHCl_3$); IR (film): 3287, 2958, 1751 cm^{-1} ; 1H NMR ($CDCl_3$, 400 MHz): $\delta = 4.18-4.01$ (m, 5H), 3.71-3.66 (m, 1H), 3.39-3.31 (m, 1H), 2.47-2.34 (m, 2H), 2.26-2.18 (m, 1H), 1.74-1.63 (m, 1H), 1.42-1.34 (m, 1H), 1.25-1.17 (m, 4H), 0.89-0.85 (m, 9H), 0.79 (d, $J = 7.2$ Hz, 3H); ^{13}C NMR ($CDCl_3$, 100 MHz): $\delta = 172.5, 159.0, 62.7, 61.3, 60.7, 54.5, 42.6, 39.1, 27.3, 25.1, 22.9, 22.8, 17.9, 15.0, 14.4$. HRMS Calcd for $C_{15}H_{28}N_2O_4$ ($M+Na$) $^+$: 323.1941; Found: 323.1942.

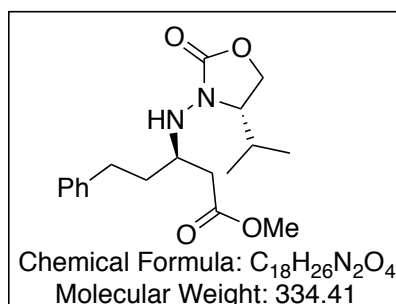
Ethyl-3-((S)-4-isopropyl-2-oxooxazolidin-3-ylamino)-4-methylpentanoate (2.117c).



Colorless oil; $[a]_D^{23} = -11.9$ ($c = 1.63$ in $CHCl_3$); IR (film): 3421, 2961, 1750 cm^{-1} ; 1H NMR ($CDCl_3$, 400 MHz): $\delta = 4.24-4.23$ (m, 1H), 4.18-4.09 (m, 3H), 4.05-4.02 (m, 1H), 3.69-3.66 (m, 1H), 3.27-3.20 (m, 1H), 2.42-

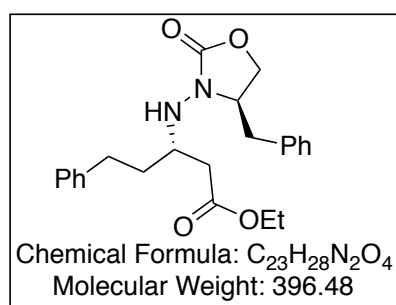
2.30 (m, 2H), 2.29-2.21 (m, 1H), 1.90-1.81 (m, 1H), 1.24 (t, $J = 7.2$ Hz, 3H), 0.92-0.86 (m, 9H), 1.24 (d, $J = 6.8$ Hz, 3H); ^{13}C NMR (CDCl_3 , 100 MHz): $\delta = 173.0, 158.7, 62.7, 61.2, 60.9, 60.8, 34.7, 29.6, 27.4, 18.9, 17.9, 17.3, 15.1, 14.4$. HRMS Calcd for $\text{C}_{14}\text{H}_{26}\text{N}_2\text{O}_4$ ($\text{M}+\text{Na}$) $^+$: 309.1785; Found: 309.1795.

Methyl-3-((S)-4-isopropyl-2-oxooxazolidin-3-ylamino)-5-phenylpentanoate (2.118a).



Colorless oil; $[\alpha]_{\text{D}}^{23} = -11$ ($c = 0.8$ in MeOH); IR (film): 3290, 2956, 1751 cm^{-1} ; ^1H NMR (CDCl_3 , 400 MHz): $\delta = 7.28-7.24$ (m, 2H), 7.18-7.15 (m, 3H), 4.18-4.14 (m, 2H), 4.05 (dd, $J = 8.8, 4.0$ Hz, 1H), 3.69-3.64 (m, 4H), 3.38-3.32 (m, 1H), 2.76-2.64 (m, 2H), 2.55-2.45 (m, 2H), 2.27-2.19 (m, 1H), 1.90-1.71 (m, 2H), 0.87 (d, $J = 7.2$ Hz, 3H), 0.79 (d, $J = 7.2$ Hz, 3H); ^{13}C NMR (CDCl_3 , 100 MHz): $\delta = 172.7, 159.1, 141.7, 128.7, 128.5, 126.2, 62.7, 61.5, 56.1, 51.9, 38.3, 34.7, 32.2, 27.3, 17.9, 15.0$. HRMS Calcd for $\text{C}_{18}\text{H}_{26}\text{N}_2\text{O}_4$ ($\text{M}+\text{Na}$) $^+$: 357.1785; Found: 357.1775.

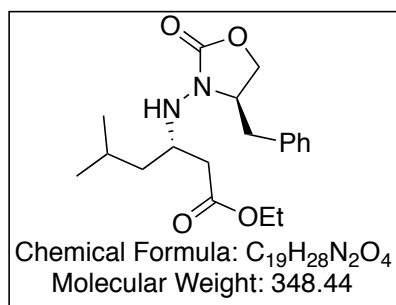
Ethyl-3-((R)-4-benzyl-2-oxooxazolidin-3-ylamino)-5-phenylpentanoate (2.117l).



Colorless oil; $[\alpha]_{\text{D}}^{24} = -24.8$ ($c = 0.52$ in CHCl_3); IR (film): 3437, 2929, 1756, 1643 cm^{-1} ; ^1H NMR (CDCl_3 , 400 MHz): $\delta = 7.32-7.23$ (m, 5H), 7.21-7.16 (m, 3H), 7.15-7.12 (m, 2H), 4.29 (d, $J = 6.4$ Hz, 1H), 4.18-4.11 (m, 2H), 4.09-4.07 (m, 1H), 3.99 (dd, $J = 8.8, 4.8$ Hz, 1H), 3.94-3.89 (m, 1H), 3.48-3.39 (m, 1H), 3.28 (dd, $J = 13.9, 3.6$ Hz, 1H), 2.74 (t, $J = 8.0$ Hz, 2H), 2.60-2.50 (m, 3H), 1.91-1.74 (m, 2H), 1.25 (t, $J = 7.2$ Hz, 3H); ^{13}C NMR (CDCl_3 , 100 MHz): $\delta = 172.2, 159.0, 141.7, 136.1, 129.3, 129.1, 128.7, 128.6, 127.3, 126.3, 66.1, 60.9, 59.3, 56.4, 38.6, 36.9, 34.8, 32.2, 14.4$. HRMS Calcd for $\text{C}_{23}\text{H}_{28}\text{N}_2\text{O}_4$ ($\text{M}+\text{Na}$) $^+$: 419.1941;

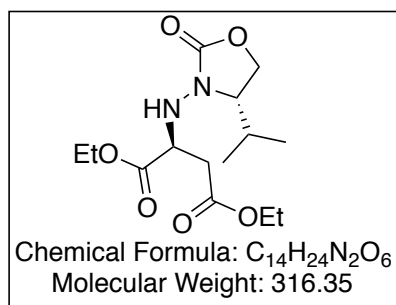
Found: 419.1956.

Ethyl-3-((R)-4-benzyl-2-oxooxazolidin-3-ylamino)-5-methylhexanoate (2.117m).



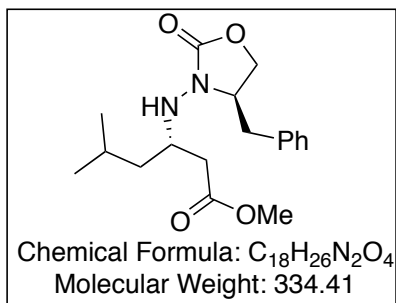
Colorless oil; $[a]_D^{23} = -25.4$ ($c = 1.36$ in $CHCl_3$); IR (film): 3434, 2927, 1756, 1640 cm^{-1} ; 1H NMR ($CDCl_3$, 400 MHz): $\delta = 7.32-7.28$ (m, 2H), 7.25-7.23 (m, 1H), 7.16-7.13 (m, 2H), 4.16-4.11 (m, 3H), 4.10-4.07 (m, 1H), 4.01 (dd, $J = 8.8, 4.8$ Hz, 1H), 3.96-3.89 (m, 1H), 3.49-3.42 (m, 1H), 3.99 (dd, $J = 13.6, 3.6$ Hz, 1H), 2.60 (dd, $J = 13.6, 9.6$ Hz, 1H), 2.53-2.37 (m, 2H), 1.80-1.69 (m, 1H), 1.44-1.37 (m, 1H), 1.32-1.23 (m, 4H), 0.95 (d, $J = 6.8$ Hz, 3H), 0.91 (d, $J = 6.8$ Hz, 3H); ^{13}C NMR ($CDCl_3$, 100 MHz): $\delta = 172.5, 159.0, 136.2, 129.3, 129.1, 127.3, 66.1, 60.7, 59.2, 54.7, 42.6, 39.2, 37.0, 25.2, 23.1, 22.8, 14.4$. HRMS Calcd for $C_{19}H_{28}N_2O_4$ ($M+Na$) $^+$: 371.1941; Found: 371.1960.

Diethyl-2-((S)-4-isopropyl-2-oxooxazolidin-3-ylamino)succinate (2.117f)



Colorless oil; IR (film): 3446, 2982, 1734 cm^{-1} ; 1H NMR ($CDCl_3$, 500 MHz): $\delta = 4.76$ (d, $J = 5.0$ Hz, 1H), 4.27-4.23 (m, 3H), 4.21-4.08 (m, 4H), 3.79-3.76 (m, 1H), 2.80 (d, $J = 5.5$ Hz, 2H), 2.30-2.23 (m, 1H), 1.33-1.27 (m, 6H), 0.91 (d, $J = 7.0$ Hz, 3H), 0.85 (d, $J = 7.0$ Hz, 3H); ^{13}C NMR ($CDCl_3$, 125 MHz): $\delta = 171.1, 170.9, 158.7, 63.1, 61.8, 61.7, 61.2, 58.8, 36.3, 27.6, 17.9, 15.2, 14.4, 14.2$.

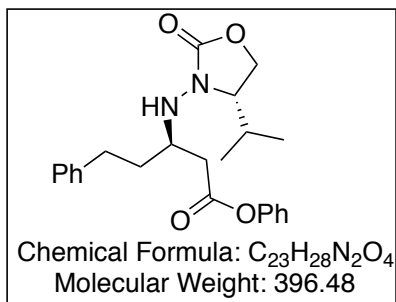
Methyl-3-((R)-4-benzyl-2-oxooxazolidin-3-ylamino)-5-methylhexanoate (2.118m)



Colorless oil; $[\alpha]_D^{23} = -32.1$ ($c = 1.18$ in MeOH); IR (film): 3434, 2955, 1757 cm^{-1} ; ^1H NMR (CDCl_3 , 500 MHz): $\delta = 7.36\text{-}7.26$ (m, 3H), 7.20-7.17 (m, 2H), 4.17-4.12 (m, 2H), 4.07-4.04 (m, 1H), 3.99-3.95 (m, 1H), 3.72 (s, 3H), 3.52-3.47 (m, 1H), 3.32 (dd, $J = 9.5, 4.0$ Hz, 1H),

2.63 (dd, $J = 13.5, 9.5$ Hz, 1H), 2.58-2.45 (m, 2H), 1.82-1.73 (m, 1H), 1.48-1.41 (m, 1H), 1.34-1.28 (m, 1H), 0.99 (d, $J = 6.5$ Hz, 3H), 0.95 (d, $J = 6.5$ Hz, 3H); ^{13}C NMR (CDCl_3 , 125 MHz): $\delta = 173.0, 159.1, 136.2, 129.4, 129.2, 127.3, 66.2, 59.2, 54.8, 51.9, 42.6, 39.0, 37.0, 25.2, 23.0, 22.8$. HRMS Calcd for C₁₈H₂₆N₂O₄ (M+Na)⁺: 357.1785; Found: 357.1783.

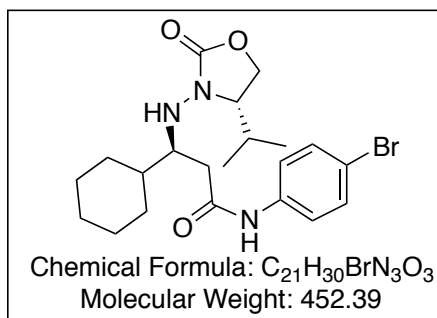
Methyl-3-((R)-4-isopropyl-2-oxooxazolidin-3-ylamino)-3-cyclohexylpropanoate (2.119a).



Colorless oil; $[\alpha]_D^{23} = -14.7$ ($c = 1.8$ in MeOH); IR (film): 3480, 3291, 2961, 1744 cm^{-1} ; ^1H NMR (CDCl_3 , 400 MHz): $\delta = 7.38\text{-}7.34$ (m, 2H), 7.30-7.26 (m, 2H), 7.24-7.17 (m, 4H), 7.10-7.08 (m, 2H), 4.23 (d, $J = 7.2$ Hz, 1H), 4.17-4.13 (m, 1H), 4.05 (dd, $J = 9.2, 4.0$ Hz, 1H),

3.70-3.65 (m, 1H), 3.49-3.44 (m, 1H), 2.82-2.73 (m, 4H), 2.31-2.23 (m, 1H), 1.20-1.84 (m, 2H), 0.87 (d, $J = 6.8$ Hz, 3H), 0.82 (d, $J = 6.8$ Hz, 3H); ^{13}C NMR (CDCl_3 , 100 MHz): $\delta = 170.9, 159.2, 150.8, 141.6, 129.7, 128.8, 128.6, 126.3, 126.1, 121.8, 62.7, 61.4, 56.0, 38.7, 34.8, 32.3, 27.3, 17.9, 15.0$. HRMS Calcd for C₂₃H₂₈N₂O₄ (M+Na)⁺: 419.1941; Found: 419.1920.

***N*-(4-bromophenyl)-3-cyclohexyl-3-((*R*)-4-isopropyl-2-oxooxazolidin-3-ylamino)propanamide (2.132h)**



White solid: m.p = 38 - 40 °C; $[\alpha]_D^{23} = 46.9$ (c = 1.0 in CHCl₃); IR (film): 3480, 3291, 2961, 1744 cm⁻¹; ¹H NMR (CDCl₃, 400 MHz): $\delta = 7.38-7.34$ (m, 2H), 7.30-7.26 (m, 2H), 7.24-7.17 (m, 4H), 7.10-7.08 (m, 2H), 4.23 (d, *J* = 7.2 Hz, 1H), 4.17-4.13 (m, 1H), 4.05 (dd, *J* = 9.2, 4.0 Hz, 1H), 3.70-3.65 (m, 1H), 3.49-3.44 (m, 1H), 2.82-2.73 (m, 4H), 2.31-2.23 (m, 1H), 1.20-1.84 (m, 2H), 0.87 (d, *J* = 6.8 Hz, 3H), 0.82 (d, *J* = 6.8 Hz, 3H); ¹³C NMR (CDCl₃, 100 MHz): $\delta = 170.9, 159.2, 150.8, 141.6, 129.7, 128.8, 128.6, 126.3, 126.1, 121.8, 62.7, 61.4, 56.0, 38.7, 34.8, 32.3, 27.3, 17.9, 15.0$. HRMS Calcd for C₂₁H₃₀BrN₃O₃ (M+Na)⁺: 474.1363; Found: 474.1358.

2.5. References

- (1) Smyth, W. F.; Ramachandran, V.; O’Kane, E.; Coulter, D., Characterisation of selected drugs with nitrogen-containing saturated ring structures by use of electrospray ionisation with ion-trap mass spectrometry. *Analytical and BioAnalytical Chem.*, **2004**, 378 (5), 1305-1312.
- (2) Kobayashi, S.; Ishitani, H., Catalytic enantioselective addition to imines. *Chem. Rev.*, **1999**, 99 (5), 1069-1094.
- (3) (a) Garigipati, R. S.; Cordova, R.; Parvez, M.; Weinreb, S. M., Diastereoselective synthesis of Highly Functionalized Homoallylic Amine Derivatives Via Diels-Alder Adducts of N-Sulfinyl Dienophiles. *Tetrahedron* **1986**, 42 (11), 2979-2983. (b) Armstrong, S. K.; Collington, E. W.; Knight, J. G.; Naylor, A.; Warren, S., A New

- Method for Stereoselective Homoallylic Amine Synthesis. *J. Chem. Soc. Perk. Trans I.*, **1993**, (13), 1433-1447. (c) Ding, H.; Friestad, G. K., Asymmetric addition of allylic nucleophiles to imino compounds. *Synthesis-Stuttgart* **2005**, (17), 2815-2829. (d) Kolodney, G.; Sklute, G.; Perrone, S.; Knochel, P.; Marek, I., Diastereodivergent synthesis of enantiomerically pure homoallylic amine derivatives containing quaternary carbon stereocenters. *Angew. Chem. Int. Ed.*, **2007**, 46 (48), 9291-9294. (e) Kim, S. H.; Lee, S.; Kim, Y. M.; Kim, J. N., Regioselective Introduction of Homoallylic Amine Moiety to Quinolines: Preparation of Reissert Compound Followed by In-Mediated Allylation of Nitrile. *Bull. Korean Chem. Soc.* **2010**, 31 (12), 3822-3825.
- (4) (a) Scheideman, M.; Shapland, P.; Vedejs, E., A mechanistic alternative for the intramolecular hydroboration of homoallylic amine and phosphine borane complexes. *J. Am. Chem. Soc.*, **2003**, 125 (35), 10502-10503. (b) Friestad, G. K.; Korapala, C. S.; Ding, H., Dual activation in asymmetric allylsilane addition to chiral N-acylhydrazones: Method development, mechanistic studies, and elaboration of homoallylic amine adducts. *J. Org. Chem.*, **2006**, 71 (1), 281-289. (c) Chang, C. L.; Chen, K. M., Diastereoselective three component reaction of N-glyoxyloyl camphorpyrazolidinone, amine and allyltributylstannane: Facile synthesis of homoallylic amines. *J Chin Chem Soc-Taip.*, **2007**, 54 (6), 1591-1594.
- (5) (a) Shen, Z.-L.; Loh, T.-P., Indium,àCopper-Mediated Barbier,àGrignard-Type Alkylation Reaction of Imines in Aqueous Media. *Org. Lett.*, **2007**, 9 (26), 5413-

5416. (b) Kobayashi, S.; Ishitani, H., Catalytic enantioselective addition to imines. *Chem. Rev.*, **1999**, 99 (5), 1069-1094.
- (6) Bocoum, A.; Boga, C.; Savoia, D.; Umani-Ronchi, A., Diastereoselective allylation of chiral imines. Novel application of allylcopper reagents to the enantioselective synthesis of homoallyl amines. *Tetrahedron. Lett.*, **1991**, 32 (10), 1367-1370.
- (7) Tanaka, H.; Inoue, K.; Pokorski, U.; Taniguchi, M.; Torii, S., A novel η^5 -Ti(O) η^5 -induced allylation of imines in a TiCl₄ (cat.)/Al bimetal system. Chirality transfer of l-valine to homoallylamine. *Tetrahedron Lett.*, **1990**, 31 (21), 3023-3026.
- (8) Zwierzak, A.; Napieraj, A., Synthesis of $E\pm$ -Arylalkylamines by Addition of Grignard Reagents to N-(Diethoxyphosphoryl)aldimines. *Synthesis* **1999**, 1999 (06), 930-934.
- (9) Alvaro, G.; Boga, C.; Savoia, D.; Umani-Ronchi, A., Diastereoselective addition of allylmetal compounds to imines derived from (S)-1-phenylethanamine. *J. Chem. Soc: Perk. Trans I.*, **1996**, (9), 875-882.
- (10) Friestad, G. K., Chiral N-Acylhydrazones: Versatile Imino Acceptors for Asymmetric Amine Synthesis. *Eur. J. Org. Chem.*, **2005**, 2005 (15), 3157-3172.
- (11) Cook, G. R.; Maity, B. C.; Kargbo, R., Highly diastereoselective indium-mediated allylation of chiral hydrazones. *Org. Lett.*, **2004**, 6 (11), 1741-1743.
- (12) Cook, G. R.; Kargbo, R.; Maity, B., Catalytic Enantioselective Indium-Mediated Allylation of Hydrazones. *Org. Lett.* **2005**, 7 (13), 2767-2770.
- (13) Kargbo, R.; Takahashi, Y.; Bhor, S.; Cook, G. R.; Lloyd-Jones, G. C.; Shepperson, I. R., Readily Accessible, Modular, and Tuneable BINOL 3,3'-

- Perfluoroalkylsulfones: Highly Efficient Catalysts for Enantioselective In-Mediated Imine Allylation. *J. Am. Chem. Soc.* **2007**, *129* (13), 3846-3847.
- (14) Araki, S.; Kamei, T.; Hirashita, T.; Yamamura, H.; Kawai, M., A New Preparative Method for Allylic Indium(III) Reagents by Reductive Transmetalation of α -Allylpalladium(II) with Indium(I) Salts. *Organic Letters* **2000**, *2* (6), 847-849.
- (15) Wang, Z., Tsuji-Trost Reaction. In *Comprehensive Organic Name Reactions and Reagents*, John Wiley & Sons, Inc.: **2010**.
- (16) Jiang, J. J.; Wang, D.; Wang, W. F.; Yuan, Z. L.; Zhao, M. X.; Wang, F. J.; Shi, M., Pd(II)-catalyzed and diethylzinc-mediated asymmetric umpolung allylation of aldehydes in the presence of chiral phosphine-Schiff base type ligands. *Tetrahedron-Asymm.*, **2010**, *21* (16), 2050-2054.
- (17) Trost, B. M.; Herndon, J. W., Inversion of the electronic reactivity of allyl acetates using an aluminum-tin reagent. *J. Am. Chem. Soc.* **1984**, *106* (22), 6835-7.
- (18) Kimura, M.; Kiyama, I.; Tomizawa, T.; Horino, Y.; Tanaka, S.; Tamaru, Y., Allylation of aldehydes via Umpolung of pi-allylpalladium(II) with triethylborane. *Tetrahedron. Lett.*, **1999**, *40* (37), 6795-6798.
- (19) (a) Ochiai, M.; Arimoto, M.; Fujita, E., Umpolung of Reactivity of Allylsilane, Allylgermane, and Allylstannane Via Their Reaction with Thallium (Iii) Salt - a New Allylation Reaction for Aromatic Compound. *Tetrahedron Lett.*, **1981**, *22* (45), 4491-4494. (b) Ochiai, M.; Fujita, E.; Arimoto, M.; Yamaguchi, H., Umpolung of Reactivity of Allylsilane, Allylgermane, and Allylstannane - Allylation of Aromatic-Compounds with Allylmetal and Arylthallium

- Bis(Trifluoroacetate). *Chemical & Pharmaceutical Bulletin* **1982**, *30* (11), 3994-3999.
- (20) (a) Wallner, O. A.; Szabo, K. J., Regioselective palladium-catalyzed electrophilic allylic substitution in the presence of hexamethylditin. *Org.Lett.*, **2002**, *4* (9), 1563-1566. (b) Sebelius, S.; Wallner, O. A.; Szabo, K. J., Palladium-catalyzed coupling of allyl acetates with aldehyde and imine electrophiles in the presence of bis(pinacolato)diboron. *Org. Lett.*, **2003**, *5* (17), 3065-3068.
- (21) Cesario, C.; Miller, M. J., Pd(0)/InI-Mediated Allylic Additions to 4-Acetoxy-2-azetidinone: New Route to Highly Functionalized Carbocyclic Scaffolds. *Org. Lett.*, **2009**, *11* (6), 1293-1295.
- (22) Cesario, C.; Miller, M. J., Palladium(0)/indium iodide-mediated allylations of electrophiles generated from the hydrolysis of Eschenmoser's salt: one-pot preparation of diverse carbocyclic scaffolds. *Tetrahedron Lett.*, **2010**, *51* (23), 3050-3052.
- (23) (a) Cleghorn, L. A. T.; Cooper, I. R.; Grigg, R.; MacLachlan, W. S.; Sridharan, V., Additive effects in palladium-indium mediated Barbier-type allylations. *Tetrahedron Lett.*, **2003**, *44* (43), 7969-7973. (b) Miyabe, H.; Yamaoka, Y.; Naito, T.; Takemoto, Y., Regioselectivity in palladium-indium iodide-mediated allylation reaction of glyoxylic oxime ether and N-sulfonylimine. *J. Org. Chem.*, **2003**, *68* (17), 6745-6751. (c) Miyabe, H.; Yamaoka, Y.; Naito, T.; Takemoto, Y., Palladium-indium iodide-mediated allylation and propargylation of glyoxylic oxime ether and

- hydrazone: the role of water in directing the diastereoselective allylation. *J. Org. Chem.*, **2004**, *69* (4), 1415-1418.
- (24) (a) Steinke, T.; Gemel, C.; Winter, M.; Fischer, R. A., [Pd₃(InCp*)₄(μ₂-InCp*)₄]: Three Linearly Arranged Palladium Atoms Wrapped into a Fluxional Shell of Eight InCp* Ligands. *Angew. Chem. Int. Ed.*, **2002**, *41* (24), 4761-4763. (b) Gemel, C.; Steinke, T.; Weiss, D.; Cokoja, M.; Winter, M.; Fischer, R. A., [M(GaCp*)₄] (M = Pd, Pt) as Building Blocks for Dimeric Homoleptic Cluster Compounds of the Type [MPt(GaCp*)₅]. *Organometallics.*, **2003**, *22* (13), 2705-2710. (c) Steinke, T.; Gemel, C.; Winter, M.; Fischer, R. A., The Clusters [Ma(ECp*)_b] (M=Pd, Pt; E=Al, Ga, In): Structures, Fluxionality, and Ligand Exchange Reactions. *Chemistry – A European Journal.*, **2005**, *11* (5), 1636-1646.
- (25) Reformatsky, S., Neue Synthese zweiatomiger einbasischer Säuren aus den Ketonen. *Berichte Der Deutschen Chemischen Gesellschaft.*, **1887**, *20* (1), 1210-1211.
- (26) Nakamura, E.; Aoki, S.; Sekiya, K.; Oshino, H.; Kuwajima, I., Carbon-carbon bond-forming reactions of zinc homoenolate of esters. A novel three-carbon nucleophile with general synthetic utility. *J. Am. Chem. Soc.*, **1987**, *109* (26), 8056-8066.
- (27) Ocampo, R.; Dolbier Jr, W. R., The Reformatsky reaction in organic synthesis. Recent advances. *Tetrahedron.*, **2004**, *60* (42), 9325-9374.
- (28) Rieke, R. D.; Hanson, M. V., New organometallic reagents using highly reactive metals. *Tetrahedron.*, **1997**, *53* (6), 1925-1956.

- (29) Parrish, J. D.; Shelton, D. R.; Little, R. D., Titanocene(III)-Promoted Reformatsky Additions. *Org. Lett.*, **2003**, 5 (20), 3615-3617.
- (30) Lei, B.; Fallis, A. G., Cadmium chloride mediated regiocontrol of dienolates and ketene thioacetals: $\text{C}=\text{C}$ condensation with aldehydes. *Can. J. Chem.*, **1991**, 69 (9), 1450-1456.
- (31) Kagoshima, H.; Hashimoto, Y.; Oguro, D.; Saigo, K., An Activated Germanium Metal-Promoted, Highly Diastereoselective Reformatsky Reaction. *J. Org. Chem.*, **1998**, 63 (3), 691-697.
- (32) Nair, V.; Ros, S.; Jayan, C. N.; Pillai, B. S., Indium- and gallium-mediated carbon-carbon bond-forming reactions in organic synthesis. *Tetrahedron.*, **2004**, 60 (9), 1959-1982.
- (33) Nelson, C. G.; Burke, T. R., Samarium Iodide-Mediated Reformatsky Reactions for the Stereoselective Preparation of α -Hydroxy- β -amino Acids: Synthesis of Isostatine and Dolaisoleucine. *J. Org. Chem.*, **2012**, 77 (1), 733-738.
- (34) Lin, N.; Chen, M.-M.; Luo, R.-S.; Deng, Y.-Q.; Lu, G., Indolinylmethanol catalyzed enantioselective Reformatsky reaction with ketones. *Tetrahedron: Asymm.*, **2010**, 21 (23), 2816-2824.
- (35) Imamoto, T.; Kusumoto, T.; Tawarayama, Y.; Sugiura, Y.; Mita, T.; Hatanaka, Y.; Yokoyama, M., Carbon-carbon bond-forming reactions using cerium metal or organocerium(III) reagents. *J. Org. Chem.*, **1984**, 49 (21), 3904-3912.
- (36) (a) Baldoli, C.; Del Buttero, P.; Licandro, E.; Papagni, A.; Pilati, T., Tricarbonyl chromium(0) complexes as chiral auxiliaries: asymmetric synthesis of aminoesters

- and lactams by Reformatskii condensation. *Tetrahedron* **1996**, 52 (13), 4849-56. (b)
- Wessjohann, L.; Gabriel, T., ChemInform Abstract: Chromium(II)-Mediated Reformatsky Reactions of Carboxylic Esters with Aldehydes. *ChemInform* **1997**, 28 (45).
- (37) Orsini, F., Reformatsky-type Co-mediated synthesis of hydroxyphosphonates. *Tetrahedron Lett.*, **1998**, 39 (11), 1425-1428.
- (38) Ashwood, M. S.; Cottrell, I. F.; Cowden, C. J.; Wallace, D. J.; Davies, A. J.; Kennedy, D. J.; Dolling, U. H., Copper-mediated reaction of 2-halopyridines with ethyl bromodifluoroacetate. *Tetrahedron Lett.*, **2002**, 43 (50), 9271-9273.
- (39) Cahiez, G. r.; Chavant, P.-Y., Organomanganese (II) reagents XX: Manganese mediated Barbier and Reformatsky like reactions an efficient route to homoallylic alcohols and α -acetoxyesters. *Tetrahedron Lett.*, **1989**, 30 (52), 7373-7376.
- (40) Tarui, A.; Ozaki, D.; Nakajima, N.; Yokota, Y.; Sokeirik, Y. S.; Sato, K.; Omote, M.; Kumadaki, I.; Ando, A., Rhodium-catalyzed Reformatsky-type reaction for asymmetric synthesis of difluoro- α -lactams using menthyl group as a chiral auxiliary. *Tetrahedron Lett.*, **2008**, 49 (24), 3839-3843.
- (41) Chattopadhyay, A.; Dubey, A. K., A Simple and Efficient Procedure of Low Valent Iron- or Copper-Mediated Reformatsky Reaction of Aldehydes. *J. Org. Chem.*, **2007**, 72 (24), 9357-9359.
- (42) Chattopadhyay, A.; Dubey, A. K., A Simple and Efficient Procedure of Low Valent Iron- or Copper-Mediated Reformatsky Reaction of Aldehydes. *J. Org. Chem.*, **2007**, 72 (24), 9357-9359.

- (43) Chattopadhyay, A.; Dubey, A. K., A Simple and Efficient Procedure of Low Valent Iron- or Copper-Mediated Reformatsky Reaction of Aldehydes. *J. Org. Chem.*, **2007**, 72 (24), 9357-9359.
- (44) Bieber, L. W.; Storch, E. C.; Malvestiti, I.; da Silva, M. F., Silver catalyzed zinc Barbier reaction of benzylic halides in water. *Tetrahedron Lett.*, **1998**, 39 (51), 9393-9396.
- (45) (a) Cozzi Pier, G., A catalytic, Me₂Zn-mediated, enantioselective reformatsky reaction with ketones. *Angew. Chem. Int. Ed.*, **2006**, 45 (18), 2951-4.
- (46) (a) Fernandez-Ibanez, M. A.; Macia, B.; Minnaard Adriaan, J.; Feringa Ben, L., Catalytic enantioselective reformatsky reaction with aldehydes. *Angew. Chem. Int. Ed.*, **2008**, 47 (7), 1317-9. (b) Fernandez-Ibanez, M. A.; Macia, B.; Minnaard, A. J.; Feringa, B. L., Catalytic Enantioselective Reformatsky Reaction with ortho-Substituted Diarylketones. *Org. Lett.*, **2008**, 10 (18), 4041-4044. (c) Fernandez-Ibanez, M. A.; Macia, B.; Minnaard, A. J.; Feringa, B. L., Catalytic enantioselective Reformatsky reaction with ketones. *Chem. Commun.*, (Cambridge, United Kingdom) **2008**, (22), 2571-2573.
- (47) Cozzi, P. G., A catalytic enantioselective imino-Reformatsky reaction. *Adv. Synth & Cat.*, **2006**, 348 (15), 2075-2079.
- (48) Rieke, R. D.; Hanson, M. V., New organometallic reagents using highly reactive metals. *Tetrahedron.*, **1997**, 53 (6), 1925-1956.

- (49) Kloetzing, R. J.; Thaler, T.; Knochel, P., An Improved Asymmetric Reformatsky Reaction Mediated by (-)-N,N-Dimethylaminoisoborneol. *ChemInform.*, **2006**, 37 (30), no-no.
- (50) A palladium-catalyzed and ultrasonic promoted Sonogashira coupling/1,3-dipolar cycloaddition of acid chlorides, terminal acetylenes, and sodium azide in one pot enables an efficient synthesis of 4,5-disubstituted-1,2,3-(NH)-triazoles in excellent yields. J. Li, D. Wang, Y. Zhang, J. Li, B. Chen, *Org. Lett.*, **2009**, 11, 3024-3027.
- (51) (a) Luche, J. L.; Petrier, C.; Gemal, A. L.; Zikra, N., Ultrasound in Organic-Synthesis .2. Formation and Reaction of Organocopper Reagents. *J. Org. Chem.*, **1982**, 47 (19), 3805-3806. (b) Luche, J. L.; Petrier, C.; Lansard, J. P.; Greene, A. E., Ultrasound in Organic-Synthesis .4. A Simplified Preparation of Diarylzinc Reagents and Their Conjugate Addition to Alpha-Enones. *J. Org. Chem.*, **1983**, 48 (21), 3837-3839. (c) Luche, J. L.; Petrier, C.; Dupuy, C., Ultrasound in Organic-Synthesis .5. Preparation and Some Reactions of Colloidal Potassium. *Tetrahedron Lett.*, **1984**, 25 (7), 753-756. (d) Luche, J. L.; Kagan, H. B., Stereochemistry in Beta-Lactam Series .V. Secondary Isotopic Effect of Deuterium and Mechanism of Reformatsky and Ketene Reactions on Schiff Bases. *Bulletin De La Societe Chimique De France.*, **1969**, (5), 1680. (e) Luche, J. L.; Kagan, H. B., Stereochemistry in Beta-Lactam Series .6. Reformatsky Reaction with Schiff Bases. *Bulletin De La Societe Chimique De France* **1969**, (10), 3500. (f) Luche, J. L.; Kagan, H. B., Some Comments on Addition of Reformatsky Reagents to Benzalaniline. *Bulletin De La Societe Chimique De France* **1971**, (6), 2260.

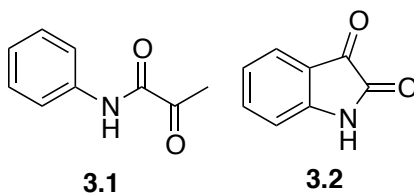
- (52) (a) Gopalaiah, K.; Kagan, H. B., Use of samarium diiodide in the field of asymmetric synthesis. *New Journal of Chemistry.*, **2008**, 32 (4), 607-637. (b) Kagan, H. B., Twenty-five years of organic chemistry with diiodosamarium: an overview. *Tetrahedron.*, **2003**, 59 (52), 10351-10372.
- (53) Mukaiyama, T.; Shiina, I.; Iwadare, H.; Saitoh, M.; Nishimura, T.; Ohkawa, N.; Sakoh, H.; Nishimura, K.; Tani, Y.-i.; Hasegawa, M.; Yamada, K.; Saitoh, K., Asymmetric Total Synthesis of Taxol R. *Chemistry – A European Journal.*, **1999**, 5 (1), 121-161.
- (54) Soengas, R. G.; Estevez, A. M., Indium-mediated allylation and Reformatsky reaction on glyoxylic oximes under ultrasound irradiation. *Ultrasonics: Sonochemistry.*, **2012**, 19 (4), 916-920.
- (55) Cozzi, P. G.; Rivalta, E., Highly enantioselective one-pot, three-component imino-Reformatsky reaction. *Angew. Chem. Int. Ed.*, **2005**, 44 (23), 3600-3603
- (56) (a) Babu, S. A.; Yasuda, M.; Shibata, I.; Baba, A., In- or In(I)-employed diastereoselective Reformatsky-type reactions with ketones: H-1 NMR investigations on the active species. *Org. Lett.*, **2004**, 6 (24), 4475-4478. (b) Babu, S. A.; Yasuda, M.; Shibata, I.; Baba, A., In- or In(I)-employed tailoring of the stereogenic centers in the Reformatsky-type reactions of simple ketones, alpha-alkoxy ketones, and beta-keto esters. *J. Org. Chem.*, **2005**, 70 (25), 10408-10419. (c) Babu, S. A.; Yasuda, M.; Okabe, Y.; Shibata, I.; Baba, A., High chelation control of three contiguous stereogenic centers in the Reformatsky reactions of

indium enolates with alpha-hydroxy ketones: Unexpected stereochemistry of lactone formation. *Org. Lett.*, **2006**, 8 (14), 3029-3032.

CHAPTER 3. STEREOSELECTIVE NUCLEOPHILIC ADDITION TO α -KETOAMIDES

3.1. Introduction

The α -ketoamide functionality and their derivatives are abundant in natural products and synthetic drug molecules.¹ Ketoamides have often been used as synthetic building blocks in developing inhibitors for peptidases such as HDACs², peptidyl prolyl isomerases (PPlases), serine proteases³, cysteine proteases⁴, HIV⁵ and FIV proteases. FK506 is one of many popular immunosuppressant drugs containing a α -ketoamide functionality.⁶ Numerous reports on the synthesis of α -ketoamides and its derivatives have been reported, due to their importance in the field of medicine. Based on the structure they can be simply categorized into linear α -ketoamides **3.1** and cyclic α -ketoamides **3.2** (Scheme 3.1).



Scheme 3.1. Linear and Cyclic α -ketoamides

A well-known cyclic α -ketoamide is isatin **3.2**.⁷ α -Ketoamides in general have a highly electrophilic carbonyl group due to the presence of the neighboring amide. Nucleophilic addition to this group results in useful molecules. Functionalizing isatin at the carbonyl carbon produces 3-substituted-3-hydroxy oxindole, which forms a core structure of numerous natural products.⁸ Interestingly, functionalized linear α -ketoamides and their applications are relatively less explored compared to their cyclic analogues. We have

developed enantioselective allylation methods for linear and cyclic α -ketoamides that will be discussed in this chapter.

3.2. Cyclic- α -Ketoamides: Isatin

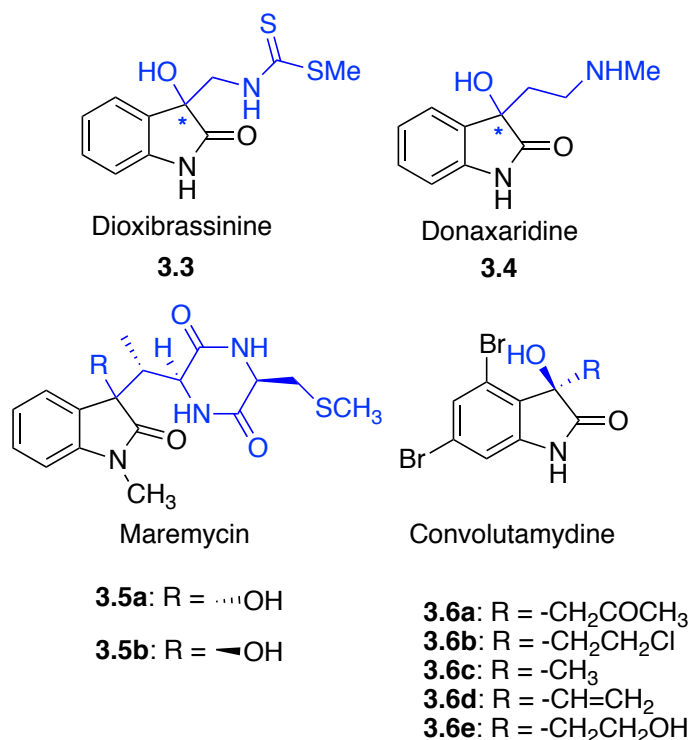
Synthetic interest in isatin and oxindole derived structures stems from a huge number of biologically active compounds and metabolites that includes isatin and oxindole as a principle core in their structure.⁹ For instance, 5-hydroxyoxindole, known as a urinary metabolite of indole has been identified to be associated with cerebro-spinal fluid. Increased amounts of oxindole and isatin in human blood and urine are associated with human neuropsychiatric syndromes. A systematic administration of isatin and oxindole could produce sedation and reversible coma.¹⁰ It is interesting to note that, it is not just isatin or oxindole that are active, but also the numerous natural products associated with them display biological activity. The molecules we find in nature evolved along with their respective targets allowing them to intersect the biological space effectively and often in a controlled fashion. Oxindoles are not an exception to this nature. The spectrum of biological activity, in addition to the synthetic challenges in constructing the oxindole frameworks resulted in a flurry of publications over the past decade. This showcases our efforts towards developing useful methodology using isatin and application of it toward the syntheses of some oxindole natural products.

3.2.1. 3-Substituted-3-hydroxy oxindoles from Isatin

3-Substituted-3-hydroxy oxindole is found to be the principal structure in variety of biologically active compounds and natural products.¹¹ It has been shown through different studies that the stereocenter at the 3-position has a great influence on their activity and could be used as a starting material for the synthesis of oxindole based molecules. As a

result of research over the past two decades, a clear understanding on the underlying cellular pathways for these molecules have been well established.¹² Several drug discovery programs working on these molecules enjoy this advantage in designing new libraries.

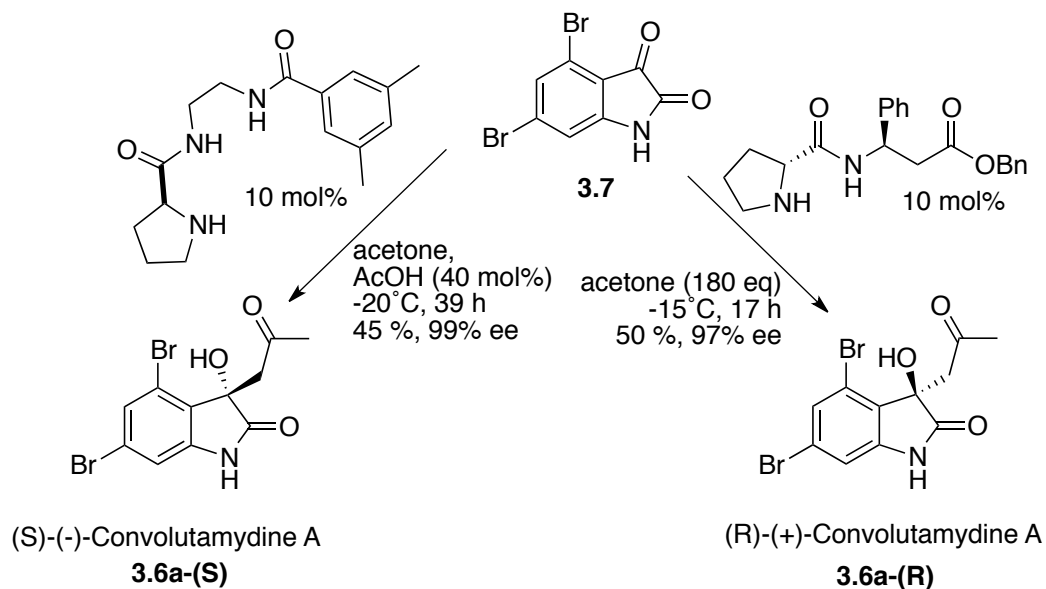
Scheme 3.2. illustrates some molecules based on 3-substituted-3-hydroxyoxindole skeleton. Convolutamydines A-E **3.6** is the first group of oxindole natural products isolated from marine bryozoan having anti-proliferative activity.¹³ The bromoindole moiety is often found in oxindole alkaloids extracted from marine organisms and believed to be involved in their repellent and antifeedant mechanism.¹⁴ Paratunamides A-D bearing secologanin units are architecturally unique oxindoles. They are the chief constituents of bio-active Brazilian ‘paratude’ plant used as a stomachic.¹⁵ Another unique oxindole alkaloid is arundaphine with bis-indole structure. Mareymicins are diketopiperazine alkaloids having some useful biological activity.



Scheme 3.2. 3-Substituted-3-Hydroxyoxindole Based Molecules

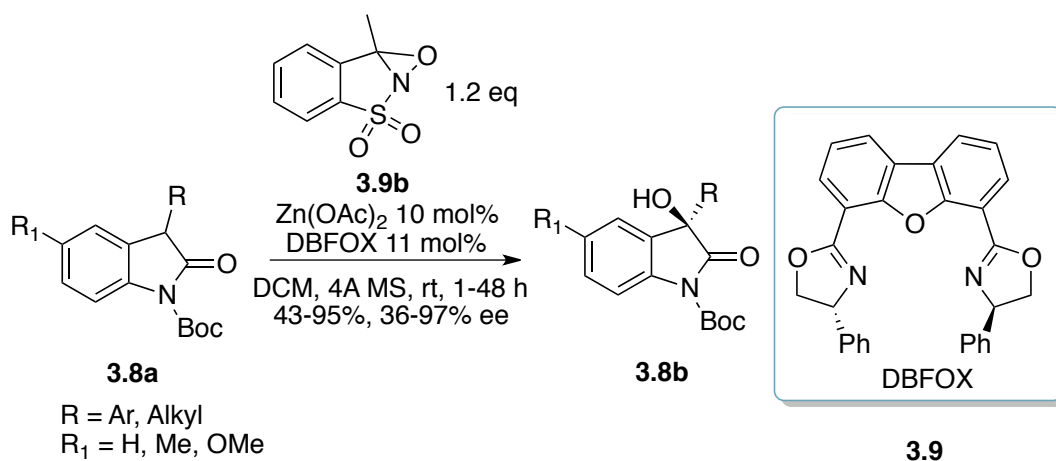
In the past decade, numerous strategies have been reported for the synthesis of these molecules. This includes metal mediated reactions and organocatalytic reactions. These reactions could be categorized broadly as 1) nucleophilic addition to isatins, 2) intramolecular arylations and 3) hydroxylation of 3-oxindoles. Most of these reports demonstrated total syntheses of useful molecules.

One of the profoundly used carbon-carbon bond forming reaction with oxindoles is aldol reaction.¹⁶ Great progress has been achieved with aldol reactions in the case of isatin substrates. However, only a limited number of molecules could be made from the aldol product of isatin. In addition to that, most of the methods require low temperatures and specially designed ligands. The reaction often produced low yield due to the highly unstable product that facile retro-aldol reaction. Tomasini reported a highly enantioselective aldol reaction with dibromo isatin **3.7** for the preparation of the biologically active natural product convolutamydin A **3.6a**. The enantioselectivity was achieved at low temperature using the specially designed proline based ligand to supply the chiral information (Scheme 3.3).¹⁷



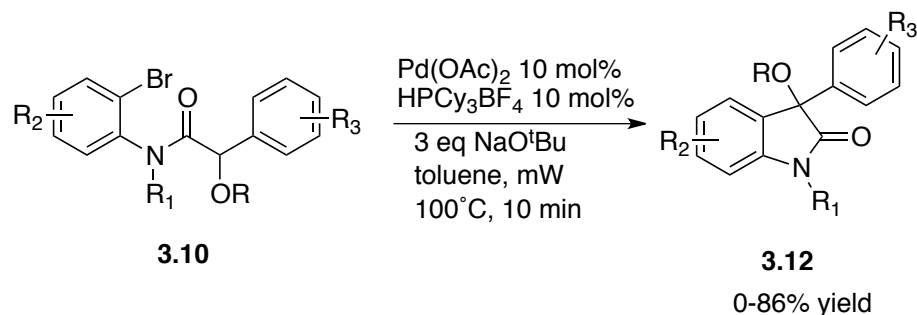
Scheme 3.3. Preparation of Convolutamydine A through Aldol reaction on Dibromoisatin

Recently, much attention has been paid to the asymmetric hydroxylation of oxindoles, another method for the synthesis of 3-substituted-3-hydroxy oxindoles. This procedure is not so attractive by the fact that not all 3-substituted oxindoles are available readily. Simple 3-methyl and 3-phenyl derivatives could be procured from commercial sources. In order to have functionalities for further expansion of the molecular structure, one would have to perform couple of synthetic transformations from parent oxindole prior to applying this methodology. Recently, Shibata and Toru reported a catalytic enantioselective hydroxylation of *N*-protected oxindoles using oxaziridine **3.9b** as a stoichiometric oxidant. In the presence of catalytic amount of Zn-DBFOX, 3-hydroxyl oxindole **3.8b** were obtained in enantioselectivities ranging from 36-97% (Scheme 3.4).¹⁸



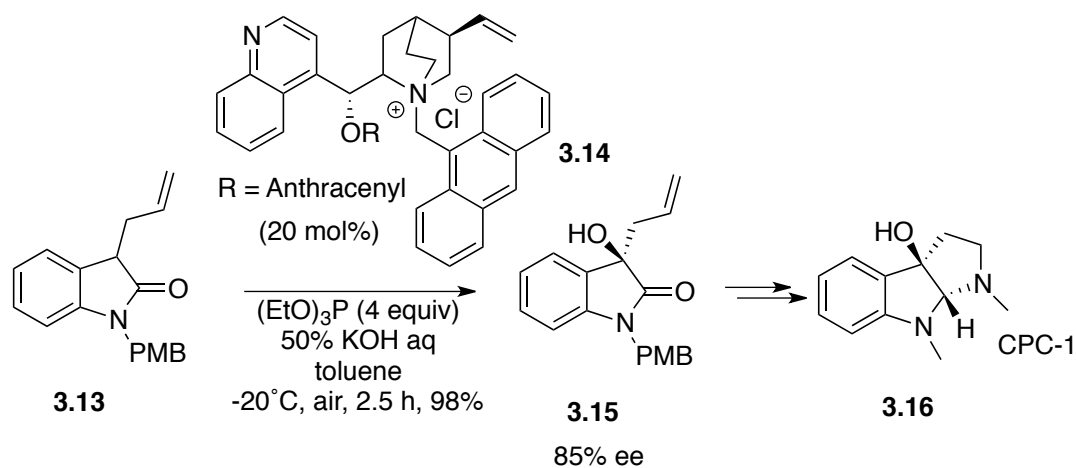
Scheme 3.4. 3-Hydroxylation of Oxindole Using Zinc acetate as Catalyst

Arylation of 3-hydroxy oxindoles is another interesting method to prepare 3-substituted-3-hydroxy oxindoles. This procedure involves intramolecular aryl transfer from aryl bromides to the C-3 carbon. This intramolecular aryl transfer has also been demonstrated on ketone carbons in an enantioselective fashion.¹⁹ This process is fundamentally interesting from a mechanistic point of view. For the practical applications preparation of the substrate is tedious. In addition to that these processes involves toxic and expensive transition metals. A Palladium catalyzed intramolecular arylation is described in Scheme 3.5. The enolate **3.10** is derived from 2-bromoaniline and mandelic acid (Scheme 3.5).²⁰



Scheme 3.5. Palladium Catalyzed Intramolecular Arylation of Oxindoles

A recent achievement with the asymmetric hydroxylation methodology towards the synthesis of useful natural products is hydroxylation of 3-allyl oxindole. A chinconidine derived phase transfer catalyst **3.14** has also been exploited for hydroxylation of *N*-Protected 3-allyl oxindole towards the synthesis of 3-allyl-3-hydroxy oxindole. A notable disadvantage is the required four equivalents of triethyl phosphite to achieve high yields. CPC-1 **3.16**, a tryptamine-derived alkaloid isolated along with several major constituents from the seeds and rinds of *C. praecox* f. *concolor*, was synthesized successfully using this methodology (Scheme 3.6).²¹

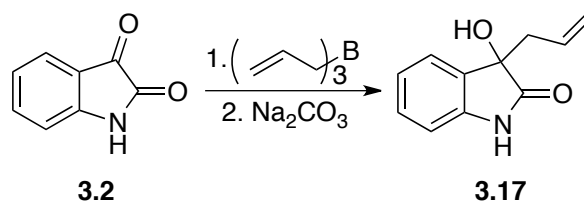


Scheme 3.6. Hydroxylation of 3-allyl oxindole

With the various methods available such as hydroxylation, arylation and aldol reaction, allylation is a versatile procedure. The terminal double bond is especially useful in syntheses involving sequentially increasing complexity. Metal-mediated entries for allylation are well-known procedures. The effectiveness of this allylation serves as a key for successful total synthesis of natural products and biologically active molecules since it involves the installation of the first stereocenter in oxindole nucleus. Being the first step of an elaborate synthesis they are often performed in a large scale.

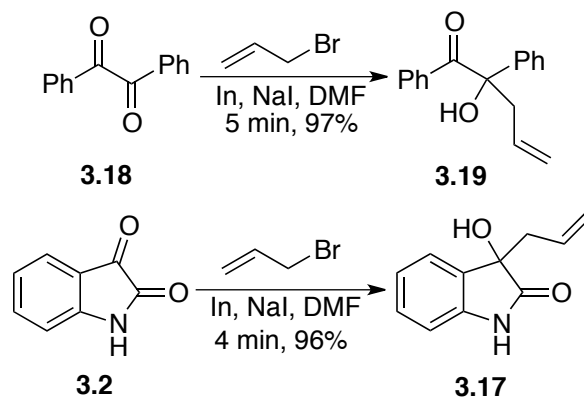
3.2.2. Allylation of Isatin

Asymmetric carbonyl allylation represents a versatile tool in the syntheses of stereo defined carbon frameworks. The product terminal alkene formed from the reaction could be converted to a variety of functional groups. One of the earliest reports that disclosed an effective way for allylation of isatin is allyl boration.²² Treatment of isatin **3.2** with triallylboron at 20°C under argon atmosphere followed by deboration upon treatment with sodium carbonate solution resulted in 67% yield of allyl isatin **3.17** (Scheme 3.7). The yields are not attractive and this method produced racemic product.



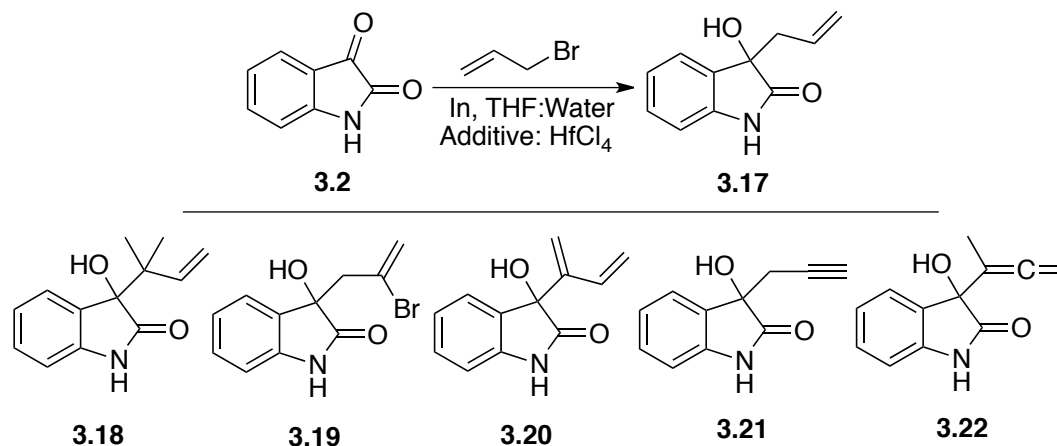
Scheme 3.7. Allylboration of Isatin

Nair and Jayan in 2001 prepared a variety of organoindium reagents in-situ using indium and allylic halides and reacted with a series of diketo compounds (Scheme 3.8).²³ Allyl, cinnamyl, propargyl and benzyl bromides reacted under indium-mediated condition in the presence of sodium iodide to produce racemic homoallylic alcohols.



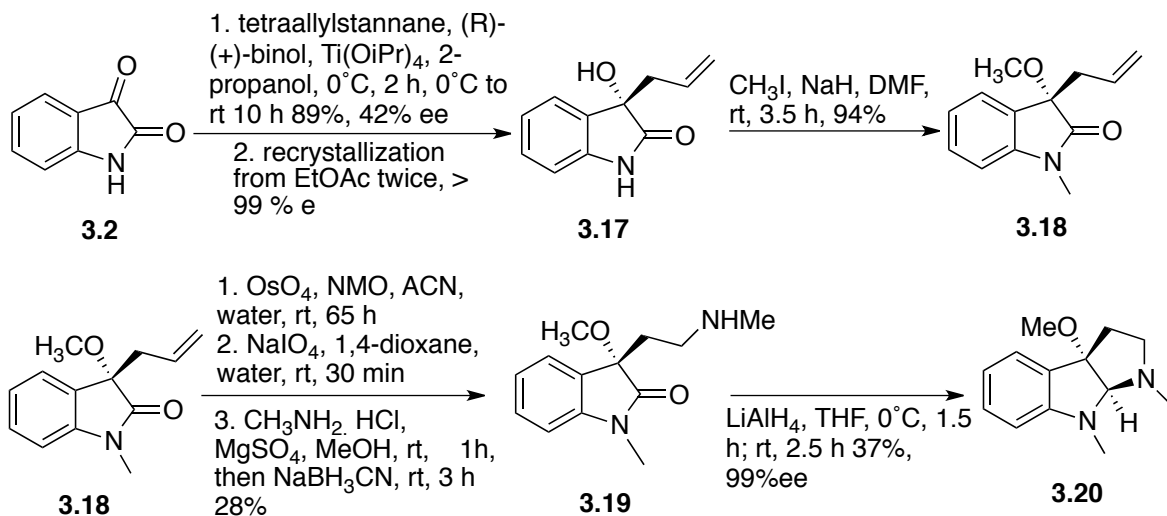
Scheme 3.8. Indium-Mediated Allylation of Isatin

Alcaide and co-workers reported an indium-mediated method for 3-substituted-3-hydroxyindolin-2-ones. Good control of regioselectivity was achieved in aqueous-THF.²⁴ The reaction required additives such as hafnium chloride, ammonium chloride or hydrobromic acid. Interesting insights into the regioselectivity issues in metal-mediated allylations have been presented in this report (Scheme 3.9).



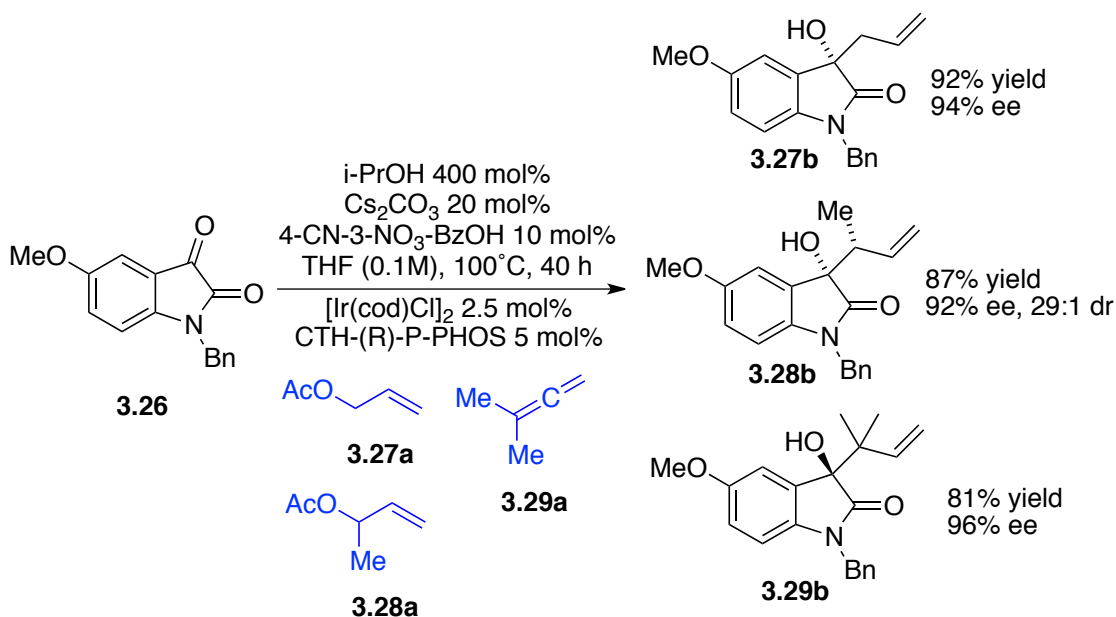
Scheme 3.9. Alkylation of Isatin in Aqueous-Solvent Mixtures

An enantioselective total synthesis of CPC **3.20** has been reported starting from isatin **3.2**. The synthesis involved an asymmetric allylation method using Ti-BINOL developed by Walsh and co-workers (Scheme 3.10). The method was not highly effective, requiring recrystallization to obtain more optically pure **3.17** and uses toxic tin reagent.



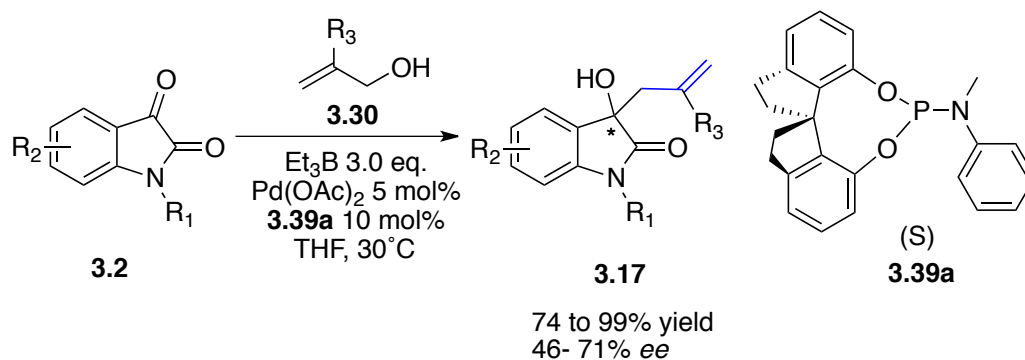
Scheme 3.10. Syntheses of a CPC Analogue Through Allylation of Isatin

In a departure from other procedures, Krishe reported a synthesis of allyl isatin using a transfer hydrogenation approach mediated by isopropanol (Scheme 3.11).²⁵ This method works effectively for N-protected isatins. This method suffers a disadvantage of using expensive iridium catalyst and a chiral phosphine.



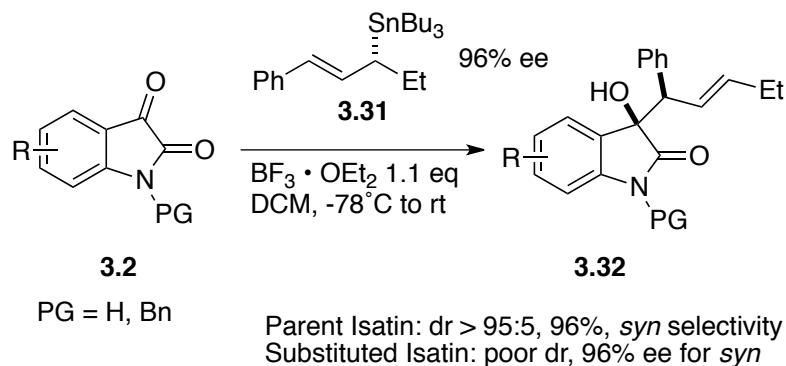
Scheme 3.11. Allylation of Isatins Through Transfer Hydrogenation

High temperature and long reaction times compromise the average yield and appreciable *ee* obtained through this method. Following these reports, Zhou and co-workers reported a highly alluring palladium catalyzed asymmetric allylation of isatins using spiro phosphoramidite ligand **3.39a** (Scheme 3.12).²⁶ The reaction uses allylic alcohols as the allyl donor. High enantioselectivity was achieved only with *N*-methyl isatin **3.2** ($R^1 = \text{CH}_3$) whereas other substituted isatins gave poor enantioselectivity. The use of expensive *P*, *N*-ligand under palladium catalyzed asymmetric allylation could not be envisioned as an effective starting point for a multistep synthesis of oxindole natural products.



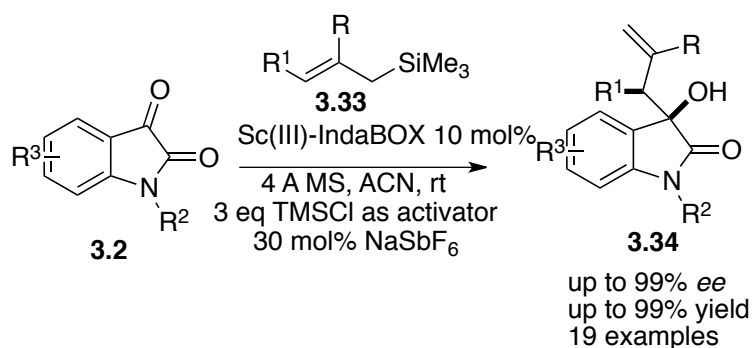
Scheme 3.12. Palladium-Catalyzed Asymmetric Allylation of Isatin

Vyas and co-workers reported stereoselective allylation of isatins using a chiral-allyltin reagent (Scheme 3.13).²⁷ The reaction required the used of a strong Lewis Acid, anhydrous atmosphere and low temperature and it is specific only to the parent isatin. Above all tin is a toxic metal, hence the protocol is not an attractive one for the synthesis of 3-substituted-3-hydroxy oxindoles.



Scheme 3.13. Alkylation of Isatin Using Chiral-Allyltin Reagent

Alkylation of carbonyl compounds using allylic silanes is also commonly referred to as Hosomi-Sakurai reaction. Franz and co-workers recently described a highly enantioselective method for the synthesis of allyl isatin through a scandium-IndaBOX catalyst (Scheme 3.14).²⁸ This is the first alkylation method that has been described in a gram scale. In spite of these attractive features, this protocol suffers disadvantages such as use of acetonitrile as solvent, requirement of additives and anhydrous reaction conditions.



Scheme 3.14. Hosomi-Sakurai type Allylation of Isatin using a Scandium Complex

It is evident from the above discussion that a significant progress has been made in the past two decades in the field of asymmetric allylation of isatins. Although a number of examples have achieved significant enantioselectivities, there is still a problem of operational simplicity and safety. Not even a single example involving reactions with low environmental impact has been reported till now. With substantial knowledge on

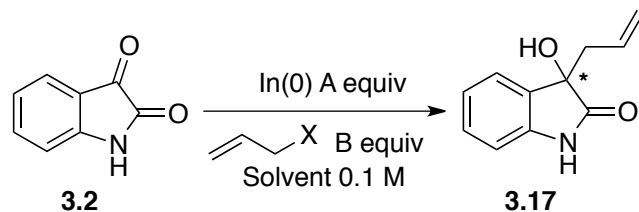
enantioselective allylation using indium metal and collective knowledge on oxindole chemistry, we sought to address this challenge to synthesize 3-allyl-3-hydroxyoxindoles in an environmentally benign fashion.

3.2.3. Results and Discussion

3.2.3.1. Solvent Screening and Optimization

Indium-mediated allylation reactions are known to proceed under aqueous solvent mixture conditions. The aim of this project is to develop such a reaction in a stereoselective fashion to obtain 3-allyl-3-hydroxyoxindoles in high optical purity. We began our screening with 2.0 equivalents of indium powder and 3.0 equivalents of allyl bromide and screened different solvents for the allylation of simple isatin **3.2** (Table 3.1). Polar aprotic solvents such as THF, acetonitrile, DMSO and DMF (Table 3.1. entry 1, 3, 6 and 8) did not facilitate the reaction. The allylation proceeded effectively resulting in near quantitative yield of allyl isatin in methanol. Interestingly the reaction did not proceed in absolute ethanol (Table 3.1. entry 5). No conversion was observed with DCM and chloroform at room temperature (Table 3.1. entry 7 and 9). The normal reaction time in methanol was 45 minutes and product formation could be indicated by the distinct color change in the reaction mixture from the bright orange color of isatin to colorless.

Table 3.1. Optimizing Indium-mediated Allylation of Isatins



Entry ^a	In(0) (A)	X	AllylHalide (B)	Solvent	%Yield ^b
1	2.0	Br	3.0	THF	0
2	2.0	Br	3.0	CH ₃ OH	>99
3	2.0	Br	3.0	CH ₃ CN	0
4	2.0	Br	3.0	Water	70
5	2.0	Br	3.0	C ₂ H ₅ OH	0
6	2.0	Br	3.0	DMF	0
7	2.0	Br	3.0	DCM	0
8	2.0	Br	3.0	DMSO	0
9	1.5	Br	2.0	CHCl ₃	0
10	3.0	Br	3.0	CH ₃ OH	>99
11	2.0	Br	2.0	CH ₃ OH	>99
12	1.5	Br	2.0	CH ₃ OH	>99
13	1.2	Br	2.0	CH ₃ OH	>99
14	1.5	I	2.0	CH ₃ OH	>99

^a reactions performed at rt and monitored until completion by tlc. ^b Isolated yields.

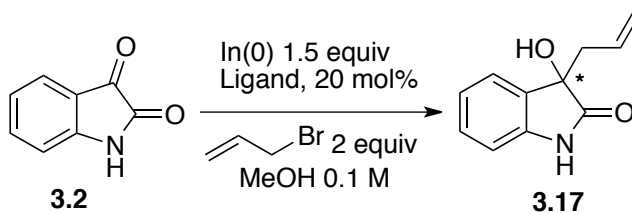
Methanol is considered as a green solvent; it can be obtained from non-fossil sources. Hence, we decided to continue our study with methanol. The reaction requires stoichiometric amount of indium metal but it is always attractive to use the minimum amount of metal. Table 3.1. Entry 10, 11, 12 and 13 indicates that we could achieve quantitative yield with as low as 1.2 equivalents of indium metal and 2.0 equivalents of allyl bromide. Allyl iodide is as effective as allyl bromide as a nucleophilic precursor.

Compared to allyl iodide allyl bromide is cheap and readily available in large quantities in relatively pure form. Hence we decided to optimize this method with allyl bromide.

3.2.3.2. Ligand Screening

Through a proper ligand screening we decided to identify a suitable ligand for the allylation of isatin substrates. The identified ligand will impart chiral information on the 3-position of the isatin molecule through a proper binding to the substrate and the allylindium reagent. Our quest for high enantioselectivity began by screening various ligands shown in Table 3.2. We screened chiral thiourea, P-N- ligand, amino alcohol derived ligand **3.35** and chiral diamine **3.40**. The reaction was carried out with 20-mol % of chiral additive, 1.5 equivalents of indium powder and 2.0 equivalents of allyl bromide with simple isatin in methanol. None of the ligand indicated in Table 3.2 gave enantioselectivity. In all the entries described in Table 3.2, the product allylisatin **3.17** was observed in near quantitative yield. But there was no stereo induction. This observation could be inferred as the failure of the chiral ligand to bind to the substrate effectively. Additionally, if the ligand interferes in the process of the formation of the organoindium reagent, it would be evident from the yield of the reaction. This was also not observed through the ligand screening experiment since all the trials gave us near quantitative yield.

Table 3.2. Initial Ligand Screening for Allylation of Isatins

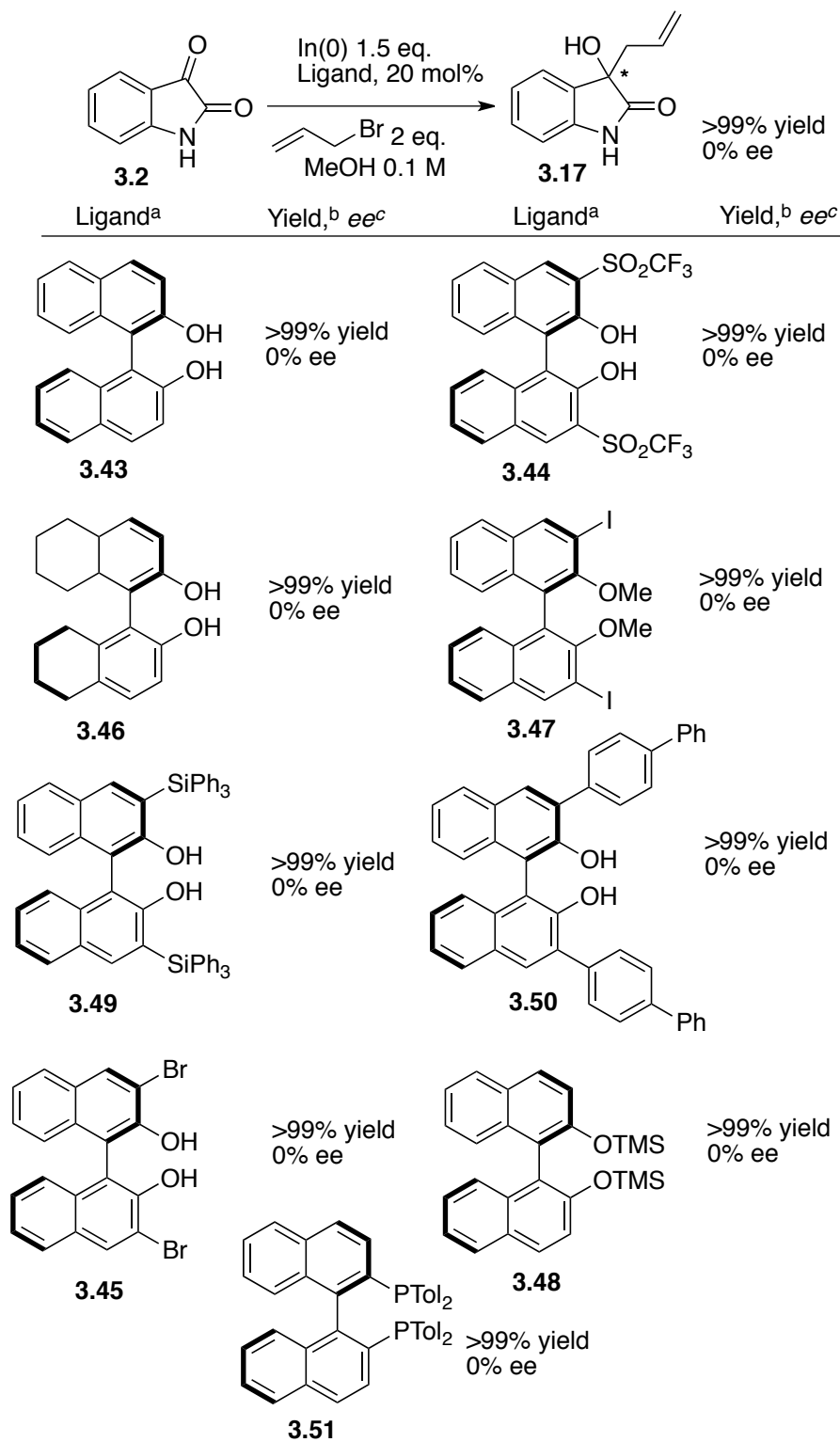


Ligand ^a	Yield, ^b ee ^c	Ligand ^a	Yield, ^b ee ^c
 3.40	>99%, 0% ee	 3.36	>99%, 0% ee
 3.39b	>99%, 0% ee	 3.42	>99%, 0% ee
 3.35	>99%, 0% ee	 3.41	>99%, 0% ee
 3.38	>99%, 0% ee	 3.37	>99%, 0% ee

^a reactions performed at rt and monitored until completion by TLC. ^b Isolated yields. ^c ee was determined by chiral HPLC

Our group has achieved remarkable success with chiral BINOL ligand for indium-mediated allylation. We have previously shown that BINOL based ligands, CF₃ and SO₂CF₃ BINOLs produce excellent enantioselectivity for indium-mediated allylation of imines.²⁹ From the discussion in the previous section on allylation of isatins, literature report using titanium Lewis acid and simple BINOL has been discussed. These facts motivated us to perform a ligand screening with some chiral BINOLs (Table 3.3). Electronic modification by incorporating withdrawing groups did not affect the enantioselectivity. In the case of imine substrates, we found that highly electron deficient BINOLS **3.44** provided us the homoallylic amine product in high optical purity. But the same ligand did not impart any chiral information the product in this reaction. We screened some sterically modified BINOLS such as **3.50** and **3.49** produced only racemic product **3.17**. Use of protected BINOLS **3.47** and **3.48** also resulted in failure. In a final attempt we used chiral BINAP as to see if the phosphines would be compatible with indium-mediated allylation. Dissapointingly they did not impart any chirality on the product as well. Thus none of the BINOLs gave any enantioselectivity in the indium-mediated allylation of isatins.

Table 3.3. Ligand Screening- BINOL Derivatives



^a reactions performed at rt and monitored until completion by TLC. ^b Isolated yields. ^c ee was determined by chiral HPLC

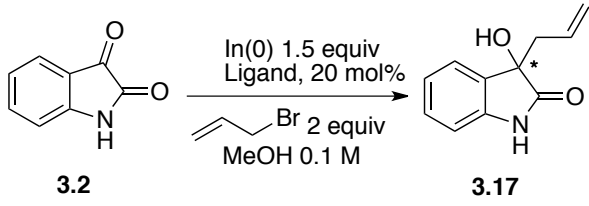
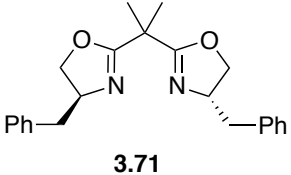
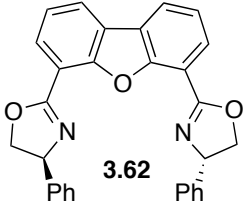
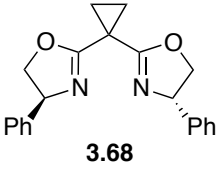
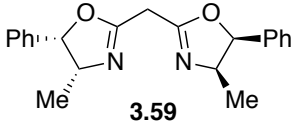
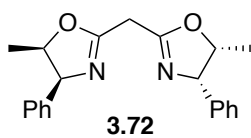
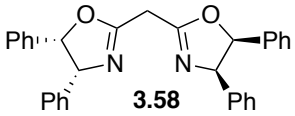
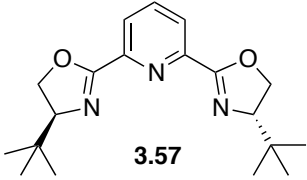
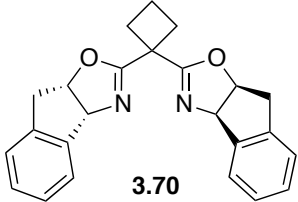
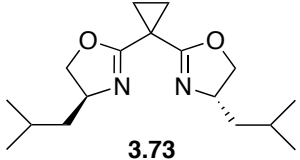
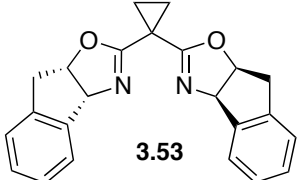
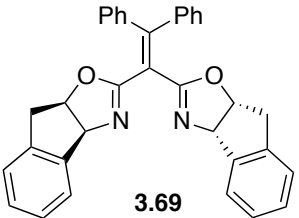
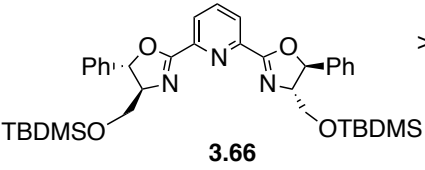
Another set of ligand that was available in our ligand library was the chiral bisoxazoline ligand. The choice of bis-oxazoline ligands was dictated by our results from bismuth-mediated allylation of isatins. Also from Table 3.2, ligands **3.55** and **3.42** are chiral oxazoline ligands, which did not impart any chiral information on the product. Hence, the further screening of the oxazoline ligand was confined to bis oxazoline ligands. The availability of a variety of bis-oxazoline ligands with varying steric volumes increased our ligand screening entries. The Ligand screening is presented in two tables Table 3.4 and Table 3.5. We screened a series of bi dentate bis oxazoline ligands such as **3.52**, **3.60**, **3.54**, **3.55**, **3.71**, **3.68**, **3.72**, **3.73**, **3.69**, **3.53**, **3.70**, **3.58**, **3.59**. The bi dentate bis oxazoline produced only the racemic product **3.17**. In the screening of tridentate bis oxazoline ligands, we found interestingly that isopropyl PYBOX **3.57** gave us 30% *ee*. We increased the steric bulk by using the TBDMS protected bis-oxazoline **3.66**, which induce the enantioinduction only up to 20%. To our delight (S)-Ph-PyBOX **3.65** gave us 54% *ee* for simple isatin. The modification of phenyl-PyBOX, a *p*-methoxy derivative **3.67** gave us 33% enantioselectivity. The use of other tridentate ligand from furan, DBFOX **3.62** did not induce optical purity. The furan analog of Ph-PyBOX, ligand **3.63** induced 30% enantioselectivity. Based on these results we decided to proceed with phenyl-PyBOX ligand for the methodology.

Table 3.4. Ligand Screening- BOX Ligands

Ligand ^a	Yield, ^b ee ^c	Ligand ^a	Yield, ^b ee ^c
	>99%, 0% ee		>99%, 0% ee
	>99%, 0% ee		>99%, 0% ee
	>99%, 0% ee		>99%, 35% ee
	>99%, 0% ee		>99%, 54% ee
	>99%, 33% ee		>99%, 54% ee

^a reactions performed at rt and monitored until completion by TLC. ^b Isolated yields. ^c ee was determined by chiral HPLC

Table 3.5. Ligand Screening- BOX Ligands

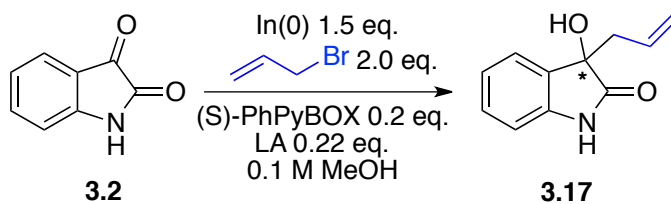
			
Ligand ^a	Yield, ^b ee ^c	Ligand ^a	Yield, ^b ee ^c
 <p>3.71</p>	>99%, 0% ee	 <p>3.62</p>	>99%, 0% ee
 <p>3.68</p>	>99%, 0% ee	 <p>3.59</p>	>99%, 0% ee
 <p>3.72</p>	>99%, 0% ee	 <p>3.58</p>	>99%, 0% ee
 <p>3.57</p>	>99%, 30% ee	 <p>3.70</p>	>99%, 7% ee
 <p>3.73</p>	>99%, 10% ee	 <p>3.53</p>	>99%, 13% ee
 <p>3.69</p>	>99%, 0% ee	 <p>3.66</p>	>99%, 20% ee

^a reactions performed at rt and monitored till completion by TLC. ^b Isolated yields. ^c ee was determined by chiral HPLC

3.2.3.3. Survey of Lewis Acids

After determining an appropriate source of chirality, the next and most important focus of our study was to evaluate the effect of the Lewis acid in the reaction. The range of Lewis acids were confined to indium and bismuth. Surprisingly enough we found that indium Lewis acids such as InCl_3 , InBr_3 , InF_3 gave the same level of enantioselectivity as compared to the reaction in the absence of added Lewis acid (Table 3.5. entry 1, 2 and 3). We speculated that an *in situ* generated chiral-indium-Lewis acid was responsible for the asymmetric induction. Addition of indium(I) and indium(II) salts did not enhance the selectivity either (Table 3.5. entry 5, 6 and 7). Addition of indium triflate (Table 3.5. entry 4) on the other hand decreased the enantioselectivity. We attribute the possible generation of triflic acid *in situ* as a reason for the acceleration of background reaction and hence the observed erosion in optical purity. Bismuth Lewis acids decreased the enantioselectivity. There could be a possible competition between indium and bismuth Lewis acids for binding with the ligand. This competition could be very well the reason for the decrease in *ee*. Yet another reason to confine the screening to indium and bismuth Lewis acids is to preserve the “green” character of the procedure.

Table 3.6. Lewis Acid Screening



Entry ^a	LA	% Yield ^b	% ee ^c
1	InBr ₃	>99	53
2	InCl ₃	>99	55
3	InF ₃	>99	53
4	In(OTf) ₃	>99	20
5	InBr	>99	54
6	InCl ₂	>99	54
7	InI	>99	54
8	BiBr ₃	>99	19
9	BiF ₃	>99	20
10	BiI ₃	>99	15
11	BiCl ₃	>99	20
12	Bi(OTf) ₃	>99	36

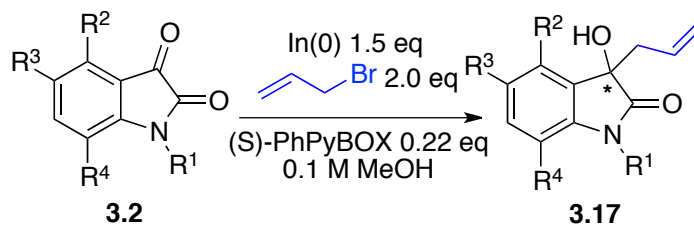
^a Reactions performed at rt and monitored until completion by TLC. ^b Isolated yields. ^c ee by chiral HPLC.

3.2.3.4. Scope of Isatins

The role of the substituent on the *N*-1 nitrogen was first evaluated in the indium-mediated allylation of isatins. The first set of experiments utilized *N*-methyl and *N*-phenyl isatin. When we used electron-donating substituents on the *N*-1 nitrogen, we found erosion in enantioselectivity. *N*-phenyl isatin and *N*-methyl isatin gave 30% and 35% respectively (Table 3.7. entry 1 and 2) *N*-allyl isatin gave 33% enantioselectivity (Table 3.7. entry 13). These results clearly indicated that the *N*-substitution has a strong effect on the enantioselection. With the use of *N*-acetyl isatin as a substrate (Table 3.7, entry 3) we

observed deacetylation. Reasons for this nature of the method are not probed completely. When unprotected isatins were used, an increase in the enantioselectivity was observed. A series of 5-substituted isatins were procured from commercial sources and subjected to indium mediated allylation conditions.

Table 3.7. Substrate Scope for Isatins



Entry ^a	SM	R ¹	R ²	R ³	R ³	Product	% Yield ^b	% ee ^c
1	3.2a	CH ₃	H	H	H	3.17a	>99	35
2	3.2b	C ₆ H ₅	H	H	H	3.17b	90	30
3 ^d	3.2c	Acetyl	H	H	H	3.17c	0	NA
4	3.2d	H	H	Br	H	3.17d	>99	45
5	3.2e	H	H	CH ₃	H	3.17e	>99	41
6	3.2f	H	H	I	H	3.17f	95	57
7	3.2g	H	H	OCF ₃	H	3.17g	90	55
8	3.2h	H	H	F	H	3.17h	92	50
9	3.2i	H	CH ₃	H	CH ₃	3.17i	>99	90
10	3.2j	H	Br	H	H	3.17j	95	88
11	3.2k	H	H	H	t-butyl	3.17k	90	40
12	3.2l	H	H	H	H	3.17l	>99	54
13	3.2m	Allyl	H	H	H	3.17m	>99	30

^a reactions performed at rt and monitored until completion by TLC. ^b Isolated yields. ^c ee by chiral HPLC. ^d Deacetylation occurred.

The 5-position on the oxindole core had moderate effect on the selectivity. Substrates **3.2d**, **3.2e**, **3.2f**, **3.2g**, **3.2h** were purchased from commercial sources. The modification of electron donating and electron withdrawing groups did not have a significant effect on the enantioselection. It is worth to mention that electron-donating

methyl group on the 5-position (Table 3.7, entry 5) affected the optical purity of the product to some extent compared to the other five substituted isatins. 5-nitro isatin not specified in this table was also subjected to the reaction condition. Interestingly the reaction did not proceed. We believe that the nitro group present on the substrate is probably interfering in the formation of the allyl indium reagent.

After investigating the 5-position we probed the method by using 4-substituted isatins. When the commercially known 4-bromo isatin **3.2j** is used in the methodology interestingly we found that the reaction produced the allylated product in 88% enantioselectivity. This remarkable increase in the enantiopurity of the product motivated us to prepare the 4,7-dimethyl isatin **3.2i**. The 4,7 derivative gave us 90% enantioselectivity. Probing the 7- position was unfruitful; the 7-tert-butyl isatin **3.2k** gave poor enantioselectivity (Table 3.7, entry 11). Thus the generality of this methodology was probed using sterically as well as the electronically modified isatins. The yield of the reaction was appreciably high. Near quantitative yield was obtained for most of the isatins. The difference in the enantioinduction could be studied by probing into the nature of the chiral-Lewis acid complex that is presumably generated *in situ*. The major isomer from the allylation methodology developed was identified as (*R*), when (*S*)-Ph-PyBOX was used as a ligand (Figure 3.1). The product structure was studied using X-ray crystallography and the absolute configuration was confirmed with the optical rotation value from the literature

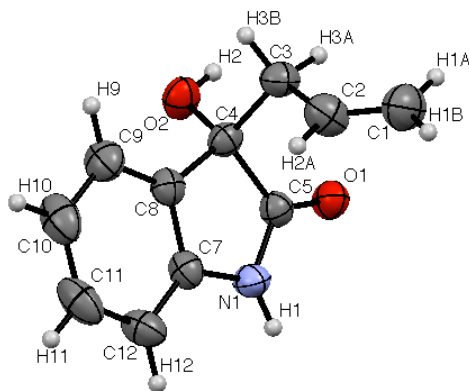


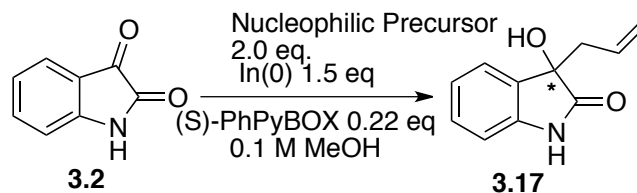
Figure 3.1. Thermal Ellipsoid Plot of (*R*)- Allyl isatin at 50% Probability Level

3.2.3.5. Scope of Nucleophilic Precursors: Preliminary Results

We were pleased with the results from the substrate screening of isatins, but wished to expand the nucleophilic precursor scope to include other substituted allylic bromides. This would also expand the scope of useful molecules constructed from the obtained 3-substituted-3-hydroxy oxindole. Introducing additional substituents also introduces the issue of regioselectivity. The regioselectivity in most of the metal-mediated processes is a function of the nature of both the metal and the nucleophilic precursor. Thus keeping the nucleophilic precursor the same, different regioselectivity could be achieved using different metals. Introducing additives plays a crucial role in changing the regioselectivity. For instance, propargylic halide upon reaction with indium metal produces two species that are in equilibrium- allenyl and propargyl indium. The reaction of the allenyl indium species with the electrophile produces the propargylated product. The reaction of the propargyl indium species with the electrophile produces allenylated product. In our investigation we observed complete regioselectivity for propargylated product **3.76** and **3.77** when we used TMS as well as methyl propargyl bromide. In most of the cases, 50:50 ratio of both the

regioisomers were observed. Literature evidence also suggests that using substituents on the propargyl halide could change this regioselectivity.³⁰ In the case of crotylation we observed an excellent stereocontrol with 4-bromoisatin. The product **3.75** was obtained in 3:1 diastereoselectivity. We were able to obtain the crystal structure of the major isomer (Figure 3.2.).

Table 3.8. Scope of Nucleophilic Precursors



Nucleophilic Precursor	Product
	<p>Quant. Yield 63% <i>ee</i></p> <p>3.18</p>
	<p>Quant. Yield 63% <i>ee</i></p> <p>3.74</p>
	<p>Quant. Yield 3:1 dr (87%, 47% <i>ee</i>)</p> <p>3.75</p>
	<p>Quant. Yield 0% <i>ee</i></p> <p>3.76</p>
	<p>Quant. Yield 0% <i>ee</i></p> <p>3.7</p>

^a reactions performed at rt and monitored until completion by tlc. ^b Isolated yields. ^c *ee* by chiral HPLC.

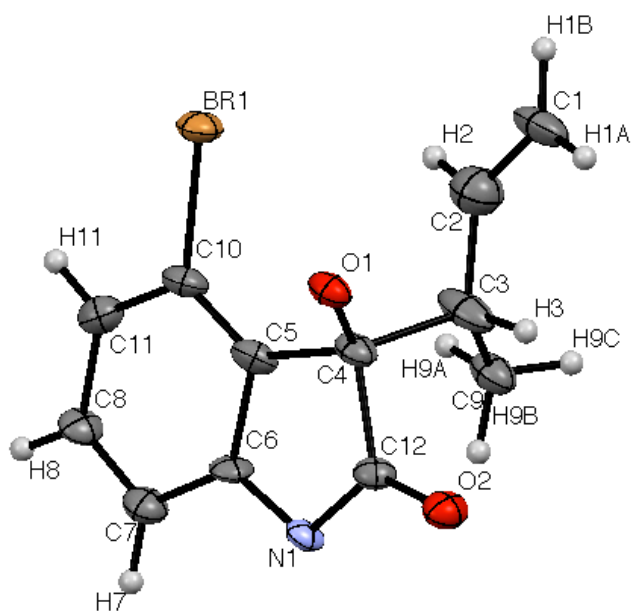
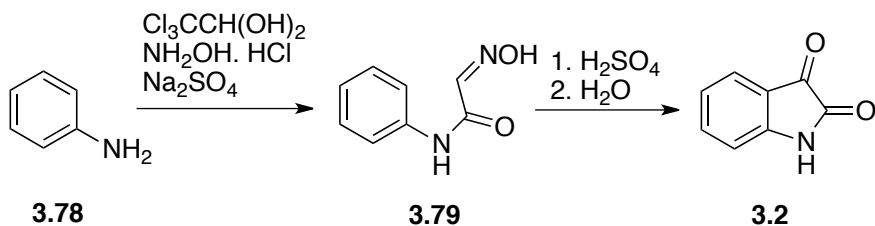


Figure 3.2. Thermal Ellipsoid Plot of Crotylated Product at 50% Probability Level

3.2.3.6. Synthesis of Isatins

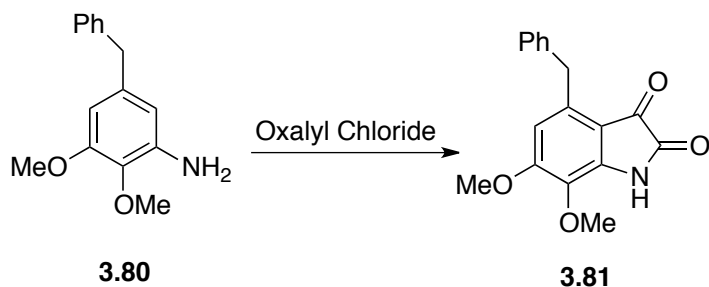
Isatin was first prepared by oxidation of indigo using chromium oxidants.³¹ The oldest procedure for large-scale synthesis of isatin is the one developed by Sandmeyer.³² The reaction involves preparation of isonitrosoacetaniline by the action of hydroxylamine and sodium sulfate on aniline. Subsequent treatment of this intermediate with sulfuric acid gives isatin in appreciable yields. This procedure has been modified many times over the years, but the principal reaction remains the same: preparation of a suitable intermediate from aniline and treat it with a Lewis acid or a Bronsted acid to perform an electrophilic addition to the aromatic ring resulting in cyclization.



Scheme 3.15. Sandmeyer's Synthesis

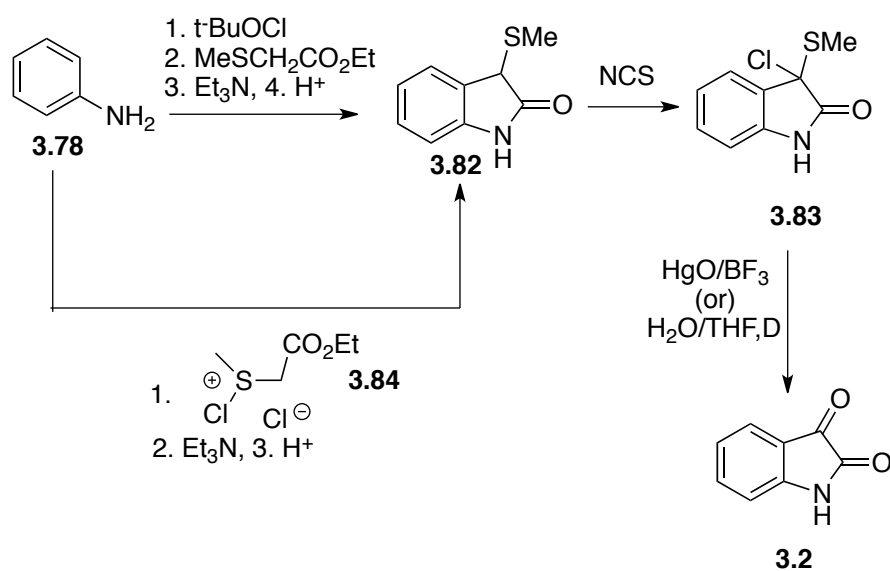
The use of microwave irradiation instead of heating has been reported for both the steps. The yields of Sandmeyer's protocol differed based upon the electronic nature of the aniline. Sandmeyer's protocol failed if the aniline was appreciably electron rich. *N*-Substituted anilines gave poor yield or did not undergo the reaction using this method. Meta-substituted anilines produced isomeric products. One of the main reagents in the above transformation is chloral hydrate, used in anesthesia for a long time and currently regulated in the United States and several other countries. The purity and the state of chloral hydrate are vital for this reaction. An alternate for chloral hydrate includes 2,2-diacetoxy acetylchloride prepared from glyoxalic acid in 2 steps and is effective than chloral hydrate for some substrates. All these modifications still suffer limitations such as low yields and use of a strong acid such as sulfuric acid for the second step of the reaction that involves the Friedel-Crafts cyclization.

To overcome all these difficulties of using chloral and its alternatives as well as sulfuric acid, Stolle reported a convenient method with oxalyl chloride. In Stolle's procedure chlorooxalyl anilide was prepared by the action of oxalyl chloride on aniline. The cyclization of this acyl chloride could also be facilitated by Lewis acids such as TiCl_4 , $\text{BF}_3 \cdot \text{Et}_2\text{O}$ or anhydrous AlCl_3 . Yet again the reaction was not general and required optimization based on each aniline substrate. For example, Melosatin A was synthesized in 5% yield (Scheme 3.16).³³



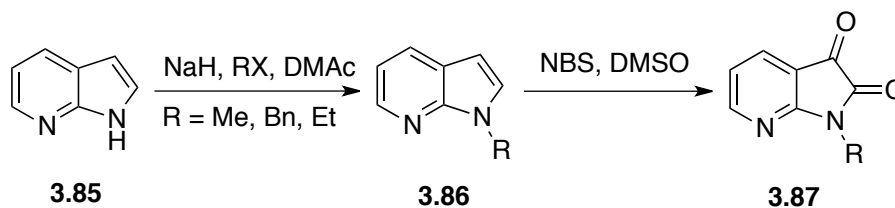
Scheme 3.16. Stolle's Procedure For Synthesis of Melosatin A

It has been observed from our group and others that the choice of Lewis acid in the cyclization step improves the yield considerably. While both Stolle's method and Sandmeyer's method involve the use of electrophilic cyclization, Gassmann introduced a new method involving 3-methylthio oxindole (Scheme 3.17).³⁴ Aniline is converted into 3-methylthio oxindole **3.82** through a series of steps. Oxidation of **3.82** could be achieved effectively using *N*-chloro succinimide. The intermediate **3.83** formed after this step is hydrolyzed to produce isatin. This procedure is effective but involves multiple steps.



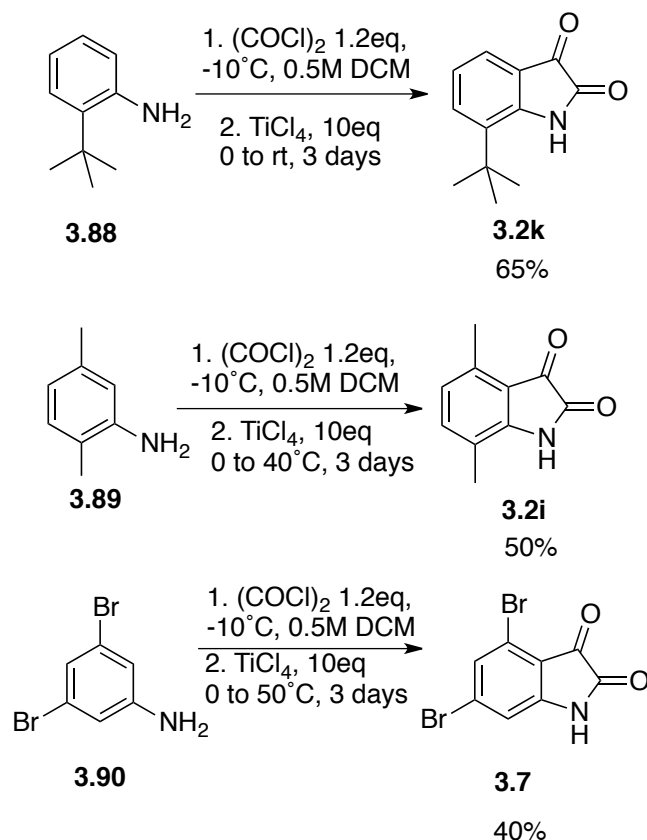
Scheme 3.17. Gassmann's Procedure

Izawa and co-workers reported an efficient one-pot method for conversion of indoles to isatins (Scheme 3.18). A drawback in this process was the requirement for the protection of the indole nitrogen.³⁵



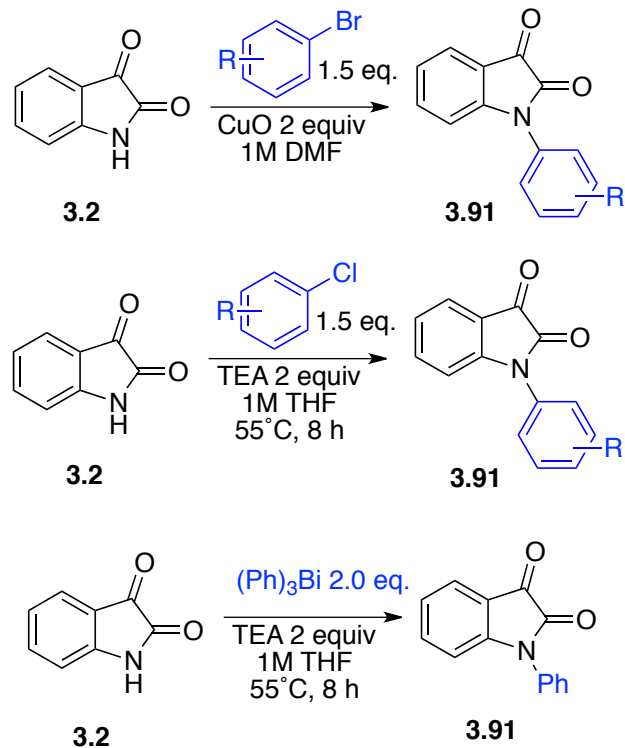
Scheme 3.18. Synthesis of Isatins from Indole

Presently numerous reports exist in literature for the synthesis of isatin.³⁶ In connection with the present research, we were in need of unusual isatins to study substituent effects. To solve this substrate requirement and to keep the procedure simple we decided to use the traditional approach of electrophilic cyclization. Through modified Stolle's procedure we were able to successfully synthesize three different isatins as shown in the Scheme 3.23. We screened Lewis acid and conditions for the second step and found that titanium tetrachloride was efficient to effect the cyclization. The temperature of the reaction was optimized to achieve appreciable yield of the isatins **3.2k**, **3.2i** and **3.7**.



Scheme 3.19. Modified Stolle's Procedure

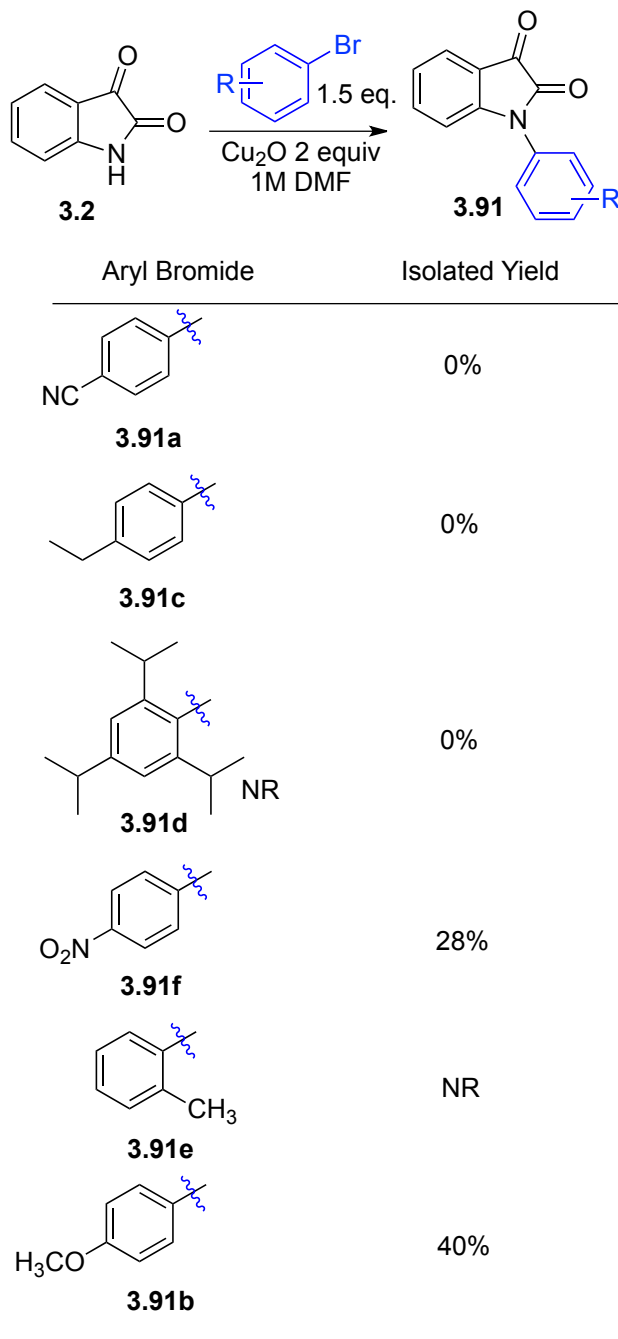
During the later part of the development of this project, we decided to prepare a series of *N*-arylisatins. The modified Stolle's procedure would work for these substrates but will require additional steps to prepare the aniline-starting material. It would also result in regioisomeric mixtures during the cyclization step. To approach this problem through a different route we decided to use *N*-arylate isatins. Procedures for *N*-arylation of amides in the literature are not abundant.³⁷ The intrinsic non-nucleophilic character of the amides make the conditions that will work for amines fail when applied to amides. Among the few reports, we found a protocol that uses copper oxide and could be applied to our desired substrates.



Scheme 3.20. Common N-Arylation Procedures

Using slightly modified conditions from the one reported in the literature, we were able to prepare few N-substituted isatins in appreciable yields. The modified condition uses copper (I) oxide instead of copper (II) oxide. Table 3.8 describes the different N-arylated isatins prepared through this protocol. We were successful in synthesizing *p*-methoxyphenyl **3.91b** and *p*-nitrophenyl **3.91f** substituted isatins (Table 3.9).

Table 3.9. Synthesis of *N*-Arylated Isatins



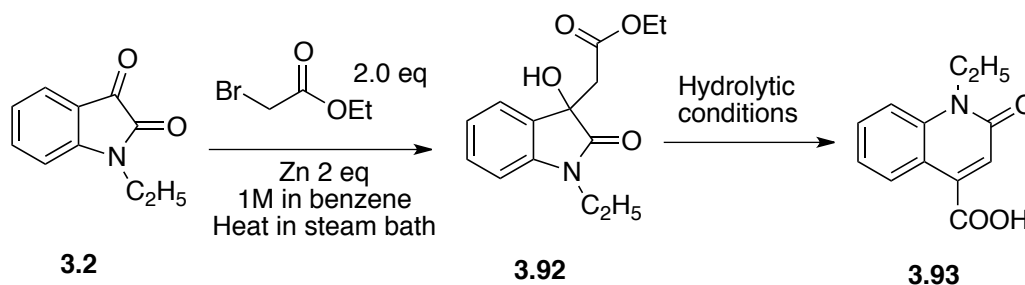
3.2.4. Summary of Isatin Alkylation

A characteristic of this methodology is that there was not a necessity for *N*-protection of isatin unlike the other existing methods. Evaluation of the scope and limitations of this methodology allowed us to devise and execute synthetic protocols for

different oxindole natural products in a relatively easier fashion. The reaction used neither chlorinated solvents nor anhydrous conditions. Perhaps serving as a defining example of the often-used term “environmentally benign” process; additionally this methodology offers an operationally simple protocol to make 3-allyl-3-hydroxy oxindoles.

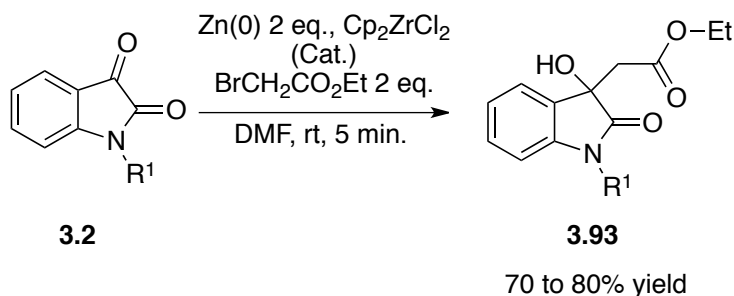
3.3. Expanding the Utility: Addition of Enolates to Isatin

In an effort to dramatically increase the scope of indium-mediated Reformatsky reaction, isatins were employed as electrophiles. Myers and Lindwall have reported Reformatsky reactions on isatin as early as 1936.³⁵ Unprotected simple isatins did not react under this classical condition using zinc metal and ethyl bromoacetate and refluxing in benzene. They also demonstrated that under aqueous conditions the β -hydroxy ester could be converted into 2-quinolone **3.93** as shown in step 2 (Scheme 3.21).



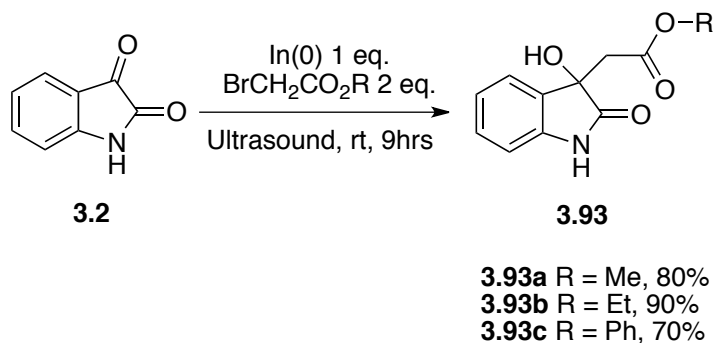
Scheme 3.21. Reformatsky Reaction of N-Protected Isatins

A recent report by Nair and co-workers demonstrated the use of zinc-mediated Reformatsky reaction promoted by catalytic amount of zirconocene complex in DMF (Scheme 3.22). The reaction was complete within few minutes to produce racemic **3.93**. This is the only other report that exists in the literature other than the original report by Myers and Lindwall. This procedure also requires the *N*-protection of isatins to participate in the reaction



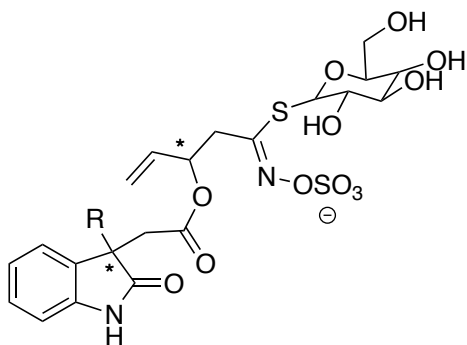
Scheme 3.22. Zinc-Mediated Reformatsky Reaction on Isatin

We have utilized our indium mediated Reformatsky reaction for isatins. In 8 to 9 hours with various α -bromoacetates at room temperature, we were able to isolate up to 85% of β -hydroxy esters of isatins (Scheme 3.23.). For the first time we were able to isolate the Reformatsky products of parent isatin **3.93**.



Scheme 3.23. Indium-Mediated Reformatsky Reaction on Isatin

This methodology could be potentially applied to the total synthesis of an interesting molecule- *glucoisatisin* **3.94**. This molecule is isolated from *Isatis tinctoria* L, a common plant in Mediterranean countries to produce indigo dye (Scheme 3.24.). The interesting architecture of *glucoisatisin* could be directly addressed using our Reformatsky reaction. The total synthesis of this molecule is currently under way in our group.



3.94a R = H, glucoisatisin (*R*) and epiglucoisatisin (*S*)
3.94b R = OH, 3'-glucoisatisin (*R*) and 3'-hydroxyepiglucoisatisin (*S*)

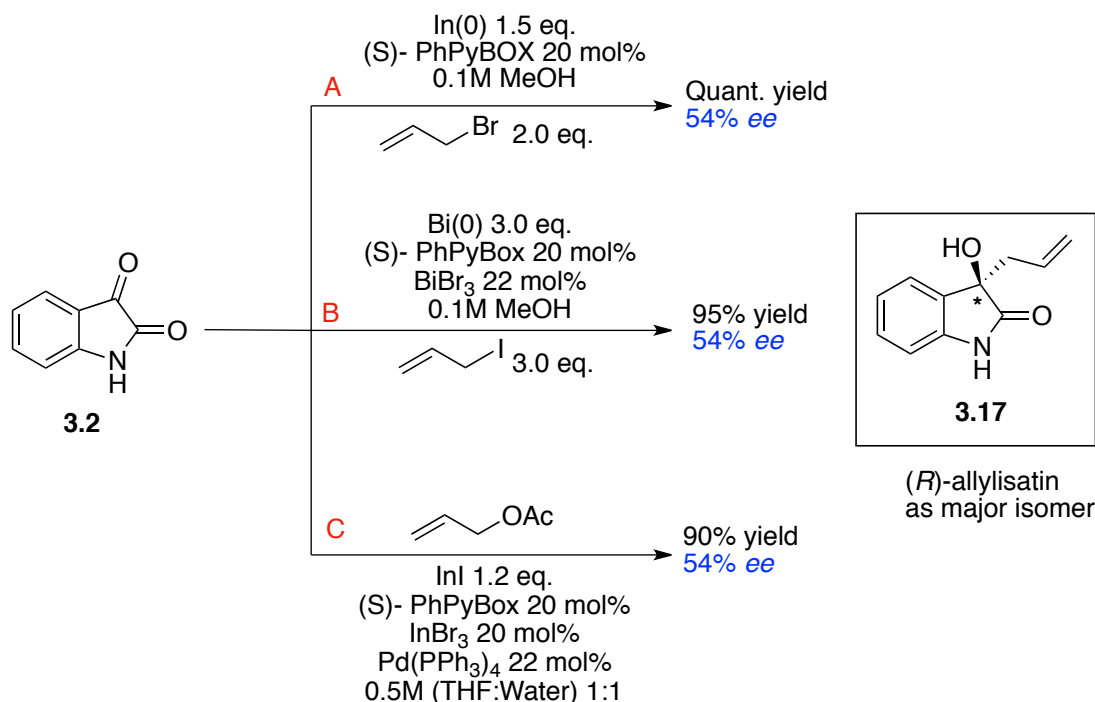
Scheme 3.24. Potential Targets from Reformatsky Reaction on Isatins

3.4. Mechanistic Studies in Allylation of Isatins

The use of asymmetric reactions to produce optically active compounds is one of the impressive transformations developed in the last century of the organic synthesis.³⁸ Achieving defined three-dimensional orientation around a carbon involves control of many parameters. Hence it is important not just to develop methods for chiral molecules but also to decipher the underlying mechanism by which they are created. In the case of asymmetric organometallic reactions, this systematic investigation will not only help us understand the nature of the active species and the atmosphere around the metal, but will also dictate the design of an effective metal-ligand complex for complete stereocontrol. In the present scenario, these investigations will help us understand the mechanism of asymmetric indium and bismuth-mediated reactions.

Scheme 3.25 compares the different methods developed in our laboratory for the asymmetric allylation of isatin. Method A uses a Barbier-type allylation using indium discussed in detail in chapter three. Method B is the bismuth-mediated allylation developed in our laboratory. Method C is the ümpolung allylation method used for chiral hydrazones applied to isatin. It is interesting that all three methods produced (*R*)-allylisatin **3.17** in

54% *ee*. Upon observing these stereochemical similarities in indium and bismuth-mediated allylations, we decided to probe the mechanism and active catalyst involved in the reaction.



Scheme 3.25. Stereochemical Similarities in $\text{In}(0)$ and $\text{Bi}(0)$ -Mediated Reactions

3.4.1. Non-Linear Effects

In asymmetric synthesis, enantiomeric excess of the product should be proportional to the enantiomeric excess of the auxiliary (or ligand) used in the reaction. This, however, may not be true in all cases. Sometimes a deviation from the linearity may be observed (Figure 3.3). This is called the non-linear effect. The chiral auxiliary or the ligand is often derived from a starting material that is not necessarily enantiopure. If the two isomers present in the system do not interact with each other; it is easy to predict the enantiomeric excess of the product using the enantiomeric excess of the ligand as described by the equation 3.1.³⁹

$$ee_{\text{prod}} = ee_{\text{max}} \times ee_{\text{auxiliary}} \quad (3.1)$$

ee_{max} is the ee provided by one of the isomer of the catalyst
 (+)-catalyst will provide $+ee_{\text{max}}$ and (-) -catalyst will provide $-ee_{\text{max}}$

ee_{prod} is the ee obtained at the end of the reaction

$ee_{\text{auxiliary}}$ is the ee of the auxiliary or the ligand used in the reaction

A non-linear effect could be positive (Curve A, Figure 3.3) or negative (Curve B, Figure 3.3) depending on the catalytic system. When the enantiomeric excess of the product is higher than expected it has a positive nonlinear effect (Curve A). If the enantiomeric excess of the product is lower than predicted it has a negative non-linear effect (Curve B).

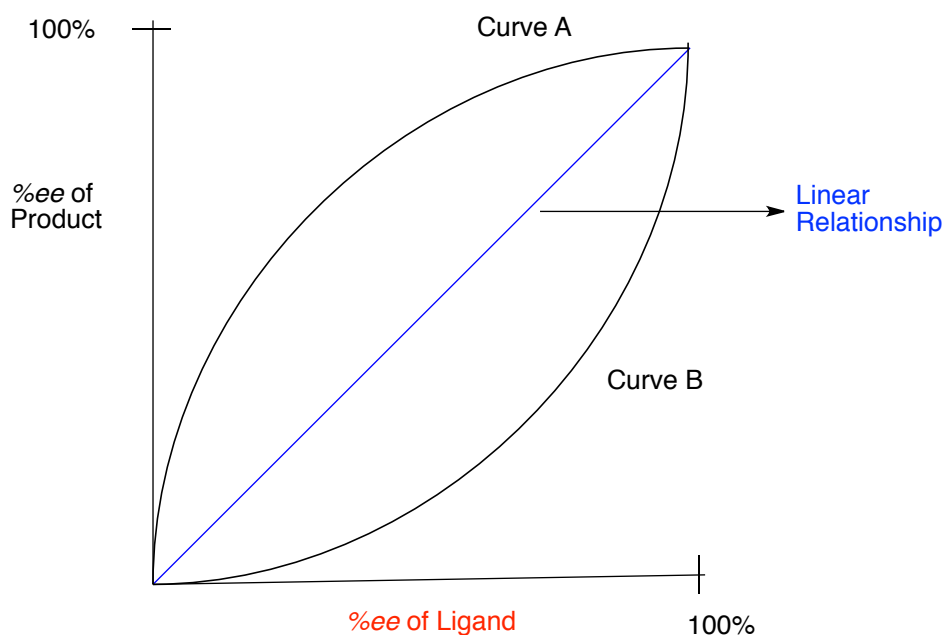


Figure 3.3. Non-Linear Effects in Asymmetric Catalysis

Aggregation of the ligands to form homochiral and heterochiral species is often observed. This adds complication to the system as well as the prediction of theoretical

models. Kagan and co-workers established and revised a mathematical model for non-linear effects in asymmetric catalysis.⁴⁰ Along with Kagan's work other groups reported studies on non-linear effects in asymmetric synthesis and autocatalysis.⁴¹

Several models have been proposed to explain the non-linear effects.⁴² For the sake of simplicity and relevance to the present investigation two major models are discussed in this section, the asymmetric model and reservoir model. In the asymmetric model there is rapid ligand exchange between two reactive species involving two ligands per metal center.

According to this system there are three possible species: ML_RL_R , ML_SL_S that are the homochiral species and ML_SL_R that is the heterochiral species or the meso catalyst. The homochiral species produces enantiomerically pure product where as the heterochiral species produces racemic product (Figure 3.4).

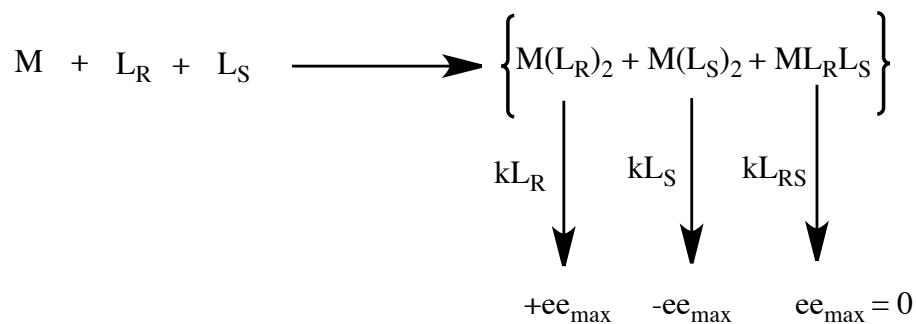


Figure 3.4. Asymmetric Model

Assuming a steady state for the formation of the complexes, the rate constant for the three species involved are k_{RR} , k_{SS} and k_{RS} . With these reaction rates one could calculate the ee of the product using the equation 3.2.

$$EE_{\text{prod}} = EE_0 ee_{\text{aux}} \frac{1 + \beta}{1 + g\beta} \quad (3.2)$$

From the equation, β is an expression for the ratio between meso complex (ML_RL_S) and homochiral complexes (ML_RL_R , ML_SL_S). The parameter g is defined as the relative

rate between the meso complex and homochiral complex ($k_{RR} = k_{SS}$). By this model if $g > 1$, then we will observe a negative non-linear effect. In the case of positive non-linear effect we will observe $g < 1$ and ee_{prod} will be higher than expected. An assumption of this model is that it assumes there is a fast ligand exchange before the final step of the catalytic cycle and it is irreversible. The non-linear effect is stronger when the diastereomeric complexes are formed irreversibly compared to when they are formed reversibly.

The second model is the reservoir model. It is applicable when numerous metal complexes are generated during the preparation of the catalyst. Among them there is one notable species that is catalytically active. In this model the meso species formed is not an active catalyst and serves as a reservoir. This allows the active catalyst in solution to have a higher effective optical purity. Reservoir effects are often confused with asymmetric model. Two common methods are employed to differentiate the models: performing kinetic studies to understand the reaction rates and NMR studies on the diastereomeric complexes formed. Reservoir effect is described in Figure 3.5. The meso complex ML_RL_S is not catalytically active and therefore no product is formed unlike in the case of asymmetric model where the meso complex gives rise to racemic product.

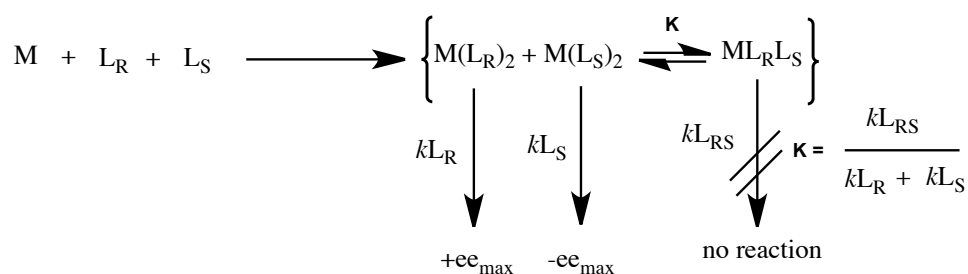


Figure 3.5. Reservoir Model

Blackmond and co-workers extensively studied the effect of non-linearity on reaction rates. In comparison with the enantiopure chiral ligand system, if there is a small

amount of impurity ($ee < 100\%$) the overall reaction rate is affected. In the case of the ‘reservoir model’ when there is more amount of the active chiral ligand locked in the meso complex, less amount of catalyst is available to the system and therefore a decrease in the reaction rate is observed.

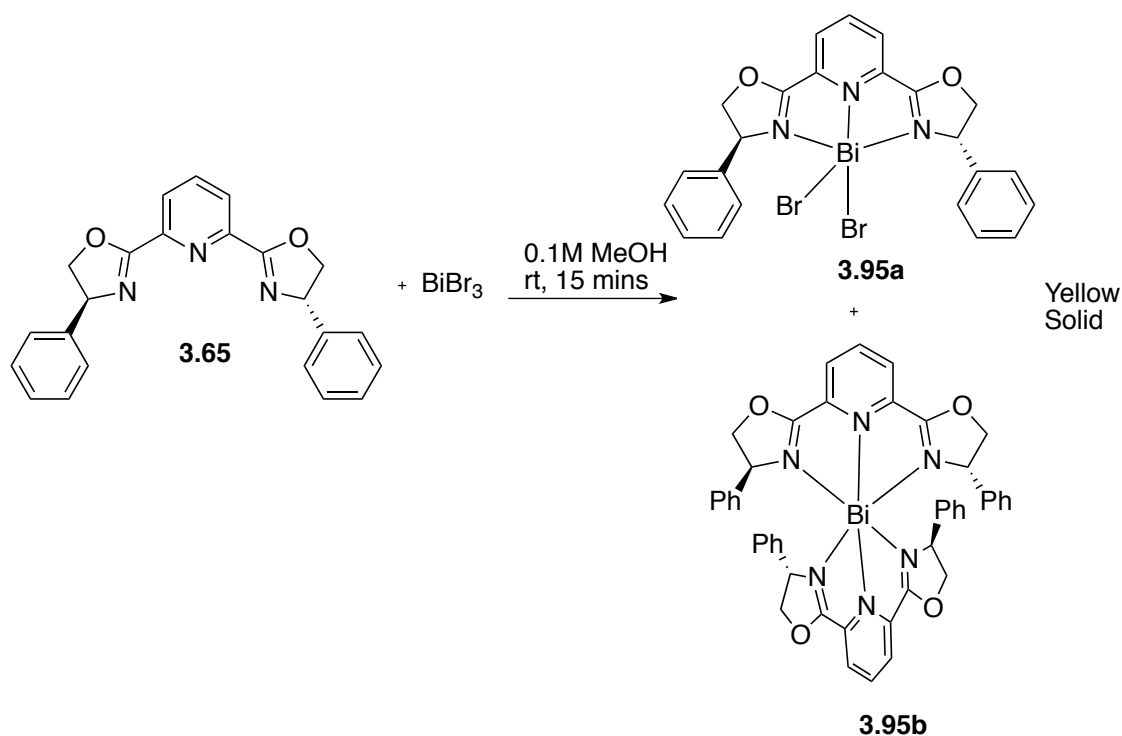
Investigating non-linear effects in asymmetric synthesis has become a common practice to understand the mechanism. Non-linear effects help in identifying the catalytically active species in the reaction. Combining the information from non-linear effects and other kinetic studies helps the synthetic chemist devise a suitable strategy for maximum enantio-control in the product.

3.4.2. Mechanism of Bismuth-Mediated Reactions

The understanding of the mechanism of bismuth-mediated reactions is still in its infancy. The generally accepted mechanism for reactions involving bismuth metal is an initiation via single electron transfer mechanism. This has been demonstrated by simple particle size variation experiments. Reactions involving certain moles of bismuth spheres have equivalent reactivity to a reaction having a lower equivalent of moles with a smaller particle size. This difference has been discussed in chapter one under the title bismuth-mediated allylation through a suitable example. Reactions involving bismuth reagents generated by reducing bismuth(III) salts often proceed through a nanometer bismuth particle thereby maximizing the total surface area available for single electron transfer process to occur. Despite the “green” property of bismuth, the amount of information about its mechanistic role is scarce in the literature. Our attempt here is to decipher the stereochemical path of the bismuth-mediated allylation of isatins developed in our laboratory.

3.4.3. Studies Towards Understanding Chiral-Bismuth Lewis Acids

The experimental procedure developed initially for bismuth mediated allylation required the pre-generation of a bismuth(III)-ligand complex. The ligand and bismuth tribromide were mixed together in a scintillation vial in 0.1M methanol and stirred. After fifteen minutes there was formation of a yellow precipitate. Initial study of the mixture revealed the existence of at least two distinct species **3.95a** and **3.95b** in solution along with a yellow solid (Scheme 3.26). The supernatant liquid and the precipitate were separated and analyzed using $^1\text{H-NMR}$ and mass spectrometry.



Scheme 3.26. Pre-generation of the Catalyst

The major product seemed to be a symmetrical complex, probably containing one ligand per bismuth with two bromines (Figure 3.6). The mass spectral analysis supported this observation (Figure 3.7). There is a minor amount of another detectable complex,

which could be one with two ligands per bismuth giving rise to the unsymmetrical signals for the protons present in the oxazoline ring of the ligand.

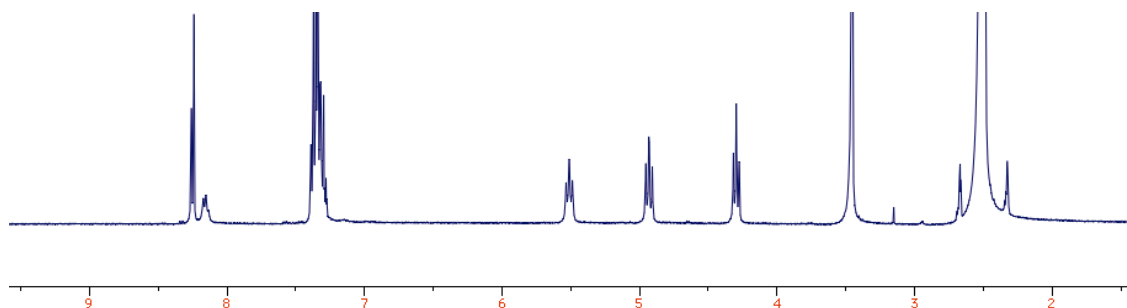


Figure 3.6. ^1H -NMR Showing Symmetric Complex in Methanol- d_4

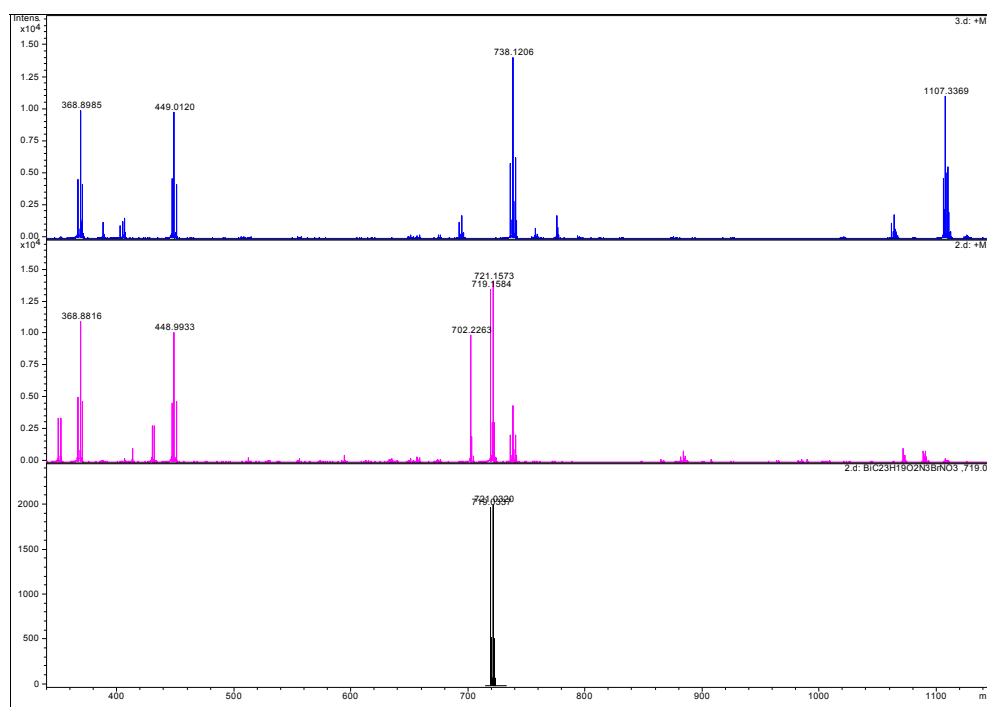
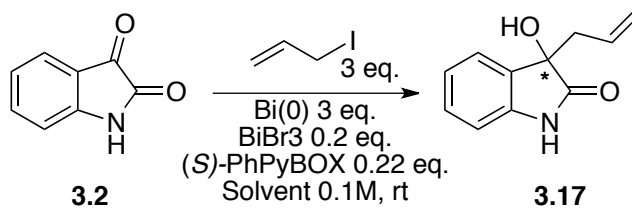


Figure 3.7. Mass Spectral Analysis of Symmetrical Complex

In order to verify if the nature of the species changes we decided to switch the solvent to acetonitrile. The objective of using acetonitrile was to determine if the active catalyst differs with respect to the solvents (Table 3.10). Another reason to investigate acetonitrile was to probe the complexes in a solvent that afforded low *ee* and yield.

Table 3.10. Solvent Screening in Bismuth-Mediated Allylation of Isatins



Entry ^a	Solvent ^b	Time	Yield ^c	%ee ^d
1	MeOH	24h	>99%	54
2	Acetonitrile	80h	30%	20

^a Catalyst was pre-generated ^b HPLC grade solvents were used

^c Isolated yields ^d ee was analyzed by HPLC

The physical appearances of the reaction in methanol are similar to that of acetonitrile, a clear solution on the top with yellow precipitate. Analyzing the ¹H-NMR spectra of the mixture revealed that unlike in methanol, the major product was the unsymmetrical (2:1 ligand to metal) complex (Figure 3.8). The mass spectral analysis confirmed this observation (Figure 3.9).

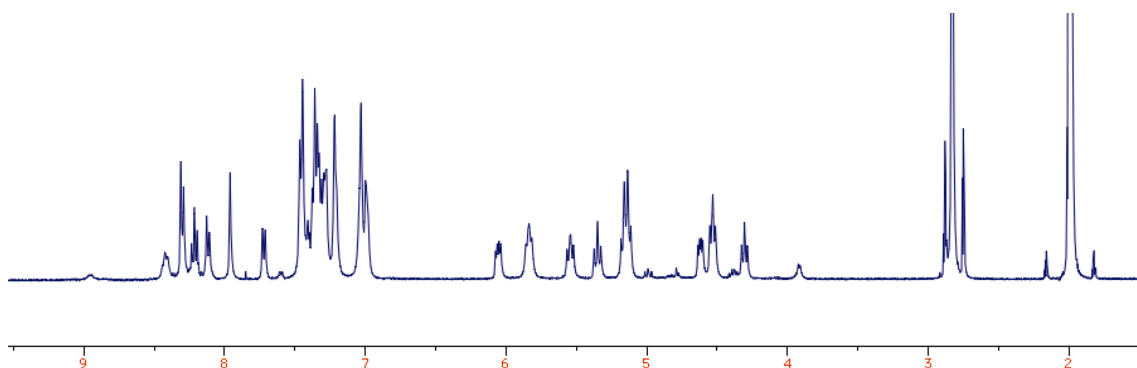


Figure 3.8. ¹H-NMR of Bi-Lewis Acid Complex in Acetonitrile-*d*₃

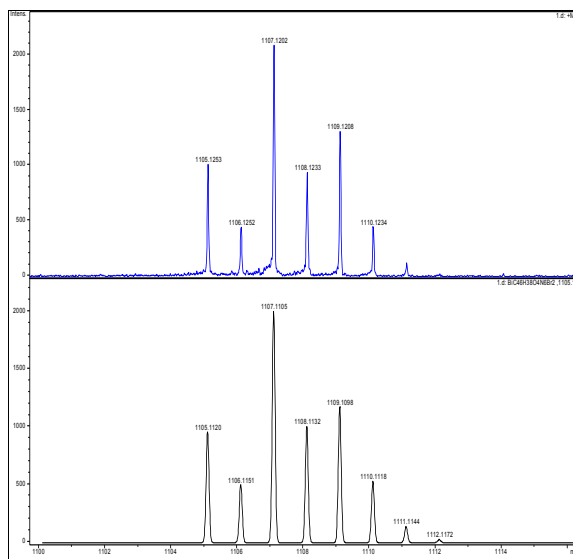


Figure 3.9. Mass spectra of Unsymmetrical Bi-Complex

The yellow solid presumably is a polymeric by-product from bis oxazoline ligands which was insoluble in most of the organic solvents. This complicated our attempts to analyze this part. The heterogeneity of the reaction could also be attributed to this insoluble solid. Upon allowing the mixture to remain in methanol- d_4 for 24 hours resulted in new signals that could not be interpreted (Figure 3.10).

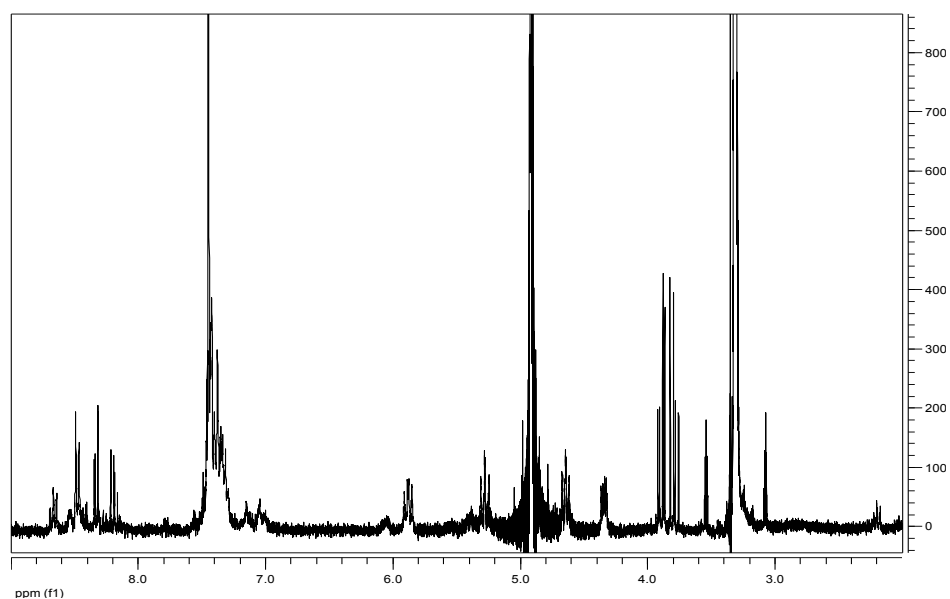


Figure 3.10. $^1\text{H-NMR}$ of the Reaction Mixture After 24h in Methanol- d_4

The yellow solid formed from mixing bismuth tribromide and the ligand was filtered from the rest of the reaction and part of the solid was dissolved in deuterated-DMF. The insoluble portions were dissolved by sonication. The $^1\text{H-NMR}$ spectra (Figure 3.10) was more complex than that of the solution. The region between 3.7 ppm to 4.0 ppm indicated a probable presence of the parent amino alcohol of the ligand bound to bismuth, (*S*)-Phenyl glycinol (Figure 3.11).

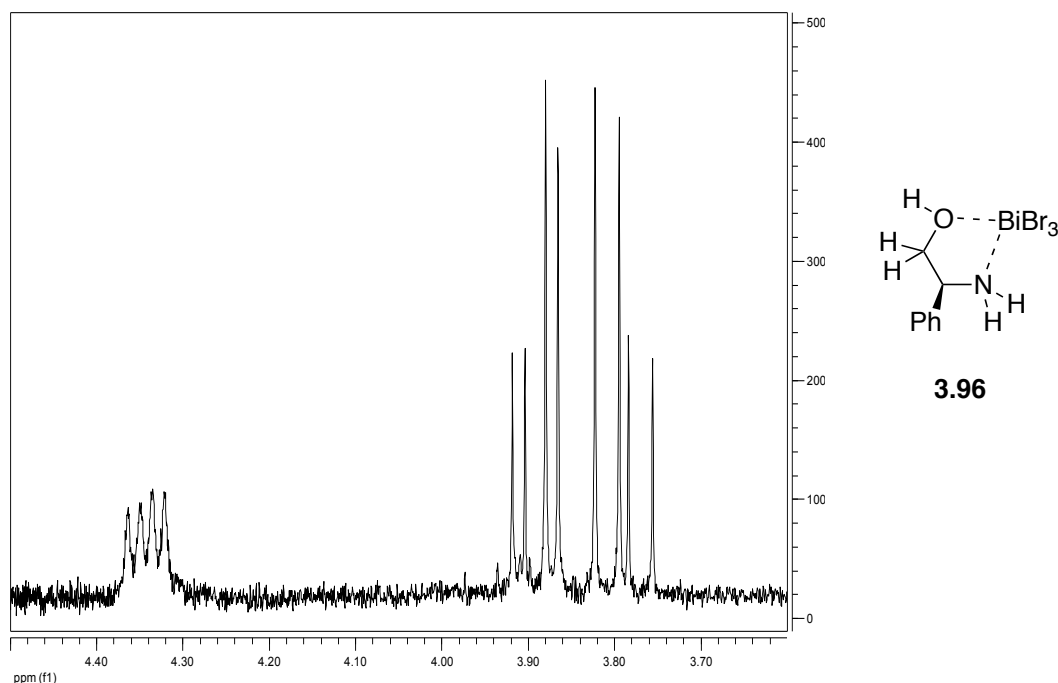
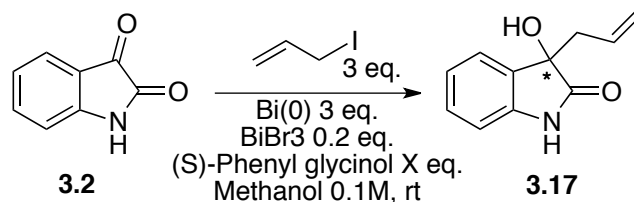


Figure 3.11. $^1\text{H-NMR}$ showing Possible Presence of Phenyl glycinol

This observation made us question if the amino alcohol formed from the hydrolysis of the ligand by the Lewis acid was responsible for enantio-induction. Experiments using (*S*)-Phenyl glycinol did not produce any enantioselectivity (Table 3.11). Thus we concluded that this hydrolysis product was not responsible for the observed catalysis.

Table 3.11. Trials with (*S*)-Phenyl glycinol



Entry ^a	X	Time	Yield ^b	%ee ^c
1	0.22	24h	Quant	0
2	0.44	24h	Quant	0

^a Catalyst was pre-mixed ^b Isolated yields ^c ee was analyzed by HPLC

From the solvent studies, we understood that there are two species formed in the reaction. One is a 1:1 complex and another is a 2:1 complex of ligand to metal. The complex containing 1:1 ligand to metal is most likely the active catalyst as it is the major product in the methanol. The 2:1 complex that was formed in a large amount in acetonitrile was most likely an inactive species, as it was coordinatively saturated. This is consistent with the lower yield and ee observed when the reaction was performed in acetonitrile. Observation of a mixture of both the complexes in methanol indicates that there could be equilibrium between these two species and the rate of the equilibrium could be a factor in the enantioselectivity. Attempts to crystallize the 1:1 complex resulted in isolation of a two ligands per bismuth complex (Figure 3.12).

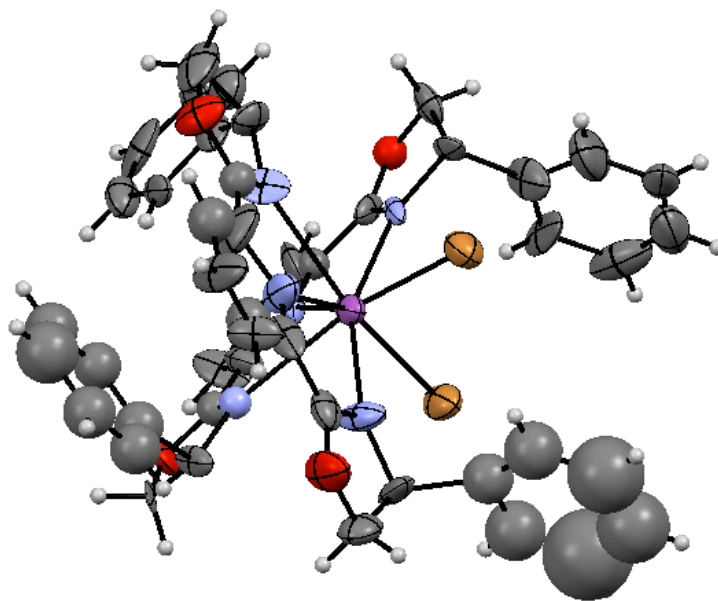


Figure 3.12. Thermal Ellipsoid Plot of (S)-Ph PyBOX -BiBr₃ at 50% Probability

The isolation of a 2:1 complex indicated us that the 2:1 structure is the most likely one to form and more stable. Attempts to isolate the racemic form of the 2:1 complex where bismuth is coordinated with (*R*)-Ph-PyBOX and (*S*)-Ph-PyBOX. This attempt made was successful and we were able to isolate and characterize the racemic complex (Figure 3.13).

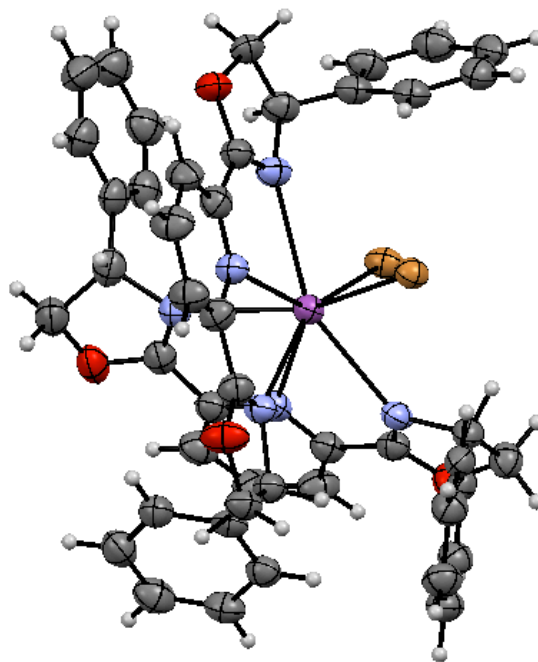


Figure 3.13. Thermal Ellipsoid Plot of Racemic Complex at 50% Probability

3.4.4. Non-Linear Effects in Bismuth-Mediated Allylation

The species we encountered during our NMR and mass spectral studies tempted us to probe into a possible non-linear effect in bismuth mediated allylation. We prepared solutions containing different ratios of (*R*)-Ph-PyBOX and (*S*)-Ph-PyBOX and utilized them in the bismuth-mediated allylation reaction. The enantiomeric excess of the product was determined by chiral HPLC and the results were plotted as ligand *ee* vs product *ee*. We observed a strong positive non-linear effect in bismuth-mediated allylation of isatin (Figure 3.14).

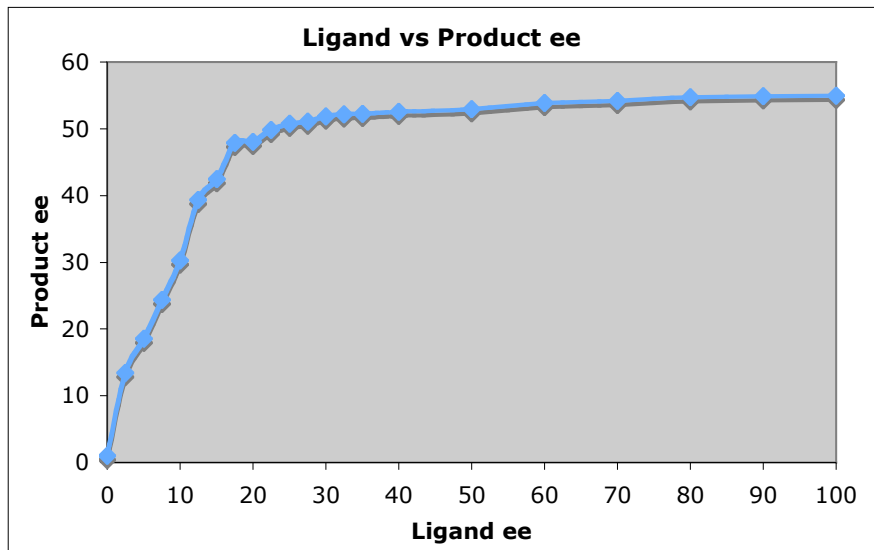
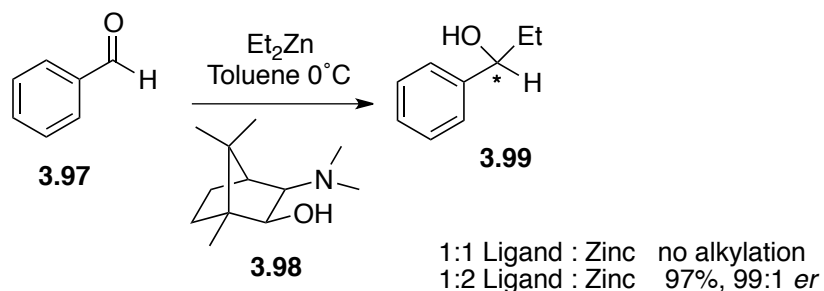


Figure 3.14. Non-Linear Effect Observed in Bismuth-Mediated Allylation

This non-linear graph resembled the one obtained in the asymmetric 1,2- and 1,4-addition of organozincs to benzaldehyde using β -amino alcohols as ligands reported by Noyori and Oguni (Scheme 3.27) (Figure 3.15). After extensive mechanistic study, Noyori concluded that there was formation of a meso dimer (ML_RL_S), which was thermodynamically favored and catalytically inactive. The chiral dimers ($M(L_R)_2$ and $M(L_S)_2$) on the other hand were in equilibrium with the catalytically active ML species. The computer-generated curve in the case of organozinc additions had a perfect fit with the experiment. The NMR and mass spectral data for our Bi-mediated allylation suggests that the meso ML_SL_R complex is a reservoir and the ML_S or ML_R complex is the active catalyst.



Scheme 3.27. Alkylation of Benzaldehyde with Et_2Zn

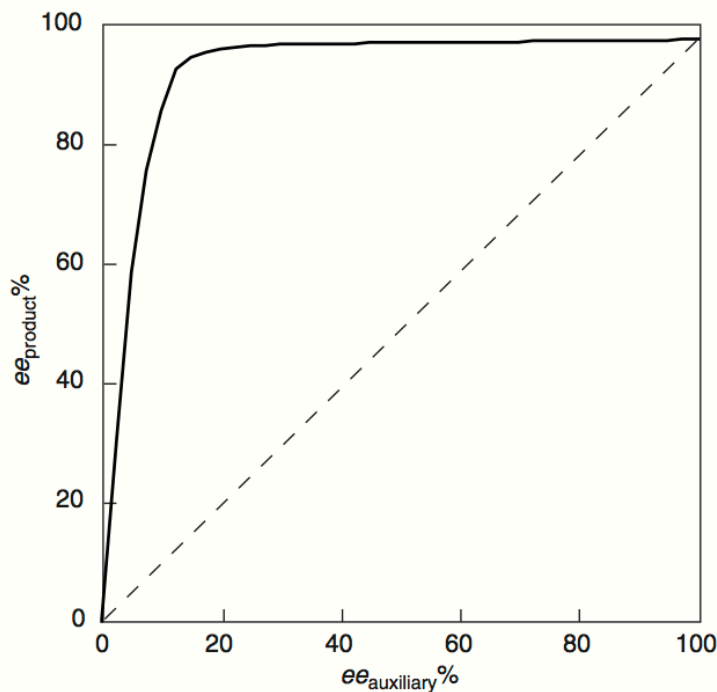


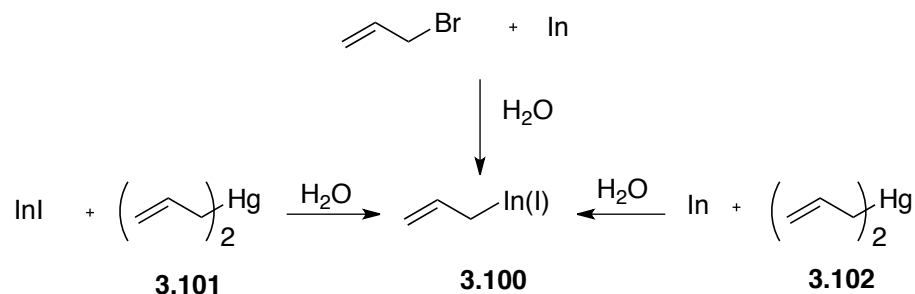
Figure 3.15. Positive Non-Linear Effect in Reaction of Et_2Zn with Benzaldehyde

As Kagan described, in the reservoir effect, part of the ee is stored in the unproductive complexes. In our case the insoluble complex could very well be the reservoir of the catalytically active species. A key factor is that the unreactive ML_RL_S complex enhances the ee of the major enantiomer and ML in solution producing a positive non-linear effect. The observation of the racemic complex or the ML_RL_S complex during our X-ray studies indicates that this is a viable pathway. More work need to be done to have a clear picture of this catalytic system. First and foremost additional evidence to explain the kinetic data supporting the reservoir effect and a computer-generated graph would be additional evidence to explain the mechanism.

3.4.5. Mechanism of Indium-Mediated Reaction

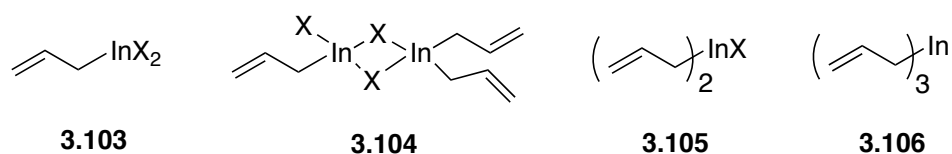
Indium-mediated reactions could be generally classified into any of the following classes. Indium Lewis acid mediated addition of allyl organometallics to electrophiles,

indium-mediated Grignard type allylations, or indium-mediated Barbier-type allylations. Chan and Yang established a generalized idea about indium-mediated allylation using Grignard or Barbier method.⁴³ They reported the formation of allylindium(I) reagent irrespective of the method followed. Using diallyl mercury, generation of allylindium(I) reagent was achieved using indium metal as well as indium(I) iodide (Scheme 3.28).



Scheme 3.28. Generation of Allylindium(I) through Different Methods

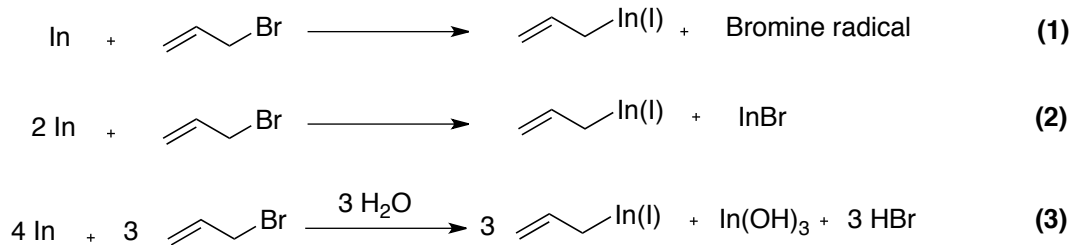
This could be understood by considering the low first ionization potential of indium metal where as the second and third ionization potentials are relatively higher. Formation of allyl radical anions is also not excluded. Prior to this report Araki and Butsugan reported the formation of allylindium diiodide from allyl iodide and indium(I) iodide in THF-*d*₈, Chan and Yang's report contradicted that diindium sesquhalide species **3.104** is actually a misinterpretation of the mixture of allylindium(I) **3.100** and allylindium dibromide **3.103** (Scheme 3.29). In the same report Chan suggested the formation of indium(III) species in organic solvents.



Scheme 3.29. Proposed Active Species in Indium-Mediated Allylation

The stoichiometry of indium mediated allylations played a crucial role in the nature of the species formed. Cook and Kargbo reported the necessity for 1:1.5 ratio of indium to allyl bromide for the generation of allyl indium species in 0.17M dry THF for their enantioselective imine allylation. The ratio of indium to allyl bromide has been stressed in several literature reports but little is known about the role in ratio and concentration plays in In-mediated allylation.

A hypothetical equation for the formation of allylindium species has been proposed (Scheme 3.30).⁴⁴ In a mixture of 1:1 indium:allylbromide, allylindium(I) could be formed giving a bromine radical which would combine with another bromine radical to produce bromine. This bromine would further oxidize indium metal. In aqueous conditions indium bromide is known to undergo disproportionation to form indium hydroxide.⁴⁵

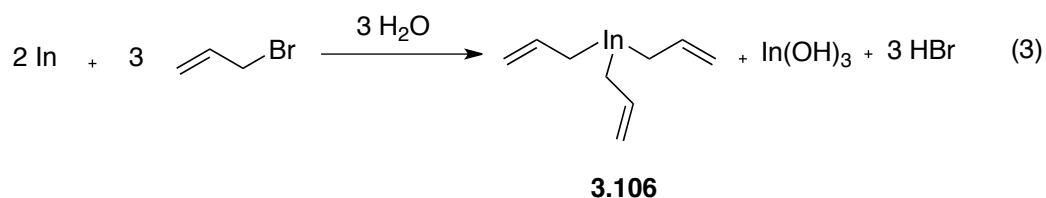
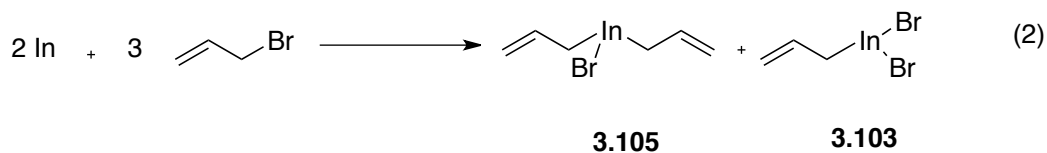
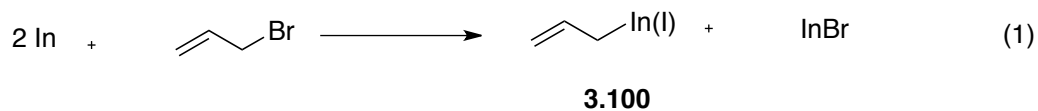


3.100

Scheme 3.30. Proposed Equations for Organoindium(I) Formation

In the case of organic solvents, indium(III) species are often presumed to be the active species (Scheme 3.31).⁴⁶ Several groups explain the formation of indium sesquihalide. Recently Bowyer investigated the reaction in 60% deuterated ethanol:D₂O mixture and monitored the consumption of allyl bromide by ¹H-NMR. The results indicated that the ratio of consumption is 2:3. The result was supporting evidence for the existence of indium(III) complexes in the system. In connection to our indium mediated allylation of isatins, we found that the reaction proceeded effectively in several

compositions of ethanol and water mixtures. This observation could very well be applied to our scenario.



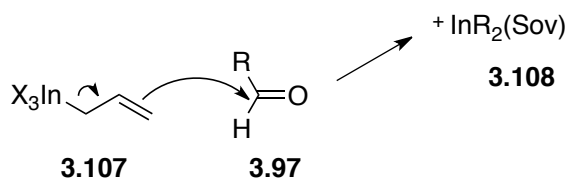
Scheme 3.31. Proposed Equations for Organoindium(III) Formation

Overall the mechanism of indium-mediated allylation is more complicated than it appears at first glance. More investigation on the nature of the allylindium reagent was not performed until 2010. An extensive report by Koszinowski⁴⁷ suggested the different organoindium species that are formed and their reactions in different solvents. In his conclusions he argued that allylindium chemistry is dominated by indium(III) species but the formation or the detection of indium(I) species could not be denied. However, they are transient in nature and not responsible for the nucleophilic addition. In conclusion, it is understood that there are two allylindium species that are commonly accepted.

1. Sesquihalide species **3.104** in organic solvents
2. Allylindium(I) species in water

The mechanism for the formation of diallylindium bromide or monoallylindium dibromide is not clear. In the case of enantioselective reactions, there is added complication to the system. The nature of the species differs based on indium coordination to the chiral

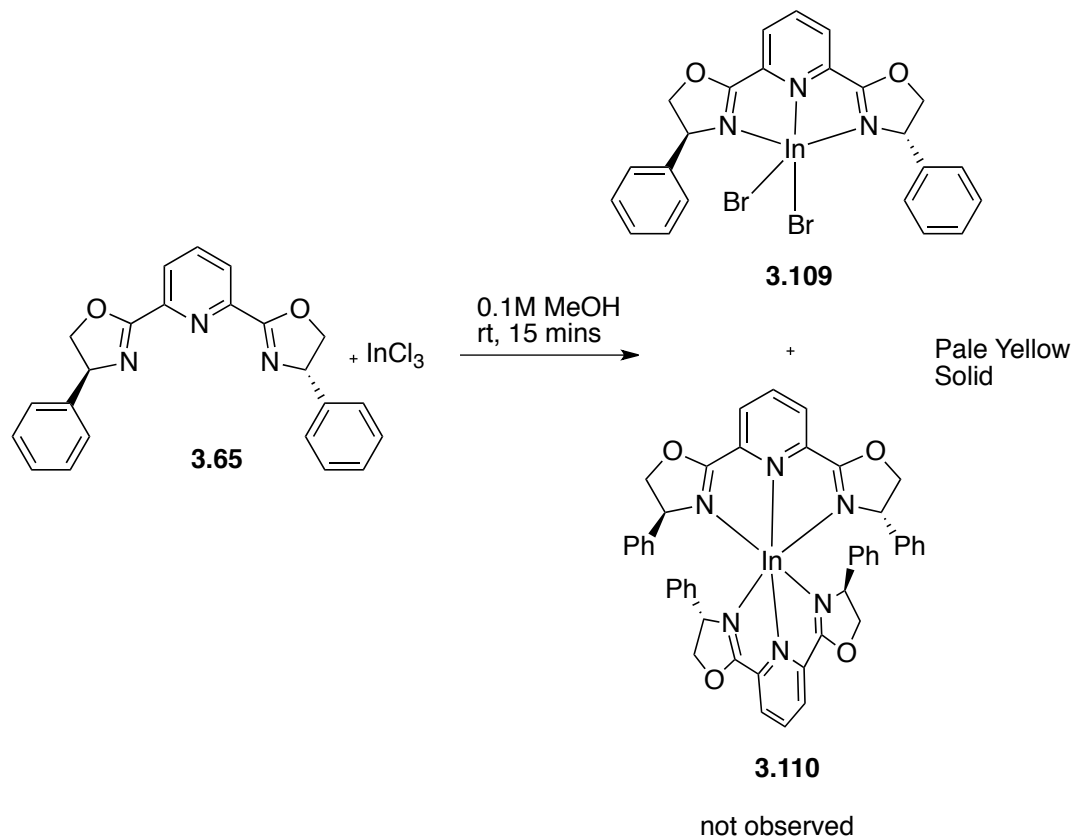
ligand. The stoichiometric experiments were conducted in the absence of an electrophile. The presence of an electrophile would of course change the course of the formation and the nature of the active species. Kosznowski, suggested a possible coordination of the carbonyl oxygen to a cationic indium species, thereby activating the electrophile for allylation (Scheme.3.32). The cationic indium species **3.108** are shown to be stable in DMF, water and other polar solvent in which the allylation using indium metal is often conducted.



Scheme 3.32. Activation of Electrophile by Cationic Indium

3.4.6. Studies Towards Understanding Chiral-Indium Lewis Acids

Our goal was to investigate the active species in asymmetric indium-mediated allylations; we hypothesized that a chiral indium Lewis acid generated in-situ was responsible for the stereochemical information transfer. To investigate this, we attempted to prepare indium complexes with our ligand, (*S*)-Ph-PyBOX. One equivalent of indium trichloride was mixed with one equivalent of the ligand and stirred in 0.1M of methanol-*d*₄. After fifteen minutes, the solution became turbid with the formation of a pale yellow precipitate (Scheme 3.33).



Scheme 3.33. Pre-generation of Chiral Indium-Lewis acid

¹H-NMR of the mixture revealed there was formation of a single species. A clear shift in the signals of the oxazoline protons were observed and the complex seemed to be symmetric based on NMR (Figure 3.16).

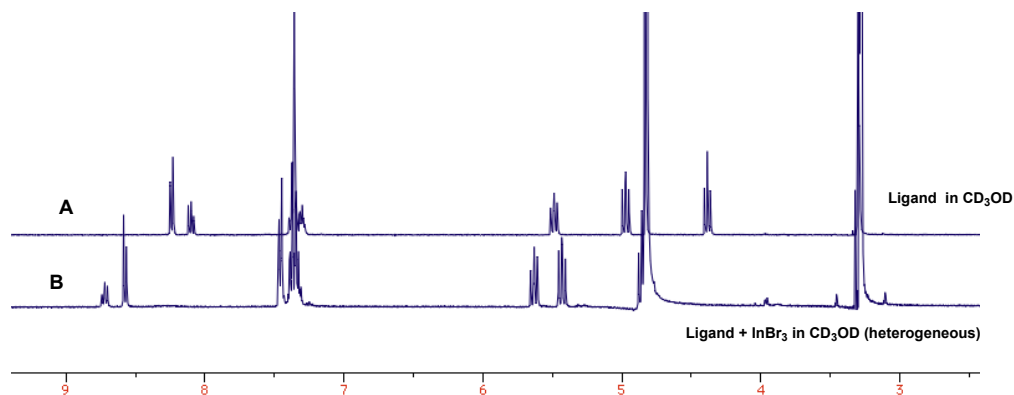


Figure 3.16. Indium-PyBOXComplex-Formation Monitored by ¹H-NMR

Based on this we assigned the structure of the complex as **3.109**. The mass spectral analysis on the other hand gave very small amount of 1:1 complex of ligand to metal with 2 bromine atoms (Figure 3.17). The majority of the compound in the solution was just the ligand. This observation did not correlate with the $^1\text{H-NMR}$ analysis since a complete shift of the signals was observed.

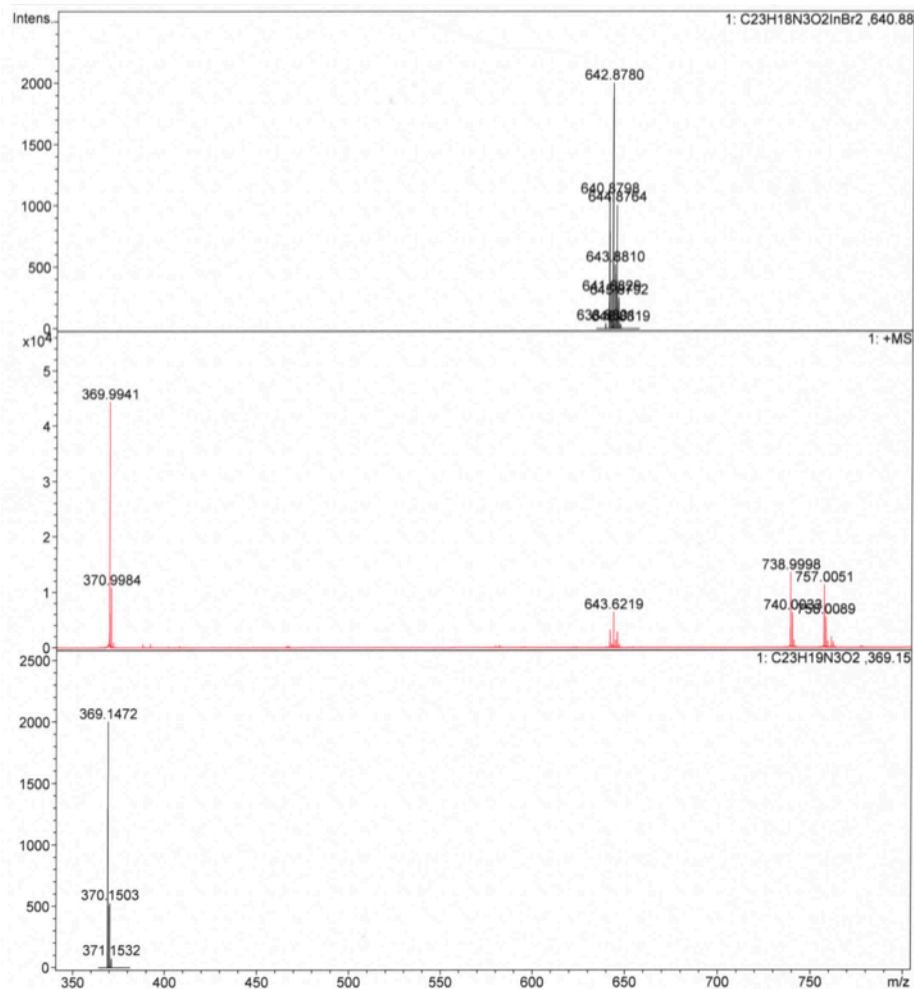


Figure 3.17. Mass Spectra of Ligand + InBr_3 in Methanol- d_4

To investigate further, we decided to do solvent studies. Ligand and Lewis acid were mixed in CD_2Cl_2 and stirred for few minutes to form a pale yellow precipitate. The solution was analyzed using $^1\text{H-NMR}$, revealing two sets of signals present in the system. One set belonged to the parent ligand and other to the formed complex. The yellow

precipitate was filtered and a small amount was dissolved in CD_2Cl_2 with the aid of sonication. Trace B in Figure 3.19 clearly shows the presence of the complex in the solid that precipitated out. Attempts to change the Lewis acid from InCl_3 to InBr_3 did not produce any notable change in the NMR spectra (Figure 3.18, Figure 3.19).

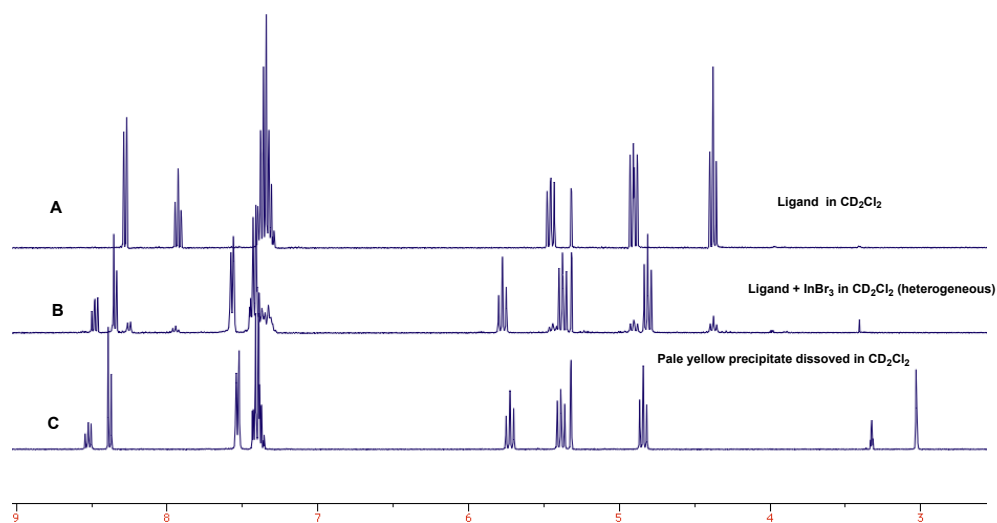


Figure 3.18. Complex-Formation in CD_2Cl_2

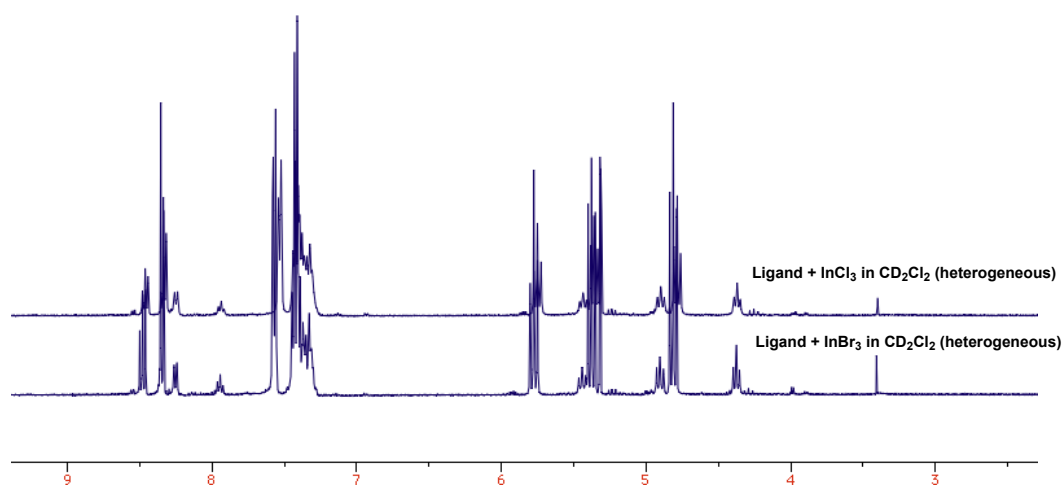


Figure 3.19. Two Species Observed with InCl_3 and InBr_3

A comprehensive analysis of ^1H -NMR and mass spectra of the mixture were performed. The ^1H -NMR did not reveal much information except showing symmetric peaks and a shift from the ligand signals. In mass spectral analysis, we found that in dichloromethane and chloroform the 1:1 complex was formed in a large amount compared to methanol (Figure 3.20 and Figure 3.21). This information did not have much relevance to the present scope since indium-mediated allylation did not proceed in halogenated solvents.

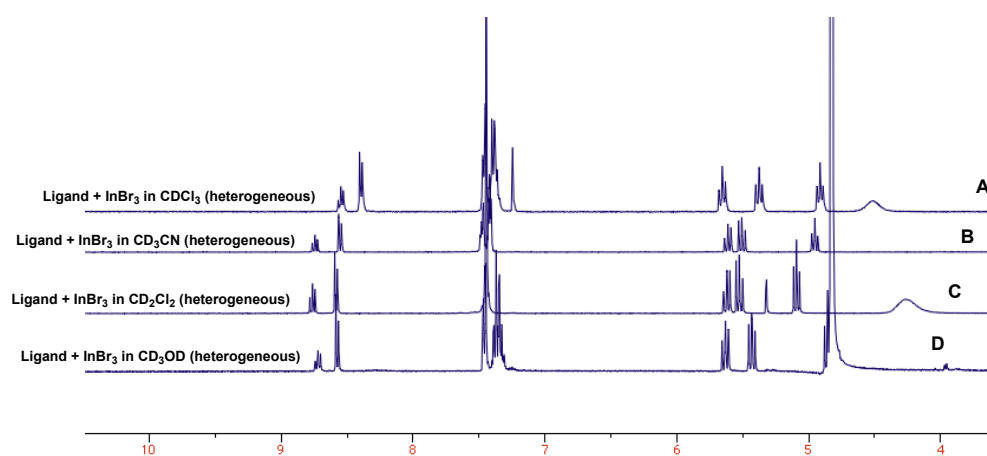


Figure 3.20. Complexes Observed in ^1H -NMR in Different Solvents

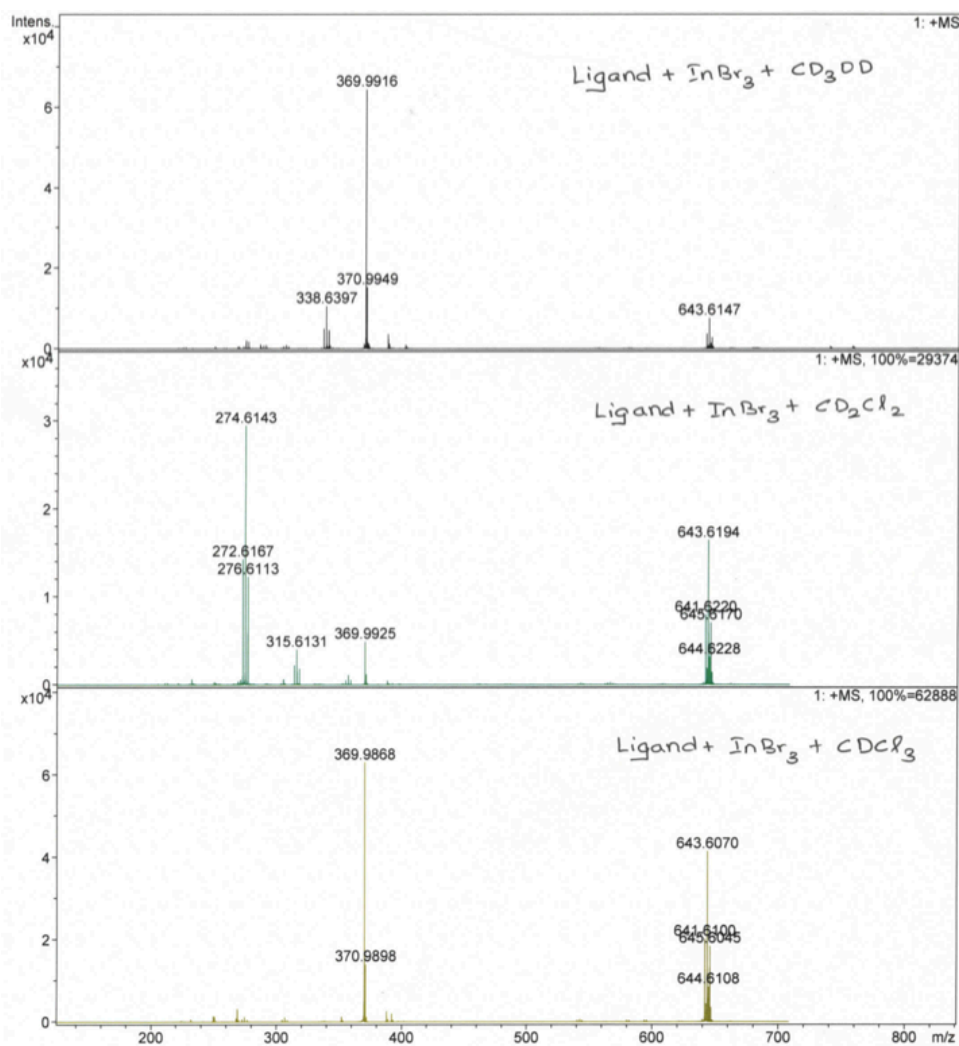


Figure 3.21. Mass Spectra of Various Indium Complexes

Attempts were still under progress for studying the complex formed after the reaction of indium metal with allyl bromide. A similar attempt as in the case of bismuth-mediated allylation, we decided to isolate the potential chiral Lewis acid complex. The ligand and indium tribromide were mixed together in methanol and the solutions were layered with non-polar solvents. The solution layered with MTBE yielded fine crystals of **3.110** in 45 days. Isolation and analysis of the crystal showed a 2:1 ligand to metal complex.

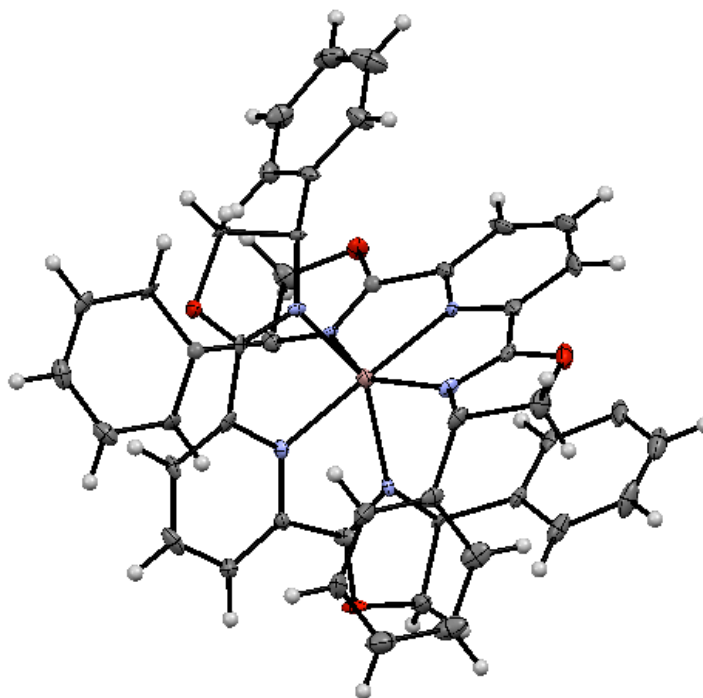


Figure 3.22. Thermal Ellipsoid Plot of 2:1 Ligand:Indium Complex at 50% Probability

3.4.7. Non-Linear Effects in Indium-Mediated Allylation

It is interesting to note that both In(0)- and Bi(0) Lewis acidic species show similar behavior by $^1\text{H-NMR}$ and mass spectral analysis. Compared to bismuth-mediated allylation we would expect a non-linearity based on the complexes observed by the spectroscopy and mass-spectrometry.

Even though there are similarities in the stereochemical outcome and the formation of complexes with the chiral ligand utilized, indium and bismuth-mediated allylation of isatins do differ in certain aspects. The reaction became homogeneous after a few minutes in the case of indium. The bismuth-mediated reaction, on the other hand, remains heterogeneous from the beginning to the end. Utilizing an added Lewis acid was

unnecessary in the case of indium-mediated allylation. Attempts to analyze the by-products and the remaining mass in bismuth reaction were unfruitful. In an earlier investigation, it has been disclosed that water has significant effect in the enantioselectivity. However, this has not been adequately investigated.

3.4.8. Summary

Allylation reactions are a valuable asset in a synthetic organic chemist's arsenal.⁴⁸ Considering the benefits of indium and bismuth-mediated reactions, explained in previous chapters, it is understood how important these mechanistic studies would be for the benefit of the development of novel asymmetric methods using these metals. Our present investigation is in its early stages. A non-linear effect was observed in bismuth-mediated allylation of isatins, but indium-mediated allylation did not show a non-linear effect. Kinetic aspects of the non-linear behavior of bismuth-mediated allylations are still under investigation. Probing the reaction using ReactIR could be beneficial. The change of enantioselectivity over time could provide us additional details on the non-linear effect. However, this has not been adequately investigated.

3.5. Linear α -Ketoamides

A variety of structurally intriguing and biologically significant oxindoles could be prepared through the above-discussed methodology. It is also worth to note that this arena is already crowded with research groups competing on selectivity and operational simplicity. Instead of further proceeding with the cyclic ketoamides we paused for a moment and started investigating linear ketoamides. The linear α -ketoamide structural motif has been found in a number of biologically important natural products, such as FK 506 and cyclotheonamide. The facile formation of stable tetrahedral adducts between the

highly electrophilic α -oxo group and nucleophilic residues (OH, SH) at the active sites of enzymes made these molecules an excellent basis for the development of enzyme inhibitors. Indeed, this structural motif has often found incorporated strategically at the P1 position of designed protease inhibitors.

We envisioned that allylation of linear ketoamides could be achieved using our indium mediated enantioselective allylation. The product, an enantiomerically pure α -allylated- α -hydroxy ketoamide could be converted to α -allylated- α -hydroxy acid. Synthesis of such an attractive intermediate is relatively unexplored territory in asymmetric organic synthesis. Combined with this motivation, the innate fascination of an organic chemist to synthesize unnatural compounds motivated us to develop enantioselective allylation of linear- α -ketoamides.

3.5.1. Biological Significance of Linear α -Ketoamides

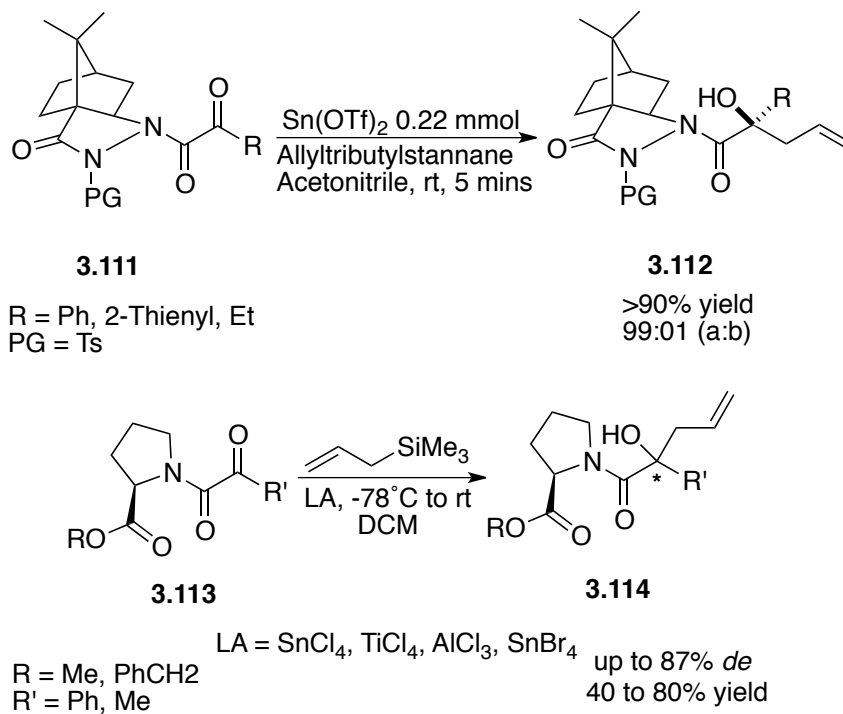
In addition to our research on developing novel In(0) and Bi(0)- mediated allylations, our group was involved in developing isoform selective HDAC inhibitors. To this end, we found that some α -ketoamides could be used as HDAC inhibitors. The main strategy is to develop functionality that will possess appreciable half-life and bioavailability. In 2003, Wada reported some ketoamide analogues of HDAC inhibitors. The results were attractive and the described structures were able to inhibit a mixture of HDAC 1 and HDAC 2 up to 0.11 μ M (IC₅₀). This would be a potential area where our allylation methodology could be readily applied in generating small molecule libraries based on ketoamides.

Another arena is metastasis. Mortality due to tumor invasion and distant metastasis is drastically higher than cancer itself. It has been stated in literature, if not multiple times

that more attention should be paid to developing strategies to prevent malignant cells from spreading and producing secondary metastatic colonies rather than to arrest the tumor growth. Cathepsin S (Cat S) is a cellular protease necessary for the invasion and angiogenesis of cancer cells. Monitoring Cat S level in blood can predict whether a person is dying because of the risk of heart disease or cancer. Inhibition of Cat S is closely related to various immune disorders. Ketoamides are by far the most potent inhibitors of Cat S reported. A recent report also indicates that α -ketoamides could be used as inhibitors for Dengue virus protease.⁴⁹ This is another niche where our methodologies could be applied in developing compounds from ketoamides and investigates their potency against Cat S or HDAC's.

3.5.2. Allylation of Linear α -Ketoamides

Soai and co-workers reported the first useful allylation method for this ketoamides. His group has reported a diastereoselective allylation method for chiral α -ketoamides derived from proline esters with allyl trimethylsilane to yield homoallylic alcohol as early as 1984.⁵⁰ Another highly diastereoselective allylation of camphor pyrazolidinone derived α -ketoamides have been reported with allyltributyl tin and various Lewis acids by Chen (Scheme 3.34). Chiral ketoamide **3.111** undergoes tin triflate catalyzed allylation using allylstannane effectively to produce one diastereomer **3.112** in high yield.⁵¹ To the best of our knowledge, these are the only allylation protocols known in literature for linear α -ketoamides.



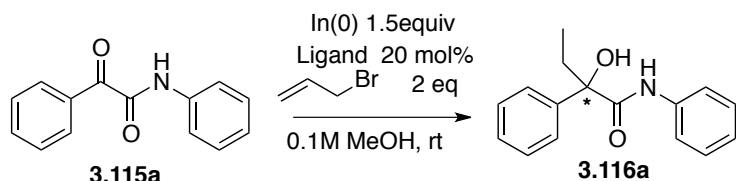
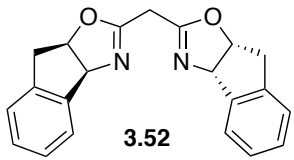
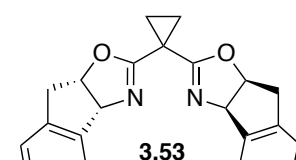
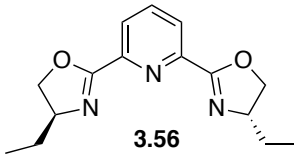
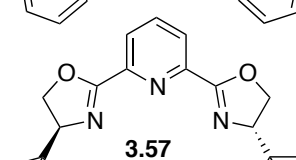
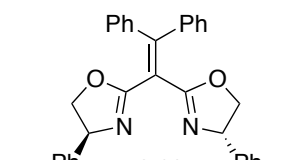
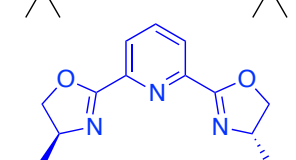
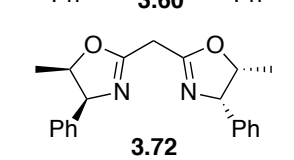
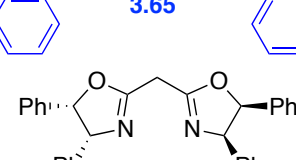
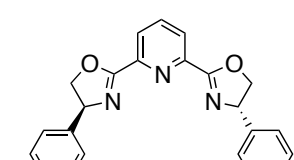
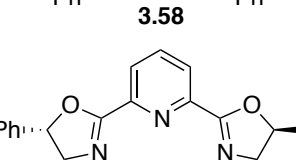
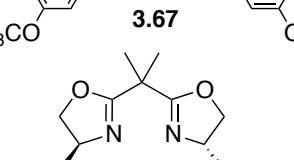
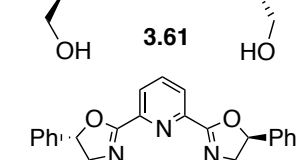
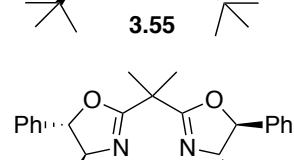
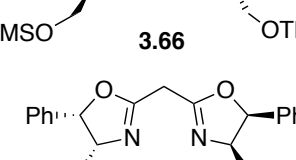
Scheme 3.34. Diastereoselective Allylation of Ketoamides

3.5.3. Results and Discussion

3.5.3.1. Ligand Screening

With most of the conditions screened for isatin, we decided to investigate similar condition for linear- α -ketoamides. With 1.5 eq. and 2.0 eq. allyl bromide, our previous experiments showed that amino alcohol based BOX ligands are effective for chiral information transfer. Our study in linear ketoamide began by screening our BOX ligand library. These studies revealed that phenyl-PyBOX served as a suitable ligand for chiral induction (Table 3.12).

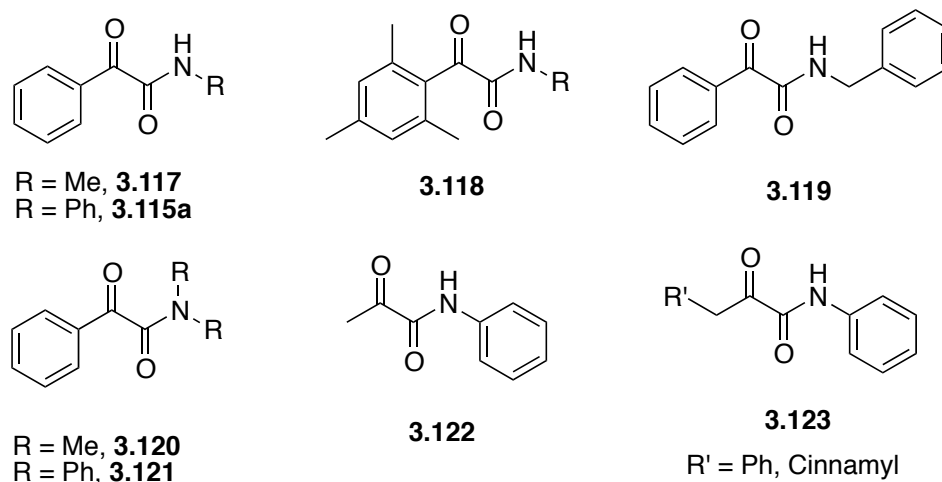
Table 3.12. Ligand Screening for Linear Ketoamides

			
Ligand ^a	Yield, ^b ee ^c	Ligand ^a	Yield, ^b ee ^c
	>99%, 0% ee		88%, 15% ee
	>99%, 7% ee		95, 9% ee
	97%, 0% ee		>95%, 75% ee
	>90%, 60% ee		95%, 9% ee
	92%, 49% ee		>99%, 3% ee
	>99%, 18% ee		97%, 30% ee
	>99%, 0% ee		>99%, 0% ee

^a reactions performed at rt and monitored until completion by TLC. ^b Isolated yields. ^c ee was determined by chiral HPLC

3.5.3.2. Substrate Scope

Unlike isatins, in the case of linear ketoamides there are a lot of variables to explore in substrate scope and evaluate the generality of the reaction. The functional groups could be modified at the keto-group end as well as the amide end. Substrates **3.117**, **3.115** could be derived from benzoyl formic acid. Compound **3.118** was prepared from mesityl glyoxalic acid. Ketoamides derived from pyruvic acid **3.102** could be used effectively in indium-mediated allylation (Scheme 3.35).

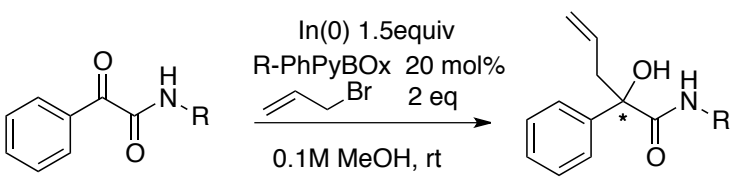
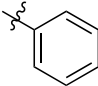
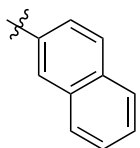
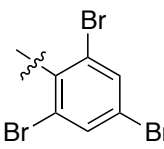
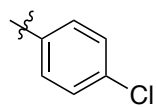
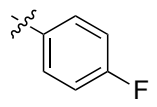
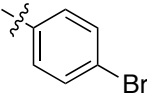
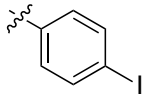
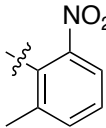
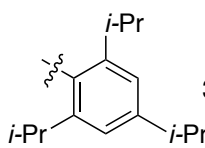
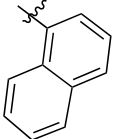


Scheme 3.35. Substrate Scope for Linear Ketoamides

We initially investigated benzoyl formamides and were able to obtain appreciable enantioselectivities as summarized in Table 3.10. The possible variable with this substrate modification is preparation by varying the functionality with aniline. The sterics around the amide nitrogen did not have much positive effect on the enantioselectivity. Most of the functionalities are well tolerated under the indium mediated allylation condition. Substrates containing a nitro group did not react as seen in the case of isatin substrates and *N,N*-disubstituted ketoamides **3.120** and **3.121** did not react under the indium mediated allylation condition.

Modifying the substrate with naphthyl derivatives increased the enantioselectivity to some extent. Substitution of the anilines with different halogens gave similar ee and yield to that of the parent substrate. Having bulkier isopropyl groups did not have a significant impact in the enantioselectivity **3.115k**. It is interesting to note that substrate derived from 2, 4, 6-tribromoaniline gave a lower enantioselectivity compared to the other substrates **3.115b**. The ligand screening was performed only for benzoyl formamides. To expand the scope of the project to other substrates, a ligand screening would be inevitable for pyruvic acid derived substrates **3.125**.

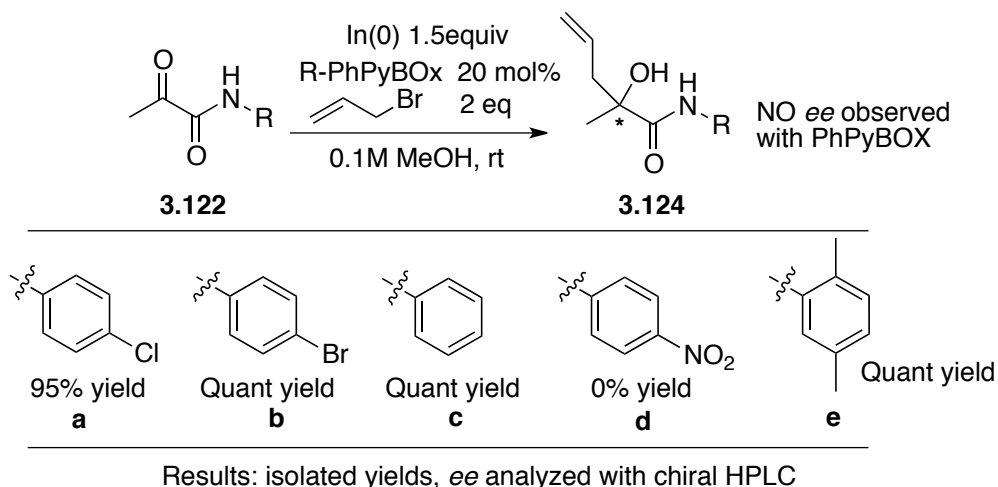
Table 3.13. Allylation of Linear Ketoamides: Substrate Scope

							
R	3.115	% yield ^a	% ee ^b	R	3.116	% yield ^a	% ee ^b
	3.115a	97 (3.116a)	75		3.115g	Quant (3.116g)	78
	3.115b	85 (3.116b)	53		3.115h	95 (3.116h)	73
-NR ₂ = -NH ₂	3.115c	95 (3.116c)	74		3.115i	90 (3.116i)	75
	3.115d	95 (3.116d)	76		3.115j	95 (3.116j)	75
	3.115e	No Reaction	NA		3.115k	90 (3.116k)	73
	3.115f	88 (3.116f)	78				

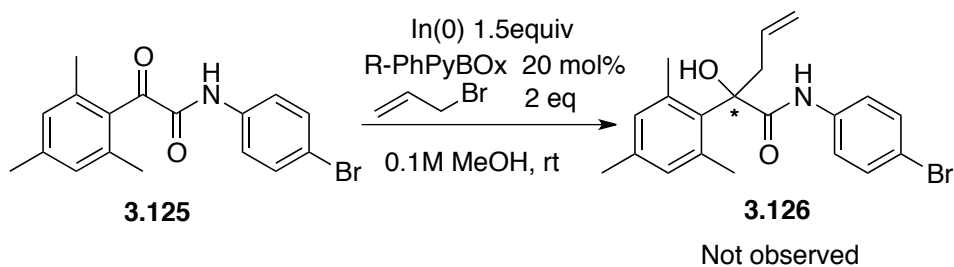
^a Isolated yields, ^b ee determined by HPLC

A series of linear ketoamides were prepared from pyruvic acid (Table 3.14). The indium-mediated allylation of various pyruvanilides successfully yielded allylated product in excellent yield. The enantioinduction on the other hand was not successful with phenyl-PyBOX as ligand (Table 3.14, **3.122a** to **3.122e**).

Table 3.14. Alkylation of Pyruvanilides



After exploring substrates with benzoyl formic acid and pyruvic acid with mixed success and failures, we decided to modify the sterics close to the electrophilic site. A linear ketoamide **3.125** from mesityl glyoxalic acid was prepared with *p*-bromoaniline (Scheme 3.36). The substrate did not react under indium-mediated allylation condition.

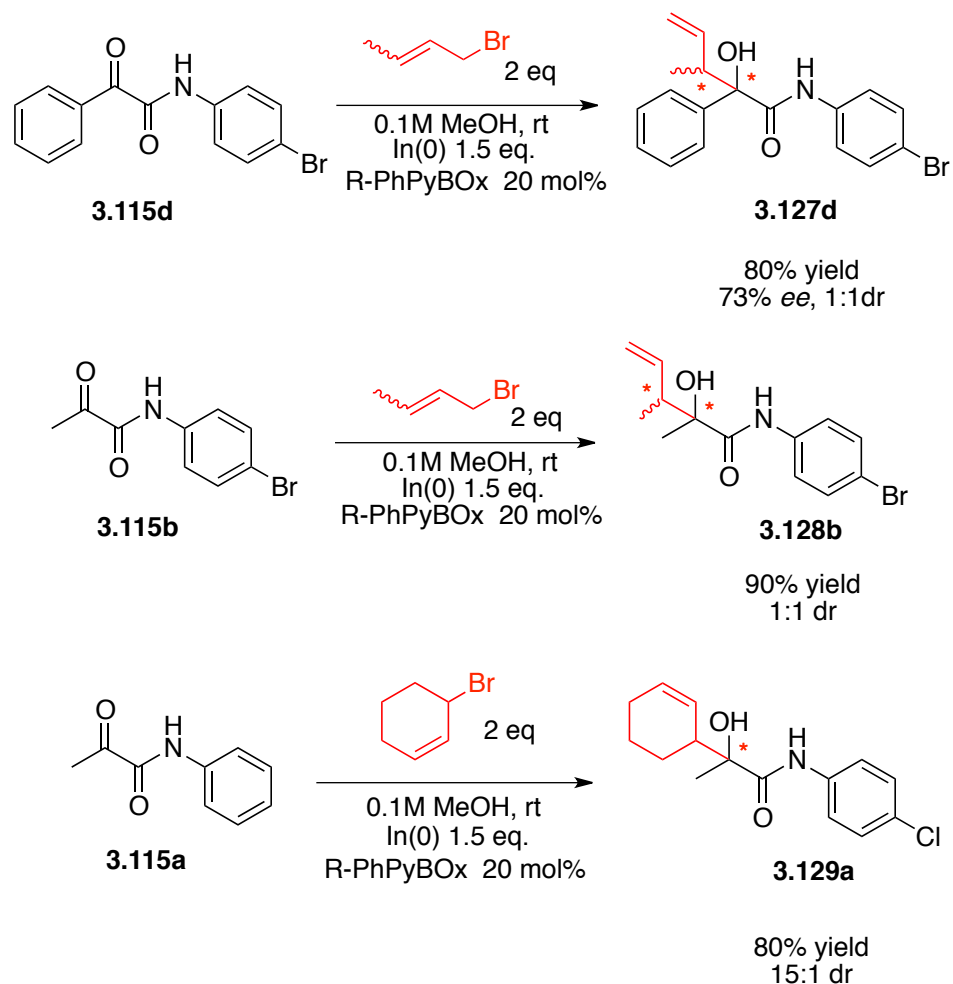


Scheme 3.36. Alkylation of Mesityl glyoxalic Acid Derived Ketoamide

3.5.3.3. Choice of Nucleophilic Precursors

Till this point in the development of enantioselective ketoamides allylations, all substrates utilized allyl bromide as the nucleophilic precursor. In the next stage, we could consider other nucleophilic precursors, similar to our experiments on isatins. A reaction of pyruvaniline with cyclohexenyl bromide under the indium mediated allylation conditions gave the product **3.129a** in 15:1 dr. This promising result would lead us to

expand this system to various allylic bromides. The crotylation experiment with linear ketoamide from benzoyl formic acid **3.115d** and pyruvic acid **3.115b** did not produce any diastereoselectivity (Scheme 3.37).

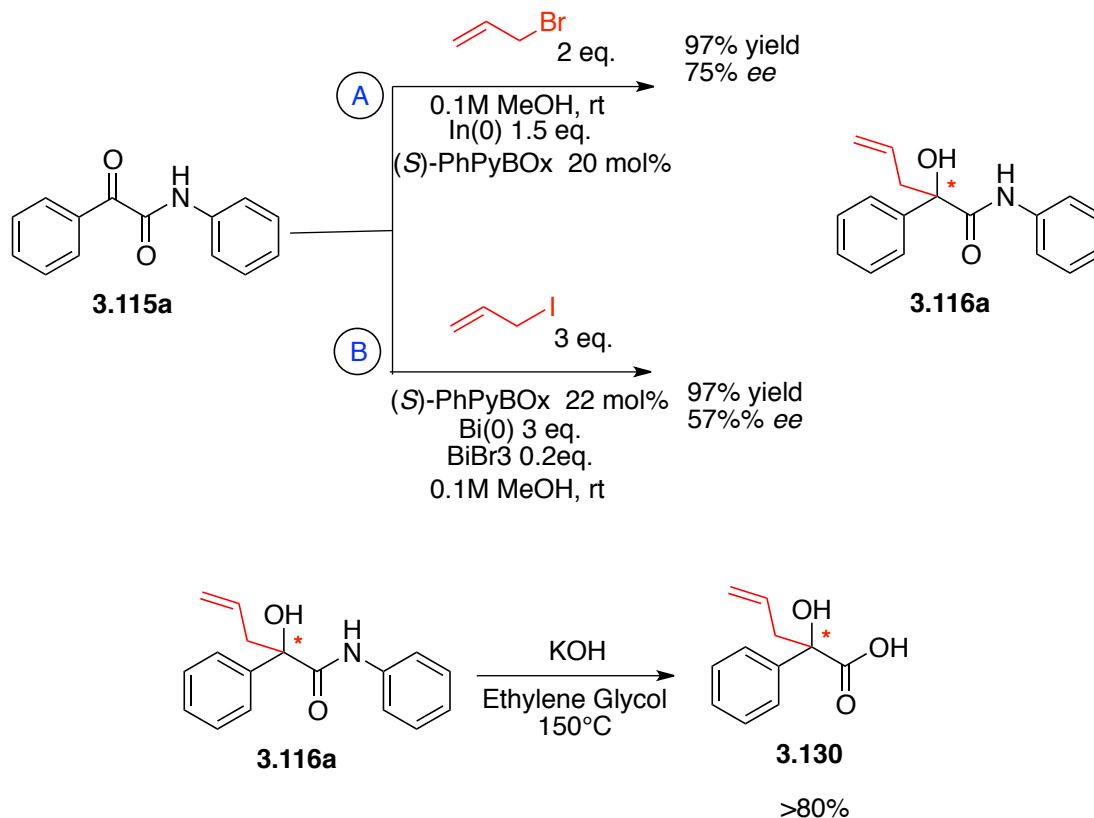


Scheme 3.37. Nucleophilic Precursor scope with Linear Ketoamide

3.6. Stereochemical Reasoning

In the course of allylation we found that when we use (*S*)-Ph-PYBOX, the major isomer observed was (*R*)-allyl isatin. Similarly in the case of linear ketoamides **3.115a**, we observed that when (*S*)-Ph-PYBOX was used, the (*R*)-product **3.116a** was observed as major isomer in the case of indium mediated allylation as well as bismuth-mediated allylation that was developed prior to this research in our group. Both of these absolute

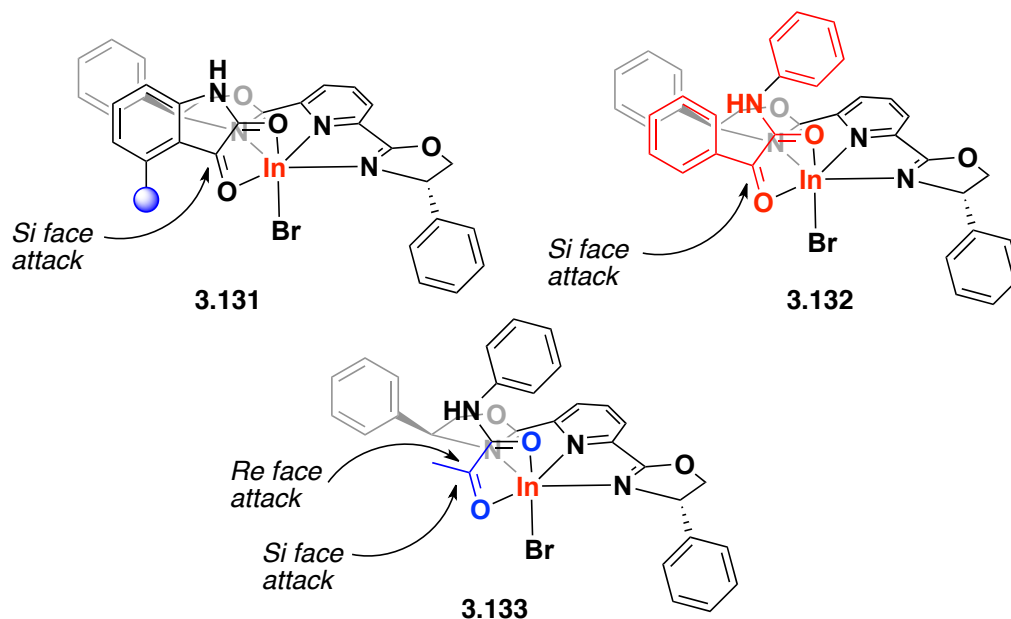
configurations were established based on combination of information obtained from X-ray crystal data and optical rotation values of established compound **3.130** from the literature (Scheme 3.38).



Scheme 3.38. Alkylation of Linear Ketoamides with Indium and Bismuth

We reasoned that the isatin as well as the linear ketoamide bind to the chiral Lewis acid in a specific configuration **3.131**. Isatin molecule binds to the chiral Lewis acid in such a way that the more basic amide carbonyl assumes the axial position and relatively less basic ketone carbonyl assumes the equatorial position. Hypothesizing this as a most favored conformation, compared to the other possibilities, one would be able to reason that the *Si-face* attack by the nucleophile would result in the (*R*)-isomer as observed from the experiment. If the 4-position in the substrate is substituted with an atom relatively larger like bromide or a methyl group which is bigger than a hydrogen atom there is effective

blocking of the attack from the *Re* face, there is effective facial selectivity, and thus this conformation explains why the 4- substituted isatins gave a high enantioselection (Scheme 3.39).



Scheme 3.39. Proposed Modes of Binding for Substrates to Chiral-Lewis acid

Similar to the discussion on isatins we use the similar analogy for linear ketoamides. The proposed binding mode would explain the reason for the observed absolute configuration of the major isomer. The *Si*-face attack results in (*R*)-isomer, which is observed as the major isomer. Now moving to the pyruvic acid derived ketoamides, they produced racemic homoallylic alcohols under indium mediated allylation condition using phenyl-PyBOX ligand. With the hypothesized models **3.131** and **3.132** one could assume that this would be the similar case with the pyruvanilides **3.133**. The lack of substantial amount of supporting information makes it hard at this present moment to claim that this would be the most possible way the nucleophilic attack is occurring. Also in structures **3.131** and **3.132** it seems like the phenyl ring on the substrate could have possible π -stacking

interaction with the phenyl group in the PyBOX. Probing this allylation with other nucleophiles such as allylsilanes and stannanes could give us some insight into the plausibility of these conformations. It is also worth to mention that in the case of bismuth, a similar situation could be envisioned. Both indium and bismuth behaved very similarly in the allylation of isatins and linear ketoamides. The stereochemical similarities suggest us that probing into the mechanism and modes of reactivity would benefit us in developing new green chemical methods using these environmentally benign non-toxic metal.

3.7. Conclusion

We have demonstrated the first enantioselective allylation of ketoamides in aqueous solvent mixtures. Allylation of ketoamides, both cyclic and linear, with a variety of nucleophilic precursors gave homoallylic alcohols in high yields and enantioselectivities. We observed that in order to achieve high enantioselectivity in allylation of isatins, 4-substitution was necessary. The substrate scope of linear ketoamides could be expanded to a great extent as discussed in the respective section. With access to highly enantioenriched 3-substituted-3-hydroxy oxindoles at hand, they are likely to attract additional interest as highly functionalized chiral building blocks in the synthesis of oxindole natural products with surreal complexities. Elaborate studies should be conducted to understand the nature of the chiral Lewis acid generated *in situ* as the enormity of this project began to sink in.

3.8. Supporting Information

Isatins were purchased from Aldrich. (*S*)- and (*R*)-PhPyBOX were prepared through a modified literature procedure. Nucleophilic precursors were purchased from Aldrich. Indium powder was purchased from STREM chemicals. Flash chromatography was

performed using EM Science silica gel 60 (230-400 mesh). All glassware were oven dried, assembled hot and cooled under a stream of argon before use.

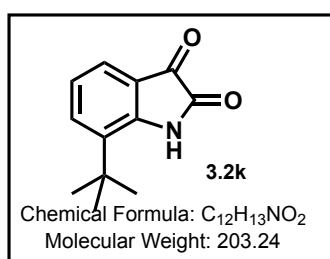
Thin Layer Chromatography (TLC) was performed on a silica gel Whatman-60F glass plates, and components were visualized by illumination of UV light at 254 nm or by staining with iodine vapors or ammonium molybdate solution or vanillin solution or potassium permanganate solution, Melting points were measured with a Fisher-Johns melting point apparatus and are uncorrected. $^1\text{H-NMR}$ was recorded on a Varian Inova-500NB (500MHz), Varian Inova-400NB (400MHz), or Varian Mercury-300 (300MHz). Chemical shifts are reported in parts per million (ppm) downfield from TMS, using residual CDCl_3 (7.24ppm) as an internal standard. Data are reported as follows: Chemical shift, multiplicity (s = singlet, d = doublet, t = triplet, q = quartet, m = multiplet), coupling constant and integration. $^{13}\text{C-NMR}$ was recorded on Varian Inova-500 NB (125 MHz), Varian Inova-400 NB (100MHz), and Varian Mercury-300 (75MHz) spectrometers, using broadband proton decoupling. Chemical shifts are reported in parts per million (ppm) downfield from TMS, using the middle resonance of CDCl_3 (77.9 ppm) as an internal standard. HPLC analyses were carried out on Waters 515 HPLC pump and 2487 dual lambda detector or Waters e2695 separation module with 2487 dual lambda detector connected to a PC with a Empower workstation. Rotations were recorded on a JASCO-DIP-370 instrument and JASCO. High Resolution Mass Spectra (HRMS) (ESI+) were obtained on a BioToF mass spectrometer.

3.8.1. General Procedure for the Preparation of Isatins

A mixture of aniline 100 mmol is dissolved in 10 mL of dry dichloromethane was added slowly at -10°C to 100 mmol of oxalyl chloride. After 15 minutes the color of the

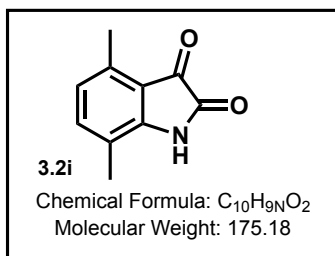
solution becomes pale green. The solution was evaporated to dryness in a rotary evaporator under vacuum. The solid is dissolved in 20 mL of dry dichloromethane and cooled to 0°C. To this solution 200 mmol of titanium tetrachloride in dichloromethane was added dropwise and the solution is warmed to room temperature. The crude reaction mixture is washed with water and the product is extracted with ethyl acetate. The product is purified by recrystallizing with a mixture of hexane and ethyl acetate (1:1).

Orange crystals; m.p = 215-218 °C; IR (film): 3430, 1743, 2957, 1599, 1694, 1489, 1464,



1422, 1323, 1266, 777, 705 cm⁻¹; ¹H NMR (400 MHz, Acetone-d₆): δ 1.43 (s, 9H), 2.04 (m, 1H), 7.07-7.11(t, 1H, *J* = 7.4 Hz), 7.40-7.42 (d, 1H, *J* = 7.4 Hz), 7.61-7.63 (d, 1H, *J* = 7.3 Hz), 9.63 (s, 1H); ¹³C NMR (Acetone-D₆, 125 MHz): δ

206.4, 206.2, 185.1, 159.9, 136.3, 135.2, 124.0, 123.2, 119.8, 34.6.



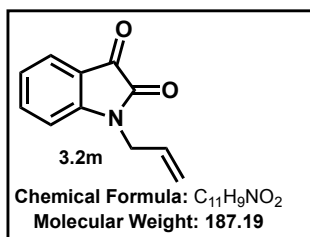
Orange solid; m.p = 240-243 °C; IR (film): 3448, 2530, 2096, 1791, 1717, 1652, 1621, 1273, 1251 cm⁻¹; ¹H NMR (400 MHz, Acetone-d₆): δ 2.61 (dd, 1H, *J* = 8.5, 13.2 Hz), 2.75 (dd, 1H, *J* = 6.3, 13.2 Hz), 3.65 (s, 1H), 5.10 (d, 1H, *J* = 18.1 Hz), 5.11 (d,

1H, *J* = 8.8 Hz), 5.65 (m, 1H), 6.88(d, 1H, *J* = 7.6 Hz), 7.07 (t, 1H, *J* = 7.6 Hz), 7.25 (t, 1H, *J* = 7.3 Hz), 7.36 (d, 1H, *J* = 7.3 Hz); ¹³C NMR (DMSO-D₆, 100 MHz): δ = 185.2, 133.2, 131.9, 130.5, 124.2, 119.3, 118.0, 116.3, 41.3, 16.6, 15.6. HRMS Calcd for C₁₀H₉NO₂ (M+Na)⁺: 198.1670; Found: 198.1685.

3.8.2. General Procedure for the Preparation of 1-Aryl-1*H*-indole-2,4-diones

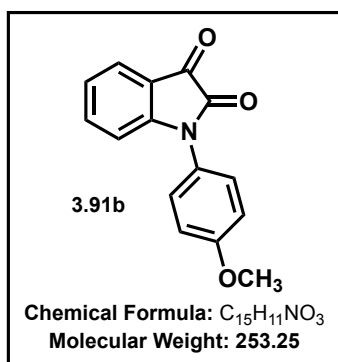
A mixture of 0.04 mole of isatin and 0.08 mole of the corresponding aryl bromide and 10 g of cupric oxide in dimethyl formamide was sonicated for 15 minutes at room

temperature and followed by which, the reaction mixture was heated under reflux for 10 hours. The hot solution was filtered to remove any inorganics present. The filtrate was poured into cold water and the resulting precipitate was filtered and dried. Further purification could be performed using flash column chromatography. The product was recrystallized from a mixture of ethyl acetate and hexane.



1-(2-Propen-1-yl)-*H*-Indole-2,3-dione⁵², Red crystals; M. p = 89–91 °C (recrystallized ethanol); IR: 1734, 1606 cm⁻¹; ¹H NMR (CDCl₃): δ 4.24 (dd, 2H), 5.19 (m, 2H), 5.70 (m, 1H); 6.81–7.46 (m, 4H); ¹³C NMR (CDCl₃): 42.4, 118.5, 130.,

110.9, 123.8, 125.2, 138.4, 117.4, 156.7, 157.9, 183.2.



1-(4-Methoxyphenyl)-*H*-Indole-2,3-dione Orange solid; M.p = 163–165 °C; IR (film): 3439, 1733, 1683, 1614, 1515, 1466, 1368, 1297, 1251, 1184, 1101, 821 cm⁻¹; ¹H NMR (DMSO-*d*₆, 400 MHz): δ = 12.83 (s, 1H), 11.68 (s, 1H), 8.07 (s, 1H), 7.97 (d, *J* = 7.6 Hz, 2H), 7.77 (d, *J* = 8.8 Hz, 1H), 7.68–7.59 (m, 2H), 7.55–7.51 (m, 2H), 6.35 (s, 1H), 2.42 (s, 3H); ¹³C NMR

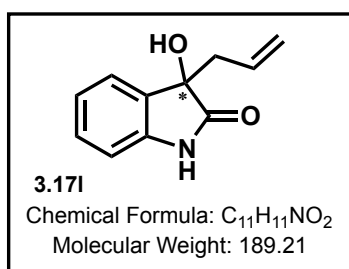
(DMSO-*d*₆, 100 MHz): δ = 151.4, 137.0, 127.0, 125.1, 123.4, 122.5, 116.7, 113.8, 109.8,

54.0. HRMS Calcd for C₁₅H₁₁NO₃ (M+Na)⁺: 276.2240; Found: 276.2219.

3.8.3. General Procedure for Indium-Mediated Allylation of Isatins

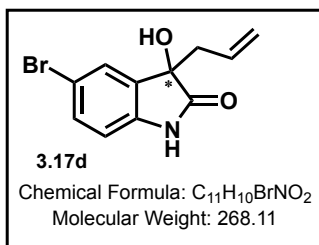
Isatin (0.2 mmol scale, 1 equiv.), indium powder (0.3 mmol, 1.5 equiv.) and (S)-PhPyBOX (0.044 mmol) were added to a 20 mL scintillation vial equipped with a magnetic pellet. Two milliliters of HPLC methanol was syringed into the vial followed by allyl bromide (0.4 mmol, 2 equiv.). The reaction mixture was stirred at room temperature until

the substrate was totally consumed. The reaction could be monitored by TLC or in many cases with the complete disappearance of the color of isatin. The reaction was then concentrated and about 10 mL of 50% ethyl acetate/hexane was added to the vial. The mixture was sonicated for 2 minutes and filtered through a 5 cm plug of silica gel. If necessary, column chromatography was performed for further purification. Enantiopure 3-Allyl-3-hydroxy-oxindoles could be obtained upon recrystallizing the product with minimum amount of hot ethyl acetate.



1,3-dihydro-3-hydroxy-3-(2-propen-1-yl)- *H*-Indol-2-one.⁵³

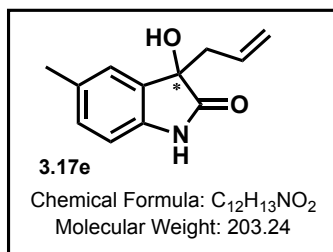
m.p = 112-115 ; IR (KBr) ν = 3332, 1721, 1624, 1474, 1190, 744, 629 cm⁻¹; ¹H NMR (300 MHz, CDCl₃ + DMSO-d₆): δ 2.61 (dd, 1H, *J* = 8.5, 13.2 Hz), 2.75 (dd, 1H, *J* = 6.3, 13.2 Hz), 3.65 (s, 1H), 5.10 (d, 1H, *J* = 18.1 Hz), 5.11 (d, 1H, *J* = 8.8 Hz), 5.65 (m, 1H), 6.88(d, 1H, *J* = 7.6 Hz), 7.07 (t, 1H, *J* = 7.6 Hz), 7.25 (t, 1H, *J* = 7.3 Hz), 7.36 (d, 1H, *J* = 7.3 Hz); ¹³C NMR (75 MHz, CDCl₃ + DMSO-d₆): δ 42.9, 76.3, 110.3, 120.4, 122.9, 124.3, 129.5, 130.06, 130.14, 140.1, 180.0. HPLC: ChiralPak-AD-H: Hexane:IPA(90:10); 1.0 ml/min, 254nm, 11.0 min and 15.1 min.



5-Bromo-1,3-dihydro-3-hydroxy-3-(2-propen-1-yl)- *2H*-Indol-2-one.⁵³

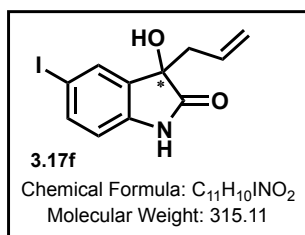
m.p = 190-192°C; IR (KBr) ν = 3246, 3177, 1706, 1619, 1472, 1440, 1182, 1082, 930, 826, 730 cm⁻¹; ¹H NMR (300 MHz, CDCl₃ + DMSO-d₆): δ 2.50-2.56 (m, 1H), 2.60-2.70 (m, 1H), 2.98 (s, 1H), 4.92-5.04 (m, 1H), 5.50-5.63 (m, 1H), 5.82 (s, 1H) 6.74 (d, 1H, *J* = 7.8 Hz), 7.30 (dd, 1H, *J* = 2.0, 6.3

Hz), 7.40 (s, 1H), 10.02 (s, 1H); ^{13}C NMR (75 MHz, $\text{CDCl}_3 + \text{DMSO-d}_6$): δ 41.7, 75.1, 110.7, 113.5, 118.5, 126.4, 130.3, 130.6, 133.0, 140.6, 177.9. HPLC: ChiralPak-AD-H: Hexane:IPA(90:10); 1.0 ml/min, 254nm, 12.3 min and 18.0 min.



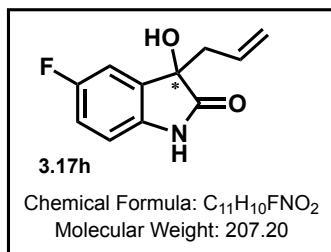
5-Methyl-1,3-dihydro-3-hydroxy-3-(2-propen-1-yl)- 2H-Indol-2-one.⁵³

White solid; m.p = 169-171°C; IR (KBr) ν = 3258, 3184, 2920, 1701, 1626, 1489, 1157, 927, 817, 733 cm^{-1} ; ^1H NMR (300 MHz, $\text{CDCl}_3 + \text{DMSO-d}_6$): δ 2.10 (s, 3H), 2.58-2.64 (m, 2H), 3.00 (s, 1H), 5.00 (dd, 2H, J = 9.6, 13.2 Hz), 5.55-5.67 (m, 1H), 6.62 (d, 1H, J = 7.7 Hz), 6.94 (d, 1H, J = 7.7 Hz), 7.08 (s, 1H), 9.80 (s, 1H); ^{13}C NMR (75 MHz, $\text{CDCl}_3 + \text{DMSO-d}_6$): δ 21.3, 47.6, 85.3, 110.1, 119.9, 127.8, 128.1, 128.4, 130.8, 131.9, 139.6, 177.6. HPLC: ChiralPak-AD-H: Hexane:IPA(90:10); 1.0 ml/min, 254nm, 12.5 min and 16.0 min.



5-Iodo-1,3-dihydro-3-hydroxy-3-(2-propen-1-yl)- 2H-Indol-2-one.⁵³

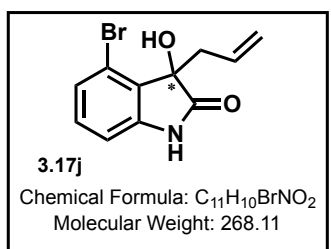
White solid; m.p = 156-158°C; IR (KBr) ν = 3248, 3166, 1710, 1615, 1468, 1439, 1175, 1060, 950, 810, 733 cm^{-1} ; ^1H NMR (300 MHz, $\text{CDCl}_3 + \text{DMSO-d}_6$): δ 2.50-2.56 (m, 1H), 2.60-2.70 (m, 1H), 2.98 (s, 1H), 4.92-5.04 (m, 1H), 5.50-5.63 (m, 1H), 5.82 (s, 1H), 6.74 (d, 1H, J = 7.8 Hz), 7.30 (dd, 1H, J = 2.0, 6.3 Hz), 7.40 (s, 1H), 10.02 (s, 1H); ^{13}C NMR (75 MHz, $\text{CDCl}_3 + \text{DMSO-d}_6$): δ 41.7, 75.1, 110.7, 113.5, 118.5, 126.4, 130.3, 130.6, 133.0, 140.6, 177.9. HPLC: ChiralPak-AD-H: Hexane:IPA(90:10); 1.0 ml/min, 254nm, 15.1 min and 17.0 min.



5-Fluoro-1,3-dihydro-3-hydroxy-3-(2-propen-1-yl)- 2H-Indol-2-one.⁵³

White solid; m.p = 211-213 °C; IR (film): 3275, 1678, 1459, 1376, 1313, 1153, 1066, 937, 851, 825, 770 cm⁻¹; ¹H NMR

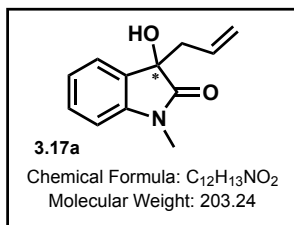
(DMSO-D₆, 400 MHz): δ = 12.83 (s, 1H), 11.68 (s, 1H), 8.07 (s, 1H), 7.97 (d, *J* = 7.6 Hz, 2H), 7.77 (d, *J* = 8.8 Hz, 1H), 7.68-7.59 (m, 2H), 7.55-7.51 (m, 2H), 6.35 (s, 1H), 2.42 (s, 3H); ¹³C NMR (DMSO-D₆, 100 MHz): δ = 184.4, 173.6, 165.2, 158.4, 158.3, 146.4, 138.7, 137.4, 134.2, 133.9, 131.1, 125.2, 122.8, 119.1, 115.9, 23.5. HPLC: ChiralPak-AD-H: Hexane:IPA(90:10); 1.0 ml/min, 254nm, 10.5 min and 16.5 min.



4-Bromo-1,3-dihydro-3-hydroxy-3-(2-propen-1-yl)- 2H-Indol-2-one.⁵³

IR (film): 3424, 2546, 2361, 2338, 2115, 1740, 1707, 1652, 1617, 1445, 1267, 1172, 927 cm⁻¹; ¹H NMR (DMSO-D₆, 400 MHz): δ = 12.83 (s, 1H), 11.68 (s, 1H), 8.07

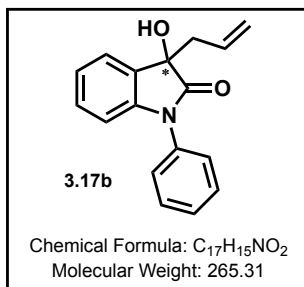
(s, 1H), 7.97 (d, *J* = 7.6 Hz, 2H), 7.77 (d, *J* = 8.8 Hz, 1H), 7.68-7.59 (m, 2H), 7.55-7.51 (m, 2H), 6.35 (s, 1H), 2.42 (s, 3H); ¹³C NMR (Acetone-D₆, 100 MHz): δ = 184.4, 173.6, 165.2, 158.4, 158.3, 146.4, 138.7, 137.4, 134.2, 133.9, 131.1, 125.2, 122.8, 119.1, 115.9, 23.5. HPLC: ChiralPak-AD-H: Hexane:IPA(90:10); 1.0 ml/min, 254nm, 15.2 min and 17.1 min.



1,3-Dihydro-3-hydroxy-1-methyl-3-(2-propen-1-yl)- H-Indol-2-one.⁵³; Mp = 154-156 °C; IR (KBr) ν = 3295, 1615, 1456, 1168,

1065, 956, 756 cm⁻¹; ¹H NMR (300 MHz, CDCl₃ + DMSO-D₆): δ 2.56-2.78 (m, 2H), 3.17 (s, 3H), 3.28 (s, 1H), 5.06-5.13 (m, 2H), 5.55-5.72 (m, 1H), 6.82 (d, 1H, *J* = 8.2 Hz), 7.10 (t, 1H, *J* = 8.2 Hz), 7.32 (t, 1H, *J* = 8.2 Hz), 7.38 (d, 1H, *J* = 8.2 Hz); ¹³C NMR (75 MHz, CDCl₃ + DMSO-D₆): δ 26.1, 42.8, 75.9,

108.4, 120.3, 123.0, 124.1, 129.6, 129.8, 130.5, 143.2, 177.9. HPLC: ChiralPak-AD-H: Hexane:IPA(90:10); 1.0 ml/min, 254nm, 10.6 min and 13.2 min.

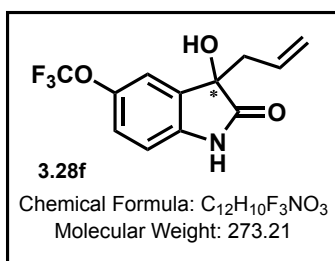


1,3-Dihydro-3-hydroxy-1-phenyl-3-(2-propen-1-yl)-H-Indol-

2-one. ⁵³IR (film): 3275, 1678, 1459, 1376, 1313, 1153, 1066, 937, 851, 825, 770 cm⁻¹; ¹H NMR (DMSO-D₆, 400 MHz): δ = 12.83 (s, 1H), 11.68 (s, 1H), 8.07 (s, 1H), 7.97 (d, *J* = 7.6 Hz, 2H), 7.77 (d, *J* = 8.8 Hz, 1H), 7.68-7.59 (m, 2H), 7.55-7.51 (m,

2H), 6.35 (s, 1H), 2.42 (s, 3H); ¹³C NMR (DMSO-D₆, 100 MHz): δ = 184.4, 173.6, 165.2, 158.4, 158.3, 146.4, 138.7, 137.4, 134.2, 133.9, 131.1, 125.2, 122.8, 119.1, 115.9, 23.5.

HPLC: ChiralPak-AD-H: Hexane:IPA(90:10); 1.0 ml/min, 254nm, 14.3 min and 17.7 min.

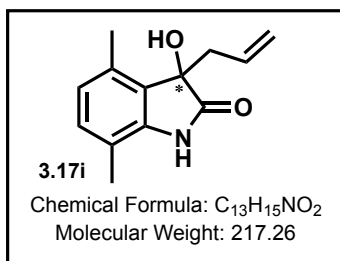


4-Trifluoromethoxy-1,3-dihydro-3-hydroxy-3-(2-propen-

1-yl)- 2H-Indol-2-one. ⁵³IR (film): 3438, 1771, 1716, 1638, 1652, 1635, 1558, 1456, 1472, 1266, 667 cm⁻¹; ¹H NMR (400 MHz, CDCl₃): δ 2.56-2.76 (m, 2H), 3.04 (s, 1H), 5.12-5.18

(dd, 2H, *J* = 9.5, 13.1 Hz), 5.64-5.75 (m, 1H), 6.86-6.88 (d, 1H, *J* = 7.6 Hz), 7.13-7.15 (d, 1H, *J* = 7.6 Hz), 7.90 (s, 1H); ¹³C NMR (DMSO-D₆, 100 MHz): δ = 178.3, 147.3, 143.6, 139.8, 132.0, 130.2, 121.8, 119.1, 117.7, 110.0, 75.6, 42.0. HPLC: ChiralPak-AD-H:

Hexane:IPA(90:10); 1.0 ml/min, 254nm, 12.6 min and 16.4 min.

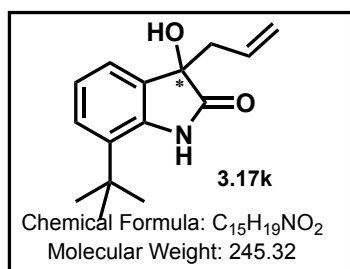


4,7-Dimethyl-1,3-dihydro-3-hydroxy-3-(2-propen-1-yl)-

2H-Indol-2-one. IR (film): 3400, 2538, 2105, 1638, 1652, 1633, 1558, 1248, 1202, 1068 cm⁻¹; ¹H NMR (300 MHz, CDCl₃): δ 2.17 (s, 3H), 2.42 (s, 3H), 2.76-2.93 (m, 2H), 3.27

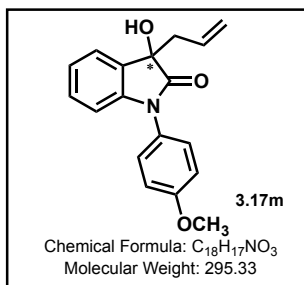
(s, 1H), 4.97-5.10 (dd, 2H, *J* = 9.2, 13.4 Hz), 5.38-5.49 (m, 1H), 6.74-6.76 (d, 1H, *J* = 7.6

Hz), 6.93-6.95 (dd, 1H, $J = 7.5$ Hz), 8.52 (s, 1H); ^{13}C NMR (Acetone- D_6 , 100 MHz): $\delta = 185.2, 133.2, 131.9, 130.5, 124.2, 119.3, 118.0, 116.3, 41.3, 16.6, 15.6$. HRMS Calcd for $\text{C}_{13}\text{H}_{15}\text{NO}_2$ ($\text{M}+\text{Na}$) $^+$: 240.2355 Found: 240.2364. HPLC: ChiralPak-AD-H: Hexane:IPA(90:10); 1.0 ml/min, 254nm, 14.2 min and 19.5 min.



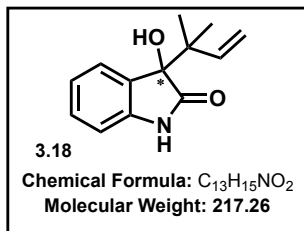
7-*t*-Butyl-1,3-dihydro-3-hydroxy-3-(2-propen-1-yl)-2H-Indol-2-one. IR (film): 3275, 1678, 1459, 1376, 1313, 1153, 1066, 937, 851, 825, 770 cm^{-1} ; ^1H NMR (DMSO- D_6 , 400 MHz): $\delta = 12.83$ (s, 1H), 11.68 (s, 1H), 8.07 (s, 1H), 7.97 (d,

$J = 7.6$ Hz, 2H), 7.77 (d, $J = 8.8$ Hz, 1H), 7.68-7.59 (m, 2H), 7.55-7.51 (m, 2H), 6.35 (s, 1H), 2.42 (s, 3H); ^{13}C NMR (DMSO- D_6 , 220 MHz): $\delta = 184.4, 173.6, 165.2, 140.6, 139.6, 128.2, 127.8, 123.9, 39.0, 34.54$. HPLC: ChiralPak-AD-H: Hexane:IPA(90:10); 1.0 ml/min, 254nm, 14.3 min and 16.4 min.

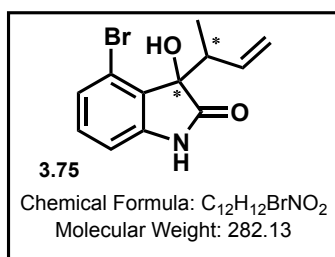


1,3-Dihydro-3-hydroxy-1-(4-methoxyphenyl)-3-(2-propen-1-yl)-H-Indol-2-one. ^{53}IR (film): 3398, 2360, 2337, 1843, 1791, 1716, 1514, 1465, 1249, 1180, 1107, 1029, 922 cm^{-1} ; ^1H NMR (CDCl_3 , 400 MHz): $\delta = 7.60$ (s, 2H), 7.40-7.42 (d, $J = 7.0$ Hz

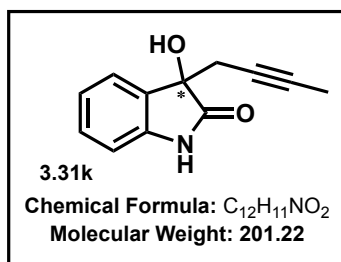
2H), 7.16-7.20 (t, $J = 7.0$ Hz, 1H), 7.11-7.13 (d, $J = 7.4$ Hz, 2H), 6.81-6.83 (d, $J = 6.8$ Hz, 1H), 3.86 (s, 3H), 2.83 (s, 3H), 2.03 (s, 1H); ^{13}C NMR (CDCl_3 , 100 MHz): $\delta = 205.3, 178.3, 160.1, 144.6, 131.3, 130.4, 130.1, 128.7, 127.4, 125.1, 124.2, 121.4, 115.8, 110.4, 76.8, 56.4, 44.2$. HRMS Calcd for $\text{C}_{18}\text{H}_{17}\text{NO}_3$ ($\text{M}+\text{Na}$) $^+$: 318.2720; Found: 318.2710. HPLC: ChiralPak-AD-H: Hexane:IPA(90:10); 1.0 ml/min, 254nm, 15.9 min and 19.5 min.



1,3-dihydro-3-hydroxy-3-(1-methyl-2-propen-1-yl)-*H*-Indol-2-one.⁵⁴ Mp 188-190°C; IR(KBr) ν = 3366, 1706, 1621, 1472, 1185, 1115, 916, 771, 755, 732, 672 cm⁻¹; ¹H NMR (400 MHz, CDCl₃) δ 1.12 (s, 3H), 1.18 (s, 3H), 2.84 (s, 1H), 5.15 (dd, 1H, J = 1.2, 17.4 Hz), 5.24 (dd, 1H, J = 1.2, 10.8 Hz), 6.19 (dd, 1H, J = 10.8, 17.4 Hz), 6.81 (d, 1H, J = 7.6 Hz), 7.02 (td, 1H, J = 0.9, 7.6 Hz), 7.25 (td, 1H, J = 1.3, 7.6 Hz), 7.37 (1H, dd, J = 0.7, 7.6 Hz); ¹³C-NMR (100 MHz, CDCl₃ + DMSO-d₆): δ 21.1, 22.4, 43.7, 80.0, 109.9, 113.6, 121.6, 126.6, 129.6, 132.0, 143.1, 144, 179.8. HPLC: ChiralPak-AD-H: Hexane:IPA(90:10); 1.0 ml/min, 254nm, 20.1 min and 26.2 min.



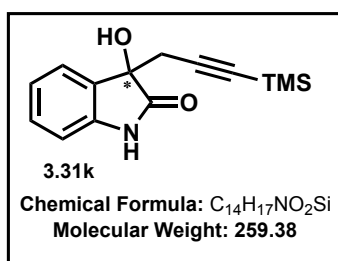
4-Bromo-1,3-dihydro-3-hydroxy-3-(1-methyl-2-propen-1-yl)-*H*-Indol-2-one. (Major isomer isolated by recrystallization using ethylacetate) IR (film): 3444, 2964, 1706, 1652, 1616, 1443, 1376, 1376, 1341, 1247, 1168, 1140, 993 cm⁻¹; ¹H NMR (DMSO-D₆, 400 MHz): δ = 9.16, 9.05 (s, 1H), 6.77-6.84 (m, 4H), 6.48-6.50 (t, J = 3.3 Hz, 1H), 6.56-6.57 (m, 1H), 5.94-6.01 (q, J = 8.1 Hz, 1H), 5.05-5.16 (q, J = 8.0 Hz, 1H), 4.78-4.86 (m, 1H), 2.59, 2.56 (s, 1H), 1.01-1.03 (d, J = 7.0 Hz, 3H), 0.45-0.47 (d, J = 7.0 Hz, 3H); ¹³C NMR (DMSO-D₆, 100 MHz): δ = 184.4, 173.6, 165.2, 158.4, 158.3, 146.4, 138.7, 137.4, 134.2, 133.9, 131.1, 125.2, 122.8, 119.1, 115.9, 23.5. HRMS Calcd for C₁₂H₁₂BrNO₂ (M+Na)⁺: 304.1455; Found: 304.1465. HPLC: ChiralPak-AD-3: Hexane:IPA(95:5); 1.0 ml/min, 254nm, 23.5; 31.8 mins and 26.8, 27.8 mins. Major isomer is the peak at 27.8 min.



3-(2-butyn-1-yl)-1,3-dihydro-3-hydroxy- *H*-Indol-2-one.⁵⁵

IR (film): 3420, 1843, 1792, 1716, 1652, 1576, 1342, 1185, 1115, 667. cm⁻¹; ¹H NMR (Acetone-D₆, 400 MHz): δ = 8.79 (s, 1H), 7.24 (s, 1H), 6.92-6.94 (d, *J* = 7.0 Hz, 1H), 6.82-6.86

(t, *J* = 7.1 Hz, 1H), 6.60-6.64 (t, *J* = 7.0 Hz, 1H), 6.82-6.86 (d, *J* = 7.9 Hz, 1H), 4.48 (s, 3H), 4.20 (s, 1H), 2.39 (s, 2H); ¹³C NMR (Acetone-D₆, 100 MHz): δ = 205.7, 178.2, 141.8, 130.8, 129.6, 124.9, 122.5, 110.2, 100.9, 78.7, 76.7, 13.7. HRMS Calcd for C₁₂H₁₁NO₂ (M+Na)⁺: 224.2110 Found: 224.1954. HPLC: ChiralPak-AD-H: Hexane:IPA(90:10); 1.0 ml/min, 254nm, 21.1 min and 25.0 min.



3-(3-Trimethylsilyl-2-butyn-1-yl)-1,3-dihydro-3-hydroxy- *H*-Indol-2-one.⁵⁵

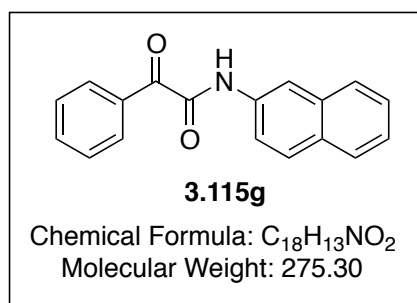
IR (film): 3378, 2970, 2900, 2522, 2106, 1931, 1698, 1622, 1472, 1333, 1249, 838 cm⁻¹; ¹H NMR (Acetone-D₆, 400

MHz): δ = 9.21 (s, 1H), 7.16-7.24 (m, 2H), 6.94-6.98 (t, *J* = 7.5 Hz, 1H), 6.84-6.88 (d, *J* = 7.6 Hz, 1H), 4.90 (s, 1H), 4.45-4.46 (d, *J* = 3.1 Hz, 2H); ¹³C NMR (Acetone-D₆, 100 MHz): δ = 209.5, 178.5, 142.3, 133.8, 129.8, 125.6, 122.5, 110.3, 110.2, 72.7. HRMS Calcd for C₁₄H₁₇NO₂Si (M+Na)⁺: 282.2430 Found: 282.2426. HPLC: ChiralPak-AD-H: Hexane:IPA(90:10); 1.0 ml/min, 254nm, 15.5 min and 19.5 min.

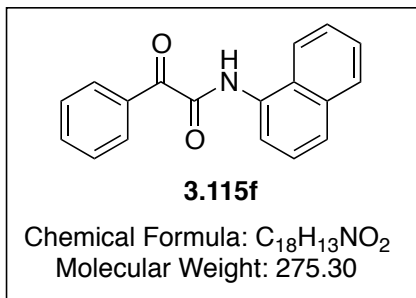
3.8.4 General Procedure for Preparation of Linear Ketoamides

To a 100mL, three-necked round-bottomed flask equipped with magnetic stirrer, pressure equalizing addition funnel, vacuum-take-off adapter and a glass adapter with a stopper connected to a bubbler. The whole apparatus was purged under argon. The flask is charged with benzoyl formic acid (0.20 mmol, 1 equiv.) and 25 mL of dichloro methane.

To this solution oxalyl chloride (0.20 mmol, 1.1 equiv.) was added slowly through an addition funnel over 10 minutes at 0°C. Followed by the addition 200 μL of DMF was added and the glass stopper connected to a bubbler is opened to enable the hydrogen chloride gas to escape. The solution was allowed to stir until the evolution stops. After an additional 30 minutes the apparatus is disassembled. The round –bottomed flask was kept at 0°C under argon while a solution of the aniline (0.20 mmol, 1 equiv.) and triethyl amine (0.22 mmol, 1.1 equiv.) in 20 mL dichloro methane is charged in a clean addition funnel. The reaction is continued with a similar assembly as before. The reaction was allowed to stir for 5 to 8 h or until the aniline was consumed by TLC. Following the completion of the reaction, the mixture was washed with water and dried with sodium sulfate. The resulting organic layer was concentrated under vacuum and purified by flash silica gel chromatography. The ketoamides could also be purified by recrystallization with 30%ethyl acetate/hexane mixture.



2-Oxo-N,2-phenylacetamide. Yellow Solid, M. P = 142-144°C °C (CHCl₃); IR ν_{\max} (KBr): 1674, 1710, 3321 cm⁻¹H NMR (400 MHz CDCl₃): δ 9.12 (s, 1H), 8.42-8.45 (m, 3H), 7.79-7.85 (m, 3H), 7.60-7.67 (td, 1H), 7.58-7.63 (dd, J=7.0 Hz, 3.1 Hz 4H), 7.24-7.53 (m, 5H); ¹³C NMR (100 MHz, CDCl₃): δ 188.1, 159.8, 135.5, 134.9, 134.6, 133.9, 132.4, 131.9, 129.9, 129.4, 128.7, 128.5, 127.6, 126.4, 120.3, 117.9. HRMS Calcd for C₁₈H₁₃NO₂ (M+Na)⁺: 298.2911 Found: 298.2398.



***N*-(Naphthalene-1-yl)-2-oxo-2-phenylacetamide.** Pale

yellow solids, M. P = 92-96 °C; IR ν_{\max} (thin film):

3430, 3258, 1772, 1668, 1655, 1456, 1472, 813, 513,

503 cm⁻¹; ¹H NMR (400 MHz CDCl₃): δ 9.53 (s, 1H),

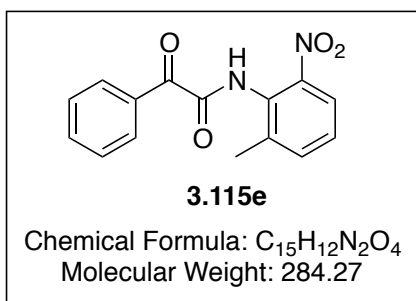
8.47-8.49 (m, 2H), 8.22-8.24 (d, J=7.2 Hz, 1H), 7.94-

7.96 (d, J=7.2 Hz, 1H), 7.88-7.90 (d, J=7.0 Hz, 1H), 7.73-7.75 (d, J=7.2 Hz, 1H), 7.64-7.68

(tt, J=7.3 Hz, 3.0 Hz, 1H), 7.50-7.60 (m, 5H); ¹³C NMR (100 MHz, CDCl₃): δ 188.4,

160.2, 135.7, 135.0, 134.1, 132.5, 139.9, 139.6, 127.6, 127.4, 127.2, 126.7, 121.1, 120.4,

113.9. HRMS Calcd for C₁₈H₁₃NO₂ (M+Na)⁺: 298.2911 Found: 292.1600.



2-Oxo-N,2-(6-methyl-2-nitro)-phenylacetamide. Pale

yellow solid, m. p = 115-118 °C (CHCl₃); IR ν_{\max}

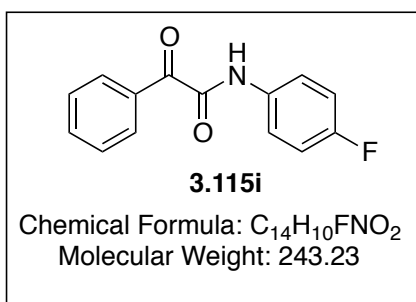
(film): 3406, 2929, 2103, 1843, 1791, 1771, 1652, 1558,

1506, 1456, 1419, 1344, 1296, 1247, 1204, 1176, 1015

cm⁻¹; ¹H NMR (400 MHz CDCl₃): δ 7.94-7.99 (m, 4H),

7.62-7.66 (m, 2H), 7.48-7.52 (m, 3H), 2.51 (s, 1H.); ¹³C NMR (100 MHz, CDCl₃): δ

205.2, 137.7, 136.0, 132.6, 131.4, 131.0, 129.8, 124.6, 18.6.



2-Oxo-N,2-(4-fluoro)-phenylacetamide White solid,

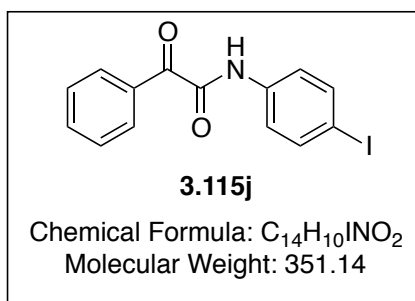
m. p = 108-110 °C (CHCl₃); IR ν_{\max} (film): 3336,

1733, 1670, 1558, 1540, 1507, 1284, 1209, 845 cm⁻¹; ¹H

NMR (400 MHz CDCl₃): δ 8.94 (s, 3H), 8.37-8.39 (d,

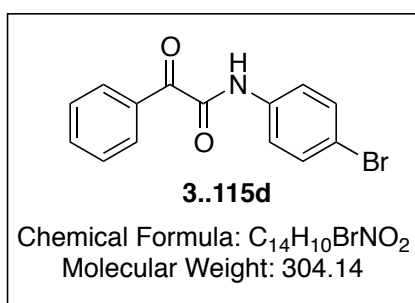
J=7.4 Hz, 2H), 7.61-7.67 (m, 3H), 7.46-7.50 (t,

J=6.9 Hz, 2H), 7.04-7.09 (dt, J=7.0 Hz, 2.9 Hz 2H); ^{13}C NMR (CDCl_3): δ 188.2, 162.0, 159.7, 159.6, 159.6, 135.6, 133.9, 133.6, 132.4, 129.5, 122.6, 122.5, 117.0, 116.8. HRMS Calcd for $\text{C}_{14}\text{H}_{10}\text{FNO}_2$ ($\text{M}+\text{Na}$) $^+$: 266.0696 Found: 266.1629.



2-Oxo-N,2-(4-iodo)-phenylacetamide Bright yellow solid; m. p = 153-155°C °C (CHCl_3); IR ν_{max} (KBr): 3343, 1771, 1733, 1575, 1521, 684 cm^{-1} ; ^1H NMR (400 MHz CDCl_3): δ 8.93 (s, 1H), 8.37-8.40 (m, 2H), 7.46-7.51 (m, 4H); ^{13}C NMR (100 MHz, CDCl_3): δ 187.9,

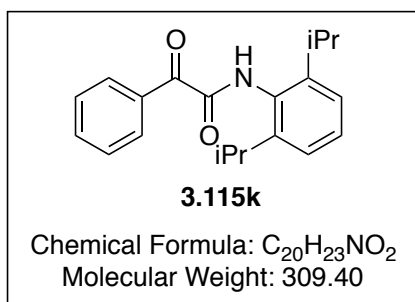
159.7, 139.1, 137.3, 135.7, 133.8, 132.4, 129.5, 122.6, 89.7. HRMS Calcd for $\text{C}_{14}\text{H}_{10}\text{INO}_2$ ($\text{M}+\text{Na}$) $^+$: 368.0920 Found: 374.0927.



2-Oxo-N,2-(4-bromo)-phenylacetamide white solid, m. p = 135-138°C °C (CHCl_3); IR ν_{max} (KBr): 1674, 1710, 3321 cm^{-1} ; ^1H NMR (400 MHz CDCl_3): δ 8.94 (s, 3H), 8.37-8.39 (d, J=7.4 Hz, 2H), 7.61-7.67 (m, 3H), 7.46-7.50 (t, J=6.9 Hz, 2H), 7.04-7.09 (dt, J=7.0 Hz, 2.9

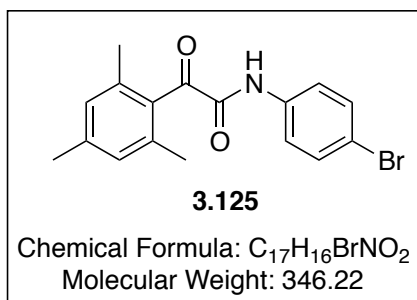
Hz 2H); ^{13}C NMR (CDCl_3): δ 188.2, 162.0, 159.7, 159.6, 159.6, 135.6, 133.9, 133.6, 132.4, 129.5, 122.6, 122.5, 117.0, 116.8. HRMS Calcd for $\text{C}_{17}\text{H}_{16}\text{BrNO}_2$ ($\text{M}+\text{Na}$) $^+$: 368.2082

Found: 368.2054.



2-Oxo-N,2-(2,6-diisopropyl)-phenylacetamide white solid, m. p = 124-126°C °C (CHCl_3); IR ν_{max} (Thin film): 3296, 3069, 2961, 2927, 2867, 2361, 2338, 1771, 1733, 1716, 1676, 1635, 1507, 936, 907 cm^{-1} ; H NMR (400 MHz, CDCl_3): δ 8.38-8.41 (m, 2H), 8.33 (s, 1H),

7.62-7.66 (tt, J=7.4 Hz, 3.1Hz, 1H), 7.48-7.52 (tt, J=7.3 Hz, 3.0 Hz, 2H), 7.32-7.35 (t, J=7.4 Hz, 1H), 7.20-7.24 (t, J=7.0 Hz, 2H), 3.04-3.11 (sep, J=7.1 Hz, 2H), 1.21-1.24 (d, J=6.8 Hz, 12H); ^{13}C NMR (100 MHz, CDCl_3): δ 188.7, 162.0, 147.0, 135.6, 134.1, 132.3, 130.6, 129.8, 129.6, 124.6, 29.9, 24.6. HRMS Calcd for $\text{C}_{20}\text{H}_{23}\text{NO}_2$ ($\text{M}+\text{Na}$) $^+$: 332.1629 Found: 332.2649.



2-Mesityl-2-oxo-N,2-(4-bromo)-phenylacetamide

White solid, m. p = 155-158°C °C ; IR ν_{max} (Thin film):

3377, 2926, 2253, 1648, 1521, 1488, 1397, 1263, 1145,

1073, 987, 911, 876, 731, 649, 667 cm^{-1} ; ^1H NMR (400

MHz, CDCl_3): δ 8.8 (s, 1H), 7.57-7.59 (td, J=7.4 Hz, 3.1

Hz, 2H), 7.46-7.49 (td, 0J=7.3 Hz, 3.2 Hz, 2H), 6.87 (s, 2H), 2.29 (s, 3H), 2.19 (s, 6H); ^{13}C

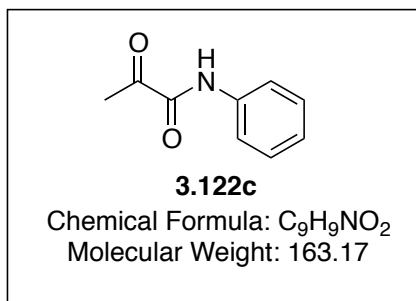
NMR (100 MHz, CDCl_3): δ 198.1, 159.1, 141.7, 1368, 133.4, 129.9, 122.4, 119.2, 22.4,

20.7. HRMS Calcd for $\text{C}_{17}\text{H}_{16}\text{BrNO}_2$ ($\text{M}+\text{Na}$) $^+$: 368.2082 Found: 368.2054.

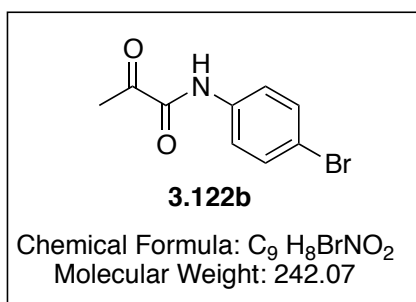
3.8.5. General Procedure for Preparation of Pyruvanilides

To a 100mL, three-necked round-bottomed flask equipped with magnetic stirrer, pressure equalizing addition funnel, vacuum-take-off adapter and a glass adapter with a stopper connected to a bubbler. The whole apparatus was purged under argon. The flask is charged with pyruvic acid (0.20 mmol, 1 equiv.) and 25 mL of dichloro methane. To this solution a,a-dichloromethyl methyl ether (0.20 mmol, 1 equiv.) was added slowly through an addition funnel over 30 minutes. Half way through the addition, the glass stopper connected to a bubbler is opened to enable the hydrogen chloride gas to escape. The solution was allowed to stir until the evolution stops. After an additional 30 minutes the apparatus is disassembled. The round –bottomed flask was kept at 0°C under argon while a

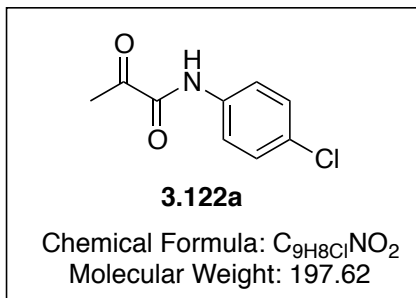
solution of the aniline (0.20 mmol, 1 equiv.) and triethyl amine (0.22 mmol, 1.1 equiv.) in 20 mL dichloro methane is charged in a clean addition funnel. The reaction is continued with a similar assembly as before. The reaction was allowed to stir for 5 to 8 h or until the aniline was consumed by TLC. Following the completion of the reaction, the mixture was washed with water and dried with sodium sulfate. The resulting organic layer was concentrated under vacuum and purified by flash silica gel chromatography. The ketoamides could also be purified by recrystallization with 30%ethyl acetate/hexane mixture.



2-Oxo-N-phenyl-propanamide.⁵⁶ White solid, m. p = 130-132°C °C; IR ν_{\max} (KBr): 1674, 1710, 3321 cm⁻¹; ¹H NMR (400 MHz CDCl₃): δ 8.70 (br s, 1H), 7.60-7.62 (d, J=9 Hz, 2H), 7.33-7.37 (t, J=7.4 Hz, 2H), 7.13-7.17 (t, J=7.4 Hz), 2.55 (s, 3H); ¹³C NMR (CDCl₃): δ 198.1, 158.4, 137.1, 130.1, 126.1, 120.5, 24.9.



N-(4-Bromophenyl)-2-oxo-propanamide.⁵⁷ White solid, m. p = 136-138°C °C; IR ν_{\max} (film): 3330, 2959, 2364, 1733, 1699, 1662, 1558, 1539, 1505, 1362, 1234, 1143, 918 cm⁻¹; ¹H NMR (400 MHz CDCl₃): δ 8.69 (br s, 1H), 7.50-7.53 (td, J=9.3, 7.0 Hz, 1H), 7.45-7.48 (td, J=9.1, 7.0 Hz, 2H), 2.54 (s, 3H); ¹³C NMR (CDCl₃): δ 205.2, 197.8, 158.3, 136.1, 133.1, 122.1, 95.2, 24.8. HRMS Calcd for C₉H₈BrNO₂ (M+Na)⁺: 263.9636 Found: 296.9600.



***N*-(4-Chlorophenyl)-2-oxo-propanamide** White solid,

m. p = 141-145°C °C; IR ν_{\max} (film): 3332, 2926, 2854,

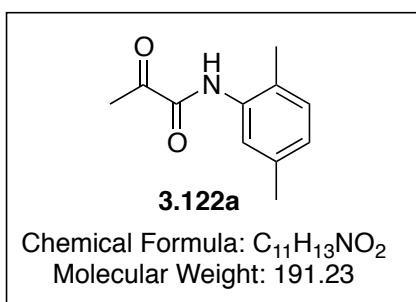
1716, 1688, 1527, 1458, 1402, 1376, 1088, 1012,

906 cm⁻¹; ¹H NMR (400 MHz CDCl₃): δ 8.70 (br s, 1H),

7.56-7.59 (td, J=9 Hz, 7 Hz, 2H), 7.29-7.33 (td, J=9.0

Hz, 7.4 Hz, 2H), 2.53 (s, 3H); ¹³C NMR (CDCl₃): δ 197.8, 158.3, 131.3, 130.2, 121.8, 95.3,

24.8. HRMS Calcd for C₉H₈ClNO₂ (M+Na)⁺: 220.1087 Found: 220.0141.



***N*-(2,5-dimethylphenyl)-2-oxo-propanamide.** White

solid, m. p = 162-164°C °C; IR ν_{\max} (thin film): 3338,

1772, 1733, 1666, 1506, 1271, 1226, 1005, 852 cm⁻¹;

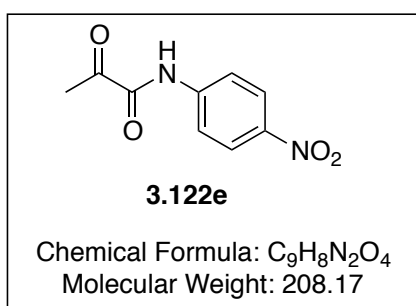
¹H NMR (400 MHz CDCl₃): δ 8.65 (br s, 1H), 7.88 (s,

1H), 7.05-7.07 (d, J=7.6 Hz, 2H), 6.89-6.91 (d, J=7.7

Hz, 1H), 2.53 (s, 3H), 2.31 (s, 3H), 2.24 (s, 3H); ¹³C NMR (CDCl₃): δ 198.4, 158.3, 137.6,

134.9, 131.3, 127.1, 126.0, 122.6, 24.9, 22.0, 17.8. HRMS Calcd for C₁₁H₁₃NO₂ (M+Na)⁺:

214.2162 Found: 214.1816.



***N*-(4-nitrophenyl)-2-oxo-propanamide** White solid,

m. p = 183-188°C °C; IR ν_{\max} (film): 3446, 1699, 1652,

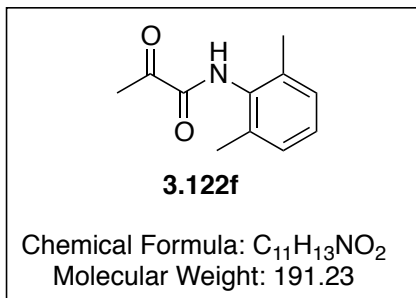
1540, 1506, 1411, 1343 cm⁻¹; ¹H NMR (400 MHz

CDCl₃): δ 8.70 (br s, 1H), 8.23-8.26 (td, J=8.9 Hz, 7.0

Hz, 2H), 7.79-7.82 (td, J=8.8 Hz, 7.1 Hz, 2H), 2.57 (s,

3H); ¹³C NMR (CDCl₃): δ 205.3, 197.1, 158.5, 126.1, 120.3, 24.7. HRMS Calcd for

C₉H₈N₂O₄ (M+Na)⁺: 231.1606 Found: 231.1580.



***N*-(2,5-dimethylphenyl)-2-oxo-propanamide.** White

solid, m. p = sublimes above 225°C; IR ν_{\max} (KBr):

1674, 1710, 3321 cm⁻¹ ¹H NMR (400 MHz CDCl₃): δ

9.32 (s, 1H), 7.92 (s, 1H), 7.09-7.11 (d, J=7.2 Hz, 1H),

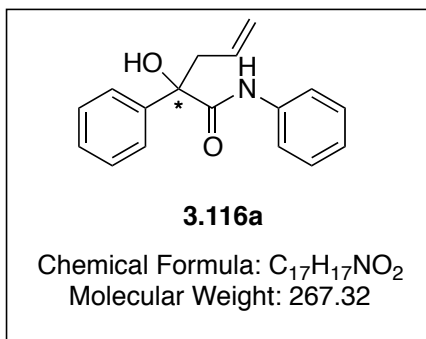
6.93-9.94 (d, J=7.2 Hz, 1H), 2.34 (s, 3H), 2.31 (s, 6H;

¹³C NMR (100 MHz, CDCl₃): δ 158.5, 137.7, 135.0, 131.3, 127.4, 126.0, 122.5, 22.1, 17.8.

HRMS Calcd for C₁₁H₁₃NO₂ (M+Na)⁺: 214.2162 Found: 214.2104.

3.8.6. General Procedure for Indium-Mediated Allylation of Linear Ketoamides

α -ketoamide (0.2 mmol scale, 1 equiv.), indium powder (0.3 mmol, 1.5 equiv.) and (S)-PhPyBOX (0.044 mmol) were added to a 20 mL scintillation vial equipped with a magnetic pellet. Two milliliters of HPLC methanol was syringed into the vial followed by allyl bromide (0.4 mmol, 2 equiv.). The reaction mixture was stirred at room temperature until the substrate was totally consumed. The reaction could be monitored by TLC. Upon completion the reaction was then concentrated and about 10 mL of 50% ethyl acetate/hexane was added to the vial. The mixture was sonicated for 2 minutes and filtered through a 5 cm plug of silica gel. If necessary, column chromatography was performed for further purification. Enantiopure 3-Allyl-3-hydroxy-oxindoles could be obtained upon recrystallizing the product with minimum amount of hot ethyl acetate.



***N*-phenyl- α -2-propen-1-yl- phenylacetamide.**⁵⁸

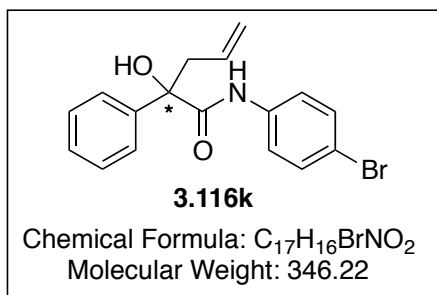
[α]_D -47.6° [c 0.9, CHCl₃ (75% ee)]; ¹H NMR (400

MHz, CDCl₃) δ 8.61 (1H, br s, NH), 7.71-7.68 (2H, m,

Ar-H), 7.54 (2H, dd, J = 8.6, 1.2 Hz, Ar-H), 7.39-7.35

(2H, m, Ar-H), 7.32-7.27 (3H, m, Ar-H), 7.08 (1H, t, J

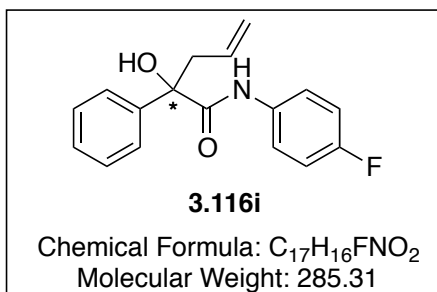
= 7.6 Hz, Ar-H), 5.81-5.71 (1H, m, CH₂HC=CH₂), 5.33-5.28 (2H, m, C=CH₂), 3.23 (1H, dd, J = 14.0, 7.2 Hz, CH₂), 3.01 (1H, s, OH), 2.84 (1H, dd, J = 14.0, 8.0 Hz, CH₂); ¹³C NMR (100 MHz, CDCl₃) δ 170.8, 141.0, 137.2, 132.4, 128.7, 128.2, 127.6, 125.0, 124.1, 121.6, 119.3, 77.7, 44.8; IR (neat) 3370, 1668, 1599, 1522, 1443, 1314, 1240, 1177, 1032, 922, 754, 729, 692, 669 cm⁻¹. HPLC: Chiralcel-OJ-H: Hexane:IPA(90:10); 1.0 ml/min, 254nm, 10.5 min and 12.3 min.



***N*-phenyl- α -2-propen-1-yl-(4-bromo)**

phenylacetamide. ¹H NMR (400 MHz, CDCl₃) δ 8.60 (bs, 1H), 7.65-7.668 (m, 2H), 7.45-7.49 (m, 2H), 7.26-7.37 (m, 3H), 6.94-6.98 (m, 2H), 5.67-5.77 (m, 1H), 5.25-5.31 (m, 2H), 3.15-3.20 (dd, J = 7.1 Hz, 2H),

2.80-2.85 (dd, J = 7.1 Hz, 2H), 1.60 (s, 1H); ¹³C NMR (100 MHz, CDCl₃) δ 172.9, 146.7, 142.1, 133.3, 131.1, 128.9, 128.7, 128.3, 125.6, 123.8, 121.9, 78.6, 44.8, 29.0, 24.0, 23.8; IR (neat) 3379, 3071, 2952, 2854, 1771, 1733, 1669, 1509, 1447, 1212, 1156, 1212, 1156, 1100, 1071, 911 cm⁻¹ HRMS Calcd for C₁₇H₁₆BrNO₂ (M+Na)⁺: 368.2049; Found: 368.2056. HPLC: ChiralPak-AD-3: HPLC: Chiralcel-OJ-H: Hexane:IPA(90:10); 1.0 ml/min, 254nm, 11.3 min and 13.5 min.

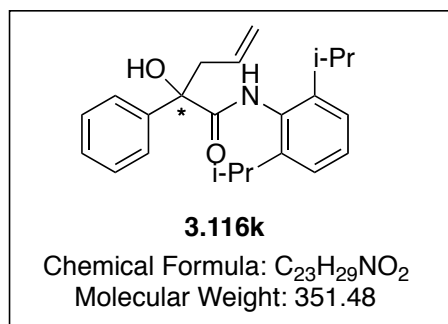


***N*-phenyl- α -2-propen-1-yl- (4-**

fluoro)phenylacetamide. ¹H NMR (400 MHz, CDCl₃) δ 8.60 (bs, 1H), 7.65-7.668 (m, 2H), 7.45-7.49 (m, 2H), 7.26-7.37 (m, 3H), 6.94-6.98 (m, 2H), 5.67-5.77 (m, 1H), 5.25-5.31 (m, 2H), 3.15-3.20 (dd, J = 7.1

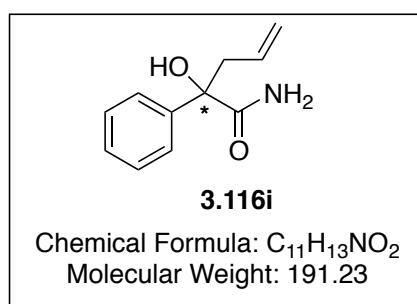
Hz, 2H), 2.80-2.85 (dd, J = 7.1 Hz, 2H), 1.60 (s, 1H); ¹³C NMR (100 MHz, CDCl₃) δ 172.9,

146.7, 142.1, 133.3, 131.1, 128.9, 128.7, 128.3, 125.6, 123.8, 121.9, 78.6, 44.8, 29.0, 24.0, 23.8; IR (neat) 3379, 3071, 2952, 2854, 1771, 1733, 1669, 1588, 1509, 1436, 1212, 1156, 1212, 1156, 1100, 1071, 911 cm^{-1} HRMS Calcd for $\text{C}_{17}\text{H}_{16}\text{FNO}_2$ ($\text{M}+\text{Na}$) $^+$: 308.1855; Found: 308.1841. HPLC: Chiralcel-OJ-H: Hexane:IPA(90:10); 1.0 ml/min, 254nm, 8.9 min and 10.5 min..



***N*-phenyl- α -2-propen-1-yl- (2,6-diisopropyl)phenylacetamide** M.p. = 199-201 $^{\circ}\text{C}$; ^1H NMR (400 MHz, CDCl_3) δ 7.81 (bs, 1H), 7.69-7.72 (m, 2H), 7.35-7.39 (m, 2H), 7.31-7.32 (m, 2H), 7.19-7.21 (d, $J = 8\text{ Hz}$, 2H), 7.07-7.09 (d, $J = 8\text{ Hz}$, 2H),

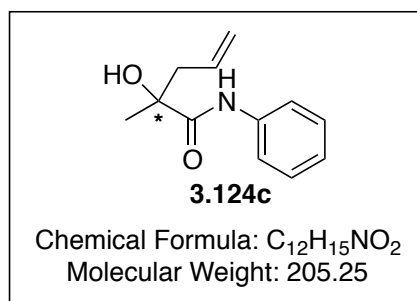
5.79-5.90 (m, 1H), 5.29-5.35 (m, 2H), 3.24-3.30 (dd, $J = 7.0, 7.2\text{ Hz}$, 1H), 2.77-2.83 (dd, $J = 7.3, 7.1\text{ Hz}$, 1H), 2.71 (bs, 1H); ^{13}C NMR (100 MHz, CDCl_3) δ 172.9, 146.7, 142.1, 133.3, 131.1, 128.9, 128.7, 128.3, 125.6, 123.8, 121.9, 78.6, 44.8, 29.0, 24.0, 23.8; IR (neat) 3330, 2959, 1733, 1699, 1662, 1558, 1539, 1505, 1362, 1234, 1143, 918 cm^{-1} HRMS Calcd for $\text{C}_{23}\text{H}_{29}\text{NO}_2$ ($\text{M}+\text{Na}$) $^+$: 374.3620; Found: 374.3623. HPLC: Chiralcel-OJ-H: Hexane:IPA(90:10); 1.0 ml/min, 254nm, 12.9 min and 14.1 min..



***N*-phenyl- α -2-propen-1-yl-acetamide** IR (neat) 3384, 1791, 1733, 1653, 1576, 1521, 1418, 1143, 1028, 997 cm^{-1} ; ^1H NMR (400 MHz, CDCl_3) δ 7.58-7.61 (m, 2H), 7.23-7.35 (s, 4H), 6.61 (s, 1H), 5.65-5.76 (m, 1H), 5.20-5.25 (m, 2H), 3.02-3.14 (dd, $J = 7.1\text{ Hz}, 7.0\text{ Hz}$, 1H),

3.02-3.14 (dd, $J = 7.1\text{Hz}$, 7.0 Hz , 1H) 1.8 (bs, 1H ; ^{13}C NMR (100 MHz, CDCl_3) δ 177.1, 142.2, 133.5, 129.2, 128.7, 126.1, 122.1, 18.4, 45.2. HPLC: Chiralcel-OJ-H:

Hexane:IPA(90:10); 1.0 ml/min, 254nm, 15.9 min and 19.0 min.



2-Hydroxy-2-methyl-N-phenyl-4-pentenamide.⁵⁹ IR

(neat) 3370, 1668, 1599, 1522, 1443, 1314, 1240, 1177,

1032, 922, 754, 729, 692, 669 cm^{-1} ; ^1H NMR (400

MHz, CDCl_3) δ 8.61 (1H, br s, NH), 7.71-7.68 (2H, m,

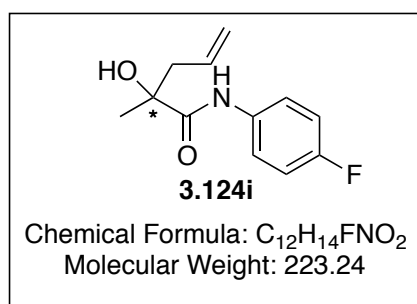
Ar-H), 7.54 (2H, dd, $J = 8.6, 1.2\text{ Hz}$, Ar-H), 7.39-7.35

(2H, m, Ar-H), 7.32-7.27 (3H, m, Ar-H), 7.08 (1H, t, $J = 7.6\text{ Hz}$, Ar-H), 5.81-5.71 (1H, m, $\text{CH}_2\text{HC}=\text{CH}_2$), 5.33-5.28 (2H, m, $\text{C}=\text{CH}_2$), 3.23 (1H, dd, $J = 14.0, 7.2\text{ Hz}$, CH_2), 3.01 (1H, s, OH), 2.84 (1H, dd, $J = 14.0, 8.0\text{ Hz}$, CH_2); ^{13}C NMR (100 MHz, CDCl_3) δ 170.8,

141.0, 137.2, 132.4, 128.7, 128.2, 127.6, 125.0, 124.1, 121.6, 119.3, 77.7, 44.8; HRMS

Calcd for $\text{C}_{12}\text{H}_{15}\text{NO}_2$ ($\text{M}+\text{Na}$)⁺: 304.1455; Found: 304.1465. HPLC: ChiralPak-AD-H:

Hexane:IPA(95:5); 1.0 ml/min, 254nm, 15.1 min and 18.6 min.



2-Hydroxy-2-methyl-N-(4-fluorophenyl)-4-

pentenamide. IR (neat) 3370, 1668, 1599, 1522, 1443,

1314, 1240, 1177, 1032, 922, 754, 729, 692, 669 cm^{-1} ;

^1H NMR (400 MHz, CDCl_3) δ 8.61 (1H, br s, NH),

7.71-7.68 (2H, m, Ar-H), 7.54 (2H, dd, $J = 8.6, 1.2\text{ Hz}$,

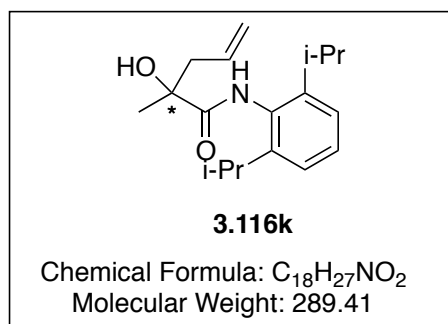
Ar-H), 7.39-7.35 (2H, m, Ar-H), 7.32-7.27 (3H, m, Ar-H), 7.08 (1H, t, $J = 7.6\text{ Hz}$, Ar-

H), 5.81-5.71 (1H, m, $\text{CH}_2\text{HC}=\text{CH}_2$), 5.33-5.28 (2H, m, $\text{C}=\text{CH}_2$), 3.23 (1H, dd, $J = 14.0, 7.2$

Hz, CH_2), 3.01 (1H, s, OH), 2.84 (1H, dd, $J = 14.0, 8.0\text{ Hz}$, CH_2); ^{13}C NMR (100 MHz,

CDCl_3) δ 172.0, 161.4, 159.0, 142.0, 134.3, 133.3, 129.3, 128.8, 126.0, 122.7, 122.2, 122.1,

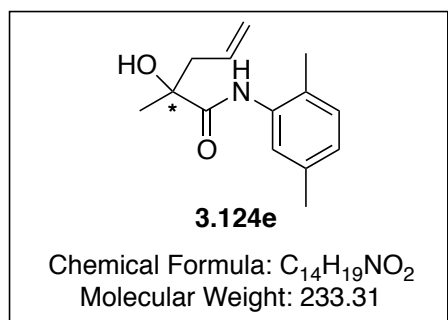
116.5, 116.3, 78.6, 45.6. HRMS Calcd for $C_{12}H_{12}BrNO_2$ ($M+Na$)⁺: 304.1455; Found: 304.1465. HPLC: ChiralPak-AD-H: Hexane:IPA(95:5); 1.0 ml/min, 254nm, 16.0 min and 17.1 min.



2-Hydroxy-2-methyl-N-(2,6-diisopropyl)phenyl-4-

pentenamide. IR (neat) 3370, 1668, 1599, 1522, 1443, 1314, 1240, 1177, 1032, 922, 754, 729, 692, 669 cm^{-1} ; 1H NMR (400 MHz, $CDCl_3$) δ 8.68, 8.60 (1H, br s, NH), 7.41-7.49 (8H, m, Ar-H), 5.81-5.92

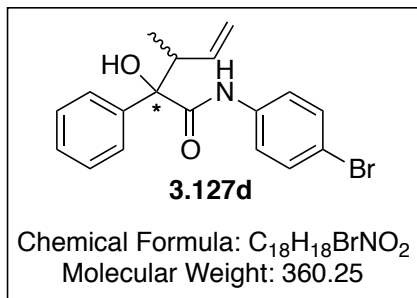
(2H, m), 5.13-5.25 (2H, m), 2.71-2.79 (2H, m), 2.46, 2.28 (1H, s, OH), 1.46, 1.47 (1H, s), 1.11-1.13 (3H, d, 7.0 Hz), 1.03-1.05 (3H, d, 7.0 Hz); ^{13}C NMR (100 MHz, $CDCl_3$) δ 177.1, 142.2, 133.5, 129.2, 128.7, 126.1, 122.1, 18.4, 45.2; HRMS Calcd for $C_{18}H_{27}BNO_2$ ($M+Na$)⁺: 304.1455; Found: 304.1465. HPLC: ChiralPak-AD-H: Hexane:IPA(95:5); 1.0 ml/min, 254nm, 18.0 min and 20.1 min.



2-Hydroxy-2-methyl-N-(2,5-dimethyl)phenyl-4-

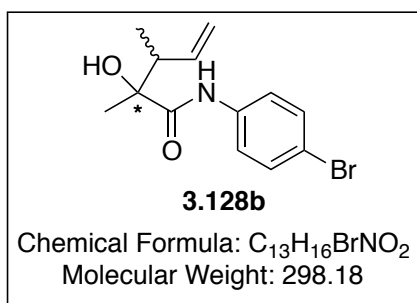
pentenamide. IR (neat) 3386, 2251, 1716, 1652, 1539, 1489, 1394, 1289, 1175, 809 cm^{-1} ; 1H NMR (400 MHz, $CDCl_3$) δ 8.52 (br s, 1H), 7.79 (s, 1H), 7.02-7.04 (d, $J = 14Hz$, 1H), 6.84-6.68 (d, $J = 14Hz$,

1H), 5.77-5.86 (m, 1H), 5.19-5.24 (m, 1H), 2.32 (s, 1H), 2.19 (s, 1H), 1.50 (s, 1H); ^{13}C NMR (100 MHz, $CDCl_3$) δ 174.1, 137.4, 133.3, 131.0, 126.4, 126.0, 123.2, 121.6, 76.4, 45.3, 27.1, 22.0, 18.0 HRMS Calcd for $C_{14}H_{19}NO_2$ ($M+Na$)⁺: 256.2551; Found: 256.2564. HPLC: ChiralPak-AD-H: Hexane:IPA(99:1); 1.0 ml/min, 254nm, 15.5 min and 19.2 min.



Mixture of both diastereomers IR (neat) 3370, 1668, 1599, 1522, 1443, 1314, 1240, 1177, 1032, 922, 754, 729, 692, 669 cm⁻¹; ¹H NMR (400 MHz, CDCl₃) δ 7.63-7.67 (m, 2H), 7.57-7.60 (m, 1H), 7.47-7.51 (m, 2H), 7.39-7.44 (m, 2H), 7.34-7.39 (m, 3H), 5.65-5.76 (m,

2H), 5.26-5.31 (m, 2H), 3.14-3.20 (dd, J = 7.1 Hz, 7 Hz, 1H), 2.80-2.85 (1H, dd, J = 7.1 Hz, 7 Hz, 1H), 1.55 (1H, s); ¹³C NMR (100 MHz, CDCl₃) δ 171.7, 141.5, 137.0, 135.3, 132.9, 132.8, 132.4, 132.0, 129.1, 129.0, 128.7, 122.5, 122.0, 121.7, 117.5, 94.9, 78.4, 45.3; HRMS Calcd for C₁₂H₁₂BrNO₂ (M+Na)⁺: 304.1455; Found: 304.1465.



Mixture of both diastereomers; IR (neat) 3370, 1668, 1599, 1522, 1443, 1314, 1240, 1177, 1032, 922, 754, 729, 692, 669 cm⁻¹; ¹H NMR (400 MHz, CDCl₃) δ 8.68, 8.60 (1H, br s, NH), 7.41-7.49 (8H, m, Ar-H), 5.81-5.92 (2H, m), 5.13-5.25 (2H, m), 2.71-2.79 (2H, m), 2.46,

2.28 (1H, s, OH), 1.46, 1.47 (1H, s), 1.11-1.13 (3H, d, 7.0 Hz), 1.03-1.05 (3H, d, 7.0 Hz); ¹³C NMR (100 MHz, CDCl₃) δ 173.5, 173.2, 138.5, 137.8, 136.4, 131.9, 121.2, 118.1, 117.4, 116.9, 116.8, 45.1, 44.9, 29.7, 25.6, 23.8, 14.3, 12.7. HRMS Calcd for C₁₂H₁₂BrNO₂ (M+Na)⁺: 304.1455; Found: 304.1465.

3.9. References

- (1) Lockman, J. W.; Reeder, M. D.; Robinson, R.; Ormonde, P. A.; Cimbor, D. M.; Williams, B. L.; Willardsen, J. A., Oxindole derivatives as inhibitors of TAK1 kinase. *Bioorg Med Chem Lett.*, 21 (6), 1724-7.

- (2) Glaser, K. B.; Li, J.; Pease, L. J.; Staver, M. J.; Marcotte, P. A.; Guo, J.; Frey, R. R.; Garland, R. B.; Heyman, H. R.; Wada, C. K.; Vasudevan, A.; Michaelides, M. R.; Davidsen, S. K.; Curtin, M. L., Differential protein acetylation induced by novel histone deacetylase inhibitors. *Biochem. Biophys. Commun.*, **2004**, *325* (3), 683-690.
- (3) Welsch, C.; Schweizer, S.; Shimakami, T.; Domingues, F. S.; Kim, S.; Lemon, S. M.; Antes, I., Ketoamide resistance and hepatitis C virus fitness in Val55 variants of the NS3 serine protease. *Antimicro. Ag. and Chemo.*, *56* (4), 1907-1915. Powers, J. C. Preparation of peptidyl ketoamides as serine protease and cysteine protease inhibitors. 1995-539946 5610297, 19951006., 1997. Chen, K. X.; Njoroge, F. G.; Sannigrahi, M.; Nair, L. G.; Yang, W.; Vibulbhan, B.; Venkatraman, S.; Arasappan, A.; Bogen, S. L.; Bennett, F.; Girijavallabhan, V. M. Preparation of novel peptidyl ketoamides with cyclic p4s as inhibitors of NS3 serine protease of hepatitis C virus. 2005-US59242005085242, 20050224., 2005.
- (4) (a) Blandino, C. M.; Coffen, D. L.; Chipman, S. D.; Cheng, H. Combinatorial synthesis and screening of α -ketoamide-derivative cysteine protease inhibitors. 1998-US7747 9846559, 19980416., **1998**. (b) Powers, J. C. Preparation of tripeptide α -ketoamides as serine and cysteine protease inhibitors. 1996-7773546235929, 19961227., **2001**.
- (5) Sheha, M. M.; Mahfouz, N. M.; Hassan, H. Y.; Youssef, A. F.; Mimoto, T.; Kiso, Y., Synthesis of di- and tripeptide analogues containing α -ketoamide as a new core structure for inhibition of HIV-1 protease. *E. J. Org. Chem.*, **2000**, *35* (10), 887-894. Tam, T. F.; Carriere, J.; MacDonald, I. D.; Castelhana, A. L.; Pliura, D. H.; Dewdney, N. J.; Thomas, E. M.; Bach, C.; Barnett, J.; et al., Intriguing structure-

- activity relations underlie the potent inhibition of HIV protease by norstatine-based peptides. *J. Med. Chem.*, **1992**, *35* (7), 1318-20.
- (6) Ireland, R. E.; Highsmith, T. K.; Gegnas, L. D.; Gleason, J. L., Synthesis of the 9,10-acetonide of 9-dihydro-FK-506. *J. Org. Chem.*, **1992**, *57* (19), 5071-3.
- (7) Sumpter, W. C., The chemistry of oxindole. *Chem Rev* **1945**, *37*, 443-79. da Silva, J. F. M.; Garden, S. J.; Pinto, A. C., The chemistry of isatins: a review from 1975 to 1999. *J. Braz. Chem. Soc.*, **2001**, *12* (3), 273-U86.
- (8) Sumpter, W. C., The chemistry of oxindole. *Chem Rev* **1945**, *37*, 443-79.
 Strigacova, J.; Hudecova, D.; Mikulasova, M.; Varecka, L.; Lasikova, A.; Vegh, D., Novel oxindole derivatives and their biological activity. *Folia Microbiol (Praha)*, **2001**, *46* (3), 187-92. Lockman, J. W.; Reeder, M. D.; Robinson, R.; Ormonde, P. A.; Cimborá, D. M.; Williams, B. L.; Willardsen, J. A., Oxindole derivatives as inhibitors of TAK1 kinase. *Bioorg Med Chem Lett.*, **2011**, *21* (6), 1724-7.
 Lockman, J. W.; Reeder, M. D.; Robinson, R.; Ormonde, P. A.; Cimborá, D. M.; Williams, B. L.; Willardsen, J. A., Oxindole derivatives as inhibitors of TAK1 kinase. *Bioorg Med. Chem. Lett.*, *21* (6), 1724-1727.
- (9) Peterson, A. C.; Cook, J. M., Studies on the enantiospecific synthesis of oxindole alkaloids. *Tetrahedron Lett.*, **1994**, *35* (17), 2651-4.
- (10) (a) Crumeyrolle-Arias, M.; Medvedev, A.; Cardona, A.; Tournaire, M. C.; Glover, V., Endogenous oxidized indoles share inhibitory potency against [H-3]isatin binding in rat brain. *J. Neu. Trans.*, **2007**, (72), 29-34. (b) Carpenedo, R.; Mannaioni, G.; Moroni, F., Oxindole, a sedative tryptophan metabolite,

- accumulates in blood and brain of rats with acute hepatic failure. *J Neurochem.*, **1998**, *70* (5), 1998-2003.
- (11) Peddibhotla, S., 3-Substituted-3-hydroxy-2-oxindole, an emerging new scaffold for drug discovery with potential anti-cancer and other biological activities. *Curr. Bioact. Compd.*, **2009**, *5* (1), 20-38.
- (12) Whatmore, J. L.; Swann, E.; Barraja, P.; Newsome, J. J.; Bunderson, M.; Beall, H. D.; Tooke, J. E.; Moody, C. J., Comparative study of isoflavone, quinoxaline and oxindole families of anti-angiogenic agents. *Angiogenesis.*, **2002**, *5* (1-2), 45-51.
- Tokunaga, T.; Hume, W. E.; Umezome, T.; Okazaki, K.; Ueki, Y.; Kumagai, K.; Hourai, S.; Nagamine, J.; Seki, H.; Taiji, M.; Noguchi, H.; Nagata, R., Oxindole derivatives as orally active potent growth hormone secretagogues. *J. Med. Chem.*, **2001**, *44* (26), 4641-9.
- Carpenedo, R.; Mannaioni, G.; Moroni, F., Oxindole, a sedative tryptophan metabolite, accumulates in blood and brain of rats with acute hepatic failure. *J Neurochem.*, **1998**, *70* (5), 1998-2003.
- (13) Nakamura, T.; Shirokawa, S.; Hosokawa, S.; Nakazaki, A.; Kobayashi, S., Enantioselective Total Synthesis of Convolutamydines B and E. *Org. Lett.*, **2006**, *8* (4), 677-679.
- (14) Carletti, I.; Banaigs, B.; Amade, P.; Matemone, a new bioactive bromine-containing oxindole alkaloid from the Indian Ocean sponge *Iotrochota purpurea*. *J. Nat. Prod.*, **2000**, *63* (7), 981-983.
- (15) Kagata, T.; Saito, S.; Shigemori, H.; Ohsaki, A.; Ishiyama, H.; Kubota, T.; Kobayashi, J., Paratunamides A-D, oxindole alkaloids from *Cinnamodendron axillare*. *J. Nat. Prod.*, **2006**, *69* (10), 1517-21.

- (16) Nakamura, T.; Shirokawa, S.; Hosokawa, S.; Nakazaki, A.; Kobayashi, S., Enantioselective Total Synthesis of Convolutamydines B and E. *Org. Lett.*, **2006**, *8* (4), 677-679.
- (17) Luppi, G.; Monari, M.; Correa, R. J.; Violante, F. d. A.; Pinto, A. C.; Kaptein, B.; Broxterman, Q. B.; Garden, S. J.; Tomasini, C., The first total synthesis of (R)-convolutamydine A. *Tetrahedron.*, **2006**, *62* (51), 12017-12024.
- (18) Ishimaru, T.; Shibata, N.; Nagai, J.; Nakamura, S.; Toru, T.; Kanemasa, S., Lewis Acid-Catalyzed Enantioselective Hydroxylation Reactions of Oxindoles and α -Keto Esters Using DBFOX Ligand. *J. Am. Chem. Soc.*, **2006**, *128* (51), 16488-16489.
- (19) Yin, L.; Kanai, M.; Shibasaki, M., A Facile Pathway to Enantiomerically Enriched 3-Hydroxy-2-Oxindoles: Asymmetric Intramolecular Arylation of α -Keto Amides Catalyzed by a Palladium–DifluorPhos Complex. *Angew. Chem. Int. Ed.*, **2011**, *50* (33), 7620-7623.
- (20) Liu, L.; Ishida, N.; Ashida, S.; Murakami, M., Synthesis of Chiral N-Heterocyclic Carbene Ligands with Rigid Backbones and Application to the Palladium-Catalyzed Enantioselective Intramolecular α -Arylation of Amides. *Org. Lett.*, **2011**, *13* (7), 1666-1669.
- (21) Smith, C. D.; Zilfou, J. T.; Stratmann, K.; Patterson, G. M.; Moore, R. E., Welwitindolinone analogues that reverse P-glycoprotein-mediated multiple drug resistance. *Mol. Pharm.*, **1995**, *47* (2), 241-247.
- (22) Mikhaylovsky, A. G.; Ignatenko, A. V.; Bubnov, Y. N., Allylboration of isatin and 2,3-dioxopyrrolo[2,1- α]isoquinolines. *Khimiya Geterotsiklicheskikh Soedinenii.*, **1998**, (7), 908-915.

- (23) Nair, V.; Jayan, C. N.; Ros, S., Novel reactions of indium reagents with 1,2-diones: a facile synthesis of alpha-hydroxy ketones. *Tetrahedron.*, **2001**, *57* (46), 9453-9459.
- (24) Alcaide, B.; Almendros, P.; Rodriguez-Acebes, R., Metal-mediated entry to functionalized 3-substituted 3-hydroxyindolin-2-ones via regiocontrolled carbonylallylation, bromoallylation, 1,3-butadien-2-ylation, propargylation, or allenylation reactions of isatins in aqueous media. *J. Org. Chem.*, **2005**, *70* (8), 3198-3204.
- (25) Itoh, J.; Han, S. B.; Krische, M. J., Enantioselective Allylation, Crotylation, and Reverse Prenylation of Substituted Isatins: Iridium-Catalyzed C-C Bond-Forming Transfer Hydrogenation. *Angew. Chem. Int. Ed.*, **2009**, *48* (34), 6313-6316.
- (26) Qiao, X. C.; Zhu, S. F.; Zhou, Q. L., From allylic alcohols to chiral tertiary homoallylic alcohol: palladium-catalyzed asymmetric allylation of isatins. *Tetrahedron Asymm.*, **2009**, *20* (11), 1254-1261.
- (27) Vyas, D. J.; Frohlich, R.; Oestreich, M., Stereochemical Surprises in the Lewis Acid-Mediated Allylation of Isatins. *J. Org. Chem.*, **2010**, *75* (19), 6720-6723.
- (28) Hanhan, N. V.; Tang, Y. C.; Tran, N. T.; Franz, A. K., Scandium(III)-Catalyzed Enantioselective Allylation of Isatins Using Allylsilanes. *Org. Lett.*, **2012**, *14* (9), 2218-2221.
- (29) Cook, G. R.; Maity, B. C.; Kargbo, R., Highly diastereoselective indium-mediated allylation of chiral hydrazones. *Organic Letters* **2004**, *6* (11), 1741-1743. Cook, G. R.; Kargbo, R.; Hallman, J. In *New developments in palladium- and indium-mediated allylation*, American Chemical Society: 2003; pp ORGN-577.

- (30) Nair, V.; Ros, S.; Jayan, C. N.; Viji, S., Indium-mediated allylation and propargylation of isatins: A facile synthesis of 3-substituted 3-hydroxyoxindoles. *Synthesis.*, **2003**, (16), 2542-2546.
- (31) Henesey, F., Preparation of Isatin by Oxidation of Indigo. *J. Soc. Dy. & Col.*, **1937**, 53 (9), 347-348.
- (32) Wang, Z., Sandmeyer Isatin Synthesis. In *Comprehensive Organic Name Reactions and Reagents*, John Wiley & Sons, Inc.
- (33) da Silva, J. F. M.; Garden, S. J.; Pinto, A. C., The chemistry of isatins: a review from 1975 to 1999. *J. Braz. Chem. Soc.*, **2001**, 12 (3), 273-U86.
- (34) Gassman, P. G.; Cue, B. W.; Luh, T.-Y., A general method for the synthesis of isatins. *J. Org. Chem.*, **1977**, 42 (8), 1344-1348.
- (35) Jiro Tatsugi, Tong Zhiwei and Yasuji Izawa., An improved preparation of isatins from indoles (01-227BP)
- (36) Sumpter, W. C., The Chemistry of Isatin. *Chem. Rev.*, **1944**, 34 (3), 393-434.
- (37) Shaughnessy, K. H.; Hamann, B. C.; Hartwig, J. F., Palladium-catalyzed inter- and intramolecular C \pm -arylation of amides. Application of intramolecular amide arylation to the Synthesis of oxindoles. *J. Org. Chem.*, **1998**, 63 (19), 6546-6553.
- (38) Gant, T. G.; Meyers, A. I., The chemistry of 2-oxazolines (1985, Äipresent). *Tetrahedron.*, **1994**, 50 (8), 2297-2360.
- (39) (a) Puchot, C.; Samuel, O.; Dunach, E.; Zhao, S.; Agami, C.; Kagan, H. B., Nonlinear effects in asymmetric synthesis. Examples in asymmetric oxidations and aldolization reactions. *J. Am. Chem. Soc.* **1986**, 108 (9), 2353-7. (b) Kagan, H. B. In

Nonlinear effects in asymmetric synthesis: Recent results, American Chemical Society: 1996; pp ORGN-316.

- (40) (a) Girard, C.; Kagan, H. B., Nonlinear effects in asymmetric synthesis and stereoselective reactions: ten years of investigation. *Angew. Chem., Int. Ed.*, **1998**, *37* (21), 2923-2959. (b) Kagan, H. B., Practical consequences of non-linear effects in asymmetric synthesis. *Adv. Synth. Catal.*, **2001**, *343* (3), 227-233.
- (41) Blackmond, D. G., Mathematical models of nonlinear effects in asymmetric catalysis: New insights based on the role of reaction rate. *J. Am. Chem. Soc.*, **1997**, *119* (52), 12934-12939. (a) Blackmond, D. G., Kinetic Implications of Nonlinear Effects in Asymmetric Synthesis. *J. Am. Chem. Soc.*, **1998**, *120* (51), 13349-13353. (b) Palmans, A. R. A.; Meijer, E. W., Amplification of chirality in dynamic supramolecular aggregates. *Angew. Chem., Int. Ed.*, **2007**, *46* (47), 8948-8968.
- (42) Satyanarayana, T.; Abraham, S.; Kagan, H. B., Nonlinear Effects In Asymmetric Catalysis. *Angew Chem Int Ed.*, **2009**, *48* (3), 456-494.
- (43) (a) Chan, T. H.; Li, C. J.; Lee, M. C.; Wei, Z. Y., 1993 R.U. Lemieux Award Lecture Organometallic-type reactions in aqueous media, "A new challenge in organic synthesis. *Can. J. Chem.*, **1994**, *72* (5), 1181-1192. (b) Li, C.-J.; Zhang, W.-C., Unexpected Barbier, "Grignard Allylation of Aldehydes with Magnesium in Water. *J. Am. Chem. Soc.*, **1998**, *120* (35), 9102-9103. (c) Chan, T. H.; Yang, Indium-Mediated Organometallic Reactions in Aqueous Media: "The Nature of the Allylindium Intermediate. *J. Am. Chem. Soc.*, **1999**, *121* (13), 3228-3229.
- (44) On oxidation states of indium: Olson, I. A.; Sessler, A. M.; Connell, J. L.; Giordano, E.; Baez, S. Y. Y.; Zavaleta, S. W.; Bowyer, W. J., Measurement of

- Heterogeneous Reaction Rates during Indium-Mediated Allylation. *J. Phys. Chem. A.*, **2009**, *113* (12), 2801-2808. Wang, Z.; Hammond, G. B., Fluorinated Building Blocks. The Discovery of a Stable Difluoroallenyl Indium and the Synthesis of gem-Difluoroallenyl and -propargyl Synthons in Aqueous Media. *J. Org. Chem.*, **2000**, *65* (20), 6547-6552.
- (45) (a) Tuck, D. G., The lower oxidation states of indium. *Chem. Soc. Rev.*, **1993**, *22* (4), 269-76. Pardoe, J. A. J.; Downs, A. J., Development of the Chemistry of Indium in Formal Oxidation States Lower than +3. *Chem. Rev.*, **2007**, *107* (1), 2-45. (b) Visco, R. E., The indous ion: an intermediate in the electrochemical oxidation of indium metal. *J. Electrochem. Soc.*, **1965**, *112* (9), 932-7. (c) Visco, R. E., Kinetics and equilibriums of the system indium(III)-indium(I)-indium(0) in acidic solution. *J. Phys. Chem.*, **1965**, *69* (1), 202-7. (d) Miller, B.; Visco, R. E., Ring-disk amperometry, indium dissolution. *J. Electrochem. Soc.*, **1968**, *115* (3), 251-8. (e) Thompson, L. C. A.; Pacer, R., The solubility of indium hydroxide in acidic and basic media at 25°C. *J. Inorg. Nucl. Chem.*, **1963**, *25* (8), 1041-4.
- (46) (a) Kim, E.; Gordon, D. M.; Schmid, W.; Whitesides, G. M., Tin- and indium-mediated allylation in aqueous media: application to unprotected carbohydrates. *J. Org. Chem.*, **1993**, *58* (20), 5500-7. (b) Peckermann, I.; Raabe, G.; Spaniol, T. P.; Okuda, J., Tris(allyl) indium compounds: Synthesis and structural characterization. *Chem. Commun.*, **2011**, *47* (17), 5061-5063. (c) Koszinowski, K., Oxidation State, Aggregation, and Heterolytic Dissociation of Allyl Indium Reagents. *J. Am. Chem. Soc.*, **2011**, *132* (17), 6032-6040.

- (47) Koszinowski, K., Oxidation State, Aggregation, and Heterolytic Dissociation of Allyl Indium Reagents. *J. Am. Chem. Soc.*, **2011**, *132* (17), 6032-6040.
- (48) Haddad, T. D.; Hirayama, L. C.; Singaram, B., Indium-Mediated Asymmetric Barbier-Type Allylations: Additions to Aldehydes and Ketones and Mechanistic Investigation of the Organoindium Reagents. *J. Org. Chem.* *75* (3), 642-649.
- (49) Steuer, C.; Gege, C.; Fischl, W.; Heinonen, K. H.; Bartenschlager, R.; Klein, C. D., Synthesis and biological evaluation of α -ketoamides as inhibitors of the Dengue virus protease with antiviral activity in cell-culture. *Bioorg. Med Chem. Lett.*, **2011**, *19* (13), 4067-4074.
- (50) (a) Soai, K.; Ishizaki, M., Asymmetric synthesis of functionalized tertiary homoallyl alcohols by diastereoselective allylation of chiral α -keto amides derived from (S)-proline esters: control of stereochemistry based on saturated coordination of Lewis acid. *J. Org. Chem.*, **1986**, *51* (17), 3290-3295. (b) Soai, K.; Ishizaki, M., Diastereoselective asymmetric allylation of chiral [small alpha]-keto-amides with allyltrimethylsilane. Preparation of protected homoallylic alcohols. *J. Chem. Soc.: Chem. Commun.*, **1984**, (15), 1016-1017.
- (51) (a) Wang, S.-G.; Tsai, H. R.; Chen, K., Lewis acid mediated diastereoselective allylation of camphorpyrazolidinone derived α -ketoamides. *Tetrahedron Letters* **2004**, *45* (32), 6183-6185. (b) Kulkarni, N. A.; Wang, S.-G.; Lee, L.-C.; Tsai, H. R.; Venkatesham, U.; Chen, K., Highly diastereoselective allylation and reduction of chiral camphor-derived α -ketoamides. *Tetrahedron: Asymm.*, **2006**, *17* (3), 336-346.

- (52) Al, M. K.; Ennajih, H.; Zouihri, H.; Bouhfid, R.; Ng, S. W.; Essassi, E. M., Synthesis of novel dispiro-oxindoles via 1,3-dipolar cycloaddition reactions of azomethine ylides. *Tetrahedron Lett.*, **2010**, *53* (18), 2328-2331.
- (53) Wu, H.; Xue, F.; Xiao, X.; Qin, Y., Total Synthesis of (+)-Perophoramidine and Determination of the Absolute Configuration. *J. Am. Chem. Soc.*, **2010**, *132* (40), 14052-14054.
- (54) Higuchi, K.; Saito, K.; Hirayama, T.; Watanabe, Y.; Kobayashi, E.; Kawasaki, T., Claisen rearrangement through enolization of 2-allyloxyindolin-3-ones: construction of adjacent carbon stereocenters in 3-hydroxyindolin-2-ones. *Synthesis.*, **2010**, (21), 3609-3614.
- (55) Alcaide, B.; Almendros, P.; Rodriguez-Acebes, R., Metal-mediated entry to functionalized 3-substituted 3-hydroxyindolin-2-ones via regiocontrolled carbonylallylation, bromoallylation, 1,3-butadien-2-ylation, propargylation, or allenylation reactions of isatins in aqueous media. *J. Org. Chem.*, **2005**, *70* (8), 3198-3204.
- (56) Kaur, P.; Singh, P.; Kumar, S., Regio- and stereochemical aspects in synthesis of 2-allyl derivatives of glycolic, mandelic and lactic acids and their iodocyclisations to 3-hydroxy-3,4-dihydrofuran-2(5H)-ones. *Tetrahedron.*, **2005**, *61* (34), 8231-8240.
- (57) Bryant, W. M. D.; Mitchell, J., Jr., Optical crystallographic studies with the polarizing microscope. II. Identification of the p-bromoanilides of some lower aliphatic acids. *J. Am. Chem. Soc.*, **1938**, *60*, 2748-51.

- (58) Ooi, T.; Fukumoto, K.; Maruoka, K., Construction of enantiomerically enriched tertiary C^{\pm} -hydroxycarboxylic acid derivatives by phase-transfer-catalyzed asymmetric alkylation of diaryloxazolidine-2,4-diones. *Angew. Chem., Int. Ed.*, **2006**, *45* (23), 3839-3842.
- (59) Merino, O.; Santoyo, B. M.; Montiel, L. E.; Jimenez-Vazquez, H. A.; Zepeda, L. G.; Tamariz, J., Versatile synthesis of quaternary 1,3-oxazolidine-2,4-diones and their use in the preparation of C^{\pm} -hydroxyamides. *Tetrahedron Lett.*, **2010**, *51* (29), 3738-3742.

APPENDIX A. X-RAY ANALYSIS OF ALLYLISATIN 3.17

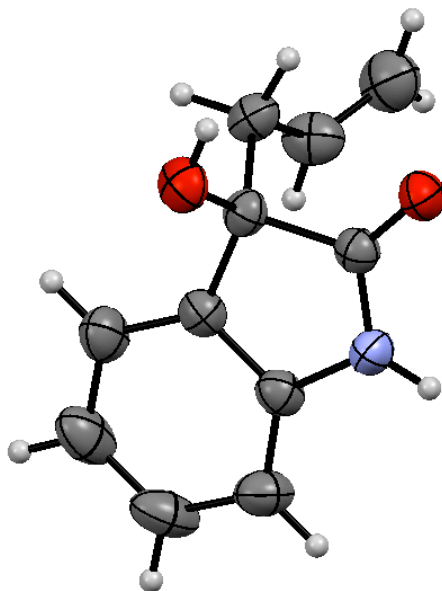


Figure A.1. Thermal Ellipsoid Plot of Allylisatin 3.17

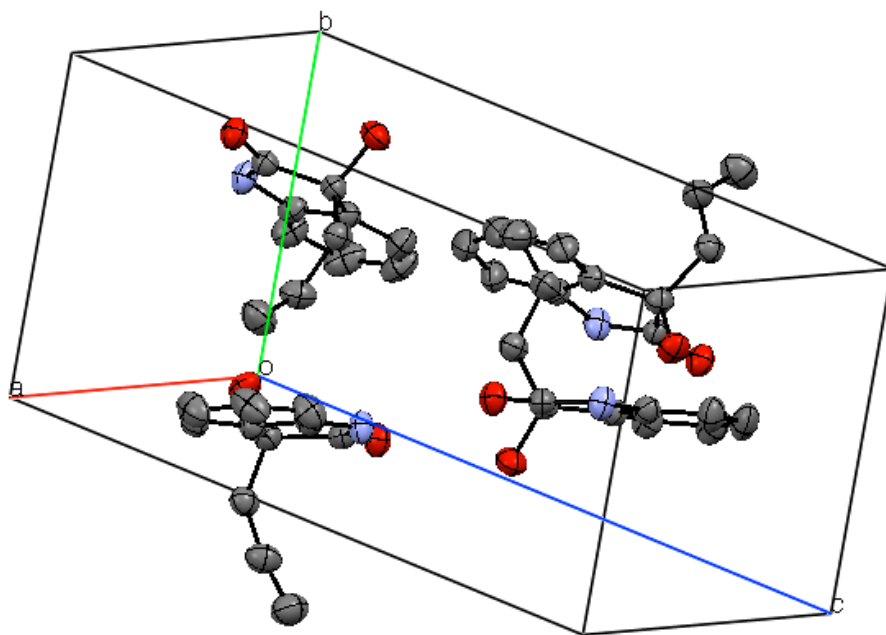


Figure A.2. Crystal Packing of Allylisatin 3.17

A.1. Crystal Data and Structure Refinement for Allylisatin 3.17

_chemical_formula_sum 'C11 H11 N O2'
_chemical_formula_weight 189.21
_symmetry_cell_setting Orthorhombic
_symmetry_space_group_name_H-M P2(1)2(1)2(1)
_cell_length_a 7.517(9)
_cell_length_b 7.543(9)
_cell_length_c 17.06(2)
_cell_angle_alpha 90.00
_cell_angle_beta 90.00
_cell_angle_gamma 90.00
_cell_volume 967(2)
_cell_formula_units_Z 4
_cell_measurement_temperature 260(2)
_cell_measurement_reflns_used 808
_cell_measurement_theta_min 2.95
_cell_measurement_theta_max 24.77
_exptl_crystal_description rod
_exptl_crystal_colour colorless
_exptl_crystal_size_max 0.62
_exptl_crystal_size_mid 0.40
_exptl_crystal_size_min 0.28
_exptl_crystal_density_meas ?
_exptl_crystal_density_diffn 1.299
_exptl_crystal_density_method 'not measured'
_exptl_crystal_F_000 400
_exptl_absorpt_coefficient_mu 0.090
_exptl_absorpt_correction_type numerical
_exptl_absorpt_correction_T_min 0.793881
_exptl_absorpt_correction_T_max 1.000000
_exptl_absorpt_process_details ?
_diffn_ambient_temperature 260(2)
_diffn_radiation_wavelength 0.71073
_diffn_radiation_type MoK\alpha
_diffn_radiation_source 'fine-focus sealed tube'
_diffn_radiation_monochromator graphite
_diffn_measurement_device_type 'CCD area detector'
_diffn_measurement_method 'phi and omega scans'
_diffn_detector_area_resol_mean ?
_diffn_standards_number ?
_diffn_standards_interval_count ?
_diffn_standards_interval_time ?
_diffn_standards_decay_% ?
_diffn_reflns_number 5541
_diffn_reflns_av_R_equivalents 0.0348

```

_diffrn_reflns_av_sigmaI/netI  0.0308
_diffrn_reflns_limit_h_min     -9
_diffrn_reflns_limit_h_max      7
_diffrn_reflns_limit_k_min     -9
_diffrn_reflns_limit_k_max      8
_diffrn_reflns_limit_l_min     -16
_diffrn_reflns_limit_l_max      21
_diffrn_reflns_theta_min       2.39
_diffrn_reflns_theta_max       26.23
_reflns_number_total           1140
_reflns_number_gt              995
_reflns_threshold_expression    >2sigma(I)
_refine_ls_structure_factor_coef Fsqd
_refine_ls_matrix_type         full
_refine_ls_weighting_scheme     calc
_atom_sites_solution_primary    direct
_atom_sites_solution_secondary difmap
_atom_sites_solution_hydrogens  geom
_refine_ls_hydrogen_treatment  constr
_refine_ls_extinction_method    SHELXL
_refine_ls_extinction_coef      0.085(8)
_refine_ls_abs_structure_details .
_refine_ls_abs_structure_Flack .
_chemical_absolute_configuration syn
_refine_ls_number_reflns       1140
_refine_ls_number_parameters    128
_refine_ls_number_restraints    0
_refine_ls_R_factor_all         0.0385
_refine_ls_R_factor_gt         0.0314
_refine_ls_wR_factor_ref       0.0847
_refine_ls_wR_factor_gt       0.0814
_refine_ls_goodness_of_fit_ref  1.054
_refine_ls_restrained_S_all    1.054
_refine_ls_shift/su_max        0.000
_refine_ls_shift/su_mean       0.000
_diffrn_measured_fraction_theta_max 0.990
_diffrn_reflns_theta_full      26.23
_diffrn_measured_fraction_theta_full 0.990
_refine_diff_density_max       0.124
_refine_diff_density_min      -0.126
_refine_diff_density_rms       0.029

```

Table A.1. Atomic Coordinates and Equivalent Isotropic Displacement Parameters for Allylisatin 3.17

Number	Label	Xfrac + ESD	Yfrac + ESD	Zfrac + ESD	Uequiv
1	O1	0.24795(18)	0.7122(2)	-0.01102(7)	0.0421
2	O2	0.01742(18)	0.78615(19)	0.12770(8)	0.0448
3	H2	-0.0423	0.7977	0.0878	0.0670
4	C5	0.2751(2)	0.6754(3)	0.05834(10)	0.0343
5	N1	0.4346(2)	0.6663(2)	0.09274(8)	0.0399
6	H1	0.5341	0.6810	0.0687	0.0480
7	C4	0.1297(2)	0.6368(3)	0.11990(11)	0.0347
8	C8	0.2397(3)	0.6136(3)	0.19231(10)	0.0362
9	C7	0.4186(3)	0.6294(3)	0.17367(11)	0.0372
10	C10	0.3208(3)	0.5652(3)	0.32501(12)	0.0579
11	H10	0.2893	0.5450	0.3770	0.0700
12	C12	0.5508(3)	0.6131(3)	0.22809(12)	0.0494
13	H12	0.6701	0.6244	0.2145	0.0590
14	C3	0.0210(3)	0.4743(3)	0.09707(12)	0.0412
15	H3A	-0.0720	0.4575	0.1358	0.0490
16	H3B	-0.0364	0.4975	0.0472	0.0490
17	C11	0.4984(4)	0.5789(3)	0.30489(12)	0.0577
18	H11	0.5847	0.5649	0.3435	0.0690
19	C9	0.1897(3)	0.5813(3)	0.26870(11)	0.0476
20	H9	0.0702	0.5706	0.2821	0.0570
21	C2	0.1234(3)	0.3074(3)	0.09033(13)	0.0497
22	H2A	0.1967	0.2776	0.1323	0.0600
23	C1	0.1206(3)	0.1998(4)	0.03193(14)	0.0617
24	H1A	0.0493	0.2242	-0.0113	0.0740
25	H1B	0.1898	0.0977	0.0329	0.0740

Table A.2. Symmetry Operations for AllylIsatin 3.17

Number	Symm. Op.	Description	Detailed Description	Order	Type
1	x,y,z	Identity	Identity	1	1
2	$1/2-x,-y,1/2+z$	Screw axis (2-fold)	2-fold screw axis with direction [0, 0, 1] at $1/4, 0, z$ with screw component [0, 0, 1/2]	2	2
3	$-x,1/2+y,1/2-z$	Screw axis (2-fold)	2-fold screw axis with direction [0, 1, 0] at $0, y, 1/4$ with screw component [0, 1/2, 0]	2	2
4	$1/2+x,1/2-y,-z$	Screw axis (2-fold)	2-fold screw axis with direction [1, 0, 0] at $x, 1/4, 0$ with screw component [1/2, 0, 0]	2	2

Table A.3. Bond Lengths for AllylIsatin 3.17

Number	Atom1	Atom2	Length
1	O1	C5	1.232(3)
2	O2	H2	0.820(2)
3	O2	C4	1.414(3)
4	C5	N1	1.337(3)
5	C5	C4	1.543(3)
6	N1	H1	0.860(2)
7	N1	C7	1.414(3)
8	C4	C8	1.497(3)
9	C4	C3	1.524(3)
10	C8	C7	1.387(4)
11	C8	C9	1.378(3)
12	C7	C12	1.365(3)
13	C10	H10	0.931(2)
14	C10	C11	1.382(4)
15	C10	C9	1.382(3)
16	C12	H12	0.930(2)
17	C12	C11	1.392(3)
18	C3	H3A	0.970(2)
19	C3	H3B	0.970(2)
20	C3	C2	1.480(3)
21	C11	H11	0.931(3)
22	C9	H9	0.930(2)
23	C2	H2A	0.931(2)
24	C2	C1	1.285(4)
25	C1	H1A	0.930(2)
26	C1	H1B	0.930(3)

Table A.4. Bond Angles for Allyllsatin 3.17

Number	Atom1	Atom2	Atom3	Angle
1	H2	O2	C4	109.5(1)
2	O1	C5	N1	125.6(2)
3	O1	C5	C4	125.3(2)
4	N1	C5	C4	109.1(2)
5	C5	N1	H1	124.3(2)
6	C5	N1	C7	111.3(2)
7	H1	N1	C7	124.4(2)
8	O2	C4	C5	109.7(1)
9	O2	C4	C8	110.2(2)
10	O2	C4	C3	110.2(2)
11	C5	C4	C8	101.1(2)
12	C5	C4	C3	111.0(2)
13	C8	C4	C3	114.4(2)
14	C4	C8	C7	109.7(2)
15	C4	C8	C9	130.6(2)
16	C7	C8	C9	119.8(2)
17	N1	C7	C8	108.9(2)
18	N1	C7	C12	128.3(2)
19	C8	C7	C12	122.8(2)
20	H10	C10	C11	119.6(2)
21	H10	C10	C9	119.7(2)
22	C11	C10	C9	120.6(2)
23	C7	C12	H12	121.6(2)
24	C7	C12	C11	116.8(2)
25	H12	C12	C11	121.6(2)
26	C4	C3	H3A	108.5(2)
27	C4	C3	H3B	108.5(2)
28	C4	C3	C2	115.2(2)
29	H3A	C3	H3B	107.5(2)
30	H3A	C3	C2	108.5(2)
31	H3B	C3	C2	108.5(2)
32	C10	C11	C12	121.4(2)
33	C10	C11	H11	119.3(2)
34	C12	C11	H11	119.3(2)
35	C8	C9	C10	118.6(2)
36	C8	C9	H9	120.7(2)
37	C10	C9	H9	120.7(2)
38	C3	C2	H2A	117.0(2)
39	C3	C2	C1	126.1(2)

Table A.4. Bond Angles for AllylIsatin 3.17 (Continued)

Number	Atom1	Atom2	Atom3	Angle
40	H2A	C2	C1	117.0(2)
41	C2	C1	H1A	119.9(3)
42	C2	C1	H1B	120.0(3)
43	H1A	C1	H1B	120.0(3)

APPENDIX B. X-RAY ANALYSIS OF CROTYLISATIN 3.75

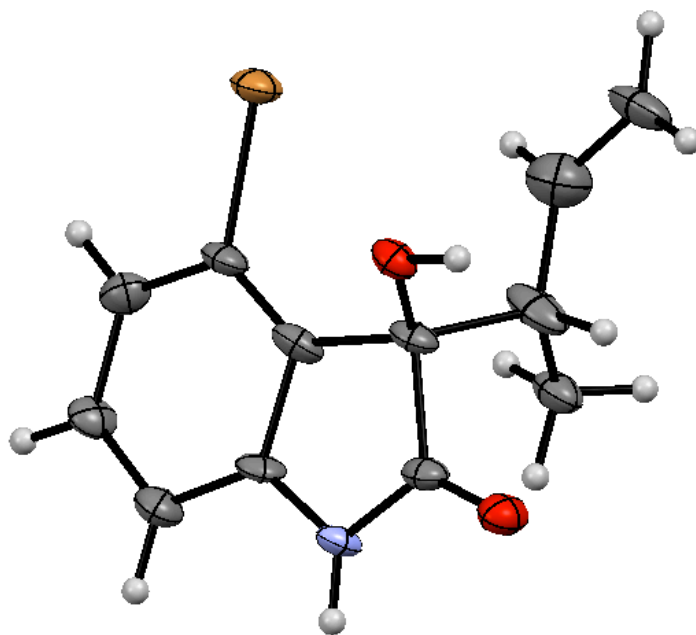


Figure B.1. Thermal Ellipsoid Plot of Crotylisatin 3.75

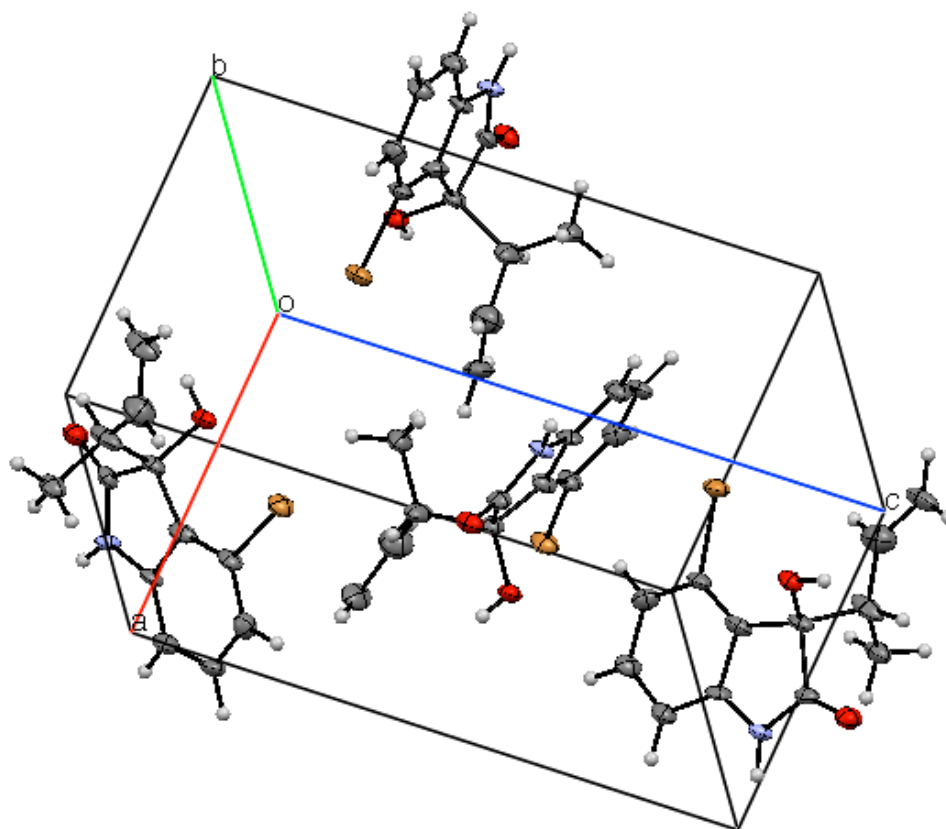


Figure B.2. Crystal Packing of Crotylisatin 3.75

B.1. Crystal Data and Structure Refinement for 3.75

_chemical_formula_moiety 'C12 H12 Br N O2'
_chemical_formula_sum 'C12 H12 Br N O2'
_chemical_formula_weight 282.14
symmetry_cell_setting Orthorhombic
symmetry_space_group_name_H-M P2(1)2(1)2(1)
space_group_name_Hall 'P 2ac 2ab'
cell_length_a 7.6498(3)
cell_length_b 10.7285(4)
cell_length_c 13.4246(5)
cell_angle_alpha 90.00
cell_angle_beta 90.00
cell_angle_gamma 90.00
cell_volume 1101.77(7)
cell_formula_units_Z 4
cell_measurement_temperature 100(2)
cell_measurement_reflns_used 3471
cell_measurement_theta_min 5.28
cell_measurement_theta_max 64.81
exptl_crystal_description plate
exptl_crystal_colour colourless
exptl_crystal_size_max 0.14
exptl_crystal_size_mid 0.08
exptl_crystal_size_min 0.02
exptl_crystal_density_meas ?
exptl_crystal_density_method 'not measured'
exptl_crystal_F_000 568
exptl_absorpt_coefficient_mu 4.962
exptl_absorpt_correction_type 'multi-scan'
exptl_absorpt_correction_T_min 0.6053
exptl_absorpt_correction_T_max 0.7526
exptl_absorpt_process_details ?
ambient_temperature 100(2)
_diffrn_radiation_wavelength 1.54178
_diffrn_radiation_type CuK α
_diffrn_radiation_source 'fine-focus sealed tube'
_diffrn_radiation_monochromator graphite
_diffrn_measurement_device_type 'Bruker APEX-II CCD'
_diffrn_measurement_method '\f and \w scans'
_diffrn_detector_area_resol_mean ?
_diffrn_reflns_number 4486
_diffrn_reflns_av_R_equivalents 0.0323
_diffrn_reflns_av_sigmaI/netI 0.0339
_diffrn_reflns_limit_h_min -7
_diffrn_reflns_limit_h_max 9

_diffn_reflns_limit_k_min -9
_diffn_reflns_limit_k_max 12
_diffn_reflns_limit_l_min -15
_diffn_reflns_limit_l_max 15
_diffn_reflns_theta_min 5.28
_diffn_reflns_theta_max 65.34
_reflns_number_total 1683
_reflns_number_gt 1625
_reflns_threshold_expression >2sigma(I)
diffn_measured_fraction_theta_max 0.944
diffn_reflns_theta_full 65.34
_diffn_measured_fraction_theta_full 0.944
_refine_diff_density_max 1.297
_refine_diff_density_min -0.570
_refine_diff_density_rms 0.130

Table B.1. Atomic Coordinates and Equivalent Isotropic Displacement Parameters for Crotylisatin 3.75

Number	Label	Xfrac + ESD	Yfrac + ESD	Zfrac + ESD	Uequiv
1	BR1	0.201438	0.194649	0.792235	0.0279
2	O1	0.210647	-0.107016	0.88461	0.0235
3	O2	0.450802	-0.245968	1.02319	0.0283
4	N1	0.641618	-0.1229	0.937734	0.0199
5	C1	-0.030128	0.056572	1.06089	0.0411
6	H1A	-0.051675	-0.023075	1.08932	0.0493
7	H1B	-0.123335	0.11427	1.05306	0.0493
8	C2	0.131224	0.087433	1.03195	0.0434
9	H2	0.148772	0.167721	1.00378	0.0521
10	C3	0.282742	0.004634	1.04111	0.0392
11	H3	0.24213	-0.067527	1.08222	0.0470
12	C4	0.348095	-0.052848	0.940735	0.0237
13	C5	0.461547	0.029977	0.873642	0.0240
14	C6	0.634652	-0.014202	0.87828	0.0213
15	C7	0.770584	0.038863	0.827032	0.0281
16	H7	0.885197	0.005036	0.830398	0.0338
17	C8	0.734997	0.143243	0.770337	0.0254
18	H8	0.827082	0.183864	0.73568	0.0305
19	C9	0.429521	0.064296	1.09995	0.0313
20	H9A	0.459218	0.145049	1.07028	0.0469
21	H9B	0.532329	0.009814	1.09859	0.0469
22	H9C	0.391983	0.076626	1.16906	0.0469
23	C10	0.43093	0.130655	0.812939	0.0248
24	C11	0.56575	0.189395	0.763518	0.0278
25	H11	0.542847	0.261629	0.724694	0.0333
26	C12	0.483429	-0.153076	0.972213	0.0213

Table B.2. Symmetry Operations for Crotylisatin 3.75

Number	Symm. Op.	Description	Detailed Description	Order	Type
1	$1/2+x, 1/2-y, -z$	Screw axis (2-fold)	2-fold screw axis with direction [1, 0, 0] at x, 1/4, 0 with screw component [1/2, 0, 0]	2	2
2	$-x, 1/2+y, 1/2-z$	Screw axis (2-fold)	2-fold screw axis with direction [0, 1, 0] at 0, y, 1/4 with screw component [0, 1/2, 0]	2	2
3	$1/2-x, -y, 1/2+z$	Screw axis (2-fold)	2-fold screw axis with direction [0, 0, 1] at 1/4, 0, z with screw component [0, 0, 1/2]	2	2

Table B.3. Bond Lengths for Crotylisatin 3.75

Number	Atom1	Atom2	Length
1	Br1	C11	1.912(7)
2	O1	C9	1.236(9)
3	O2	HO2	0.839(4)
4	O2	C5	1.419(8)
5	N1	HN1	0.879(5)
6	N1	C3	1.401(9)
7	N1	C9	1.338(9)
8	C1	H1	0.950(7)
9	C1	C2	1.38(1)
10	C1	C12	1.39(1)
11	C2	H2	0.950(8)
12	C2	C3	1.38(1)
13	C3	C4	1.413(9)
14	C4	C5	1.52(1)
15	C4	C11	1.37(1)
16	C5	C6	1.56(1)
17	C5	C9	1.56(1)
18	C6	H6	1.000(9)
19	C6	C7	1.46(1)
20	C6	C10	1.51(1)
21	C7	H7	0.95(1)
22	C7	C8	1.35(1)
23	C8	H8A	0.95(1)
24	C8	H8B	0.950(9)
25	C10	H10A	0.981(8)
26	C10	H10B	0.980(8)
27	C10	H10C	0.979(8)
28	C11	C12	1.37(1)
29	C12	H12	0.950(8)

Table B.4. Bond Angles for Crotylisatin 3.75

Number	Atom1	Atom2	Atom3	Angle
1	HO2	O2	C5	109.5(5)
2	HN1	N1	C3	124.1(6)
3	HN1	N1	C9	124.2(6)
4	C3	N1	C9	111.7(6)
5	H1	C1	C2	119.4(7)
6	H1	C1	C12	119.5(7)
7	C2	C1	C12	121.1(7)
8	C1	C2	H2	121.5(7)
9	C1	C2	C3	117.1(7)
10	H2	C2	C3	121.4(7)
11	N1	C3	C2	126.8(6)
12	N1	C3	C4	109.7(6)
13	C2	C3	C4	123.5(7)
14	C3	C4	C5	108.2(6)
15	C3	C4	C11	116.5(7)
16	C5	C4	C11	135.3(7)
17	O2	C5	C4	109.7(5)
18	O2	C5	C6	112.8(6)
19	O2	C5	C9	110.4(5)
20	C4	C5	C6	117.5(6)
21	C4	C5	C9	100.6(5)
22	C6	C5	C9	104.7(6)
23	C5	C6	H6	105.3(7)
24	C5	C6	C7	115.2(7)
25	C5	C6	C10	112.6(7)
26	H6	C6	C7	105.4(8)
27	H6	C6	C10	105.3(7)
28	C7	C6	C10	112.0(8)
29	C6	C7	H7	118.1(9)
30	C6	C7	C8	123.8(9)
31	H7	C7	C8	118(1)
32	C7	C8	H8A	120.0(9)
33	C7	C8	H8B	120.1(9)
34	H8A	C8	H8B	120(1)
35	O1	C9	N1	125.1(7)
36	O1	C9	C5	125.5(6)

Table B.4. Bond Angles for Crotylisatin 3.75 (Continued)

Number	Atom1	Atom2	Atom3	Angle
37	N1	C9	C5	109.4(6)
38	C6	C10	H10A	109.4(7)
39	C6	C10	H10B	109.5(7)
40	C6	C10	H10C	109.5(7)
41	H10A	C10	H10B	109.5(8)
42	H10A	C10	H10C	109.5(8)
43	H10B	C10	H10C	109.5(8)
44	Br1	C11	C4	121.4(5)
45	Br1	C11	C12	116.5(5)
46	C4	C11	C12	122.1(7)
47	C1	C12	C11	119.7(7)
48	C1	C12	H12	120.2(7)
49	C11	C12	H12	120.1(7)

APPENDIX C: X-RAY ANALYSIS OF REFORMATSKY PRODUCT 2.130h

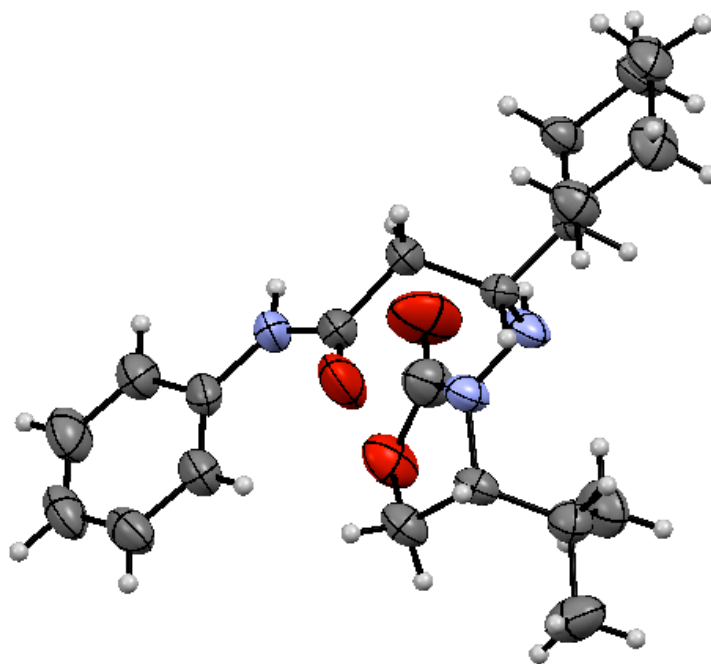


Figure C.1. Thermal Ellipsoid Plot of Reformatsky Product 2.130h

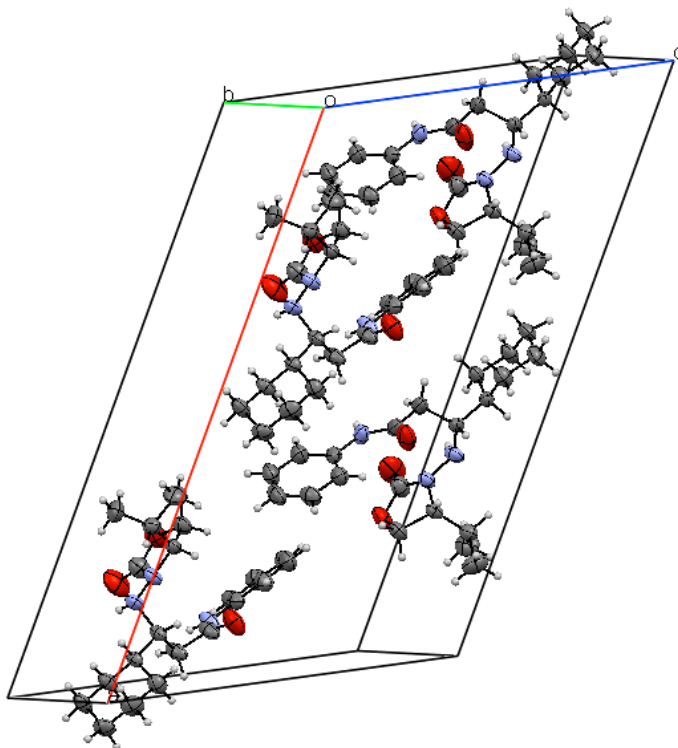


Figure C.2. Crystal Packing of Reformatsky Product 2.130h

C.1 Crystal Data and Structure Refinement for Reformatsky Product 2.130h

_chemical_formula_sum 'C21 H32 N3 O3.50'
_chemical_formula_weight 382.50
_cell_length_a 23.675(6)
_cell_length_b 6.3812(17)
_cell_length_c 15.717(4)
_cell_angle_alpha 90.00
_cell_angle_beta 119.237(4)
_cell_angle_gamma 90.00
_cell_volume 2072.0(10)
_cell_formula_units_Z 4
_cell_measurement_temperature 543(2)
_cell_measurement_reflns_used ?
_cell_measurement_theta_min ?
_cell_measurement_theta_max ?
_exptl_crystal_description ?
_exptl_crystal_colour ?
_exptl_crystal_size_max 0.60
_exptl_crystal_size_mid 0.52
_exptl_crystal_size_min 0.06
_exptl_crystal_density_meas ?
_exptl_crystal_density_diffn 1.226
_exptl_crystal_density_method 'not measured'
_exptl_crystal_F_000 828
_exptl_absorpt_coefficient_mu 0.084
_exptl_absorpt_correction_type ?
_exptl_absorpt_correction_T_min 0.9514
_exptl_absorpt_correction_T_max 0.9950
_exptl_absorpt_process_details ?
_diffn_ambient_temperature 543(2)
_diffn_radiation_wavelength 0.71073
_diffn_radiation_type MoK α
_diffn_radiation_source 'fine-focus sealed tube'
_diffn_radiation_monochromator graphite
_diffn_measurement_device_type ?
_diffn_measurement_method ?
_diffn_detector_area_resol_mean ?
_diffn_standards_number ?
_diffn_standards_interval_count ?
_diffn_standards_interval_time ?
_diffn_standards_decay_% ?
_diffn_reflns_number 6855
_diffn_reflns_av_R_equivalents 0.0228
_diffn_reflns_av_sigmaI/netI 0.0337
_diffn_reflns_limit_h_min -30

_diffn_reflns_limit_h_max	30
_diffn_reflns_limit_k_min	-8
_diffn_reflns_limit_k_max	5
_diffn_reflns_limit_l_min	-20
_diffn_reflns_limit_l_max	20
_diffn_reflns_theta_min	1.48
_diffn_reflns_theta_max	27.92
_reflns_number_total	3615
_reflns_number_gt	2882
_reflns_threshold_expression	>2sigma(I)
_refine_ls_structure_factor_coef	Fsqd
_refine_ls_matrix_type	full
_refine_ls_weighting_scheme	calc
_atom_sites_solution_primary	direct
_atom_sites_solution_secondary	difmap
_atom_sites_solution_hydrogens	geom
_refine_ls_hydrogen_treatment	mixed
_refine_ls_extinction_method	none
_refine_ls_extinction_coef	?
_refine_ls_abs_structure_Flack	0.4(16)
_refine_ls_number_reflns	3615
_refine_ls_number_parameters	277
_refine_ls_number_restraints	1
_refine_ls_R_factor_all	0.0565
_refine_ls_R_factor_gt	0.0411
_refine_ls_wR_factor_ref	0.1327
_refine_ls_wR_factor_gt	0.1123
_refine_ls_goodness_of_fit_ref	0.948
_refine_ls_restrained_S_all	0.948
_refine_ls_shift/su_max	0.000
_refine_ls_shift/su_mean	0.000
_diffn_measured_fraction_theta_max	0.995
_diffn_reflns_theta_full	27.92
_diffn_measured_fraction_theta_full	0.995
_refine_diff_density_max	0.194
_refine_diff_density_min	-0.186
_refine_diff_density_rms	0.049

Table C.1. Atomic Coordinates and Equivalent Isotropic Displacement Parameters for Reformatsky Product 2.130h

Number	Label	Xfrac + ESD	Yfrac + ESD	Zfrac + ESD	Uequiv
1	C1	0.81354(13)	0.2019(6)	0.97022(18)	0.0734
2	H1A	0.7791	0.2911	0.9641	0.1100
3	H1B	0.8413	0.2790	0.9530	0.1100
4	H1C	0.8381	0.1538	1.0363	0.1100
5	C2	0.83819(13)	-0.1353(6)	0.9109(2)	0.0770
6	H2A	0.8187	-0.2529	0.8683	0.1160
7	H2B	0.8628	-0.1838	0.9770	0.1160
8	H2C	0.8663	-0.0634	0.8928	0.1160
9	C3	0.65050(13)	0.4763(6)	0.3870(2)	0.0684
10	H3	0.6480	0.6024	0.3557	0.0820
11	C4	0.68305(12)	0.3082(6)	0.37569(18)	0.0645
12	H4	0.7022	0.3205	0.3365	0.0780
13	C5	0.77226(11)	0.2147(5)	0.75037(17)	0.0522
14	H5A	0.8191	0.2036	0.7866	0.0630
15	H5B	0.7575	0.1719	0.6836	0.0630
16	C6	0.48046(13)	-0.2284(5)	0.8388(2)	0.0620
17	H6A	0.4516	-0.3478	0.8127	0.0740
18	H6B	0.5139	-0.2635	0.9043	0.0740
19	C7	0.68690(12)	0.1249(5)	0.42214(18)	0.0612
20	H7	0.7096	0.0133	0.4152	0.0730
21	C8	0.62164(12)	0.4570(5)	0.44482(18)	0.0588
22	H8	0.5999	0.5705	0.4525	0.0710
23	C9	0.78525(10)	0.0146(4)	0.90246(16)	0.0492
24	C10	0.48419(12)	0.1549(4)	0.87394(19)	0.0552
25	H10A	0.5182	0.1396	0.9411	0.0660
26	H10B	0.4577	0.2739	0.8706	0.0660
27	C11	0.70146(13)	0.4187(5)	0.7712(2)	0.0615
28	C12	0.51165(12)	-0.1848(4)	0.77509(19)	0.0561
29	H12A	0.5375	-0.3046	0.7771	0.0670
30	H12B	0.4781	-0.1645	0.7080	0.0670
31	C13	0.44285(11)	-0.0411(5)	0.84270(19)	0.0583
32	H13A	0.4272	-0.0689	0.8883	0.0700
33	H13B	0.4056	-0.0188	0.7789	0.0700
34	C14	0.58470(11)	0.0932(5)	0.59231(17)	0.0577
35	C15	0.62502(10)	0.2696(4)	0.49119(14)	0.0488
36	C16	0.55390(10)	0.1354(5)	0.65528(16)	0.0574
37	H16A	0.5107	0.0758	0.6243	0.0690
38	H16B	0.5499	0.2856	0.6604	0.0690
39	C17	0.65782(11)	0.1000(5)	0.47976(17)	0.0566
40	H17	0.6602	-0.0274	0.5101	0.0680
41	C18	0.74179(9)	0.0777(4)	0.79646(15)	0.0397

Table C.1. Atomic Coordinates and Equivalent Isotropic Displacement Parameters for Reformatsky Product 2.130h (Continued)

Number	Label	Xfrac + ESD	Yfrac + ESD	Zfrac + ESD	Uequiv
42	C19	0.51448(10)	0.1962(4)	0.80938(16)	0.0460
43	H19A	0.4807	0.2238	0.7432	0.0550
44	H19B	0.5421	0.3190	0.8328	0.0550
45	C20	0.59331(9)	0.0429(4)	0.75740(14)	0.0403
46	C21	0.55416(8)	0.0084(3)	0.81020(13)	0.0368
47	N1	0.64905(9)	0.1733(4)	0.82252(15)	0.0513
48	N2	0.68942(8)	0.2184(3)	0.78227(14)	0.0461
49	N3	0.59463(10)	0.2613(4)	0.54935(14)	0.0586
50	O1	0.67439(13)	0.5731(4)	0.7756(2)	0.0979
51	O2	0.59891(11)	-0.0844(4)	0.58131(16)	0.0814
52	O3	0.75227(10)	0.4262(3)	0.75336(15)	0.0669
53	H1	0.5873(10)	-0.028(4)	0.8789(15)	0.0360
54	H2	0.7570(10)	-0.056(4)	0.9212(14)	0.0350
55	H31	0.6095(10)	-0.098(4)	0.7539(16)	0.0430
56	H41	0.7243(10)	-0.046(4)	0.7594(16)	0.0390
57	H5	0.6361(18)	0.280(7)	0.828(3)	0.0920
58	H6	0.5806(14)	0.382(6)	0.562(2)	0.0640
59	O4	0.5000	0.6280(13)	0.5000	0.3001
60	H71	0.4804(9)	0.607(4)	0.4497(14)	0.0060
61	H71	0.5196(9)	0.607(4)	0.5503(14)	0.0060

Table C.2. Symmetry Operations for Reformatsky Product 2.130h

Number	Symm. Op.	Description	Detailed Description	Order	Type
1	x,y,z	Identity	Identity	1	1
2	-x,y,-z	Rotation axis (2-fold)	2-fold rotation axis with direction [0, 1, 0] at 0, y, 0	2	2
3	1/2+x,1/2+y,z	Centring vector	Centring vector [1/2, 1/2, 0]	1	1
4	1/2-x,1/2+y,-z	Screw axis (2-fold)	2-fold screw axis with direction [0, 1, 0] at 1/4, y, 0 with screw component [0, 1/2, 0]	2	2

Table C.3. Bond Lengths for Reformatsky Product 2.130h

Number	Atom1	Atom2	Length
1	C1	H1A	0.960(3)
2	C1	H1B	0.960(4)
3	C1	H1C	0.960(3)
4	C1	C9	1.521(4)
5	C2	H2A	0.960(3)
6	C2	H2B	0.961(3)
7	C2	H2C	0.959(4)
8	C2	C9	1.530(4)
9	C3	H3	0.930(4)
10	C3	C4	1.382(5)
11	C3	C8	1.384(5)
12	C4	H4	0.929(3)
13	C4	C7	1.358(5)
14	C5	H5A	0.971(2)
15	C5	H5B	0.969(3)
16	C5	C18	1.523(4)
17	C5	O3	1.439(4)
18	C6	H6A	0.970(3)
19	C6	H6B	0.970(2)
20	C6	C12	1.532(5)
21	C6	C13	1.509(5)
22	C7	H7	0.930(3)
23	C7	C17	1.389(5)
24	C8	H8	0.930(3)
25	C8	C15	1.382(4)
26	C9	C18	1.524(3)
27	C9	H2	0.96(3)
28	C10	H10A	0.970(2)
29	C10	H10B	0.970(3)
30	C10	C13	1.515(4)
31	C10	C19	1.525(5)
32	C11	N2	1.339(4)
33	C11	O1	1.196(4)
34	C11	O3	1.363(5)
35	C12	H12A	0.970(3)
36	C12	H12B	0.970(2)
37	C12	C21	1.515(3)
38	C13	H13A	0.970(3)
39	C13	H13B	0.969(2)
40	C14	C16	1.513(4)

Table C.3. Bond Lengths for Reformatsky Product 2.130h (Continued)

Number	Atom1	Atom2	Length
42	C14	O2	1.218(4)
43	C15	C17	1.394(4)
44	C15	N3	1.414(4)
45	C16	H16A	0.970(2)
46	C16	H16B	0.970(3)
47	C16	C20	1.527(3)
48	C17	H17	0.930(3)
49	C18	N2	1.457(3)
50	C18	H41	0.95(2)
51	C19	H19A	0.969(2)
52	C19	H19B	0.971(2)
53	C19	C21	1.519(3)
54	C20	C21	1.532(4)
55	C20	N1	1.470(3)
56	C20	H31	0.99(3)
57	C21	H1	1.00(2)
58	N1	N2	1.410(4)
59	N1	H5	0.77(5)
60	N3	H6	0.90(4)
61	O4	H71	0.71(2)
62	O4	H71	0.71(2)

Table C.4. Bond Angles for Reformatsky Product 2.130h

Number	Atom1	Atom2	Atom3	Angle
1	H1A	C1	H1B	109.4(3)
2	H1A	C1	H1C	109.5(3)
3	H1A	C1	C9	109.5(3)
4	H1B	C1	H1C	109.4(3)
5	H1B	C1	C9	109.5(3)
6	H1C	C1	C9	109.5(3)
7	H2A	C2	H2B	109.5(3)
8	H2A	C2	H2C	109.5(3)
9	H2A	C2	C9	109.5(3)
10	H2B	C2	H2C	109.4(3)
11	H2B	C2	C9	109.5(3)
12	H2C	C2	C9	109.5(3)
13	H3	C3	C4	119.9(3)
14	H3	C3	C8	120.0(3)
15	C4	C3	C8	120.0(3)

Table C.4. Bond Angles for Reformatsky Product 2.130h (Continued)

Number	Atom1	Atom2	Atom3	Angle
16	C3	C4	H4	120.2(3)
17	C3	C4	C7	119.6(3)
18	H4	C4	C7	120.2(3)
19	H5A	C5	H5B	108.6(3)
20	H5A	C5	C18	110.5(2)
21	H5A	C5	O3	110.4(2)
22	H5B	C5	C18	110.4(2)
23	H5B	C5	O3	110.4(2)
24	C18	C5	O3	106.4(2)
25	H6A	C6	H6B	108.0(3)
26	H6A	C6	C12	109.3(3)
27	H6A	C6	C13	109.3(3)
28	H6B	C6	C12	109.4(3)
29	H6B	C6	C13	109.4(3)
30	C12	C6	C13	111.4(2)
31	C4	C7	H7	119.2(3)
32	C4	C7	C17	121.6(3)
33	H7	C7	C17	119.2(3)
34	C3	C8	H8	119.9(3)
35	C3	C8	C15	120.2(3)
36	H8	C8	C15	119.9(3)
37	C1	C9	C2	111.6(2)
38	C1	C9	C18	112.9(2)
39	C1	C9	H2	107(1)
40	C2	C9	C18	110.3(2)
41	C2	C9	H2	110(1)
42	C18	C9	H2	105(1)
43	H10A	C10	H10B	108.0(3)
44	H10A	C10	C13	109.3(2)
45	H10A	C10	C19	109.3(2)
46	H10B	C10	C13	109.3(2)
47	H10B	C10	C19	109.3(2)
48	C13	C10	C19	111.5(2)
49	N2	C11	O1	128.7(3)
50	N2	C11	O3	109.0(3)
51	O1	C11	O3	122.3(3)
52	C6	C12	H12A	109.5(3)
53	C6	C12	H12B	109.5(3)
54	C6	C12	C21	110.9(2)
55	H12A	C12	H12B	108.0(3)
56	H12A	C12	C21	109.5(2)

Table C.4. Bond Angles for Reformatsky Product 2.130h (Continued)

Number	Atom1	Atom2	Atom3	Angle
57	H12B	C12	C21	109.4(2)
58	C6	C13	C10	111.5(2)
59	C6	C13	H13A	109.3(3)
60	C6	C13	H13B	109.3(3)
61	C10	C13	H13A	109.3(3)
62	C10	C13	H13B	109.4(3)
63	H13A	C13	H13B	107.9(3)
64	C16	C14	N3	116.3(2)
65	C16	C14	O2	120.9(3)
66	N3	C14	O2	122.8(3)
67	C8	C15	C17	119.7(2)
68	C8	C15	N3	117.2(2)
69	C17	C15	N3	123.1(2)
70	C14	C16	H16A	109.2(2)
71	C14	C16	H16B	109.1(2)
72	C14	C16	C20	112.1(2)
73	H16A	C16	H16B	107.9(3)
74	H16A	C16	C20	109.2(2)
75	H16B	C16	C20	109.2(2)
76	C7	C17	C15	118.7(3)
77	C7	C17	H17	120.6(3)
78	C15	C17	H17	120.7(3)
79	C5	C18	C9	116.6(2)
80	C5	C18	N2	98.0(2)
81	C5	C18	H41	111(2)
82	C9	C18	N2	113.6(2)
83	C9	C18	H41	108(2)
84	N2	C18	H41	110(2)
85	C10	C19	H19A	109.6(2)
86	C10	C19	H19B	109.6(2)
87	C10	C19	C21	110.4(2)
88	H19A	C19	H19B	108.1(2)
89	H19A	C19	C21	109.6(2)
90	H19B	C19	C21	109.5(2)
91	C16	C20	C21	113.8(2)
92	C16	C20	N1	113.1(2)
93	C16	C20	H31	110(1)
94	C21	C20	N1	106.2(2)
95	C21	C20	H31	105(1)
96	N1	C20	H31	108(1)
97	C12	C21	C19	109.9(2)

Table C.4. Bond Angles for Reformatsky Product 2.130h (Continued)

Number	Atom1	Atom2	Atom3	Angle
98	C12	C21	C20	112.9(2)
99	C12	C21	H1	104(1)
100	C19	C21	C20	114.7(2)
101	C19	C21	H1	110(1)
102	C20	C21	H1	105(1)
103	C20	N1	N2	112.2(2)
104	C20	N1	H5	108(3)
105	N2	N1	H5	105(3)
106	C11	N2	C18	112.9(2)
107	C11	N2	N1	119.2(2)
108	C18	N2	N1	121.2(2)
109	C14	N3	C15	128.5(2)
110	C14	N3	H6	113(2)
111	C15	N3	H6	118(2)
112	C5	O3	C11	108.1(2)
113	H71	O4	H71	158(3)

APPENDIX D. X-RAY ANALYSIS OF REFORMATSKY PRODUCT 2.132h

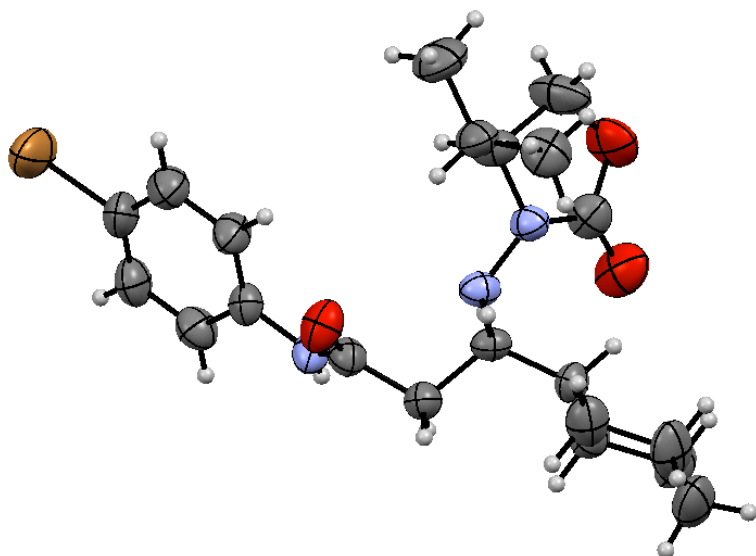


Figure D.1. Thermal Ellipsoid Plot of Reformatsky Product 2.132h

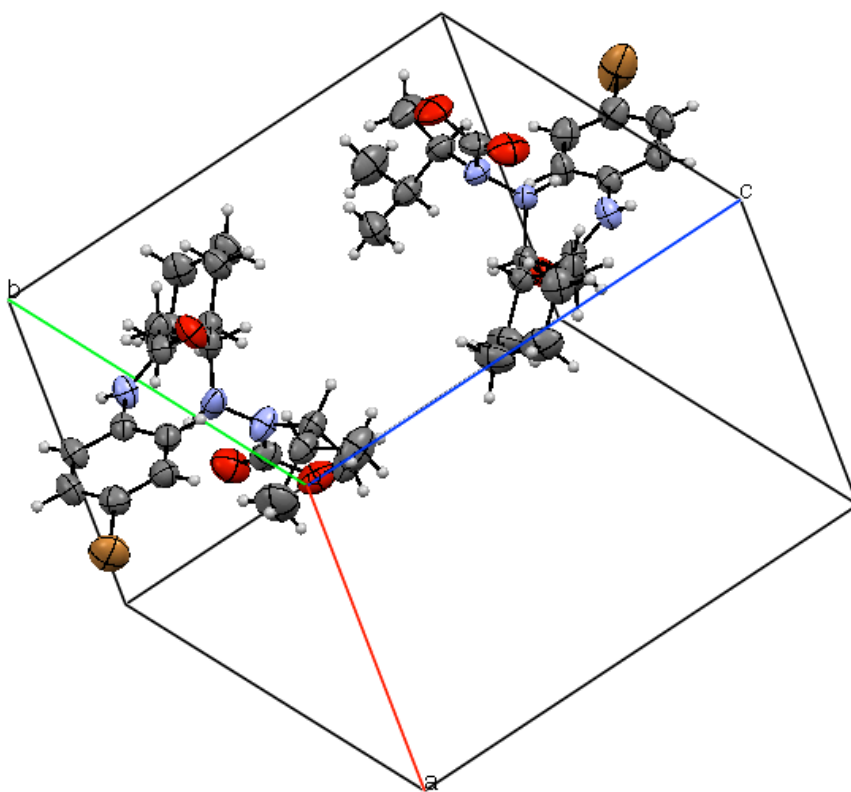


Figure D.1. Crystal Packing for Reformatsky Product 2.132h

D.1. Crystal Data and Structure Refinement Data for Reformatsky Product 2.132h

_chemical_formula_sum 'C21 H30 Br N3 O3'
_chemical_formula_weight 452.39
_symmetry_cell_setting Triclinic
_symmetry_space_group_name_H-M P1
_cell_length_a 8.491(2)
_cell_length_b 12.277(3)
_cell_length_c 12.770(3)
_cell_angle_alpha 109.458(4)
_cell_angle_beta 102.837(4)
_cell_angle_gamma 107.632(4)
_cell_volume 1116.3(5)
_cell_formula_units_Z 2
_cell_measurement_temperature 273(2)
_cell_measurement_reflns_used 2016
_cell_measurement_theta_min 2.59
_cell_measurement_theta_max 24.06
_exptl_crystal_description plate
_exptl_crystal_colour colorless
_exptl_crystal_size_max 0.44
_exptl_crystal_size_mid 0.28
_exptl_crystal_size_min 0.16
_exptl_crystal_density_meas ?
_exptl_crystal_density_diffn 1.346
_exptl_crystal_density_method 'not measured'
_exptl_crystal_F_000 472
_exptl_absorpt_coefficient_mu 1.866
_exptl_absorpt_correction_type numerical
_exptl_absorpt_correction_T_min 0.686798
_exptl_absorpt_correction_T_max 1.000000
_exptl_absorpt_process_details ?
_diffn_ambient_temperature 273(2)
_diffn_radiation_wavelength 0.71073
_diffn_radiation_type MoK\alpha
_diffn_radiation_source 'fine-focus sealed tube'
_diffn_radiation_monochromator graphite
_diffn_measurement_device_type 'CCD area detector'
_diffn_measurement_method 'phi and omega scans'
_diffn_detector_area_resol_mean ?
_diffn_standards_number ?
_diffn_standards_interval_count ?
_diffn_standards_interval_time ?
_diffn_standards_decay_% ?
_diffn_reflns_number 10413
_diffn_reflns_av_R_equivalents 0.0413

_diffn_reflns_av_sigmaI/netI	0.0888
_diffn_reflns_limit_h_min	-11
_diffn_reflns_limit_h_max	10
_diffn_reflns_limit_k_min	-16
_diffn_reflns_limit_k_max	14
_diffn_reflns_limit_l_min	-16
_diffn_reflns_limit_l_max	16
_diffn_reflns_theta_min	1.81
_diffn_reflns_theta_max	28.13
_reflns_number_total	8475
_reflns_number_gt	5523
_reflns_threshold_expression	>2sigma(I)
_refine_ls_structure_factor_coef	Fsqd
_refine_ls_matrix_type	full
_refine_ls_weighting_scheme	calc
_atom_sites_solution_primary	direct
_atom_sites_solution_secondary	difmap
_atom_sites_solution_hydrogens	geom
_refine_ls_hydrogen_treatment	mixed
_refine_ls_extinction_method	none
_refine_ls_extinction_coef	?
_refine_ls_abs_structure_Flack	-0.008(8)
_chemical_absolute_configuration	.
_refine_ls_number_reflns	8475
_refine_ls_number_parameters	545
_refine_ls_number_restraints	3
_refine_ls_R_factor_all	0.0786
_refine_ls_R_factor_gt	0.0492
_refine_ls_wR_factor_ref	0.1530
_refine_ls_wR_factor_gt	0.1342
_refine_ls_goodness_of_fit_ref	0.965
_refine_ls_restrained_S_all	0.965
_refine_ls_shift/su_max	0.003
_refine_ls_shift/su_mean	0.000

Table D.1. Atomic Coordinates and Equivalent Isotropic Displacement Parameters for Reformatsky Product 2.132h

Number	Label	Xfrac + ESD	Yfrac + ESD	Zfrac + ESD	Uequiv
1	Br1	-0.16168(8)	0.00370(5)	-0.41073(5)	0.0963
2	C1B	0.2125(7)	0.9441(5)	0.3861(4)	0.0575
3	H1B1	0.1873	0.8965	0.4321	0.0690
4	H1B2	0.1008	0.9360	0.3368	0.0690
5	C2B	0.6685(7)	0.6615(6)	0.3722(6)	0.0856
6	H2B1	0.6990	0.6952	0.4578	0.1030
7	H2B2	0.7043	0.5920	0.3469	0.1030
8	C3B	0.4704(6)	0.6158(5)	0.3100(4)	0.0561
9	C4B	0.6335(7)	0.7801(5)	0.2706(4)	0.0605
10	C5B	0.4639(7)	1.1056(5)	0.3190(5)	0.0648
11	H5B1	0.5771	1.1123	0.3645	0.0780
12	H5B2	0.4851	1.1533	0.2726	0.0780
13	C6B	0.0330(6)	0.7028(4)	0.1334(4)	0.0540
14	H6B1	-0.0488	0.7274	0.1678	0.0650
15	H6B2	0.0534	0.7439	0.0817	0.0650
16	C7B	0.3795(8)	1.1606(5)	0.4026(5)	0.0687
17	H7B1	0.2749	1.1646	0.3574	0.0820
18	H7B2	0.4617	1.2464	0.4589	0.0820
19	C8B	-0.0913(6)	0.1866(5)	-0.1770(4)	0.0592
20	H8B	-0.0832	0.1248	-0.1520	0.0710
21	C9B	0.3272(8)	1.0835(5)	0.4705(4)	0.0671
22	H9B1	0.2624	1.1173	0.5165	0.0810
23	H9B2	0.4332	1.0907	0.5255	0.0810
24	C10B	-0.0475(6)	0.5588(4)	0.0609(4)	0.0505
25	C11B	-0.0636(6)	0.3030(5)	-0.0959(4)	0.0523
26	H11B	-0.0382	0.3191	-0.0161	0.0630
27	C12B	-0.1443(7)	0.2540(5)	-0.3324(4)	0.0621
28	H12C	-0.1740	0.2369	-0.4125	0.0740
29	C13B	-0.0727(5)	0.3976(4)	-0.1305(4)	0.0458
30	C14B	0.3448(7)	0.9670(5)	0.2356(4)	0.0591
31	H14A	0.4026	0.9325	0.1839	0.0710
32	H14B	0.2347	0.9608	0.1860	0.0710
33	C15B	0.2090(6)	0.7453(4)	0.2331(4)	0.0477
34	C16B	0.3049(6)	0.8898(4)	0.3074(4)	0.0476
35	C17B	-0.1136(6)	0.3710(5)	-0.2504(4)	0.0553
36	H17C	-0.1201	0.4332	-0.2752	0.0660
37	C18B	-0.1316(7)	0.1606(5)	-0.2971(5)	0.0614
38	C19B	0.3727(7)	0.4762(5)	0.2193(4)	0.0600
39	C20B	0.3818(9)	0.3910(6)	0.2815(7)	0.0933
40	H20D	0.3184	0.3040	0.2243	0.1400
41	H20E	0.3294	0.4078	0.3411	0.1400

Table D.1. Atomic Coordinates and Equivalent Isotropic Displacement Parameters for Reformatsky Product 2.132h (Continued)

Number	Label	Xfrac + ESD	Yfrac + ESD	Zfrac + ESD	Uequiv
42	H20F	0.5033	0.4074	0.3184	0.1400
43	C21B	0.4391(13)	0.4460(8)	0.1192(7)	0.1173
44	H21D	0.4325	0.5016	0.0820	0.1750
45	H21E	0.3677	0.3598	0.0619	0.1750
46	H21F	0.5598	0.4573	0.1493	0.1750
47	N1B	0.4711(5)	0.7047(4)	0.2577(4)	0.0596
48	N2B	0.3182(5)	0.6921(4)	0.1759(3)	0.0592
49	H2B	0.2910	0.6569	0.1001	0.0710
50	N3B	-0.0359(5)	0.5211(4)	-0.0497(3)	0.0520
51	H3B	-0.0021	0.5798	-0.0727	0.0630
52	O1B	-0.1135(5)	0.4862(3)	0.0998(3)	0.0684
53	O2B	0.6742(6)	0.8556(4)	0.2306(4)	0.0841
54	O3B	0.7547(5)	0.7576(4)	0.3402(4)	0.0773
55	H2	0.422(6)	0.906(4)	0.359(4)	0.0390
56	H6	0.265(9)	0.482(6)	0.213(6)	0.0890
57	H9	0.409(6)	0.630(5)	0.379(4)	0.0590
58	H10	0.179(6)	0.697(5)	0.291(4)	0.0640
59	Br2	1.06318(10)	1.61491(6)	1.54336(6)	0.1175
60	C1A	0.9870(6)	1.2391(5)	1.3976(4)	0.0571
61	H1A	1.0005	1.1809	1.4264	0.0680
62	C2A	0.2133(6)	0.8126(5)	0.8920(5)	0.0580
63	C3A	0.4782(9)	0.4415(6)	0.7173(6)	0.0864
64	H3A1	0.3967	0.3572	0.6571	0.1040
65	H3A2	0.5856	0.4363	0.7566	0.1040
66	C4A	0.5229(8)	0.5298(6)	0.6568(5)	0.0799
67	H4A1	0.5896	0.5038	0.6082	0.0960
68	H4A2	0.4140	0.5223	0.6048	0.0960
69	C5A	0.8110(6)	0.8928(4)	1.0163(4)	0.0492
70	H5A1	0.7910	0.8525	1.0686	0.0590
71	H5A2	0.8905	0.8663	0.9806	0.0590
72	C6A	0.6309(7)	0.6678(6)	0.7476(5)	0.0667
73	H6A1	0.7478	0.6781	0.7908	0.0800
74	H6A2	0.6449	0.7215	0.7062	0.0800
75	C7A	1.0249(7)	1.3622(5)	1.4768(4)	0.0620
76	H7A	1.0625	1.3863	1.5584	0.0740
77	C8A	0.9464(7)	1.4150(5)	1.3150(5)	0.0633
78	H8A	0.9313	1.4742	1.2881	0.0760
79	C9A	0.9078(6)	1.2917(4)	1.2346(4)	0.0547
80	H9A	0.8678	1.2687	1.1532	0.0650
81	C10A	0.8939(5)	1.0346(4)	1.0870(4)	0.0480
82	C11A	0.9290(5)	1.2036(4)	1.2757(3)	0.0465

Table D.1. Atomic Coordinates and Equivalent Isotropic Displacement Parameters for Reformatsky Product 2.132h (Continued)

Number	Label	Xfrac + ESD	Yfrac + ESD	Zfrac + ESD	Uequiv
83	C12A	0.5120(7)	0.6230(5)	0.8986(4)	0.0574
84	H12A	0.4538	0.6495	0.9535	0.0690
85	H12B	0.6252	0.6294	0.9439	0.0690
86	C13A	0.5415(6)	0.7093(4)	0.8354(3)	0.0453
87	C14A	0.6348(5)	0.8520(4)	0.9187(4)	0.0417
88	C15A	1.0063(6)	1.4455(5)	1.4332(4)	0.0632
89	C16A	0.3971(8)	0.4856(5)	0.8066(5)	0.0705
90	H16A	0.3815	0.4312	0.8472	0.0840
91	H16B	0.2812	0.4788	0.7658	0.0840
92	C17A	0.1636(7)	0.9676(7)	0.8524(7)	0.0866
93	H17A	0.1238	1.0269	0.8983	0.1040
94	H17B	0.1306	0.9597	0.7716	0.1040
95	C18A	0.3645(6)	1.0132(5)	0.9083(4)	0.0575
96	C19A	0.4661(7)	1.0607(5)	0.8364(5)	0.0570
97	C20A	0.4106(8)	0.9637(6)	0.7090(5)	0.0751
98	H20A	0.4795	1.0003	0.6695	0.1130
99	H20B	0.2873	0.9388	0.6676	0.1130
100	H20C	0.4300	0.8908	0.7096	0.1130
101	C21A	0.4578(9)	1.1840(6)	0.8381(7)	0.0909
102	H21A	0.5233	1.2115	0.7926	0.1360
103	H21B	0.5083	1.2479	0.9188	0.1360
104	H21C	0.3366	1.1701	0.8041	0.1360
105	N1A	0.5308(5)	0.9047(3)	0.9846(3)	0.0457
106	N2A	0.8863(5)	1.0757(4)	1.1977(3)	0.0515
107	N3A	0.3714(4)	0.8961(3)	0.9101(3)	0.0456
108	O1A	0.9585(5)	1.1063(3)	1.0460(3)	0.0655
109	O2A	0.0861(5)	0.8469(4)	0.8530(4)	0.0818
110	O3A	0.1859(5)	0.7156(4)	0.9074(4)	0.0846
111	H1	0.423(6)	0.684(4)	0.785(4)	0.0400
112	H3	0.652(4)	0.891(3)	0.868(3)	0.0190
113	H4	0.586(6)	1.083(4)	0.880(4)	0.0540
114	H5	0.503(5)	0.869(4)	1.036(4)	0.0500
115	H7	0.864(7)	1.035(5)	1.227(5)	0.0620
116	H8	0.417(7)	1.084(6)	1.002(5)	0.0760

Table D.2. Bond Lengths for Reformatsky Product 2.132h

Number	Atom1	Atom2	Length
1	Br1	C18B	1.886(6)
2	C1B	H1B1	0.970(6)
3	C1B	H1B2	0.970(6)
4	C1B	C9B	1.528(6)
5	C1B	C16B	1.514(8)
6	C2B	H2B1	0.970(7)
7	C2B	H2B2	0.971(8)
8	C2B	C3B	1.521(7)
9	C2B	O3B	1.42(1)
10	C3B	C19B	1.535(6)
11	C3B	N1B	1.456(9)
12	C3B	H9	1.11(6)
13	C4B	N1B	1.345(7)
14	C4B	O2B	1.200(9)
15	C4B	O3B	1.362(8)
16	C5B	H5B1	0.970(6)
17	C5B	H5B2	0.970(7)
18	C5B	C7B	1.50(1)
19	C5B	C14B	1.524(6)
20	C6B	H6B1	0.970(6)
21	C6B	H6B2	0.970(6)
22	C6B	C10B	1.532(6)
23	C6B	C15B	1.538(6)
24	C7B	H7B1	0.971(7)
25	C7B	H7B2	0.970(4)
26	C7B	C9B	1.52(1)
27	C8B	H8B	0.930(7)
28	C8B	C11B	1.368(7)
29	C8B	C18B	1.395(8)
30	C9B	H9B1	0.969(7)
31	C9B	H9B2	0.970(6)
32	C10B	N3B	1.368(7)
33	C10B	O1B	1.213(7)
34	C11B	H11B	0.931(5)
35	C11B	C13B	1.390(9)
36	C12B	H12C	0.930(5)
37	C12B	C17B	1.370(7)
38	C12B	C18B	1.39(1)
39	C13B	C17B	1.390(7)
40	C13B	N3B	1.410(6)
41	C14B	H14A	0.969(6)

Table D.2. Bond Lengths for Reformatsky Product 2.132h (Continued)

Number	Atom1	Atom2	Length
42	C14B	H14B	0.971(6)
43	C14B	C16B	1.542(9)
44	C15B	C16B	1.540(6)
45	C15B	N2B	1.473(7)
46	C15B	H10	1.12(6)
47	C16B	H2	0.98(5)
48	C17B	H17C	0.930(7)
49	C19B	C20B	1.52(1)
50	C19B	C21B	1.49(1)
51	C19B	H6	0.93(8)
52	C20B	H20D	0.960(6)
53	C20B	H20E	0.960(9)
54	C20B	H20F	0.960(7)
55	C21B	H21D	0.96(1)
56	C21B	H21E	0.960(7)
57	C21B	H21F	0.96(1)
58	N1B	N2B	1.403(6)
59	N2B	H2B	0.859(4)
60	N3B	H3B	0.861(5)
61	Br2	C15A	1.918(5)
62	C1A	H1A	0.930(7)
63	C1A	C7A	1.397(7)
64	C1A	C11A	1.390(6)
65	C2A	N3A	1.333(6)
66	C2A	O2A	1.330(8)
67	C2A	O3A	1.233(9)
68	C3A	H3A1	0.970(5)
69	C3A	H3A2	0.970(8)
70	C3A	C4A	1.53(1)
71	C3A	C16A	1.49(1)
72	C4A	H4A1	0.970(7)
73	C4A	H4A2	0.969(7)
74	C4A	C6A	1.528(7)
75	C5A	H5A1	0.969(6)
76	C5A	H5A2	0.970(6)
77	C5A	C10A	1.506(6)
78	C5A	C14A	1.531(6)
79	C6A	H6A1	0.969(6)
80	C6A	H6A2	0.970(8)
81	C6A	C13A	1.525(8)
82	C7A	H7A	0.930(5)
83	C7A	C15A	1.35(1)

Table D.2. Bond Lengths for Reformatsky Product 2.132h (Continued)

Number	Atom1	Atom2	Length
84	C8A	H8A	0.931(7)
85	C8A	C9A	1.403(7)
86	C8A	C15A	1.358(8)
87	C9A	H9A	0.930(5)
88	C9A	C11A	1.390(8)
89	C10A	N2A	1.357(6)
90	C10A	O1A	1.221(7)
91	C11A	N2A	1.429(6)
92	C12A	H12A	0.970(6)
93	C12A	H12B	0.970(6)
94	C12A	C13A	1.528(8)
95	C12A	C16A	1.533(6)
96	C13A	C14A	1.540(5)
97	C13A	H1	0.96(5)
98	C14A	N1A	1.490(7)
99	C14A	H3	0.94(4)
100	C16A	H16A	0.970(7)
101	C16A	H16B	0.970(7)
102	C17A	H17A	0.970(8)
103	C17A	H17B	0.970(9)
104	C17A	C18A	1.532(7)
105	C17A	O2A	1.43(1)
106	C18A	C19A	1.527(9)
107	C18A	N3A	1.464(8)
108	C18A	H8	1.11(5)
109	C19A	C20A	1.522(8)
110	C19A	C21A	1.53(1)
111	C19A	H4	0.95(5)
112	C20A	H20A	0.960(7)
113	C20A	H20B	0.960(6)
114	C20A	H20C	0.960(8)
115	C21A	H21A	0.960(9)
116	C21A	H21B	0.960(7)
117	C21A	H21C	0.960(7)
118	N1A	N3A	1.422(5)
119	N1A	H5	0.94(6)
120	N2A	H7	0.72(7)

Table D.3. Bond Angles for Reformatsky Product 2.132h

Number	Atom1	Atom2	Atom3	Angle
1	H1B1	C1B	H1B2	108.1(5)
2	H1B1	C1B	C9B	109.4(5)
3	H1B1	C1B	C16B	109.4(5)
4	H1B2	C1B	C9B	109.4(5)
5	H1B2	C1B	C16B	109.4(5)
6	C9B	C1B	C16B	111.0(5)
7	H2B1	C2B	H2B2	108.5(7)
8	H2B1	C2B	C3B	110.4(6)
9	H2B1	C2B	O3B	110.4(6)
10	H2B2	C2B	C3B	110.3(6)
11	H2B2	C2B	O3B	110.4(6)
12	C3B	C2B	O3B	106.9(5)
13	C2B	C3B	C19B	115.7(5)
14	C2B	C3B	N1B	99.9(5)
15	C2B	C3B	H9	108(3)
16	C19B	C3B	N1B	113.9(5)
17	C19B	C3B	H9	108(3)
18	N1B	C3B	H9	111(3)
19	N1B	C4B	O2B	129.1(6)
20	N1B	C4B	O3B	108.1(5)
21	O2B	C4B	O3B	122.9(6)
22	H5B1	C5B	H5B2	108.1(6)
23	H5B1	C5B	C7B	109.5(6)
24	H5B1	C5B	C14B	109.5(5)
25	H5B2	C5B	C7B	109.5(6)
26	H5B2	C5B	C14B	109.5(5)
27	C7B	C5B	C14B	110.7(5)
28	H6B1	C6B	H6B2	108.2(5)
29	H6B1	C6B	C10B	109.6(4)
30	H6B1	C6B	C15B	109.7(4)
31	H6B2	C6B	C10B	109.7(4)
32	H6B2	C6B	C15B	109.7(4)
33	C10B	C6B	C15B	109.9(4)
34	C5B	C7B	H7B1	109.1(6)
35	C5B	C7B	H7B2	109.1(6)
36	C5B	C7B	C9B	112.5(5)
37	H7B1	C7B	H7B2	107.8(6)
38	H7B1	C7B	C9B	109.1(6)
39	H7B2	C7B	C9B	109.1(6)
40	H8B	C8B	C11B	120.0(5)
41	H8B	C8B	C18B	120.0(5)
42	C11B	C8B	C18B	120.0(5)

Table D.3. Bond Angles for Reformatsky Product 2.132h (Continued)

Number	Atom1	Atom2	Atom3	Angle
43	C1B	C9B	C7B	111.3(5)
44	C1B	C9B	H9B1	109.4(5)
45	C1B	C9B	H9B2	109.4(5)
46	C7B	C9B	H9B1	109.4(5)
47	C7B	C9B	H9B2	109.3(5)
48	H9B1	C9B	H9B2	108.0(6)
49	C6B	C10B	N3B	113.8(4)
50	C6B	C10B	O1B	122.3(5)
51	N3B	C10B	O1B	123.9(5)
52	C8B	C11B	H11B	119.4(5)
53	C8B	C11B	C13B	121.2(5)
54	H11B	C11B	C13B	119.4(5)
55	H12C	C12B	C17B	119.7(6)
56	H12C	C12B	C18B	119.6(6)
57	C17B	C12B	C18B	120.7(5)
58	C11B	C13B	C17B	118.5(5)
59	C11B	C13B	N3B	123.4(4)
60	C17B	C13B	N3B	118.0(4)
61	C5B	C14B	H14A	109.5(5)
62	C5B	C14B	H14B	109.5(5)
63	C5B	C14B	C16B	110.5(5)
64	H14A	C14B	H14B	108.0(5)
65	H14A	C14B	C16B	109.6(5)
66	H14B	C14B	C16B	109.6(5)
67	C6B	C15B	C16B	113.8(4)
68	C6B	C15B	N2B	106.6(4)
69	C6B	C15B	H10	107(3)
70	C16B	C15B	N2B	112.3(4)
71	C16B	C15B	H10	111(3)
72	N2B	C15B	H10	106(3)
73	C1B	C16B	C14B	108.7(4)
74	C1B	C16B	C15B	113.6(4)
75	C1B	C16B	H2	108(3)
76	C14B	C16B	C15B	115.1(4)
77	C14B	C16B	H2	105(3)
78	C15B	C16B	H2	106(3)
79	C12B	C17B	C13B	120.6(5)
80	C12B	C17B	H17C	119.7(5)
81	C13B	C17B	H17C	119.7(5)
82	Br1	C18B	C8B	121.3(4)
83	Br1	C18B	C12B	119.7(5)
84	C8B	C18B	C12B	119.0(5)

Table D.3. Bond Angles for Reformatsky Product 2.132h (Continued)

Number	Atom1	Atom2	Atom3	Angle
85	C3B	C19B	C20B	110.1(5)
86	C3B	C19B	C21B	112.7(6)
87	C3B	C19B	H6	90(5)
88	C20B	C19B	C21B	111.3(6)
89	C20B	C19B	H6	106(5)
90	C21B	C19B	H6	125(5)
91	C19B	C20B	H20D	109.5(7)
92	C19B	C20B	H20E	109.4(7)
93	C19B	C20B	H20F	109.5(7)
94	H20D	C20B	H20E	109.5(8)
95	H20D	C20B	H20F	109.5(8)
96	H20E	C20B	H20F	109.5(8)
97	C19B	C21B	H21D	109.4(8)
98	C19B	C21B	H21E	109.5(8)
99	C19B	C21B	H21F	109.4(8)
100	H21D	C21B	H21E	109(1)
101	H21D	C21B	H21F	109(1)
102	H21E	C21B	H21F	110(1)
103	C3B	N1B	C4B	114.1(5)
104	C3B	N1B	N2B	122.7(4)
105	C4B	N1B	N2B	121.2(5)
106	C15B	N2B	N1B	113.2(4)
107	C15B	N2B	H2B	123.4(5)
108	N1B	N2B	H2B	123.4(5)
109	C10B	N3B	C13B	127.8(4)
110	C10B	N3B	H3B	116.1(5)
111	C13B	N3B	H3B	116.1(4)
112	C2B	O3B	C4B	110.6(5)
113	H1A	C1A	C7A	120.0(5)
114	H1A	C1A	C11A	120.0(5)
115	C7A	C1A	C11A	120.0(5)
116	N3A	C2A	O2A	110.7(5)
117	N3A	C2A	O3A	125.5(5)
118	O2A	C2A	O3A	123.8(6)
119	H3A1	C3A	H3A2	107.9(7)
120	H3A1	C3A	C4A	109.1(7)
121	H3A1	C3A	C16A	109.1(7)
122	H3A2	C3A	C4A	109.1(7)
123	H3A2	C3A	C16A	109.1(7)
124	C4A	C3A	C16A	112.5(6)
125	C3A	C4A	H4A1	109.2(6)
126	C3A	C4A	H4A2	109.2(6)

Table D.3. Bond Angles for Reformatsky Product 2.132h (Continued)

Number	Atom1	Atom2	Atom3	Angle
127	C3A	C4A	C6A	111.8(6)
128	H4A1	C4A	H4A2	107.9(7)
129	H4A1	C4A	C6A	109.3(6)
130	H4A2	C4A	C6A	109.3(6)
131	H5A1	C5A	H5A2	108.2(5)
132	H5A1	C5A	C10A	109.7(4)
133	H5A1	C5A	C14A	109.7(4)
134	H5A2	C5A	C10A	109.7(4)
135	H5A2	C5A	C14A	109.7(4)
136	C10A	C5A	C14A	109.9(4)
137	C4A	C6A	H6A1	109.4(6)
138	C4A	C6A	H6A2	109.3(6)
139	C4A	C6A	C13A	111.5(5)
140	H6A1	C6A	H6A2	108.0(6)
141	H6A1	C6A	C13A	109.3(6)
142	H6A2	C6A	C13A	109.3(6)
143	C1A	C7A	H7A	120.4(6)
144	C1A	C7A	C15A	119.1(5)
145	H7A	C7A	C15A	120.5(6)
146	H8A	C8A	C9A	120.9(6)
147	H8A	C8A	C15A	120.9(6)
148	C9A	C8A	C15A	118.1(5)
149	C8A	C9A	H9A	119.8(5)
150	C8A	C9A	C11A	120.5(5)
151	H9A	C9A	C11A	119.7(5)
152	C5A	C10A	N2A	114.8(4)
153	C5A	C10A	O1A	122.2(4)
154	N2A	C10A	O1A	123.1(5)
155	C1A	C11A	C9A	119.0(4)
156	C1A	C11A	N2A	118.2(4)
157	C9A	C11A	N2A	122.8(4)
158	H12A	C12A	H12B	108.2(5)
159	H12A	C12A	C13A	109.7(5)
160	H12A	C12A	C16A	109.7(5)
161	H12B	C12A	C13A	109.7(5)
162	H12B	C12A	C16A	109.8(5)
163	C13A	C12A	C16A	109.7(5)
164	C6A	C13A	C12A	110.3(4)
165	C6A	C13A	C14A	112.8(4)
166	C6A	C13A	H1	103(3)
167	C12A	C13A	C14A	114.8(4)
168	C12A	C13A	H1	101(3)

Table D.3. Bond Angles for Reformatsky Product 2.132h (Continued)

Number	Atom1	Atom2	Atom3	Angle
169	C14A	C13A	H1	113(3)
170	C5A	C14A	C13A	115.0(4)
171	C5A	C14A	N1A	104.0(4)
172	C5A	C14A	H3	111(2)
173	C13A	C14A	N1A	115.4(4)
174	C13A	C14A	H3	105(2)
175	N1A	C14A	H3	107(2)
176	Br2	C15A	C7A	118.5(4)
177	Br2	C15A	C8A	118.2(4)
178	C7A	C15A	C8A	123.3(5)
179	C3A	C16A	C12A	111.9(5)
180	C3A	C16A	H16A	109.2(6)
181	C3A	C16A	H16B	109.3(6)
182	C12A	C16A	H16A	109.2(6)
183	C12A	C16A	H16B	109.3(6)
184	H16A	C16A	H16B	108.0(6)
185	H17A	C17A	H17B	108.6(8)
186	H17A	C17A	C18A	110.5(7)
187	H17A	C17A	O2A	110.4(7)
188	H17B	C17A	C18A	110.5(7)
189	H17B	C17A	O2A	110.4(7)
190	C18A	C17A	O2A	106.3(6)
191	C17A	C18A	C19A	113.7(5)
192	C17A	C18A	N3A	99.3(5)
193	C17A	C18A	H8	112(3)
194	C19A	C18A	N3A	113.2(4)
195	C19A	C18A	H8	111(3)
196	N3A	C18A	H8	107(3)
197	C18A	C19A	C20A	114.3(5)
198	C18A	C19A	C21A	111.6(5)
199	C18A	C19A	H4	104(3)
200	C20A	C19A	C21A	110.3(5)
201	C20A	C19A	H4	111(3)
202	C21A	C19A	H4	105(3)
203	C19A	C20A	H20A	109.5(6)
204	C19A	C20A	H20B	109.5(6)
205	C19A	C20A	H20C	109.4(6)
206	H20A	C20A	H20B	109.5(7)
207	H20A	C20A	H20C	109.5(7)
208	H20B	C20A	H20C	109.5(7)
209	C19A	C21A	H21A	109.5(7)
210	C19A	C21A	H21B	109.4(7)

Table D.3. Bond Angles for Reformatsky Product 2.132h (Continued)

Number	Atom1	Atom2	Atom3	Angle
211	C19A	C21A	H21C	109.5(7)
212	H21A	C21A	H21B	109.5(8)
213	H21A	C21A	H21C	109.5(8)
214	H21B	C21A	H21C	109.4(8)
215	C14A	N1A	N3A	114.1(3)
216	C14A	N1A	H5	114(3)
217	N3A	N1A	H5	108(3)
218	C10A	N2A	C11A	126.2(4)
219	C10A	N2A	H7	124(5)
220	C11A	N2A	H7	110(5)
221	C2A	N3A	C18A	112.0(4)
222	C2A	N3A	N1A	121.7(4)
223	C18A	N3A	N1A	117.8(4)
224	C2A	O2A	C17A	109.5(5)

APPENDIX E. X-RAY ANALYSIS OF CHIRAL LIGAND-BISMUTH COMPLEX

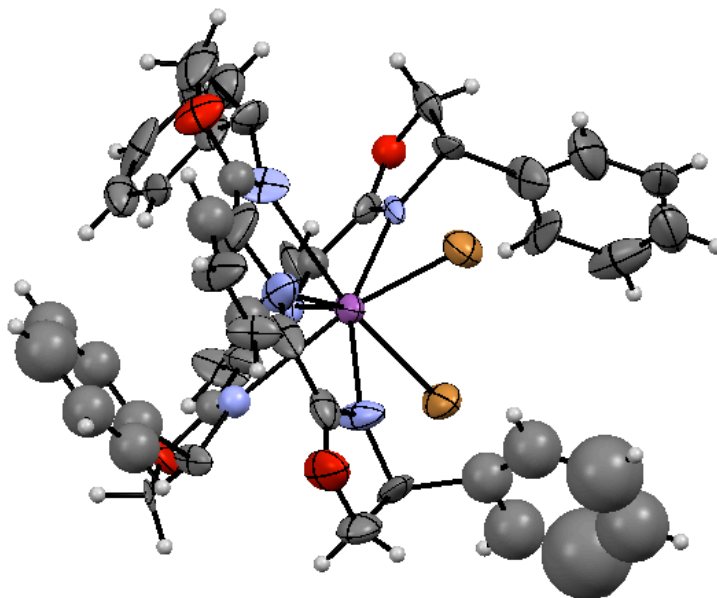


Figure E.1. Thermal Ellipsoid Plot of Chiral Ligand-Bismuth Complex

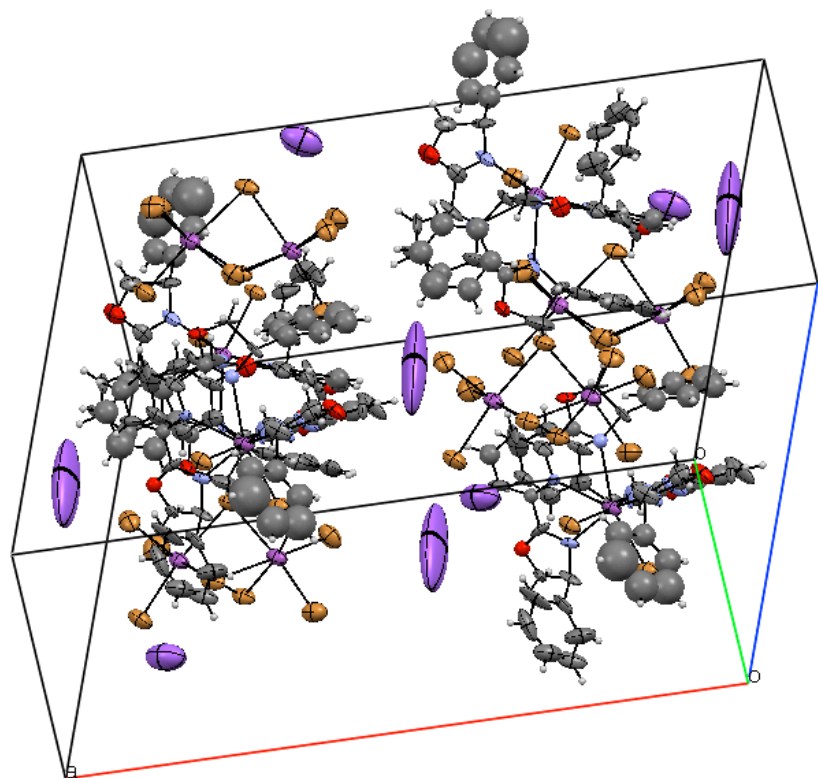


Figure E.2. Crystal Packing for Chiral Ligand-Bismuth Complex

E.1. Crystal Data and Structure Refinement for Chiral Ligand-Bismuth Complex

_chemical_formula_weight 1193.87
_symmetry_cell_setting Orthorhombic
_symmetry_space_group_name_H-M P2(1)2(1)2(1)
_cell_length_a 18.7119(3)
_cell_length_b 18.7878(2)
_cell_length_c 25.3032(3)
_cell_angle_alpha 90.00
_cell_angle_beta 90.00
_cell_angle_gamma 90.00
_cell_volume 8895.5(2)
_cell_formula_units_Z 8
_cell_measurement_temperature 100(2)
_cell_measurement_reflns_used 9997
_cell_measurement_theta_min 3.76
_cell_measurement_theta_max 65.96
_exptl_crystal_description plate
_exptl_crystal_colour colorless
_exptl_crystal_size_max .156
_exptl_crystal_size_mid .088
_exptl_crystal_size_min .02
_exptl_crystal_density_meas ?
_exptl_crystal_density_diffn 1.783
_exptl_crystal_density_method 'not measured'
_exptl_crystal_F_000 4688
_exptl_absorpt_coefficient_mu 6.115
_exptl_absorpt_correction_type multi-scan
_exptl_absorpt_correction_T_min 0.0643
_exptl_absorpt_correction_T_max 0.1639
_exptl_absorpt_process_details ?
_diffn_ambient_temperature 100(2)
_diffn_radiation_wavelength 1.54178
_diffn_radiation_type CuK α
_diffn_radiation_source 'fine-focus sealed tube'
_diffn_radiation_monochromator graphite
_diffn_measurement_device_type 'Bruker APEX-II CCD'
_diffn_measurement_method '\f and \w scans'
_diffn_detector_area_resol_mean ?
_diffn_reflns_number 67492
_diffn_reflns_av_R_equivalents 0.0608
_diffn_reflns_av_sigmaI/netI 0.0381
_diffn_reflns_limit_h_min -17
_diffn_reflns_limit_h_max 21
_diffn_reflns_limit_k_min -22
_diffn_reflns_limit_k_max 22

_diffn_reflns_limit_l_min	-29
_diffn_reflns_limit_l_max	29
_diffn_reflns_theta_min	2.93
_diffn_reflns_theta_max	66.38
_reflns_number_total	13383
_reflns_number_gt	12659
_reflns_threshold_expression	>2sigma(I)
_refine_ls_structure_factor_coef	Fsqd
_refine_ls_matrix_type	full
_refine_ls_weighting_scheme	calc
_atom_sites_solution_primary	direct
_atom_sites_solution_secondary	difmap
_atom_sites_solution_hydrogens	geom
_refine_ls_hydrogen_treatment	constr
_refine_ls_extinction_method	none
_refine_ls_extinction_coef	?
_refine_ls_abs_structure_Flack	0.00
_refine_ls_number_reflns	13383
_refine_ls_number_parameters	1105
_refine_ls_number_restraints	0
_refine_ls_R_factor_all	0.0502
_refine_ls_R_factor_gt	0.0478
_refine_ls_wR_factor_ref	0.1393
_refine_ls_wR_factor_gt	0.1366
_refine_ls_goodness_of_fit_ref	1.039
_refine_ls_restrained_S_all	1.039
_refine_ls_shift/su_max	0.013
_refine_ls_shift/su_mean	0.000
_diffn_measured_fraction_theta_max	0.901
_diffn_reflns_theta_full	66.38
_diffn_measured_fraction_theta_full	0.901
_refine_diff_density_max	1.187
_refine_diff_density_min	-1.607
_refine_diff_density_rms	0.161

Table E.1. Atomic Coordinates and Equivalent Isotropic Displacement Parameters for Chiral Ligand-Bismuth Complex

Number	Label	Xfrac + ESD	Yfrac + ESD	Zfrac + ESD	Uequiv
1	BI1	0.178557	0.945667	0.227684	0.0561
2	BI2	0.329097	0.915748	0.27207	0.0554
3	BR1	0.257461	0.99232	0.357034	0.0743
4	BR2	0.240478	0.785006	0.234127	0.0617
5	BR3	0.258893	1.01325	0.149716	0.0676
6	BR4	0.379924	0.857062	0.17016	0.0799
7	BR5	0.394842	1.04969	0.310088	0.0779
8	BR6	0.380941	0.809135	0.373922	0.0929
9	BR7	0.114534	0.89748	0.101694	0.0887
10	BR8	0.135975	1.11086	0.225035	0.087
11	BR9	0.114104	0.876114	0.302993	0.0855
12	BI3	0.312293	0.946085	0.766937	0.0433
13	BR10	0.266768	1.04552	0.855198	0.0624
14	BR11	0.366916	0.845106	0.877753	0.0627
15	O1	0.462167	1.11227	0.809897	0.0779
16	O2	0.364357	0.738208	0.610943	0.0627
17	O3	0.244249	1.16583	0.597152	0.0527
18	O4	0.164715	0.782037	0.7415	0.0413
19	N1	0.397242	0.924736	0.721832	0.0711
20	N2	0.384298	1.05595	0.813018	0.0634
21	N3	0.317305	0.817438	0.668886	0.0534
22	N4	0.242196	0.835508	0.775708	0.0377
23	N5	0.220564	0.970462	0.688612	0.033
24	N6	0.295008	1.0796	0.669195	0.0369
25	C21	0.371006	1.11068	0.602903	0.0842
26	C2	0.350113	1.05241	0.549244	0.0788
27	H2	0.315791	1.04002	0.540414	0.0946
28	C51	0.380517	1.01265	0.508783	0.0982
29	H51	0.366537	0.973656	0.472883	0.1178
30	C62	0.431815	1.03116	0.52198	0.1368
31	H62	0.452157	1.00456	0.494909	0.1641
32	C69	0.452711	1.08943	0.575637	0.0977
33	H69	0.487033	1.10182	0.584465	0.1172
34	C8	0.422307	1.12919	0.616098	0.0915
35	H8	0.436287	1.16818	0.651998	0.1097
36	C74	0.388895	1.10388	0.941202	0.0909
37	C65	0.424867	1.05625	0.988527	0.1209

Table E.1. Atomic Coordinates and Equivalent Isotropic Displacement Parameters for Chiral Ligand-Bismuth Complex (Continued)

Number	Label	Xfrac + ESD	Yfrac + ESD	Zfrac + ESD	Uequiv
38	H65	0.444575	1.01546	0.971279	0.145
39	C72	0.431383	1.06958	1.06163	0.2109
40	H72	0.45545	1.03771	1.0933	0.253
41	C54	0.401929	1.13054	1.08741	0.1873
42	H54	0.40629	1.13946	1.13633	0.2247
43	C64	0.365957	1.17818	1.04009	0.2935
44	H64	0.346252	1.21897	1.05734	0.3522
45	C56	0.359437	1.16484	0.966985	0.1299
46	H56	0.335366	1.19671	0.935322	0.1559
47	C1	0.234955	0.857188	0.549222	0.0611
48	H1	0.263861	0.890019	0.550101	0.0734
49	C3	0.12327	1.01133	0.624147	0.0717
50	H3	0.089821	1.02414	0.603542	0.086
51	C4	0.358715	0.807331	0.654213	0.0484
52	C5	0.436784	1.17881	0.842292	0.0607
53	H5A	0.429082	1.22852	0.810681	0.0729
54	H5B	0.458023	1.19806	0.886946	0.0729
55	C6	0.234815	0.778981	0.591073	0.0603
56	C7	0.434284	0.968554	0.743406	0.068
57	C9	0.487008	0.895649	0.685831	0.1101
58	H9	0.518288	0.885673	0.674894	0.1322
59	C10	0.161225	1.06764	0.616926	0.0668
60	H10	0.154622	1.11897	0.590945	0.0802
61	C11	0.189459	0.713536	0.776529	0.0431
62	H11A	0.194658	0.668545	0.743386	0.0517
63	H11B	0.170941	0.689116	0.80988	0.0517
64	C12	0.310809	0.691392	0.587556	0.0965
65	H12A	0.312406	0.630116	0.599882	0.1158
66	H12B	0.296312	0.698483	0.537049	0.1158
67	C13	0.183739	0.922861	0.69228	0.0357
68	C14	0.253573	1.09788	0.639684	0.0431
69	C15	0.281538	0.747204	0.636515	0.0491
70	C16	0.331688	1.14885	0.649975	0.0453
71	C17	0.451187	0.842955	0.659879	0.078
72	H17	0.457286	0.794407	0.63406	0.0936
73	C18	0.196155	0.847	0.737994	0.0396
74	C19	0.135503	0.936067	0.662164	0.064
75	H19	0.110898	0.895648	0.666721	0.0768

Table E.1. Atomic Coordinates and Equivalent Isotropic Displacement Parameters for Chiral Ligand-Bismuth Complex (Continued)

Number	Label	Xfrac + ESD	Yfrac + ESD	Zfrac + ESD	Uequiv
76	C22	0.425027	1.04804	0.78896	0.0501
77	C24	0.483048	0.96127	0.725836	0.0542
78	H24	0.50921	1.0003	0.741879	0.065
79	C25	0.291799	1.20596	0.603673	0.0506
80	H25A	0.291508	1.26291	0.625344	0.0607
81	H25B	0.299389	1.2133	0.556852	0.0607
82	C53	0.206557	1.0455	0.648134	0.0516
83	C55	0.205558	0.840456	0.908098	0.1034
84	H55	0.185723	0.871872	0.870983	0.1241
85	C57	0.267277	0.729126	0.954593	0.1044
86	H57	0.289725	0.685985	0.947539	0.1253
87	C58	0.185875	0.732539	0.585459	0.0657
88	H58	0.185589	0.682486	0.612601	0.0789
89	C59	0.183616	0.88103	0.503604	0.0642
90	H59	0.181234	0.931058	0.475819	0.077
91	C60	0.39962	0.860575	0.671661	0.1026
92	C61	0.233655	0.8065	1.03194	0.0924
93	H61	0.232856	0.818794	1.07916	0.1109
94	C63	0.137694	0.82974	0.500902	0.0855
95	H63	0.106581	0.843741	0.472028	0.1026
96	C66	0.203377	0.856704	0.983402	0.0915
97	H66	0.182445	0.898861	0.996331	0.1098
98	C67	0.262453	0.746512	1.02397	0.0833
99	H67	0.280019	0.714608	1.06261	0.0999
100	C68	0.385443	1.13599	0.856319	0.0674
101	C70	0.240537	0.752383	0.816505	0.0489
102	C71	0.239888	0.773563	0.894639	0.0681
103	C73	0.145712	0.75659	0.546918	0.0529
104	H73	0.117494	0.722835	0.54824	0.0634
105	NA1	0.319143	0.945454	1.01137	0.2039
106	NA2	-0.038534	0.825756	0.266266	0.7889

Table E.2. Symmetry Operations for Chiral Ligand-Bismuth Complex

Number	Symm. Op.	Description	Detailed Description	Order	Type
1	x,y,z	Identity	Identity	1	1
2	-x,y,-z	Rotation axis (2-fold)	2-fold rotation axis with direction [0, 1, 0] at 0, y, 0	2	2
3	1/2+x,1/2+y,z	Centring vector	Centring vector [1/2, 1/2, 0]	1	1
4	1/2-x,1/2+y,-z	Screw axis (2-fold)	2-fold screw axis with direction [0, 1, 0] at 1/4, y, 0 with screw component [0, 1/2, 0]	2	2

Table E.3. Bond Lengths for Chiral Ligand-Bismuth Complex

Number	Atom1	Atom2	Length
1	BI1	BR1	2.9948(4)
2	BI1	BR2	2.9752(5)
3	BI1	BR3	3.0776(5)
4	BI1	BR7	2.7568(4)
5	BI1	BR8	2.7863(5)
6	BI1	BR9	2.7159(4)
7	BI2	BR1	3.0304(4)
8	BI2	BR2	3.0988(5)
9	BI2	BR3	3.0758(4)
10	BI2	BR4	2.7742(4)
11	BI2	BR5	2.7197(4)
12	BI2	BR6	2.7018(3)
13	BI3	BR10	2.7619(3)
14	BI3	BR11	2.7873(4)
15	BI3	N1	2.6514(5)
16	BI3	N2	2.5905(4)
17	BI3	N3	2.7525(4)
18	BI3	N4	2.5838(4)
19	BI3	N5	2.6432(5)
20	BI3	N6	2.7512(4)
21	O1	C5	1.4462(2)
22	O1	C22	1.4066(2)
23	O2	C4	1.3770(2)
24	O2	C12	1.5972(3)
25	O3	C14	1.3160(2)
26	O3	C25	1.4115(3)

Table E.3. Bond Lengths for Chiral Ligand-Bismuth Complex (Continued)

Number	Atom1	Atom2	Length
27	O4	C11	1.3481(2)
28	O4	C18	1.3247(2)
29	N1	C7	1.2070(2)
30	N1	C60	1.3891(2)
31	N2	C22	1.2919(2)
32	N2	C68	1.4811(2)
33	N3	C4	1.2258(2)
34	N3	C15	1.4948(2)
35	N4	C18	1.3142(2)
36	N4	C70	1.5042(2)
37	N5	C13	1.2529(2)
38	N5	C53	1.3968(2)
39	N6	C14	1.1791(2)
40	N6	C16	1.5552(2)
41	C21	C2	1.3900(2)
42	C21	C8	1.3901(3)
43	C21	C16	1.6470(2)
44	C2	H2	0.9300(2)
45	C2	C51	1.3900(2)
46	C51	H51	0.9300(1)
47	C51	C62	1.3900(3)
48	C62	H62	0.9300(1)
49	C62	C69	1.3900(2)
50	C69	H69	0.9300(2)
51	C69	C8	1.3900(2)
52	C8	H8	0.9300(1)
53	C74	C65	1.3900(2)
54	C74	C56	1.3901(2)
55	C74	C68	1.6842(3)
56	C65	H65	0.9300(1)
57	C65	C72	1.3900(3)
58	C72	H72	0.9300(1)
59	C72	C54	1.3900(2)
60	C54	H54	0.9300(2)
61	C54	C64	1.3900(2)
62	C64	H64	0.9300(1)
63	C64	C56	1.3899(3)
64	C56	H56	0.9300(1)
65	C1	H1	0.9300(2)

Table E.3. Bond Lengths for Chiral Ligand-Bismuth Complex (Continued)

Number	Atom1	Atom2	Length
66	C1	C6	1.4461(2)
67	C1	C59	1.5222(3)
68	C3	H3	0.9300(2)
69	C3	C10	1.3752(2)
70	C3	C19	1.3699(2)
71	C4	C60	1.3619(2)
72	C5	H5A	0.9700(1)
73	C5	H5B	0.9700(1)
74	C5	C68	1.6152(3)
75	C6	C15	1.4598(2)
76	C6	C58	1.4914(3)
77	C7	C22	1.5537(2)
78	C7	C24	1.4386(3)
79	C9	H9	0.9300(2)
80	C9	C17	1.2811(2)
81	C9	C24	1.2859(2)
82	C10	H10	0.9300(1)
83	C10	C53	1.2927(2)
84	C11	H11A	0.9700(1)
85	C11	H11B	0.9700(1)
86	C11	C70	1.5522(3)
87	C12	H12A	0.9700(2)
88	C12	H12B	0.9700(2)
89	C12	C15	1.6031(2)
90	C13	C18	1.4544(2)
91	C13	C19	1.3280(3)
92	C14	C53	1.5467(3)
93	C16	C25	1.5225(2)
94	C17	H17	0.9300(1)
95	C17	C60	1.4897(3)
96	C19	H19	0.9300(1)
97	C24	H24	0.9300(1)
98	C25	H25A	0.9700(2)
99	C25	H25B	0.9700(2)
100	C55	H55	0.9300(1)
101	C55	C66	1.4792(3)
102	C55	C71	1.4477(2)
103	C57	H57	0.9300(1)
104	C57	C67	1.3906(3)

Table E.3. Bond Lengths for Chiral Ligand-Bismuth Complex (Continued)

Number	Atom1	Atom2	Length
105	C57	C71	1.4049(2)
106	C58	H58	0.9300(1)
107	C58	C73	1.2348(2)
108	C59	H59	0.9300(1)
109	C59	C63	1.4664(2)
110	C61	H61	0.9300(2)
111	C61	C66	1.3448(2)
112	C61	C67	1.2394(2)
113	C63	H63	0.9300(2)
114	C63	C73	1.4171(2)
115	C66	H66	0.9300(1)
116	C67	H67	0.9300(1)
117	C70	C71	1.5371(3)
118	C73	H73	0.9300(2)

Table E.4. Bond Angles for Chiral Ligand-Bismuth Complex

Number	Atom1	Atom2	Atom3	Angle
1	BR1	BI1	BR2	82.39
2	BR1	BI1	BR3	82.32
3	BR1	BI1	BR7	173.69
4	BR1	BI1	BR8	90.96
5	BR1	BI1	BR9	94.68
6	BR2	BI1	BR3	81.23
7	BR2	BI1	BR7	93.28
8	BR2	BI1	BR8	170.37
9	BR2	BI1	BR9	94.23
10	BR3	BI1	BR7	92.51
11	BR3	BI1	BR8	91.02
12	BR3	BI1	BR9	174.83
13	BR7	BI1	BR8	92.76
14	BR7	BI1	BR9	90.2
15	BR8	BI1	BR9	93.24
16	BR1	BI2	BR2	79.8
17	BR1	BI2	BR3	81.78
18	BR1	BI2	BR4	168.2
19	BR1	BI2	BR5	91.23
20	BR1	BI2	BR6	98.14
21	BR2	BI2	BR3	79.33

Table E.4. Bond Angles for Chiral Ligand-Bismuth Complex (Continued)

Number	Atom1	Atom2	Atom3	Angle
22	BR2	BI2	BR4	95.86
23	BR2	BI2	BR5	170.23
24	BR2	BI2	BR6	91.92
25	BR3	BI2	BR4	86.64
26	BR3	BI2	BR5	95.66
27	BR3	BI2	BR6	171.14
28	BR4	BI2	BR5	92.18
29	BR4	BI2	BR6	92.95
30	BR5	BI2	BR6	93.2
31	BI1	BR1	BI2	83.62
32	BI1	BR2	BI2	82.77
33	BI1	BR3	BI2	81.5
34	BR10	BI3	BR11	94.35
35	BR10	BI3	N1	143.46
36	BR10	BI3	N2	80.45
37	BR10	BI3	N3	155.61
38	BR10	BI3	N4	83.78
39	BR10	BI3	N5	77.23
40	BR10	BI3	N6	88.36
41	BR11	BI3	N1	79.78
42	BR11	BI3	N2	82.22
43	BR11	BI3	N3	91.39
44	BR11	BI3	N4	82.08
45	BR11	BI3	N5	142.54
46	BR11	BI3	N6	156.9
47	N1	BI3	N2	63.05
48	N1	BI3	N3	60.92
49	N1	BI3	N4	130.09
50	N1	BI3	N5	127.67
51	N1	BI3	N6	84.43
52	N2	BI3	N3	123.86
53	N2	BI3	N4	156.76
54	N2	BI3	N5	130.59
55	N2	BI3	N6	75.61
56	N3	BI3	N4	73.56
57	N3	BI3	N5	83.83
58	N3	BI3	N6	95.57
59	N4	BI3	N5	60.89
60	N4	BI3	N6	121.01

Table E.4. Bond Angles for Chiral Ligand-Bismuth Complex (Continued)

Number	Atom1	Atom2	Atom3	Angle
61	N5	BI3	N6	60.35
62	C5	O1	C22	103.94
63	C4	O2	C12	107.73
64	C14	O3	C25	103.99
65	C11	O4	C18	110.91
66	BI3	N1	C7	122.53
67	BI3	N1	C60	119.15
68	C7	N1	C60	118.32
69	BI3	N2	C22	117.22
70	BI3	N2	C68	131.02
71	C22	N2	C68	111.23
72	BI3	N3	C4	115.49
73	BI3	N3	C15	132.82
74	C4	N3	C15	111.02
75	BI3	N4	C18	120.14
76	BI3	N4	C70	134.25
77	C18	N4	C70	105.62
78	BI3	N5	C13	123.4
79	BI3	N5	C53	122.92
80	C13	N5	C53	112.87
81	BI3	N6	C14	120.67
82	BI3	N6	C16	130.41
83	C14	N6	C16	108.43
84	C2	C21	C8	120
85	C2	C21	C16	115.23
86	C8	C21	C16	124.68
87	C21	C2	H2	120
88	C21	C2	C51	120
89	H2	C2	C51	120
90	C2	C51	H51	120
91	C2	C51	C62	120
92	H51	C51	C62	120
93	C51	C62	H62	120
94	C51	C62	C69	120
95	H62	C62	C69	120
96	C62	C69	H69	120
97	C62	C69	C8	120
98	H69	C69	C8	120
99	C21	C8	C69	120

Table E.4. Bond Angles for Chiral Ligand-Bismuth Complex (Continued)

Number	Atom1	Atom2	Atom3	Angle
100	C21	C8	H8	120
101	C69	C8	H8	120
102	C65	C74	C56	120
103	C65	C74	C68	132.12
104	C56	C74	C68	103.26
105	C74	C65	H65	120
106	C74	C65	C72	120
107	H65	C65	C72	120
108	C65	C72	H72	120
109	C65	C72	C54	120
110	H72	C72	C54	120
111	C72	C54	H54	120
112	C72	C54	C64	120
113	H54	C54	C64	120
114	C54	C64	H64	120
115	C54	C64	C56	120
116	H64	C64	C56	120
117	C74	C56	C64	120
118	C74	C56	H56	120
119	C64	C56	H56	120
120	H1	C1	C6	122.96
121	H1	C1	C59	122.97
122	C6	C1	C59	114.07
123	H3	C3	C10	120.52
124	H3	C3	C19	120.52
125	C10	C3	C19	118.96
126	O2	C4	N3	117.55
127	O2	C4	C60	114.93
128	N3	C4	C60	127.35
129	O1	C5	H5A	110.34
130	O1	C5	H5B	110.34
131	O1	C5	C68	106.92
132	H5A	C5	H5B	108.57
133	H5A	C5	C68	110.34
134	H5B	C5	C68	110.34
135	C1	C6	C15	120.26
136	C1	C6	C58	117.81
137	C15	C6	C58	121.92
138	N1	C7	C22	114.09

Table E.4. Bond Angles for Chiral Ligand-Bismuth Complex (Continued)

Number	Atom1	Atom2	Atom3	Angle
139	N1	C7	C24	128.08
140	C22	C7	C24	117.46
141	H9	C9	C17	117.48
142	H9	C9	C24	117.48
143	C17	C9	C24	125.04
144	C3	C10	H10	121.73
145	C3	C10	C53	116.53
146	H10	C10	C53	121.74
147	O4	C11	H11A	110.96
148	O4	C11	H11B	110.96
149	O4	C11	C70	103.99
150	H11A	C11	H11B	108.97
151	H11A	C11	C70	110.96
152	H11B	C11	C70	110.96
153	O2	C12	H12A	112.27
154	O2	C12	H12B	112.27
155	O2	C12	C15	97.47
156	H12A	C12	H12B	109.86
157	H12A	C12	C15	112.27
158	H12B	C12	C15	112.27
159	N5	C13	C18	114.71
160	N5	C13	C19	127.59
161	C18	C13	C19	117.63
162	O3	C14	N6	121.54
163	O3	C14	C53	115.17
164	N6	C14	C53	123.29
165	N3	C15	C6	114.16
166	N3	C15	C12	105.69
167	C6	C15	C12	107.81
168	N6	C16	C21	114.15
169	N6	C16	C25	97
170	C21	C16	C25	110.44
171	C9	C17	H17	120.48
172	C9	C17	C60	119.04
173	H17	C17	C60	120.48
174	O4	C18	N4	114.67
175	O4	C18	C13	124.54
176	N4	C18	C13	120.61
177	C3	C19	C13	117.65

Table E.4. Bond Angles for Chiral Ligand-Bismuth Complex (Continued)

Number	Atom1	Atom2	Atom3	Angle
178	C3	C19	H19	121.18
179	C13	C19	H19	121.18
180	O1	C22	N2	116.59
181	O1	C22	C7	121.34
182	N2	C22	C7	121.95
183	C7	C24	C9	113.58
184	C7	C24	H24	123.21
185	C9	C24	H24	123.21
186	O3	C25	C16	108.76
187	O3	C25	H25A	109.94
188	O3	C25	H25B	109.94
189	C16	C25	H25A	109.94
190	C16	C25	H25B	109.94
191	H25A	C25	H25B	108.33
192	N5	C53	C10	126.37
193	N5	C53	C14	110.87
194	C10	C53	C14	122.61
195	H55	C55	C66	121.42
196	H55	C55	C71	121.42
197	C66	C55	C71	117.16
198	H57	C57	C67	118.4
199	H57	C57	C71	118.41
200	C67	C57	C71	123.19
201	C6	C58	H58	118.05
202	C6	C58	C73	123.9
203	H58	C58	C73	118.05
204	C1	C59	H59	118.08
205	C1	C59	C63	123.84
206	H59	C59	C63	118.08
207	N1	C60	C4	116.11
208	N1	C60	C17	114.79
209	C4	C60	C17	126.6
210	H61	C61	C66	114.75
211	H61	C61	C67	114.75
212	C66	C61	C67	130.51
213	C59	C63	H63	123.55
214	C59	C63	C73	112.91
215	H63	C63	C73	123.55
216	C55	C66	C61	115.59

Table E.4. Bond Angles for Chiral Ligand-Bismuth Complex (Continued)

Number	Atom1	Atom2	Atom3	Angle
217	C55	C66	H66	122.21
218	C61	C66	H66	122.2
219	C57	C67	C61	116.91
220	C57	C67	H67	121.55
221	C61	C67	H67	121.55
222	N2	C68	C74	106.76
223	N2	C68	C5	99.21
224	C74	C68	C5	114.19
225	N4	C70	C11	101.16
226	N4	C70	C71	109.57
227	C11	C70	C71	111.51
228	C55	C71	C57	116.56
229	C55	C71	C70	117.84
230	C57	C71	C70	125.43
231	C58	C73	C63	127.44
232	C58	C73	H73	116.28
233	C63	C73	H73	116.28

APPENDIX F. X-RAY ANALYSIS OF RACEMIC LIGAND-BISMUTH COMPLEX

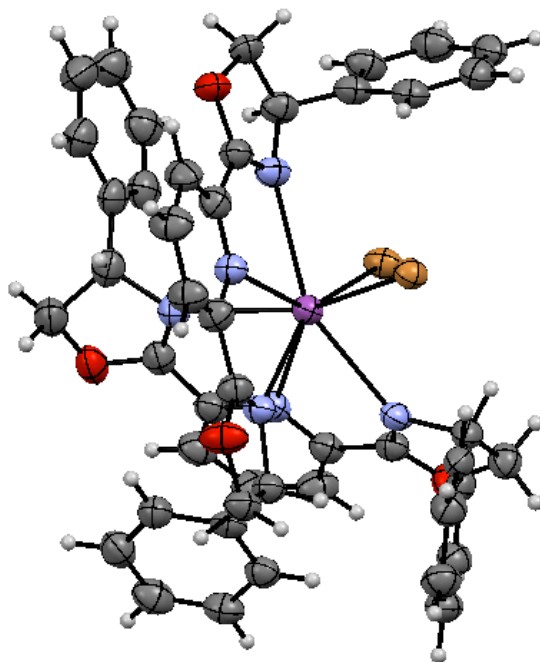


Figure F.1. Thermal Ellipsoid Plot of Racemic Ligand-Bismuth Complex

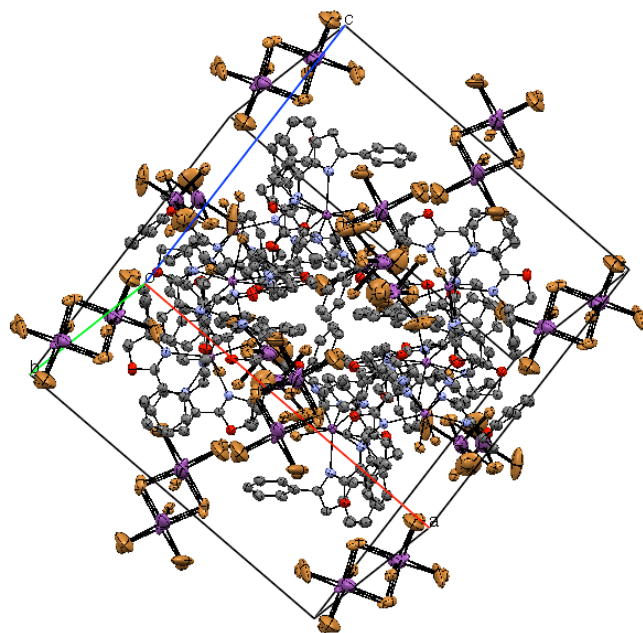


Figure F.2. Crystal Packing of Racemic Ligand-Bismuth Complex

F.1. Crystal Data and Structure Refinement for Racemic Ligand-Bismuth Complex

_chemical_formula_sum 'C46 H38 Bi2 Br6 N6 O4'
_chemical_formula_weight 1636.24
_symmetry_cell_setting ?
_symmetry_space_group_name_H-M ?
_cell_length_a 22.8761(4)
_cell_length_b 19.3719(3)
_cell_length_c 22.1917(4)
_cell_angle_alpha 90.00
_cell_angle_beta 90.00
_cell_angle_gamma 90.00
_cell_volume 9834.3(3)
_cell_formula_units_Z 8
_cell_measurement_temperature 100(2)
_cell_measurement_reflns_used ?
_cell_measurement_theta_min ?
_cell_measurement_theta_max ?
_exptl_crystal_description ?
_exptl_crystal_colour ?
_exptl_crystal_size_max 0.11
_exptl_crystal_size_mid 0.11
_exptl_crystal_size_min 0.10
_exptl_crystal_density_meas ?
_exptl_crystal_density_diffn 2.210
_exptl_crystal_density_method 'not measured'
_exptl_crystal_F_000 6112
_exptl_absorpt_coefficient_mu 19.996
_exptl_absorpt_correction_type ?
_exptl_absorpt_correction_T_min 0.2089
_exptl_absorpt_correction_T_max 0.2325
_exptl_absorpt_process_details ?
_diffn_ambient_temperature 100(2)
_diffn_radiation_wavelength 1.54178
_diffn_radiation_type CuK α
_diffn_radiation_source 'fine-focus sealed tube'
_diffn_radiation_monochromator graphite
_diffn_measurement_device_type ?
_diffn_measurement_method ?
_diffn_detector_area_resol_mean ?
_diffn_reflns_number 74406
_diffn_reflns_av_R_equivalents 0.0382
_diffn_reflns_av_sigmaI/netI 0.0197
_diffn_reflns_limit_h_min -26
_diffn_reflns_limit_h_max 26
_diffn_reflns_limit_k_min -22


```

_diffrn_reflns_limit_k_max    22
_diffrn_reflns_limit_l_min   -26
_diffrn_reflns_limit_l_max    25
_diffrn_reflns_theta_min     2.99
_diffrn_reflns_theta_max     66.52
_reflns_number_total         8505
_reflns_number_gt            7638
_reflns_threshold_expression  >2sigma(I)
_refine_ls_structure_factor_coef Fsqd
_refine_ls_matrix_type       full
_refine_ls_weighting_scheme   calc
_atom_sites_solution_primary direct
_atom_sites_solution_secondary difmap
_atom_sites_solution_hydrogens geom
_refine_ls_hydrogen_treatment mixed
_refine_ls_extinction_method  none
_refine_ls_extinction_coef    ?
_refine_ls_number_reflns     8505
_refine_ls_number_parameters  708
_refine_ls_number_restraints  782
_refine_ls_R_factor_all      0.0648
_refine_ls_R_factor_gt      0.0597
_refine_ls_wR_factor_ref     0.2006
_refine_ls_wR_factor_gt     0.1944
_refine_ls_goodness_of_fit_ref 1.095
_refine_ls_restrained_S_all   1.165
_refine_ls_shift/su_max      0.002
_refine_ls_shift/su_mean     0.000
_diffrn_measured_fraction_theta_max 0.980
_diffrn_reflns_theta_full    66.52
_diffrn_measured_fraction_theta_full 0.980
_refine_diff_density_max     3.116
_refine_diff_density_min    -3.663
_refine_diff_density_rms    0.250

```

Table F.1. Atomic Coordinates and Equivalent Isotropic Displacement Parameters for Racemic Ligand-Bismuth Complex

Number	Label	Xfrac + ESD	Yfrac + ESD	Zfrac + ESD	Uequiv
1	Bi1	0.311704(17)	0.571160(19)	0.211588(17)	0.0360
2	Br1	0.36637(5)	0.69106(5)	0.24883(5)	0.0461
3	Br2	0.36972(5)	0.48706(6)	0.29150(4)	0.0400
4	O1	0.1656(3)	0.5631(4)	0.3626(3)	0.0473
5	O2	0.4805(3)	0.6270(4)	0.1073(3)	0.0453
6	O3	0.1764(3)	0.6770(4)	0.0754(4)	0.0507
7	O4	0.2687(4)	0.3557(4)	0.1253(4)	0.0563

Table F.1. Atomic Coordinates and Equivalent Isotropic Displacement Parameters for Racemic Ligand-Bismuth Complex (Continued)

Number	Label	Xfrac + ESD	Yfrac + ESD	Zfrac + ESD	Uequiv
8	N1	0.2976(4)	0.4641(4)	0.1377(4)	0.0407
9	N2	0.4130(4)	0.5634(4)	0.1554(4)	0.0383
10	N3	0.2310(4)	0.4775(4)	0.2390(4)	0.0387
11	N4	0.2424(4)	0.5962(4)	0.3067(4)	0.0413
12	N5	0.2159(4)	0.6243(5)	0.1567(4)	0.0437
13	N6	0.3250(4)	0.6393(4)	0.1082(4)	0.0400
14	C1	0.3725(5)	0.6592(7)	0.4396(5)	0.0513
15	H1	0.3994	0.6277	0.4571	0.0610
16	C2	0.3063(5)	0.3671(6)	0.0744(5)	0.0443
17	H2A	0.2845	0.3612	0.0362	0.0530
18	H2B	0.3396	0.3344	0.0748	0.0530
19	C3	0.3584(5)	0.5190(5)	-0.0045(5)	0.0433
20	H3	0.3981	0.5121	0.0067	0.0520
21	C4	0.3797(5)	0.6536(5)	0.0889(5)	0.0407
22	C5	0.1977(5)	0.4849(6)	0.2865(5)	0.0420
23	C6	0.2290(5)	0.4174(6)	0.2094(5)	0.0453
24	C7	0.2327(5)	0.6557(5)	0.3483(5)	0.0453
25	H7	0.2160	0.6952	0.3249	0.0540
26	C8	0.2230(5)	0.6548(5)	0.1074(5)	0.0430
27	C9	0.4934(5)	0.4554(6)	0.0818(5)	0.0473
28	H9	0.5051	0.4954	0.0603	0.0570
29	C10	0.4601(4)	0.4016(6)	0.1727(5)	0.0427
30	H10	0.4491	0.4046	0.2138	0.0510
31	C11	0.4252(5)	0.6126(5)	0.1200(4)	0.0390
32	C12	0.1377(5)	0.6792(6)	0.2175(5)	0.0470
33	C13	0.1853(4)	0.6272(6)	0.3912(5)	0.0420
34	H13A	0.2018	0.6179	0.4316	0.0510
35	H13B	0.1526	0.6603	0.3953	0.0510
36	C14	0.3448(6)	0.5596(6)	-0.0545(5)	0.0500
37	H14	0.3754	0.5793	-0.0778	0.0600
38	C15	0.0755(6)	0.7163(8)	0.2990(6)	0.0657
39	H15	0.0445	0.7071	0.3263	0.0790
40	C16	0.3139(5)	0.4885(6)	0.0292(5)	0.0417
41	C17	0.2805(5)	0.6714(5)	0.0806(5)	0.0423
42	C18	0.2553(5)	0.5013(6)	0.0129(5)	0.0457
43	H18	0.2243	0.4827	0.0362	0.0550
44	C19	0.1649(6)	0.7416(6)	0.2202(5)	0.0513
45	H19	0.1959	0.7508	0.1930	0.0610
46	C20	0.4609(5)	0.3381(6)	0.1450(5)	0.0510
47	H20	0.4495	0.2980	0.1667	0.0620
48	C21	0.3905(6)	0.7028(6)	0.0446(5)	0.0527

Table F.1. Atomic Coordinates and Equivalent Isotropic Displacement Parameters for Racemic Ligand-Bismuth Complex (Continued)

Number	Label	Xfrac + ESD	Yfrac + ESD	Zfrac + ESD	Uequiv
49	H21	0.4295	0.7144	0.0338	0.0630
50	C22	0.2044(5)	0.5515(6)	0.3185(5)	0.0417
51	C23	0.2673(5)	0.4148(5)	0.1558(5)	0.0443
52	C24	0.3280(5)	0.4423(5)	0.0812(5)	0.0407
53	H24	0.3712	0.4423	0.0881	0.0490
54	C25	0.4750(4)	0.4613(6)	0.1419(5)	0.0427
55	C26	0.3254(5)	0.6347(6)	0.4064(5)	0.0437
56	H26	0.3208	0.5864	0.4005	0.0520
57	C27	0.2849(5)	0.6800(5)	0.3815(5)	0.0433
58	C28	0.2885(6)	0.7180(6)	0.0336(5)	0.0530
59	H28	0.2560	0.7380	0.0135	0.0640
60	C29	0.1519(5)	0.6262(6)	0.1697(6)	0.0507
61	H29	0.1378	0.5795	0.1824	0.0610
62	C30	0.1957(5)	0.3622(6)	0.2276(6)	0.0507
63	H30	0.1969	0.3194	0.2067	0.0610
64	C31	0.2936(6)	0.7507(6)	0.3908(5)	0.0513
65	H31	0.2666	0.7827	0.3740	0.0610
66	C32	0.4697(4)	0.5312(6)	0.1713(5)	0.0427
67	H32	0.4724	0.5260	0.2161	0.0510
68	C33	0.1597(5)	0.4332(6)	0.3088(6)	0.0513
69	H33	0.1354	0.4408	0.3429	0.0620
70	C34	0.5130(5)	0.5855(6)	0.1504(5)	0.0473
71	H34A	0.5264	0.6141	0.1847	0.0570
72	H34B	0.5474	0.5638	0.1311	0.0570
73	C35	0.4946(5)	0.3909(7)	0.0535(5)	0.0523
74	H35	0.5063	0.3873	0.0126	0.0630
75	C36	0.1038(6)	0.7804(8)	0.3009(7)	0.0647
76	H36	0.0922	0.8149	0.3289	0.0780
77	C37	0.0920(5)	0.6656(7)	0.2577(6)	0.0593
78	H37	0.0724	0.6223	0.2568	0.0710
79	C38	0.2433(6)	0.5411(6)	-0.0371(5)	0.0540
80	H38	0.2039	0.5480	-0.0492	0.0650
81	C39	0.1490(6)	0.7919(7)	0.2610(6)	0.0563
82	H39	0.1692	0.8347	0.2616	0.0680
83	C40	0.2887(6)	0.5713(6)	-0.0702(6)	0.0550
84	H40	0.2799	0.6000	-0.1038	0.0660
85	C41	0.3802(5)	0.7289(7)	0.4473(5)	0.0527
86	H41	0.4132	0.7454	0.4689	0.0630
87	C42	0.3445(6)	0.7343(7)	0.0169(5)	0.0583
88	H42	0.3512	0.7674	-0.0139	0.0700
89	C43	0.4787(5)	0.3327(6)	0.0847(6)	0.0540

Table F.1. Atomic Coordinates and Equivalent Isotropic Displacement Parameters for Racemic Ligand-Bismuth Complex (Continued)

Number	Label	Xfrac + ESD	Yfrac + ESD	Zfrac + ESD	Uequiv
90	H43	0.4797	0.2889	0.0656	0.0650
91	C44	0.3405(6)	0.7750(6)	0.4239(6)	0.0567
92	H44	0.3453	0.8231	0.4304	0.0680
93	C45	0.1599(6)	0.3714(6)	0.2785(6)	0.0557
94	H45	0.1356	0.3347	0.2919	0.0660
95	C46	0.1264(5)	0.6456(7)	0.1073(6)	0.0563
96	H46A	0.1121	0.6041	0.0858	0.0680
97	H46B	0.0938	0.6789	0.1115	0.0680
98	BiA1	0.96553(11)	0.42052(16)	0.43786(18)	0.0500
99	BiB1	1.0276(3)	0.5620(4)	0.5495(3)	0.1243
100	Br31	0.9140(4)	0.5221(6)	0.5199(6)	0.0723
101	Br41	1.0800(3)	0.4619(5)	0.4700(4)	0.0483
102	Br51	0.9686(6)	0.3323(5)	0.5331(5)	0.0363
103	Br61	1.0254(6)	0.6542(5)	0.4591(5)	0.0417
104	Br71	0.8545(3)	0.3837(4)	0.4104(4)	0.0647
105	Br81	1.0071(3)	0.3156(4)	0.3616(3)	0.0790
106	Br91	1.1360(7)	0.5960(12)	0.5864(11)	0.2000
107	Br01	0.9895(9)	0.6693(11)	0.6273(9)	0.2090
108	BiA1	1.03447(11)	0.57948(16)	0.56214(18)	0.0500
109	BiB1	0.9724(3)	0.4380(4)	0.4505(3)	0.1243
110	Br31	1.0860(4)	0.4779(6)	0.4801(6)	0.0723
111	Br41	0.9200(3)	0.5381(5)	0.5300(4)	0.0483
112	Br51	1.0314(6)	0.6677(5)	0.4669(5)	0.0363
113	Br61	0.9746(6)	0.3458(5)	0.5409(5)	0.0417
114	Br71	1.1455(3)	0.6163(4)	0.5896(4)	0.0647
115	Br81	0.9929(3)	0.6844(4)	0.6384(3)	0.0790
116	Br91	0.8640(7)	0.4040(12)	0.4136(11)	0.2000
117	Br01	1.0105(9)	0.3307(11)	0.3727(9)	0.2090
118	BiA2	0.98644(14)	0.4696(2)	0.4621(2)	0.0556
119	BiB2	1.0290(6)	0.5948(6)	0.5853(5)	0.2543
120	Br32	0.9218(6)	0.5582(9)	0.5341(8)	0.1043
121	Br42	1.0923(3)	0.5085(6)	0.5130(6)	0.1180
122	Br52	1.0050(3)	0.5678(5)	0.3709(4)	0.0780
123	Br62	1.0257(5)	0.4905(7)	0.6677(5)	0.1380
124	Br72	0.8864(4)	0.4332(7)	0.3998(5)	0.0833
125	Br82	1.0457(11)	0.3796(13)	0.3792(12)	0.2580
126	Br92	1.1332(10)	0.6448(16)	0.6276(16)	0.3323
127	BrO2	0.9818(14)	0.6792(14)	0.6814(13)	0.3050

Table F.2. Symmetry Operations for Racemic Ligand-Bismuth Complex

Number	Symm. Op.	Description	Detailed Description	Order	Type
1	x, y, z	Identity	Identity	1	1
2	$1/2+x, 1/2-y, -z$	Screw axis (2-fold)	2-fold screw axis with direction $[1, 0, 0]$ at $x, 1/4, 0$ with screw component $[1/2, 0, 0]$	2	2
3	$-x, y, 1/2-z$	Rotation axis (2-fold)	2-fold rotation axis with direction $[0, 1, 0]$ at $0, y, 1/4$	2	2
4	$1/2-x, 1/2-y, 1/2+z$	Screw axis (2-fold)	2-fold screw axis with direction $[0, 0, 1]$ at $1/4, 1/4, z$ with screw component $[0, 0, 1/2]$	2	2
5	$-x, -y, -z$	Inversion centre	Inversion at $[0, 0, 0]$	2	-1
6	$1/2-x, 1/2+y, z$	Glide plane	Glide plane perpendicular to $[1, 0, 0]$ with glide component $[0, 1/2, 0]$	2	-2
7	$x, -y, 1/2+z$	Glide plane	Glide plane perpendicular to $[0, 1, 0]$ with glide component $[0, 0, 1/2]$	2	-2
8	$1/2+x, 1/2+y, 1/2-z$	Glide plane	Glide plane perpendicular to $[0, 0, 1]$ with glide component $[1/2, 1/2, 0]$	2	-2

Table F.3. Bond Lengths for Racemic Ligand-Bismuth Complex

Number	Atom1	Atom2	Length
1	Bi1	Br1	2.764(1)
2	Bi1	Br2	2.750(1)
3	Bi1	N1	2.663(8)
4	Bi1	N2	2.636(9)
5	Bi1	N3	2.659(9)
6	Bi1	N4	2.684(9)
7	Bi1	N5	2.710(9)
8	Bi1	N6	2.664(9)
9	O1	C13	1.47(1)
10	O1	C22	1.34(1)

Table F.3. Bond Lengths for Racemic Ligand-Bismuth Complex (Continued)

Number	Atom1	Atom2	Length
11	O2	C11	1.33(1)
12	O2	C34	1.45(1)
13	O3	C8	1.35(1)
14	O3	C46	1.48(1)
15	O4	C2	1.44(1)
16	O4	C23	1.33(1)
17	N1	C23	1.25(1)
18	N1	C24	1.49(1)
19	N2	C11	1.27(1)
20	N2	C32	1.48(1)
21	N3	C5	1.31(1)
22	N3	C6	1.34(1)
23	N4	C7	1.49(1)
24	N4	C22	1.25(1)
25	N5	C8	1.25(1)
26	N5	C29	1.49(1)
27	N6	C4	1.35(1)
28	N6	C17	1.34(1)
29	C1	H1	0.95(1)
30	C1	C26	1.39(2)
31	C1	C41	1.37(2)
32	C2	H2A	0.99(1)
33	C2	H2B	0.99(1)
34	C2	C24	1.55(2)
35	C3	H3	0.95(1)
36	C3	C14	1.40(2)
37	C3	C16	1.39(2)
38	C4	C11	1.48(2)
39	C4	C21	1.39(2)
40	C5	C22	1.48(2)
41	C5	C33	1.42(2)
42	C6	C23	1.48(2)
43	C6	C30	1.37(2)
44	C7	H7	1.00(1)
45	C7	C13	1.54(2)
46	C7	C27	1.48(2)
47	C8	C17	1.48(2)
48	C9	H9	0.95(1)
49	C9	C25	1.40(2)

Table F.3. Bond Lengths for Racemic Ligand-Bismuth Complex (Continued)

Number	Atom1	Atom2	Length
50	C9	C35	1.40(2)
51	C10	H10	0.95(1)
52	C10	C20	1.38(2)
53	C10	C25	1.39(2)
54	C12	C19	1.36(2)
55	C12	C29	1.51(2)
56	C12	C37	1.40(2)
57	C13	H13A	0.99(1)
58	C13	H13B	0.99(1)
59	C14	H14	0.95(1)
60	C14	C40	1.35(2)
61	C15	H15	0.95(1)
62	C15	C36	1.40(2)
63	C15	C37	1.40(2)
64	C16	C18	1.41(2)
65	C16	C24	1.50(2)
66	C17	C28	1.39(2)
67	C18	H18	0.95(1)
68	C18	C38	1.38(2)
69	C19	H19	0.95(1)
70	C19	C39	1.38(2)
71	C20	H20	0.95(1)
72	C20	C43	1.40(2)
73	C21	H21	0.95(1)
74	C21	C42	1.36(2)
75	C24	H24	1.00(1)
76	C25	C32	1.51(2)
77	C26	H26	0.95(1)
78	C26	C27	1.39(2)
79	C27	C31	1.40(2)
80	C28	H28	0.95(1)
81	C28	C42	1.37(2)
82	C29	H29	1.00(1)
83	C29	C46	1.55(2)
84	C30	H30	0.95(1)
85	C30	C45	1.41(2)
86	C31	H31	0.95(1)
87	C31	C44	1.38(2)
88	C32	H32	1.00(1)

Table F.3. Bond Lengths for Racemic Ligand-Bismuth Complex (Continued)

Number	Atom1	Atom2	Length
89	C32	C34	1.52(2)
90	C33	H33	0.95(1)
91	C33	C45	1.37(2)
92	C34	H34A	0.99(1)
93	C34	H34B	0.99(1)
94	C35	H35	0.95(1)
95	C35	C43	1.37(2)
96	C36	H36	0.95(2)
97	C36	C39	1.38(2)
98	C37	H37	0.95(1)
99	C38	H38	0.95(1)
100	C38	C40	1.40(2)
101	C39	H39	0.95(1)
102	C40	H40	0.95(1)
103	C41	H41	0.95(1)
104	C41	C44	1.38(2)
105	C42	H42	0.95(1)
106	C43	H43	0.95(1)
107	C44	H44	0.95(1)
108	C45	H45	0.95(1)
109	C46	H46A	0.99(1)
110	C46	H46B	0.99(1)
111	BiA1	Br31	2.93(1)
112	BiA1	Br41	2.830(8)
113	BiA1	Br51	2.72(1)
114	BiA1	Br71	2.708(8)
115	BiA1	Br81	2.811(8)
116	BiA1	Br31	3.12(1)
117	BiA1	Br41	3.23(1)
118	BiA1	Br61	2.71(1)
119	BiA1	Br91	2.41(2)
120	BiA1	Br01	2.49(2)
121	BiB1	Br31	2.79(1)
122	BiB1	Br41	2.88(1)
123	BiB1	Br61	2.69(1)
124	BiB1	Br91	2.69(2)
125	BiB1	Br01	2.84(2)
126	BiB1	Br31	2.61(1)
127	BiB1	Br41	2.54(1)

Table F.3. Bond Lengths for Racemic Ligand-Bismuth Complex (Continued)

Number	Atom1	Atom2	Length
128	BiB1	Br51	2.75(1)
129	BiB1	Br71	3.03(1)
130	BiB1	Br81	3.19(1)
131	Br31	BiA1	3.12(1)
132	Br31	BiB1	2.61(1)
133	Br41	BiA1	3.23(1)
134	Br41	BiB1	2.54(1)
135	Br51	BiB1	2.75(1)
136	Br61	BiA1	2.71(1)
137	Br71	BiB1	3.03(1)
138	Br81	BiB1	3.19(1)
139	Br91	BiA1	2.41(2)
140	Br01	BiA1	2.49(2)
141	BiA1	Br31	2.93(1)
142	BiA1	Br41	2.830(8)
143	BiA1	Br51	2.72(1)
144	BiA1	Br71	2.708(8)
145	BiA1	Br81	2.811(8)
146	BiB1	Br31	2.79(1)
147	BiB1	Br41	2.88(1)
148	BiB1	Br61	2.69(1)
149	BiB1	Br91	2.69(2)
150	BiB1	Br01	2.84(2)

Table F.4. Bond Angles for Racemic Ligand-Bismuth Complex

Number	Atom1	Atom2	Atom3	Angle
1	Br1	Bi1	Br2	94.97(3)
2	Br1	Bi1	N1	153.3(2)
3	Br1	Bi1	N2	78.0(2)
4	Br1	Bi1	N3	145.0(2)
5	Br1	Bi1	N4	83.1(2)
6	Br1	Bi1	N5	100.4(2)
7	Br1	Bi1	N6	77.9(2)
8	Br2	Bi1	N1	89.7(2)
9	Br2	Bi1	N2	81.2(2)
10	Br2	Bi1	N3	77.5(2)
11	Br2	Bi1	N4	83.4(2)

Table F.4. Bond Angles for Racemic Ligand-Bismuth Complex (Continued)

Number	Atom1	Atom2	Atom3	Angle
12	Br2	Bi1	N5	154.8(2)
13	Br2	Bi1	N6	142.5(2)
14	N1	Bi1	N2	76.8(3)
15	N1	Bi1	N3	61.7(3)
16	N1	Bi1	N4	123.6(3)
17	N1	Bi1	N5	85.5(3)
18	N1	Bi1	N6	82.5(3)
19	N2	Bi1	N3	132.8(3)
20	N2	Bi1	N4	154.4(3)
21	N2	Bi1	N5	121.3(3)
22	N2	Bi1	N6	61.3(3)
23	N3	Bi1	N4	62.2(3)
24	N3	Bi1	N5	78.5(3)
25	N3	Bi1	N6	127.9(3)
26	N4	Bi1	N5	78.9(3)
27	N4	Bi1	N6	130.9(3)
28	N5	Bi1	N6	61.1(3)
29	C13	O1	C22	104.8(8)
30	C11	O2	C34	103.4(8)
31	C8	O3	C46	103.2(8)
32	C2	O4	C23	106.4(9)
33	Bi1	N1	C23	117.7(7)
34	Bi1	N1	C24	132.8(6)
35	C23	N1	C24	108.2(9)
36	Bi1	N2	C11	116.4(7)
37	Bi1	N2	C32	132.9(6)
38	C11	N2	C32	105.8(8)
39	Bi1	N3	C5	120.9(7)
40	Bi1	N3	C6	120.4(7)
41	C5	N3	C6	118.1(9)
42	Bi1	N4	C7	135.5(6)
43	Bi1	N4	C22	116.7(7)
44	C7	N4	C22	107.5(9)
45	Bi1	N5	C8	117.8(7)
46	Bi1	N5	C29	135.7(7)
47	C8	N5	C29	106.5(9)
48	Bi1	N6	C4	118.7(7)
49	Bi1	N6	C17	122.4(7)
50	C4	N6	C17	117.6(9)

Table F.4. Bond Angles for Racemic Ligand-Bismuth Complex (Continued)

Number	Atom1	Atom2	Atom3	Angle
51	H1	C1	C26	120(1)
52	H1	C1	C41	120(1)
53	C26	C1	C41	120(1)
54	O4	C2	H2A	111(1)
55	O4	C2	H2B	111(1)
56	O4	C2	C24	105.1(9)
57	H2A	C2	H2B	109(1)
58	H2A	C2	C24	111(1)
59	H2B	C2	C24	111(1)
60	H3	C3	C14	120(1)
61	H3	C3	C16	120(1)
62	C14	C3	C16	120(1)
63	N6	C4	C11	113.2(9)
64	N6	C4	C21	122(1)
65	C11	C4	C21	125(1)
66	N3	C5	C22	115(1)
67	N3	C5	C33	124(1)
68	C22	C5	C33	121(1)
69	N3	C6	C23	114(1)
70	N3	C6	C30	124(1)
71	C23	C6	C30	123(1)
72	N4	C7	H7	109.0(9)
73	N4	C7	C13	102.1(8)
74	N4	C7	C27	115.7(9)
75	H7	C7	C13	109.0(9)
76	H7	C7	C27	108.9(9)
77	C13	C7	C27	111.9(9)
78	O3	C8	N5	120(1)
79	O3	C8	C17	114.9(9)
80	N5	C8	C17	125(1)
81	H9	C9	C25	120(1)
82	H9	C9	C35	120(1)
83	C25	C9	C35	120(1)
84	H10	C10	C20	119(1)
85	H10	C10	C25	119(1)
86	C20	C10	C25	122(1)
87	O2	C11	N2	120.0(9)
88	O2	C11	C4	117.3(9)
89	N2	C11	C4	122.6(9)

Table F.4. Bond Angles for Racemic Ligand-Bismuth Complex (Continued)

Number	Atom1	Atom2	Atom3	Angle
90	C19	C12	C29	122(1)
91	C19	C12	C37	119(1)
92	C29	C12	C37	119(1)
93	O1	C13	C7	104.6(8)
94	O1	C13	H13A	110.8(9)
95	O1	C13	H13B	110.9(9)
96	C7	C13	H13A	110.8(9)
97	C7	C13	H13B	110.8(9)
98	H13A	C13	H13B	109(1)
99	C3	C14	H14	120(1)
100	C3	C14	C40	121(1)
101	H14	C14	C40	120(1)
102	H15	C15	C36	119(1)
103	H15	C15	C37	119(1)
104	C36	C15	C37	121(1)
105	C3	C16	C18	119(1)
106	C3	C16	C24	121(1)
107	C18	C16	C24	121(1)
108	N6	C17	C8	113.0(9)
109	N6	C17	C28	123(1)
110	C8	C17	C28	124(1)
111	C16	C18	H18	120(1)
112	C16	C18	C38	120(1)
113	H18	C18	C38	120(1)
114	C12	C19	H19	119(1)
115	C12	C19	C39	122(1)
116	H19	C19	C39	119(1)
117	C10	C20	H20	120(1)
118	C10	C20	C43	120(1)
119	H20	C20	C43	120(1)
120	C4	C21	H21	120(1)
121	C4	C21	C42	119(1)
122	H21	C21	C42	120(1)
123	O1	C22	N4	120(1)
124	O1	C22	C5	115.3(9)
125	N4	C22	C5	125(1)
126	O4	C23	N1	119(1)
127	O4	C23	C6	116.9(9)
128	N1	C23	C6	124(1)

Table F.4. Bond Angles for Racemic Ligand-Bismuth Complex (Continued)

Number	Atom1	Atom2	Atom3	Angle
129	N1	C24	C2	101.5(8)
130	N1	C24	C16	112.2(9)
131	N1	C24	H24	109.4(9)
132	C2	C24	C16	114.8(9)
133	C2	C24	H24	109.4(9)
134	C16	C24	H24	109(1)
135	C9	C25	C10	118(1)
136	C9	C25	C32	121(1)
137	C10	C25	C32	121.1(9)
138	C1	C26	H26	120(1)
139	C1	C26	C27	121(1)
140	H26	C26	C27	120(1)
141	C7	C27	C26	122(1)
142	C7	C27	C31	120(1)
143	C26	C27	C31	118(1)
144	C17	C28	H28	121(1)
145	C17	C28	C42	118(1)
146	H28	C28	C42	121(1)
147	N5	C29	C12	111.3(9)
148	N5	C29	H29	110(1)
149	N5	C29	C46	101.7(9)
150	C12	C29	H29	110(1)
151	C12	C29	C46	112(1)
152	H29	C29	C46	110(1)
153	C6	C30	H30	121(1)
154	C6	C30	C45	117(1)
155	H30	C30	C45	121(1)
156	C27	C31	H31	119(1)
157	C27	C31	C44	121(1)
158	H31	C31	C44	119(1)
159	N2	C32	C25	110.2(8)
160	N2	C32	H32	109.4(9)
161	N2	C32	C34	101.9(8)
162	C25	C32	H32	109.5(9)
163	C25	C32	C34	116.0(9)
164	H32	C32	C34	109.4(9)
165	C5	C33	H33	122(1)
166	C5	C33	C45	116(1)
167	H33	C33	C45	122(1)

Table F.4. Bond Angles for Racemic Ligand-Bismuth Complex (Continued)

Number	Atom1	Atom2	Atom3	Angle
168	O2	C34	C32	104.5(8)
169	O2	C34	H34A	111(1)
170	O2	C34	H34B	111(1)
171	C32	C34	H34A	111(1)
172	C32	C34	H34B	111(1)
173	H34A	C34	H34B	109(1)
174	C9	C35	H35	120(1)
175	C9	C35	C43	120(1)
176	H35	C35	C43	120(1)
177	C15	C36	H36	121(1)
178	C15	C36	C39	118(1)
179	H36	C36	C39	121(1)
180	C12	C37	C15	119(1)
181	C12	C37	H37	120(1)
182	C15	C37	H37	120(1)
183	C18	C38	H38	120(1)
184	C18	C38	C40	121(1)
185	H38	C38	C40	120(1)
186	C19	C39	C36	120(1)
187	C19	C39	H39	120(1)
188	C36	C39	H39	120(1)
189	C14	C40	C38	120(1)
190	C14	C40	H40	120(1)
191	C38	C40	H40	120(1)
192	C1	C41	H41	120(1)
193	C1	C41	C44	120(1)
194	H41	C41	C44	120(1)
195	C21	C42	C28	120(1)
196	C21	C42	H42	120(1)
197	C28	C42	H42	120(1)
198	C20	C43	C35	120(1)
199	C20	C43	H43	120(1)
200	C35	C43	H43	120(1)
201	C31	C44	C41	119(1)
202	C31	C44	H44	120(1)
203	C41	C44	H44	120(1)
204	C30	C45	C33	120(1)
205	C30	C45	H45	120(1)
206	C33	C45	H45	120(1)

Table F.4. Bond Angles for Racemic Ligand-Bismuth Complex (Continued)

Number	Atom1	Atom2	Atom3	Angle
207	O3	C46	C29	103.7(9)
208	O3	C46	H46A	111(1)
209	O3	C46	H46B	111(1)
210	C29	C46	H46A	111(1)
211	C29	C46	H46B	111(1)
212	H46A	C46	H46B	109(1)
213	Br31	BiA1	Br41	91.5(3)
214	Br31	BiA1	Br51	87.1(3)
215	Br31	BiA1	Br71	86.5(3)
216	Br31	BiA1	Br81	175.2(3)
217	Br31	BiA1	Br31	85.9(3)
218	Br31	BiA1	Br41	5.0(3)
219	Br31	BiA1	Br61	82.3(3)
220	Br31	BiA1	Br91	80.8(6)
221	Br31	BiA1	Br01	177.1(5)
222	Br41	BiA1	Br51	87.6(3)
223	Br41	BiA1	Br71	177.9(3)
224	Br41	BiA1	Br81	92.5(2)
225	Br41	BiA1	Br31	5.6(3)
226	Br41	BiA1	Br41	86.5(2)
227	Br41	BiA1	Br61	82.4(3)
228	Br41	BiA1	Br91	170.9(6)
229	Br41	BiA1	Br01	87.8(5)
230	Br51	BiA1	Br71	91.9(3)
231	Br51	BiA1	Br81	90.3(3)
232	Br51	BiA1	Br31	88.1(3)
233	Br51	BiA1	Br41	87.7(3)
234	Br51	BiA1	Br61	7.2(3)
235	Br51	BiA1	Br91	96.6(6)
236	Br51	BiA1	Br01	90.1(5)
237	Br71	BiA1	Br81	89.5(2)
238	Br71	BiA1	Br31	172.5(3)
239	Br71	BiA1	Br41	91.5(2)
240	Br71	BiA1	Br61	96.9(3)
241	Br71	BiA1	Br91	7.6(5)
242	Br71	BiA1	Br01	94.2(5)
243	Br81	BiA1	Br31	98.0(3)
244	Br81	BiA1	Br41	177.8(2)
245	Br81	BiA1	Br61	95.5(3)

Table F.4. Bond Angles for Racemic Ligand-Bismuth Complex (Continued)

Number	Atom1	Atom2	Atom3	Angle
246	Br81	BiA1	Br91	95.5(5)
247	Br81	BiA1	Br01	4.7(5)
248	Br31	BiA1	Br41	81.0(3)
249	Br31	BiA1	Br61	82.5(3)
250	Br31	BiA1	Br91	165.6(6)
251	Br31	BiA1	Br01	93.4(5)
252	Br41	BiA1	Br61	82.4(3)
253	Br41	BiA1	Br91	85.7(5)
254	Br41	BiA1	Br01	174.0(5)
255	Br61	BiA1	Br91	101.0(6)
256	Br61	BiA1	Br01	94.9(5)
257	Br91	BiA1	Br01	100.2(7)
258	Br31	BiB1	Br41	93.3(4)
259	Br31	BiB1	Br61	89.5(4)
260	Br31	BiB1	Br91	175.6(6)
261	Br31	BiB1	Br01	93.4(5)
262	Br31	BiB1	Br31	99.5(4)
263	Br31	BiB1	Br41	6.9(3)
264	Br31	BiB1	Br51	94.5(4)
265	Br31	BiB1	Br71	174.3(4)
266	Br31	BiB1	Br81	96.9(3)
267	Br41	BiB1	Br61	89.9(4)
268	Br41	BiB1	Br91	88.2(5)
269	Br41	BiB1	Br01	172.9(5)
270	Br41	BiB1	Br31	6.3(3)
271	Br41	BiB1	Br41	100.1(3)
272	Br41	BiB1	Br51	94.6(4)
273	Br41	BiB1	Br71	92.5(3)
274	Br41	BiB1	Br81	169.6(3)
275	Br61	BiB1	Br91	94.7(6)
276	Br61	BiB1	Br01	87.8(5)
277	Br61	BiB1	Br31	89.1(4)
278	Br61	BiB1	Br41	88.6(4)
279	Br61	BiB1	Br51	7.1(3)
280	Br61	BiB1	Br71	90.3(4)
281	Br61	BiB1	Br81	87.9(3)
282	Br91	BiB1	Br01	85.3(6)
283	Br91	BiB1	Br31	82.0(6)
284	Br91	BiB1	Br41	171.1(6)

Table F.4. Bond Angles for Racemic Ligand-Bismuth Complex (Continued)

Number	Atom1	Atom2	Atom3	Angle
285	Br91	BiB1	Br51	89.5(6)
286	Br91	BiB1	Br71	6.2(5)
287	Br91	BiB1	Br81	81.9(5)
288	Br01	BiB1	Br31	166.7(6)
289	Br01	BiB1	Br41	86.5(5)
290	Br01	BiB1	Br51	82.5(5)
291	Br01	BiB1	Br71	80.8(5)
292	Br01	BiB1	Br81	3.4(4)
293	Br31	BiB1	Br41	106.4(4)
294	Br31	BiB1	Br51	93.2(4)
295	Br31	BiB1	Br71	86.2(4)
296	Br31	BiB1	Br81	163.3(4)
297	Br41	BiB1	Br51	93.0(4)
298	Br41	BiB1	Br71	167.3(4)
299	Br41	BiB1	Br81	90.0(3)
300	Br51	BiB1	Br71	84.8(3)
301	Br51	BiB1	Br81	82.3(3)
302	Br71	BiB1	Br81	77.4(3)
303	BiA1	Br31	BiB1	87.6(4)
304	BiA1	Br31	BiA1	94.1(3)
305	BiA1	Br31	BiB1	7.1(2)
306	BiB1	Br31	BiA1	6.5(2)
307	BiB1	Br31	BiB1	80.5(4)
308	BiA1	Br31	BiB1	87.0(4)
309	BiA1	Br41	BiB1	87.7(3)
310	BiA1	Br41	BiA1	93.5(3)
311	BiA1	Br41	BiB1	7.9(2)
312	BiB1	Br41	BiA1	5.8(2)
313	BiB1	Br41	BiB1	79.9(3)
314	BiA1	Br41	BiB1	85.6(3)
315	BiA1	Br51	BiB1	9.8(2)
316	BiB1	Br61	BiA1	9.9(2)
317	BiA1	Br71	BiB1	6.8(2)
318	BiA1	Br81	BiB1	5.3(1)
319	BiB1	Br91	BiA1	8.3(2)
320	BiB1	Br01	BiA1	6.6(2)
321	Br31	BiA1	Br41	81.0(3)
322	Br31	BiA1	Br61	82.5(3)
323	Br31	BiA1	Br91	165.6(6)

Table F.4. Bond Angles for Racemic Ligand-Bismuth Complex (Continued)

Number	Atom1	Atom2	Atom3	Angle
324	Br31	BiA1	Br01	93.4(5)
325	Br31	BiA1	Br31	85.9(3)
326	Br31	BiA1	Br41	5.6(3)
327	Br31	BiA1	Br51	88.1(3)
328	Br31	BiA1	Br71	172.5(3)
329	Br31	BiA1	Br81	98.0(3)
330	Br41	BiA1	Br61	82.4(3)
331	Br41	BiA1	Br91	85.7(5)
332	Br41	BiA1	Br01	174.0(5)
333	Br41	BiA1	Br31	5.0(3)
334	Br41	BiA1	Br41	86.5(2)
335	Br41	BiA1	Br51	87.7(3)
336	Br41	BiA1	Br71	91.5(2)
337	Br41	BiA1	Br81	177.8(2)
338	Br61	BiA1	Br91	101.0(6)
339	Br61	BiA1	Br01	94.9(5)
340	Br61	BiA1	Br31	82.3(3)
341	Br61	BiA1	Br41	82.4(3)
342	Br61	BiA1	Br51	7.2(3)
343	Br61	BiA1	Br71	96.9(3)
344	Br61	BiA1	Br81	95.5(3)
345	Br91	BiA1	Br01	100.2(7)
346	Br91	BiA1	Br31	80.8(6)
347	Br91	BiA1	Br41	170.9(6)
348	Br91	BiA1	Br51	96.6(6)
349	Br91	BiA1	Br71	7.6(5)
350	Br91	BiA1	Br81	95.5(5)
351	Br01	BiA1	Br31	177.1(5)
352	Br01	BiA1	Br41	87.8(5)
353	Br01	BiA1	Br51	90.1(5)
354	Br01	BiA1	Br71	94.2(5)
355	Br01	BiA1	Br81	4.7(5)
356	Br31	BiA1	Br41	91.5(3)
357	Br31	BiA1	Br51	87.1(3)
358	Br31	BiA1	Br71	86.5(3)
359	Br31	BiA1	Br81	175.2(3)
360	Br41	BiA1	Br51	87.6(3)
361	Br41	BiA1	Br71	177.9(3)
362	Br41	BiA1	Br81	92.5(2)

Table F.4. Bond Angles for Racemic Ligand-Bismuth Complex (Continued)

Number	Atom1	Atom2	Atom3	Angle
363	Br51	BiA1	Br71	91.9(3)
364	Br51	BiA1	Br81	90.3(3)
365	Br71	BiA1	Br81	89.5(2)
366	Br31	BiB1	Br41	106.4(4)
367	Br31	BiB1	Br51	93.2(4)
368	Br31	BiB1	Br71	86.2(4)
369	Br31	BiB1	Br81	163.3(4)
370	Br31	BiB1	Br31	99.5(4)
371	Br31	BiB1	Br41	6.3(3)
372	Br31	BiB1	Br61	89.1(4)
373	Br31	BiB1	Br91	82.0(6)
374	Br31	BiB1	Br01	166.7(6)
375	Br41	BiB1	Br51	93.0(4)
376	Br41	BiB1	Br71	167.3(4)
377	Br41	BiB1	Br81	90.0(3)
378	Br41	BiB1	Br31	6.9(3)
379	Br41	BiB1	Br41	100.1(3)
380	Br41	BiB1	Br61	88.6(4)
381	Br41	BiB1	Br91	171.1(6)
382	Br41	BiB1	Br01	86.5(5)
383	Br51	BiB1	Br71	84.8(3)
384	Br51	BiB1	Br81	82.3(3)
385	Br51	BiB1	Br31	94.5(4)
386	Br51	BiB1	Br41	94.6(4)
387	Br51	BiB1	Br61	7.1(3)
388	Br51	BiB1	Br91	89.5(6)
389	Br51	BiB1	Br01	82.5(5)
390	Br71	BiB1	Br81	77.4(3)
391	Br71	BiB1	Br31	174.3(4)
392	Br71	BiB1	Br41	92.5(3)
393	Br71	BiB1	Br61	90.3(4)
394	Br71	BiB1	Br91	6.2(5)
395	Br71	BiB1	Br01	80.8(5)
396	Br81	BiB1	Br31	96.9(3)
397	Br81	BiB1	Br41	169.6(3)
398	Br81	BiB1	Br61	87.9(3)
399	Br81	BiB1	Br91	81.9(5)
400	Br81	BiB1	Br01	3.4(4)
401	Br31	BiB1	Br41	93.3(4)

Table F.4. Bond Angles for Racemic Ligand-Bismuth Complex (Continued)

Number	Atom1	Atom2	Atom3	Angle
402	Br31	BiB1	Br61	89.5(4)
403	Br31	BiB1	Br91	175.6(6)
404	Br31	BiB1	Br01	93.4(5)
405	Br41	BiB1	Br61	89.9(4)
406	Br41	BiB1	Br91	88.2(5)
407	Br41	BiB1	Br01	172.9(5)
408	Br61	BiB1	Br91	94.7(6)
409	Br61	BiB1	Br01	87.8(5)
410	Br91	BiB1	Br01	85.3(6)
411	BiA1	Br31	BiB1	87.0(4)
412	BiA1	Br31	BiA1	94.1(3)
413	BiA1	Br31	BiB1	6.5(2)
414	BiB1	Br31	BiA1	7.1(2)
415	BiB1	Br31	BiB1	80.5(4)
416	BiA1	Br31	BiB1	87.6(4)
417	BiA1	Br41	BiB1	85.6(3)
418	BiA1	Br41	BiA1	93.5(3)
419	BiA1	Br41	BiB1	5.8(2)
420	BiB1	Br41	BiA1	7.9(2)
421	BiB1	Br41	BiB1	79.9(3)
422	BiA1	Br41	BiB1	87.7(3)
423	BiB1	Br51	BiA1	9.8(2)
424	BiA1	Br61	BiB1	9.9(2)
425	BiB1	Br71	BiA1	6.8(2)
426	BiB1	Br81	BiA1	5.3(1)
427	BiA1	Br91	BiB1	8.3(2)
428	BiA1	Br01	BiB1	6.6(2)

APPENDIX G. X-RAY ANALYSIS OF LIGAND-INDIUM COMPLEX

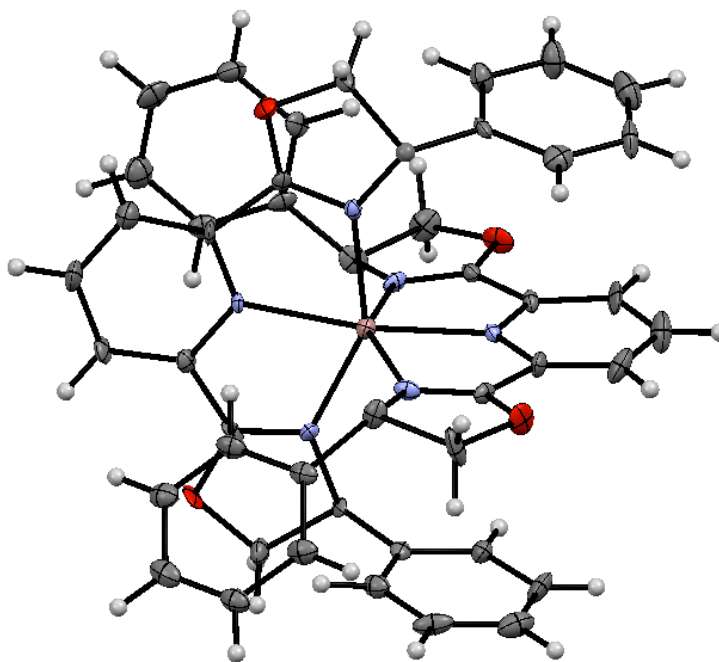


Figure G.1. Thermal Ellipsoid Plot of Ligand-Indium Complex

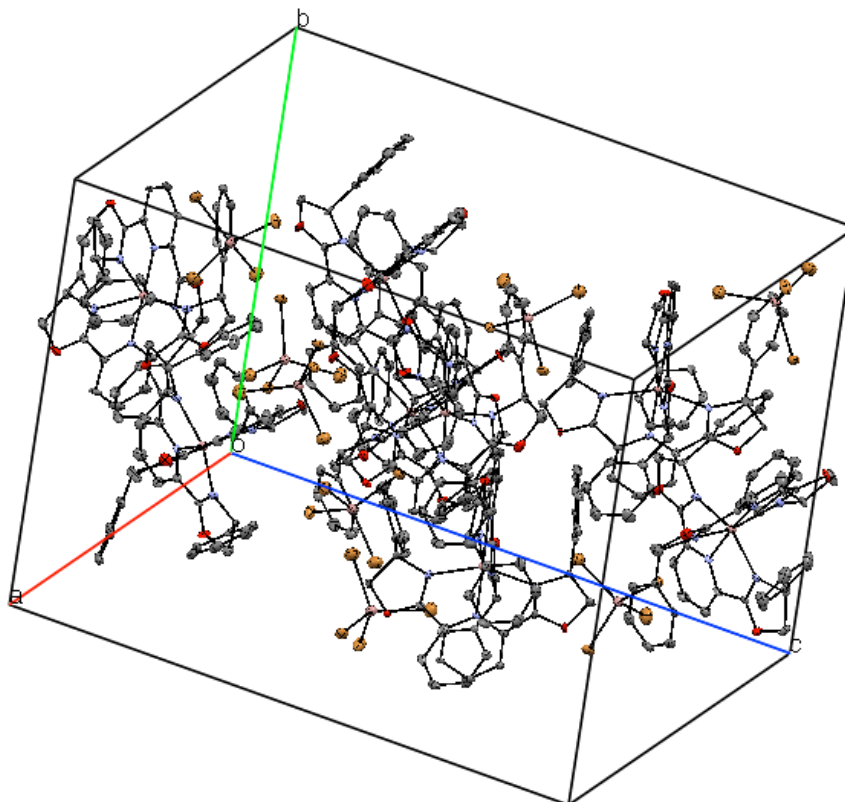


Figure G.2. Crystal Packing of Ligand-Indium Complex

G.1. Crystal Data and Structure Refinement for Ligand-Indium Complex

```
_chemical_formula_sum 'C46 H34 Br4 Ga2 N6 O4'  
_chemical_formula_weight 1193.87  
_symmetry_cell_setting Orthorhombic  
_symmetry_space_group_name_H-M P2(1)2(1)2(1)  
_cell_length_a 18.7119(3)  
_cell_length_b 18.7878(2)  
_cell_length_c 25.3032(3)  
_cell_angle_alpha 90.00  
_cell_angle_beta 90.00  
_cell_angle_gamma 90.00  
_cell_volume 8895.5(2)  
_cell_formula_units_Z 8  
_cell_measurement_temperature 100(2)  
_cell_measurement_reflns_used 9997  
_cell_measurement_theta_min 3.76  
_cell_measurement_theta_max 65.96  
_exptl_crystal_description plate  
_exptl_crystal_colour colorless  
_exptl_crystal_size_max .156  
_exptl_crystal_size_mid .088  
_exptl_crystal_size_min .02  
_exptl_crystal_density_meas ?  
_exptl_crystal_density_diffn 1.783  
_exptl_crystal_density_method 'not measured'  
_exptl_crystal_F_000 4688  
_exptl_absorpt_coefficient_mu 6.115  
_exptl_absorpt_correction_type multi-scan  
_exptl_absorpt_correction_T_min 0.0643  
_exptl_absorpt_correction_T_max 0.1639  
_exptl_absorpt_process_details ?  
_diffn_ambient_temperature 100(2)  
_diffn_radiation_wavelength 1.54178  
_diffn_radiation_type CuK\alpha  
_diffn_radiation_source 'fine-focus sealed tube'  
_diffn_radiation_monochromator graphite  
_diffn_measurement_device_type 'Bruker APEX-II CCD'  
_diffn_measurement_method '\f and \w scans'  
_diffn_detector_area_resol_mean ?  
_diffn_reflns_number 67492  
_diffn_reflns_av_R_equivalents 0.0608  
_diffn_reflns_av_sigmaI/netI 0.0381  
_diffn_reflns_limit_h_min -17  
_diffn_reflns_limit_h_max 21  
_diffn_reflns_limit_k_min -22
```

```

_diffrn_reflns_limit_k_max    22
_diffrn_reflns_limit_l_min   -29
_diffrn_reflns_limit_l_max    29
_diffrn_reflns_theta_min     2.93
_diffrn_reflns_theta_max     66.38
_reflns_number_total         13383
_reflns_number_gt            12659
_reflns_threshold_expression  >2sigma(I)
_refine_ls_structure_factor_coef Fsqd
_refine_ls_matrix_type       full
_refine_ls_weighting_scheme   calc
_atom_sites_solution_primary  direct
_atom_sites_solution_secondary difmap
_atom_sites_solution_hydrogens geom
_refine_ls_hydrogen_treatment constr
_refine_ls_extinction_method  none
_refine_ls_extinction_coef    ?
_refine_ls_abs_structure_Flack 0.00
_refine_ls_number_reflns     13383
_refine_ls_number_parameters  1105
_refine_ls_number_restraints  0
_refine_ls_R_factor_all      0.0502
_refine_ls_R_factor_gt      0.0478
_refine_ls_wR_factor_ref     0.1393
_refine_ls_wR_factor_gt     0.1366
_refine_ls_goodness_of_fit_ref 1.039
_refine_ls_restrained_S_all  1.039
_refine_ls_shift/su_max      0.013
_refine_ls_shift/su_mean     0.000
_diffrn_measured_fraction_theta_max 0.901
_diffrn_reflns_theta_full    66.38
_diffrn_measured_fraction_theta_full 0.901
_refine_diff_density_max     1.187
_refine_diff_density_min     -1.607
_refine_diff_density_rms     0.161

```

Table G.1. Atomic Coordinates and Equivalent Isotropic Displacement Parameters for Ligand-Indium Complex

Number	Label	Xfrac + ESD	Yfrac + ESD	Zfrac + ESD	Uequiv
1	IN1	0.03329(6)	0.27802(4)	0.36456(3)	0.0130
2	O21	0.1371(3)	0.4044(2)	0.47940(19)	0.0117
3	O22	-0.0658(3)	0.3995(2)	0.24281(19)	0.0153
4	O23	0.1854(3)	0.1359(2)	0.2996(2)	0.0153
5	O24	-0.1389(3)	0.1739(3)	0.4409(2)	0.0200
6	N21	-0.0636(4)	0.2589(3)	0.4112(2)	0.0113

Table G.1. Atomic Coordinates and Equivalent Isotropic Displacement Parameters for Ligand-Indium Complex (Continued)

Number	Label	Xfrac + ESD	Yfrac + ESD	Zfrac + ESD	Uequiv
7	N22	0.0242(4)	0.1665(3)	0.3702(2)	0.0087
8	N23	0.1248(4)	0.2363(3)	0.3181(2)	0.0107
9	N24	0.0926(4)	0.3090(3)	0.4346(2)	0.0097
10	N25	0.0380(4)	0.3900(3)	0.3604(2)	0.0100
11	N26	-0.0230(4)	0.3072(3)	0.2903(2)	0.0090
12	C1	-0.0320(5)	0.1387(4)	0.3930(3)	0.0140
13	C7	-0.0798(5)	0.1931(4)	0.4157(3)	0.0133
14	C9	0.2750(4)	0.3311(4)	0.3353(3)	0.0127
15	H9	0.2968	0.2883	0.3470	0.0150
16	C10	0.1026(4)	0.3773(3)	0.4374(3)	0.0097
17	C13	0.1199(5)	0.2778(3)	0.4849(3)	0.0110
18	C15	0.1601(5)	0.3409(4)	0.5104(3)	0.0150
19	H15A	0.1468	0.3461	0.5481	0.0180
20	H15B	0.2125	0.3341	0.5079	0.0180
21	C16	0.1870(5)	0.3930(4)	0.2831(3)	0.0127
22	H16	0.1480	0.3924	0.2591	0.0150
23	C19	0.0746(5)	0.1256(4)	0.3485(3)	0.0153
24	C20	0.0735(5)	0.4253(4)	0.3978(3)	0.0117
25	C21	-0.0929(5)	0.3361(4)	0.2155(3)	0.0183
26	H21A	-0.0797	0.3370	0.1776	0.0220
27	H21B	-0.1456	0.3330	0.2185	0.0220
28	C25	0.2172(5)	0.3286(3)	0.3000(3)	0.0108
29	C26	0.2211(5)	0.2144(4)	0.4365(3)	0.0193
30	H26	0.2273	0.2557	0.4154	0.0230
31	C27	0.1820(5)	0.2603(4)	0.2826(3)	0.0150
32	C29	0.2695(5)	0.4585(4)	0.3365(3)	0.0200
33	H29	0.2869	0.5027	0.3494	0.0240
34	C35	-0.0790(5)	0.1440(4)	0.2592(3)	0.0150
35	H35	-0.0336	0.1354	0.2437	0.0180
36	C36	0.1317(5)	0.1691(3)	0.3219(3)	0.0116
37	C37	0.2640(5)	0.1574(4)	0.4289(3)	0.0227
38	H37	0.2999	0.1588	0.4024	0.0270
39	C40	0.3002(5)	0.3958(4)	0.3530(3)	0.0147
40	H40	0.3393	0.3971	0.3770	0.0180
41	C41	0.2286(5)	0.1934(4)	0.2769(3)	0.0203
42	H41A	0.2395	0.1838	0.2393	0.0240
43	H41B	0.2741	0.1990	0.2964	0.0240
44	C46	0.0047(5)	0.4248(3)	0.3211(3)	0.0107
45	C48	-0.1052(4)	0.2122(4)	0.2618(3)	0.0117
46	C49	0.0690(5)	0.0522(4)	0.3492(3)	0.0197
47	H49	0.1047	0.0233	0.3332	0.0230

Table G.1. Atomic Coordinates and Equivalent Isotropic Displacement Parameters for Ligand-Indium Complex (Continued)

Number	Label	Xfrac + ESD	Yfrac + ESD	Zfrac + ESD	Uequiv
48	C52	0.2132(5)	0.4572(4)	0.3010(3)	0.0190
49	H52	0.1927	0.5005	0.2889	0.0230
50	C54	0.1678(5)	0.2129(4)	0.4749(3)	0.0157
51	C55	0.1570(5)	0.1515(4)	0.5050(3)	0.0223
52	H55	0.1195	0.1492	0.5303	0.0270
53	C56	-0.1718(5)	0.2405(4)	0.4591(3)	0.0230
54	H56A	-0.1808	0.2391	0.4976	0.0280
55	H56B	-0.2176	0.2492	0.4405	0.0280
56	C57	-0.0566(4)	0.2726(3)	0.2440(3)	0.0117
57	C59	-0.1163(5)	0.2988(4)	0.4452(3)	0.0150
58	C60	0.0427(5)	0.5350(4)	0.3561(3)	0.0200
59	H60	0.0451	0.5855	0.3544	0.0240
60	C61	0.0768(5)	0.4986(3)	0.3970(3)	0.0130
61	H61	0.1020	0.5238	0.4237	0.0160
62	C62	0.0056(5)	0.4978(4)	0.3186(3)	0.0143
63	H62	-0.0191	0.5221	0.2912	0.0170
64	C63	-0.1178(5)	0.4303(4)	0.4305(3)	0.0240
65	H63	-0.0821	0.4336	0.4570	0.0290
66	C65	-0.1444(5)	0.3646(4)	0.4172(3)	0.0160
67	C68	-0.0422(5)	0.0648(4)	0.3962(3)	0.0200
68	H68	-0.0829	0.0447	0.4131	0.0240
69	C72	-0.1422(5)	0.4928(4)	0.4059(4)	0.0263
70	H72	-0.1240	0.5380	0.4161	0.0310
71	C73	-0.1975(5)	0.3596(4)	0.3785(3)	0.0213
72	H73	-0.2167	0.3145	0.3691	0.0260
73	C74	-0.0299(5)	0.3738(3)	0.2847(3)	0.0123
74	C75	-0.2121(5)	0.1668(5)	0.3047(3)	0.0267
75	H75	-0.2572	0.1754	0.3207	0.0320
76	C76	-0.2220(6)	0.4211(4)	0.3537(3)	0.0270
77	H76	-0.2586	0.4181	0.3279	0.0320
78	C77	0.2554(6)	0.0949(4)	0.4609(4)	0.0283
79	H77	0.2864	0.0553	0.4566	0.0340
80	C79	-0.1728(5)	0.2246(5)	0.2834(3)	0.0213
81	H79	-0.1922	0.2713	0.2838	0.0260
82	C80	0.0109(6)	0.0223(4)	0.3733(3)	0.0253
83	H80	0.0065	-0.0280	0.3744	0.0310
84	C81	-0.1199(5)	0.0862(4)	0.2797(3)	0.0213
85	C82	-0.1863(6)	0.1000(5)	0.3025(3)	0.0283
86	H82	-0.2136	0.0619	0.3167	0.0340
87	C90	-0.1930(6)	0.4873(5)	0.3668(4)	0.0290
88	H90	-0.2084	0.5288	0.3486	0.0350

Table G.1. Atomic Coordinates and Equivalent Isotropic Displacement Parameters for Ligand-Indium Complex (Continued)

Number	Label	Xfrac + ESD	Yfrac + ESD	Zfrac + ESD	Uequiv
89	C91	0.2025(6)	0.0936(5)	0.4971(4)	0.0333
90	H91	0.1960	0.0519	0.5179	0.0400
91	IN2	0.51889(6)	0.26023(4)	0.12501(4)	0.0140
92	O11	0.6813(3)	0.1481(3)	0.2047(2)	0.0190
93	O12	0.5904(3)	0.4312(3)	0.0310(2)	0.0163
94	O13	0.3996(3)	0.3688(3)	0.2406(2)	0.0197
95	O14	0.3888(3)	0.1330(3)	0.0219(2)	0.0213
96	N11	0.4915(4)	0.3227(3)	0.1947(2)	0.0130
97	N12	0.4087(4)	0.2491(3)	0.1320(2)	0.0100
98	N13	0.4864(4)	0.1801(3)	0.0609(2)	0.0143
99	N14	0.5755(4)	0.1879(3)	0.1745(2)	0.0127
100	N15	0.6289(4)	0.2895(3)	0.1191(2)	0.0097
101	N16	0.5218(4)	0.3479(3)	0.0691(2)	0.0103
102	C2	0.4721(5)	0.3827(3)	0.0317(3)	0.0110
103	C3	0.7046(5)	0.0993(4)	0.0510(3)	0.0213
104	H3	0.7452	0.1238	0.0643	0.0260
105	C4	0.6427(5)	0.1350(4)	0.0419(3)	0.0190
106	H4	0.6408	0.1848	0.0481	0.0230
107	C5	0.6777(5)	0.2494(4)	0.1433(3)	0.0127
108	C6	0.4198(5)	0.1716(3)	0.0603(3)	0.0127
109	C8	0.4248(5)	0.3281(3)	0.2013(3)	0.0120
110	C11	0.5268(5)	0.0353(4)	0.1449(3)	0.0180
111	H11	0.5749	0.0374	0.1331	0.0210
112	C12	0.5816(5)	0.1000(4)	0.0236(3)	0.0153
113	C14	0.6482(4)	0.3441(4)	0.0886(3)	0.0133
114	C17	0.3708(5)	0.2068(4)	0.0992(3)	0.0150
115	C18	0.4337(5)	0.0783(4)	0.2018(3)	0.0153
116	H18	0.4177	0.1081	0.2297	0.0190
117	C22	0.3008(5)	0.2862(4)	0.1731(3)	0.0210
118	H22	0.2771	0.3149	0.1985	0.0250
119	C23	0.5041(5)	0.0797(4)	0.1867(3)	0.0130
120	C24	0.5872(5)	0.0267(4)	0.0140(3)	0.0207
121	H24	0.5467	0.0015	0.0014	0.0250
122	C28	0.4033(5)	0.4074(4)	0.0569(3)	0.0130
123	C30	0.2627(6)	0.2410(5)	0.1393(3)	0.0287
124	H30	0.2121	0.2375	0.1418	0.0350
125	C31	0.5155(5)	0.1442(4)	0.0119(3)	0.0157
126	C32	0.5198(5)	0.4431(4)	0.0083(3)	0.0180
127	H32A	0.5216	0.4400	-0.0308	0.0220
128	H32B	0.5013	0.4905	0.0184	0.0220
129	C33	0.4474(5)	0.1027(5)	-0.0077(4)	0.0280

Table G.1. Atomic Coordinates and Equivalent Isotropic Displacement Parameters for Ligand-Indium Complex (Continued)

Number	Label	Xfrac + ESD	Yfrac + ESD	Zfrac + ESD	Uequiv
130	H33A	0.4403	0.1095	-0.0461	0.0340
131	H33B	0.4521	0.0511	-0.0003	0.0340
132	C34	0.6424(5)	0.1941(4)	0.1746(3)	0.0123
133	C38	0.4623(5)	0.3960(4)	0.2666(3)	0.0233
134	H38A	0.4619	0.3833	0.3045	0.0280
135	H38B	0.4647	0.4484	0.2632	0.0280
136	C39	0.5821(5)	0.3759(3)	0.0626(3)	0.0110
137	C42	0.3854(6)	0.0335(4)	0.1763(3)	0.0243
138	H42	0.3365	0.0337	0.1864	0.0290
139	C43	0.5266(5)	0.3607(4)	0.2384(3)	0.0170
140	C44	0.7183(5)	0.3624(4)	0.0810(3)	0.0210
141	H44	0.7313	0.4024	0.0602	0.0250
142	C45	0.4799(6)	-0.0104(4)	0.1214(3)	0.0240
143	H45	0.4961	-0.0418	0.0945	0.0290
144	C47	0.5546(4)	0.1317(3)	0.2130(3)	0.0110
145	C50	0.4014(5)	0.4641(4)	0.0919(3)	0.0203
146	H50	0.4440	0.4896	0.0996	0.0250
147	C51	0.6494(5)	-0.0091(4)	0.0224(3)	0.0197
148	H51	0.6519	-0.0588	0.0154	0.0240
149	C53	0.7694(5)	0.3200(4)	0.1050(4)	0.0243
150	H53	0.8187	0.3299	0.0996	0.0290
151	C58	0.3744(5)	0.2872(4)	0.1679(3)	0.0123
152	C64	0.5843(5)	0.4104(3)	0.2182(3)	0.0163
153	C66	0.6273(5)	0.1038(4)	0.2314(3)	0.0183
154	H66A	0.6318	0.1081	0.2703	0.0220
155	H66B	0.6332	0.0531	0.2215	0.0220
156	C67	0.3001(5)	0.2009(4)	0.1017(3)	0.0230
157	H67	0.2754	0.1700	0.0784	0.0280
158	C69	0.6552(5)	0.3987(4)	0.2315(3)	0.0193
159	H69	0.6680	0.3597	0.2534	0.0230
160	C70	0.5662(5)	0.4672(4)	0.1849(3)	0.0177
161	H70	0.5178	0.4750	0.1752	0.0210
162	C71	0.3386(6)	0.4839(5)	0.1156(4)	0.0280
163	H71	0.3380	0.5229	0.1394	0.0340
164	C78	0.7495(5)	0.2629(4)	0.1372(3)	0.0170
165	H78	0.7844	0.2343	0.1543	0.0200
166	C83	0.7084(5)	0.0261(4)	0.0407(3)	0.0220
167	H83	0.7518	0.0011	0.0465	0.0270
168	C84	0.6198(5)	0.5124(4)	0.1659(3)	0.0217
169	H84	0.6075	0.5513	0.1438	0.0260
170	C85	0.4084(6)	-0.0113(4)	0.1366(3)	0.0267

Table G.1. Atomic Coordinates and Equivalent Isotropic Displacement Parameters for Ligand-Indium Complex (Continued)

Number	Label	Xfrac + ESD	Yfrac + ESD	Zfrac + ESD	Uequiv
171	H85	0.3756	-0.0426	0.1197	0.0320
172	C86	0.3399(5)	0.3716(4)	0.0463(3)	0.0223
173	H86	0.3404	0.3325	0.0225	0.0270
174	C87	0.2761(5)	0.3916(5)	0.0696(3)	0.0247
175	H87	0.2330	0.3672	0.0612	0.0300
176	C88	0.7072(6)	0.4446(4)	0.2124(3)	0.0257
177	H88	0.7557	0.4375	0.2221	0.0310
178	C89	0.6889(6)	0.5013(4)	0.1789(3)	0.0257
179	H89	0.7251	0.5317	0.1654	0.0310
180	C92	0.2758(6)	0.4472(5)	0.1050(4)	0.0310
181	H92	0.2326	0.4605	0.1222	0.0370
182	IN3	0.50409(6)	0.72723(5)	0.11380(4)	0.0195
183	Br1	0.54413(6)	0.82135(4)	0.05652(3)	0.0253
184	Br3	0.51320(7)	0.62157(5)	0.06326(4)	0.0384
185	Br4	0.57530(6)	0.71471(5)	0.18969(4)	0.0348
186	Br6	0.38255(6)	0.74858(5)	0.14303(3)	0.0271
187	IN4	0.05929(6)	0.23473(4)	0.11688(4)	0.0159
188	Br2	0.09421(6)	0.15432(5)	0.18452(4)	0.0319
189	Br5	0.08307(5)	0.35405(4)	0.14748(3)	0.0216
190	Br7	0.12864(7)	0.20831(6)	0.04226(4)	0.0392
191	Br8	-0.06643(5)	0.22306(4)	0.09609(3)	0.0184
192	H81	-0.215(5)	0.021(5)	0.268(4)	0.0260

Table G.2. Symmetry Operations for Ligand -Indium Complex

Number	Symm. Op.	Description	Detailed Description	Order	Type
1	x,y,z	Identity	Identity	1	1
2	$1/2+x,1/2-y,-z$	Screw axis (2-fold)	2-fold screw axis with direction $[1, 0, 0]$ at $x, 1/4, 0$ with screw component $[1/2, 0, 0]$	2	2
3	$x,1/2+y,1/2-z$	Screw axis (2-fold)	2-fold screw axis with direction $[0, 1, 0]$ at $0, y, 1/4$ with screw component $[0, 1/2, 0]$	2	2
4	$1/2-x,-y,1/2+z$	Screw axis (2-fold)	2-fold screw axis with direction $[0, 0, 1]$ at $1/4, 0, z$ with screw component $[0, 0, 1/2]$	2	2

Table G.3. Bond Lengths for Ligand-Indium Complex

Number	Atom1	Atom2	Length
1	IN1	N21	2.193(7)
2	IN1	N22	2.107(6)
3	IN1	N23	2.220(7)
4	IN1	N24	2.171(6)
5	IN1	N25	2.108(6)
6	IN1	N26	2.223(6)
7	O21	C10	1.344(9)
8	O21	C15	1.491(9)
9	O22	C21	1.467(9)
10	O22	C74	1.345(9)
11	O23	C36	1.31(1)
12	O23	C41	1.466(9)
13	O24	C7	1.33(1)
14	O24	C56	1.47(1)
15	N21	C7	1.28(1)
16	N21	C59	1.51(1)
17	N22	C1	1.31(1)
18	N22	C19	1.33(1)
19	N23	C27	1.47(1)
20	N23	C36	1.273(8)
21	N24	C10	1.299(8)
22	N24	C13	1.491(9)
23	N25	C20	1.33(1)
24	N25	C46	1.34(1)
25	N26	C57	1.480(9)
26	N26	C74	1.266(8)
27	C1	C7	1.47(1)
28	C1	C68	1.40(1)
29	C9	H9	0.949(8)
30	C9	C25	1.40(1)
31	C9	C40	1.38(1)
32	C10	C20	1.45(1)
33	C13	C15	1.55(1)
34	C13	C54	1.53(1)
35	C15	H15A	0.991(8)
36	C15	H15B	0.991(9)
37	C16	H16	0.949(9)
38	C16	C25	1.40(1)
39	C16	C52	1.38(1)
40	C19	C36	1.50(1)
41	C19	C49	1.38(1)

Table G.3. Bond Lengths for Ligand-Indium Complex (Continued)

Number	Atom1	Atom2	Length
42	C20	C61	1.379(9)
43	C21	H21A	0.990(8)
44	C21	H21B	0.991(9)
45	C21	C57	1.55(1)
46	C25	C27	1.51(1)
47	C26	H26	0.949(8)
48	C26	C37	1.35(1)
49	C26	C54	1.39(1)
50	C27	C41	1.54(1)
51	C29	H29	0.950(8)
52	C29	C40	1.38(1)
53	C29	C52	1.38(1)
54	C35	H35	0.950(9)
55	C35	C48	1.37(1)
56	C35	C81	1.43(1)
57	C37	H37	0.950(9)
58	C37	C77	1.44(1)
59	C40	H40	0.951(9)
60	C41	H41A	0.990(8)
61	C41	H41B	0.990(9)
62	C46	C62	1.373(9)
63	C46	C74	1.48(1)
64	C48	C57	1.52(1)
65	C48	C79	1.40(1)
66	C49	H49	0.951(8)
67	C49	C80	1.37(1)
68	C52	H52	0.950(8)
69	C54	C55	1.40(1)
70	C55	H55	0.951(9)
71	C55	C91	1.40(1)
72	C56	H56A	0.989(8)
73	C56	H56B	0.991(9)
74	C56	C59	1.55(1)
75	C59	C65	1.52(1)
76	C60	H60	0.951(8)
77	C60	C61	1.39(1)
78	C60	C62	1.37(1)
79	C61	H61	0.950(8)
80	C62	H62	0.950(8)
81	C63	H63	0.949(9)
82	C63	C65	1.37(1)

Table G.3. Bond Lengths for Ligand-Indium Complex (Continued)

Number	Atom1	Atom2	Length
83	C63	C72	1.41(1)
84	C65	C73	1.40(1)
85	C68	H68	0.952(9)
86	C68	C80	1.40(1)
87	C72	H72	0.951(8)
88	C72	C90	1.38(1)
89	C73	H73	0.951(8)
90	C73	C76	1.39(1)
91	C75	H75	0.950(9)
92	C75	C79	1.42(1)
93	C75	C82	1.35(1)
94	C76	H76	0.95(1)
95	C76	C90	1.40(1)
96	C77	H77	0.950(9)
97	C77	C91	1.35(2)
98	C79	H79	0.950(9)
99	C80	H80	0.949(8)
100	C81	C82	1.39(1)
101	C82	H82	0.95(1)
102	C90	H90	0.95(1)
103	C91	H91	0.95(1)
104	IN2	N11	2.179(5)
105	IN2	N12	2.080(8)
106	IN2	N13	2.295(6)
107	IN2	N14	2.130(6)
108	IN2	N15	2.136(7)
109	IN2	N16	2.172(5)
110	O11	C34	1.36(1)
111	O11	C66	1.47(1)
112	O12	C32	1.46(1)
113	O12	C39	1.320(8)
114	O13	C8	1.340(9)
115	O13	C38	1.44(1)
116	O14	C6	1.344(9)
117	O14	C33	1.44(1)
118	N11	C8	1.26(1)
119	N11	C43	1.47(1)
120	N12	C17	1.35(1)
121	N12	C58	1.32(1)
122	N13	C6	1.26(1)
123	N13	C31	1.51(1)
124	N14	C34	1.26(1)

Table G.3. Bond Lengths for Ligand-Indium Complex (Continued)

Number	Atom1	Atom2	Length
125	N14	C47	1.489(9)
126	N15	C5	1.33(1)
127	N15	C14	1.334(9)
128	N16	C2	1.48(1)
129	N16	C39	1.26(1)
130	C2	C28	1.51(1)
131	C2	C32	1.56(1)
132	C3	H3	0.950(9)
133	C3	C4	1.36(1)
134	C3	C83	1.40(1)
135	C4	H4	0.949(8)
136	C4	C12	1.40(1)
137	C5	C34	1.46(1)
138	C5	C78	1.38(1)
139	C6	C17	1.50(1)
140	C8	C58	1.48(1)
141	C11	H11	0.949(9)
142	C11	C23	1.41(1)
143	C11	C45	1.36(1)
144	C12	C24	1.40(1)
145	C12	C31	1.52(1)
146	C14	C39	1.52(1)
147	C14	C44	1.37(1)
148	C17	C67	1.33(1)
149	C18	H18	0.949(8)
150	C18	C23	1.37(1)
151	C18	C42	1.39(1)
152	C22	H22	0.949(8)
153	C22	C30	1.40(1)
154	C22	C58	1.38(1)
155	C23	C47	1.51(1)
156	C24	H24	0.949(9)
157	C24	C51	1.36(1)
158	C28	C50	1.39(1)
159	C28	C86	1.39(1)
160	C30	H30	0.95(1)
161	C30	C67	1.40(1)
162	C31	C33	1.57(1)
163	C32	H32A	0.992(8)
164	C32	H32B	0.989(8)
165	C33	H33A	0.99(1)
166	C33	H33B	0.991(9)

Table G.3. Bond Lengths for Ligand-Indium Complex (Continued)

Number	Atom1	Atom2	Length
167	C38	H38A	0.988(8)
168	C38	H38B	0.989(8)
169	C38	C43	1.55(1)
170	C42	H42	0.95(1)
171	C42	C85	1.38(1)
172	C43	C64	1.52(1)
173	C44	H44	0.949(8)
174	C44	C53	1.38(1)
175	C45	H45	0.950(8)
176	C45	C85	1.39(2)
177	C47	C66	1.53(1)
178	C50	H50	0.950(9)
179	C50	C71	1.37(1)
180	C51	H51	0.952(8)
181	C51	C83	1.37(1)
182	C53	H53	0.951(9)
183	C53	C78	1.40(1)
184	C64	C69	1.39(1)
185	C64	C70	1.40(1)
186	C66	H66A	0.991(8)
187	C66	H66B	0.991(8)
188	C67	H67	0.948(8)
189	C69	H69	0.949(8)
190	C69	C88	1.39(1)
191	C70	H70	0.950(9)
192	C70	C84	1.40(1)
193	C71	H71	0.95(1)
194	C71	C92	1.39(2)
195	C78	H78	0.950(8)
196	C83	H83	0.950(9)
197	C84	H84	0.949(8)
198	C84	C89	1.35(1)
199	C85	H85	0.952(9)
200	C86	H86	0.950(8)
201	C86	C87	1.38(1)
202	C87	H87	0.952(9)
203	C87	C92	1.38(1)
204	C88	H88	0.95(1)
205	C88	C89	1.40(1)
206	C89	H89	0.95(1)
207	C92	H92	0.95(1)
208	IN3	Br1	2.406(1)

Table G.3. Bond Lengths for Ligand-Indium Complex (Continued)

Number	Atom1	Atom2	Length
209	IN3	Br3	2.368(1)
210	IN3	Br4	2.349(1)
211	IN3	Br6	2.425(2)
212	IN4	Br2	2.375(1)
213	IN4	Br5	2.413(1)
214	IN4	Br7	2.344(2)
215	IN4	Br8	2.421(1)

Table G.4. Bond Angles for Ligand-Indium Complex

Number	Atom1	Atom2	Atom3	Angle
1	N21	IN1	N22	74.6(2)
2	N21	IN1	N23	149.9(2)
3	N21	IN1	N24	91.6(2)
4	N21	IN1	N25	103.0(2)
5	N21	IN1	N26	95.9(2)
6	N22	IN1	N23	75.3(2)
7	N22	IN1	N24	104.6(2)
8	N22	IN1	N25	177.5(2)
9	N22	IN1	N26	105.3(2)
10	N23	IN1	N24	97.6(2)
11	N23	IN1	N25	107.1(2)
12	N23	IN1	N26	90.3(2)
13	N24	IN1	N25	75.6(2)
14	N24	IN1	N26	150.0(2)
15	N25	IN1	N26	74.4(2)
16	C10	O21	C15	104.6(5)
17	C21	O22	C74	104.6(5)
18	C36	O23	C41	103.9(6)
19	C7	O24	C56	105.6(6)
20	IN1	N21	C7	113.7(5)
21	IN1	N21	C59	140.0(5)
22	C7	N21	C59	106.0(6)
23	IN1	N22	C1	119.5(5)
24	IN1	N22	C19	119.2(5)
25	C1	N22	C19	121.3(7)
26	IN1	N23	C27	141.1(5)
27	IN1	N23	C36	112.9(5)
28	C27	N23	C36	106.1(6)
29	IN1	N24	C10	112.5(5)
30	IN1	N24	C13	140.0(5)
31	C10	N24	C13	107.0(6)
32	IN1	N25	C20	118.8(5)
33	IN1	N25	C46	120.2(5)
34	C20	N25	C46	121.0(7)
35	IN1	N26	C57	139.7(5)
36	IN1	N26	C74	112.8(5)
37	C57	N26	C74	107.6(6)
38	N22	C1	C7	112.5(7)
39	N22	C1	C68	122.0(7)
40	C7	C1	C68	125.5(7)
41	O24	C7	N21	120.2(7)

Table G.4. Bond Angles for Ligand-Indium Complex (Continued)

Number	Atom1	Atom2	Atom3	Angle
42	O24	C7	C1	120.3(7)
43	N21	C7	C1	119.5(7)
44	H9	C9	C25	120.1(7)
45	H9	C9	C40	119.9(7)
46	C25	C9	C40	120.0(7)
47	O21	C10	N24	119.1(6)
48	O21	C10	C20	119.3(6)
49	N24	C10	C20	121.4(7)
50	N24	C13	C15	102.8(6)
51	N24	C13	C54	111.8(6)
52	C15	C13	C54	113.2(6)
53	O21	C15	C13	104.7(6)
54	O21	C15	H15A	110.8(7)
55	O21	C15	H15B	110.8(7)
56	C13	C15	H15A	110.8(7)
57	C13	C15	H15B	110.9(7)
58	H15A	C15	H15B	108.8(8)
59	H16	C16	C25	119.6(8)
60	H16	C16	C52	119.6(8)
61	C25	C16	C52	120.8(7)
62	N22	C19	C36	111.9(7)
63	N22	C19	C49	121.0(7)
64	C36	C19	C49	127.0(7)
65	N25	C20	C10	111.6(7)
66	N25	C20	C61	120.6(7)
67	C10	C20	C61	127.8(7)
68	O22	C21	H21A	110.8(7)
69	O22	C21	H21B	110.8(7)
70	O22	C21	C57	104.7(6)
71	H21A	C21	H21B	108.9(8)
72	H21A	C21	C57	110.7(7)
73	H21B	C21	C57	110.8(7)
74	C9	C25	C16	118.4(7)
75	C9	C25	C27	123.4(7)
76	C16	C25	C27	118.0(7)
77	H26	C26	C37	119.7(8)
78	H26	C26	C54	119.8(8)
79	C37	C26	C54	120.6(8)
80	N23	C27	C25	113.6(6)
81	N23	C27	C41	102.7(6)
82	C25	C27	C41	118.4(7)
83	H29	C29	C40	120.1(8)

Table G.4. Bond Angles for Ligand-Indium Complex (Continued)

Number	Atom1	Atom2	Atom3	Angle
84	H29	C29	C52	119.9(8)
85	C40	C29	C52	120.0(8)
86	H35	C35	C48	119.9(8)
87	H35	C35	C81	120.1(8)
88	C48	C35	C81	120.1(7)
89	O23	C36	N23	121.2(7)
90	O23	C36	C19	118.6(6)
91	N23	C36	C19	120.0(7)
92	C26	C37	H37	119.9(8)
93	C26	C37	C77	120.1(8)
94	H37	C37	C77	120.0(8)
95	C9	C40	C29	120.9(7)
96	C9	C40	H40	119.5(8)
97	C29	C40	H40	119.5(8)
98	O23	C41	C27	104.7(6)
99	O23	C41	H41A	110.8(7)
100	O23	C41	H41B	110.9(7)
101	C27	C41	H41A	110.9(7)
102	C27	C41	H41B	110.8(7)
103	H41A	C41	H41B	108.7(8)
104	N25	C46	C62	121.0(7)
105	N25	C46	C74	110.4(6)
106	C62	C46	C74	128.6(7)
107	C35	C48	C57	117.9(7)
108	C35	C48	C79	119.8(7)
109	C57	C48	C79	122.1(7)
110	C19	C49	H49	120.7(8)
111	C19	C49	C80	118.4(8)
112	H49	C49	C80	120.9(8)
113	C16	C52	C29	119.9(8)
114	C16	C52	H52	120.0(8)
115	C29	C52	H52	120.1(8)
116	C13	C54	C26	121.2(7)
117	C13	C54	C55	118.8(7)
118	C26	C54	C55	120.0(7)
119	C54	C55	H55	120.8(8)
120	C54	C55	C91	118.5(8)
121	H55	C55	C91	120.7(8)
122	O24	C56	H56A	111.0(7)
123	O24	C56	H56B	110.7(7)
124	O24	C56	C59	104.5(6)
125	H56A	C56	H56B	109.0(8)

Table G.4. Bond Angles for Ligand-Indium Complex (Continued)

Number	Atom1	Atom2	Atom3	Angle
126	H56A	C56	C59	110.9(7)
127	H56B	C56	C59	110.8(7)
128	N26	C57	C21	102.5(6)
129	N26	C57	C48	110.3(6)
130	C21	C57	C48	116.7(6)
131	N21	C59	C56	102.5(6)
132	N21	C59	C65	111.4(6)
133	C56	C59	C65	116.7(7)
134	H60	C60	C61	120.1(8)
135	H60	C60	C62	120.2(8)
136	C61	C60	C62	119.8(7)
137	C20	C61	C60	118.7(7)
138	C20	C61	H61	120.6(8)
139	C60	C61	H61	120.7(7)
140	C46	C62	C60	119.0(7)
141	C46	C62	H62	120.5(8)
142	C60	C62	H62	120.5(8)
143	H63	C63	C65	119.2(8)
144	H63	C63	C72	119.2(8)
145	C65	C63	C72	121.7(8)
146	C59	C65	C63	119.5(7)
147	C59	C65	C73	121.2(7)
148	C63	C65	C73	119.3(8)
149	C1	C68	H68	121.8(8)
150	C1	C68	C80	116.3(7)
151	H68	C68	C80	121.8(8)
152	C63	C72	H72	120.6(9)
153	C63	C72	C90	118.7(8)
154	H72	C72	C90	120.7(9)
155	C65	C73	H73	120.2(8)
156	C65	C73	C76	119.6(8)
157	H73	C73	C76	120.2(8)
158	O22	C74	N26	119.6(7)
159	O22	C74	C46	118.5(6)
160	N26	C74	C46	121.8(7)
161	H75	C75	C79	119.5(8)
162	H75	C75	C82	119.7(9)
163	C79	C75	C82	120.8(8)
164	C73	C76	H76	119.9(8)
165	C73	C76	C90	120.3(8)
166	H76	C76	C90	119.8(9)
167	C37	C77	H77	120.5(9)

Table G.4. Bond Angles for Ligand-Indium Complex (Continued)

Number	Atom1	Atom2	Atom3	Angle
168	C37	C77	C91	118.7(9)
169	H77	C77	C91	121(1)
170	C48	C79	C75	119.4(8)
171	C48	C79	H79	120.3(8)
172	C75	C79	H79	120.4(8)
173	C49	C80	C68	121.0(8)
174	C49	C80	H80	119.4(9)
175	C68	C80	H80	119.6(8)
176	C35	C81	C82	119.2(8)
177	C75	C82	C81	120.7(8)
178	C75	C82	H82	119.6(9)
179	C81	C82	H82	119.7(9)
180	C72	C90	C76	120.4(9)
181	C72	C90	H90	120(1)
182	C76	C90	H90	120(1)
183	C55	C91	C77	122.1(9)
184	C55	C91	H91	119(1)
185	C77	C91	H91	119(1)
186	N11	IN2	N12	75.7(2)
187	N11	IN2	N13	149.6(2)
188	N11	IN2	N14	89.1(2)
189	N11	IN2	N15	98.3(2)
190	N11	IN2	N16	97.2(2)
191	N12	IN2	N13	74.4(2)
192	N12	IN2	N14	112.3(2)
193	N12	IN2	N15	170.8(2)
194	N12	IN2	N16	99.0(2)
195	N13	IN2	N14	97.4(2)
196	N13	IN2	N15	112.0(2)
197	N13	IN2	N16	92.5(2)
198	N14	IN2	N15	74.1(2)
199	N14	IN2	N16	148.7(2)
200	N15	IN2	N16	74.6(2)
201	C34	O11	C66	104.4(6)
202	C32	O12	C39	104.6(6)
203	C8	O13	C38	104.8(6)
204	C6	O14	C33	105.1(6)
205	IN2	N11	C8	112.5(5)
206	IN2	N11	C43	139.9(5)
207	C8	N11	C43	107.6(6)
208	IN2	N12	C17	121.8(5)
209	IN2	N12	C58	119.0(5)

Table G.4. Bond Angles for Ligand-Indium Complex (Continued)

Number	Atom1	Atom2	Atom3	Angle
210	C17	N12	C58	119.1(7)
211	IN2	N13	C6	110.8(5)
212	IN2	N13	C31	140.9(5)
213	C6	N13	C31	106.9(6)
214	IN2	N14	C34	115.9(5)
215	IN2	N14	C47	134.9(5)
216	C34	N14	C47	109.0(6)
217	IN2	N15	C5	118.9(5)
218	IN2	N15	C14	120.0(5)
219	C5	N15	C14	121.0(7)
220	IN2	N16	C2	137.4(5)
221	IN2	N16	C39	115.2(5)
222	C2	N16	C39	107.2(6)
223	N16	C2	C28	113.7(6)
224	N16	C2	C32	101.8(6)
225	C28	C2	C32	115.1(6)
226	H3	C3	C4	120.2(8)
227	H3	C3	C83	120.1(8)
228	C4	C3	C83	119.8(8)
229	C3	C4	H4	119.4(8)
230	C3	C4	C12	121.4(8)
231	H4	C4	C12	119.2(8)
232	N15	C5	C34	109.9(7)
233	N15	C5	C78	120.9(7)
234	C34	C5	C78	129.2(8)
235	O14	C6	N13	120.4(7)
236	O14	C6	C17	116.7(6)
237	N13	C6	C17	122.9(7)
238	O13	C8	N11	119.4(7)
239	O13	C8	C58	119.7(7)
240	N11	C8	C58	120.8(7)
241	H11	C11	C23	119.7(8)
242	H11	C11	C45	119.9(8)
243	C23	C11	C45	120.3(8)
244	C4	C12	C24	117.3(7)
245	C4	C12	C31	118.3(7)
246	C24	C12	C31	124.3(7)
247	N15	C14	C39	109.4(6)
248	N15	C14	C44	122.3(7)
249	C39	C14	C44	128.2(7)
250	N12	C17	C6	110.0(7)
251	N12	C17	C67	122.9(8)

Table G.4. Bond Angles for Ligand-Indium Complex (Continued)

Number	Atom1	Atom2	Atom3	Angle
252	C6	C17	C67	127.1(7)
253	H18	C18	C23	119.9(8)
254	H18	C18	C42	119.7(8)
255	C23	C18	C42	120.4(8)
256	H22	C22	C30	121.4(8)
257	H22	C22	C58	121.5(8)
258	C30	C22	C58	117.2(8)
259	C11	C23	C18	119.1(7)
260	C11	C23	C47	121.5(7)
261	C18	C23	C47	119.3(7)
264	H24	C24	C51	119.3(8)
265	C2	C28	C50	121.9(7)
266	C2	C28	C86	119.8(7)
267	C50	C28	C86	118.3(7)
268	C22	C30	H30	120.5(9)
269	C22	C30	C67	119.1(8)
270	H30	C30	C67	120.3(9)
271	N13	C31	C12	112.2(6)
272	N13	C31	C33	100.8(6)
273	C12	C31	C33	116.7(7)
274	O12	C32	C2	104.9(6)
275	O12	C32	H32A	110.7(7)
276	O12	C32	H32B	110.7(7)
277	C2	C32	H32A	110.8(7)
278	C2	C32	H32B	110.9(7)
279	H32A	C32	H32B	108.8(8)
280	O14	C33	C31	104.8(7)
281	O14	C33	H33A	110.9(8)
282	O14	C33	H33B	110.8(8)
283	C31	C33	H33A	110.8(8)
284	C31	C33	H33B	110.7(8)
285	H33A	C33	H33B	108.9(9)
286	O11	C34	N14	118.3(7)
287	O11	C34	C5	120.8(7)
288	N14	C34	C5	120.9(7)
289	O13	C38	H38A	110.6(7)
290	O13	C38	H38B	110.5(7)
291	O13	C38	C43	105.7(6)
292	H38A	C38	H38B	109.0(8)
293	H38A	C38	C43	110.5(7)
294	H38B	C38	C43	110.5(7)
295	O12	C39	N16	121.0(7)

Table G.4. Bond Angles for Ligand-Indium Complex (Continued)

Number	Atom1	Atom2	Atom3	Angle
296	O12	C39	C14	118.3(6)
297	N16	C39	C14	120.6(7)
298	C18	C42	H42	119.9(8)
299	C18	C42	C85	120.2(8)
300	H42	C42	C85	119.9(9)
301	N11	C43	C38	102.0(6)
302	N11	C43	C64	111.3(6)
303	C38	C43	C64	116.4(7)
304	C14	C44	H44	121.5(8)
305	C14	C44	C53	117.1(8)
306	H44	C44	C53	121.4(8)
307	C11	C45	H45	119.8(9)
308	C11	C45	C85	120.4(8)
309	H45	C45	C85	119.8(9)
310	N14	C47	C23	109.5(6)
311	N14	C47	C66	102.0(6)
312	C23	C47	C66	117.9(6)
313	C28	C50	H50	119.8(8)
314	C28	C50	C71	120.7(8)
315	H50	C50	C71	119.5(8)
316	C24	C51	H51	119.9(8)
317	C24	C51	C83	120.3(8)
318	H51	C51	C83	119.9(8)
319	C44	C53	H53	119.6(9)
320	C44	C53	C78	120.9(8)
321	H53	C53	C78	119.5(9)
322	N12	C58	C8	111.3(7)
323	N12	C58	C22	122.7(7)
324	C8	C58	C22	125.9(7)
325	C43	C64	C69	120.1(7)
326	C43	C64	C70	120.0(7)
327	C69	C64	C70	119.9(7)
328	O11	C66	C47	106.1(6)
329	O11	C66	H66A	110.6(7)
330	O11	C66	H66B	110.5(7)
331	C47	C66	H66A	110.5(7)
332	C47	C66	H66B	110.6(7)
333	H66A	C66	H66B	108.7(8)
334	C17	C67	C30	119.0(8)
335	C17	C67	H67	120.5(8)
336	C30	C67	H67	120.5(8)
337	C64	C69	H69	120.4(8)

Table G.4. Bond Angles for Ligand-Indium Complex (Continued)

Number	Atom1	Atom2	Atom3	Angle
338	C64	C69	C88	119.2(8)
339	H69	C69	C88	120.4(8)
340	C64	C70	H70	120.2(8)
341	C64	C70	C84	119.7(7)
342	H70	C70	C84	120.1(8)
343	C50	C71	H71	120(1)
344	C50	C71	C92	120.4(9)
345	H71	C71	C92	120(1)
346	C5	C78	C53	117.8(8)
347	C5	C78	H78	121.1(8)
348	C53	C78	H78	121.1(8)
349	C3	C83	C51	119.8(8)
350	C3	C83	H83	120.0(8)
351	C51	C83	H83	120.2(8)
352	C70	C84	H84	119.7(8)
353	C70	C84	C89	120.6(8)
354	H84	C84	C89	119.7(8)
355	C42	C85	C45	119.6(8)
356	C42	C85	H85	120.2(9)
357	C45	C85	H85	120.2(9)
358	C28	C86	H86	119.2(8)
359	C28	C86	C87	121.5(8)
360	H86	C86	C87	119.3(8)
361	C86	C87	H87	120.3(8)
362	C86	C87	C92	119.1(8)
363	H87	C87	C92	120.5(9)
364	C69	C88	H88	119.5(8)
365	C69	C88	C89	120.7(8)
366	H88	C88	C89	119.7(9)
367	C84	C89	C88	119.9(8)
368	C84	C89	H89	120.2(9)
369	C88	C89	H89	120.0(9)
370	C71	C92	C87	119.9(9)
371	C71	C92	H92	120(1)
372	C87	C92	H92	120(1)
373	Br1	IN3	Br3	105.57(5)
374	Br1	IN3	Br4	112.92(5)
375	Br1	IN3	Br6	110.75(5)
376	Br3	IN3	Br4	108.47(5)
377	Br3	IN3	Br6	111.78(5)
378	Br4	IN3	Br6	107.41(5)

Table G.4. Bond Angles for Ligand-Indium Complex (Continued)

Number	Atom1	Atom2	Atom3	Angle
379	Br2	IN4	Br5	108.00(5)
380	Br2	IN4	Br7	107.07(5)
381	Br2	IN4	Br8	111.50(5)
382	Br5	IN4	Br7	110.68(5)
383	Br5	IN4	Br8	109.46(5)
384	Br7	IN4	Br8	110.11(5)